The Dissertation Committee for Bryant Allson Chambers certifies that this is the approved version of the following dissertation:

A molecular biological model describing silver nanoparticle mechanism of toxicity and associated antibiotic resistance

Committee:

Mary Jo Kirisits, Supervisor

Lynn E. Katz

Navid Saleh

Hans Hofmann

Matthew Parsek

A molecular biological model describing silver nanoparticle mechanism of toxicity and associated antibiotic resistance

By

Bryant Allson Chambers

Dissertation

Presented to the Faculty of the Graduate School of

The University of Texas at Austin

in Partial Fulfillment

of the Requirements

for the Degree of

Doctor of Philosophy

The University of Texas at Austin

May 2018

Dedication

For my family and friends, especially my grandmother, Elladean Rupert Chambers.

Thank you all for pushing.

And the millions of bacteria who gave their lives for this research….

Acknowledgements

There is no way to thank all the people who have helped me in this endeavor; I will, by the sheer number of those who have assisted, miss some of you. So, I will start here by saying thank you to all who have in some form or fashion been there for me over the last eight years. When I first came back and started this process I was very unsure, and it took a lot to figure out where I was headed. Thank you.

Thank you first to my committee for all their help in preparing this document. Navid Saleh, thank you for all the guidance and excitement; you have been mentor who I can laugh with just as easily and I can seek advice from. Lynn Katz, thank you for the great conversations about science and all the work you have done with me. I have been honored to know you and have you on my committee. Hans Hofmann, you have always brought an excitement to conversations about my work and I value your perspective; your interest has given me confidence. Matthew Parsek, thank you for your help and conversations. Planning out my work with you and your willingness to help even from such great distance led to some very successful experiments! Lastly, and most importantly, thank you, Mary Jo Kirisits, you have shown patience, guidance, and friendship over the many years it took me to figure all of this out. A sincere thank you. You also gave me the opportunity to pursue my own research ideas, an opportunity that not many students receive. I look forward to continued conversation after I finally find a place to hang my academic hat.

The family of friends I have found in the EWRE program compares to none that I have made anywhere else in my life. This is a hard program with amazing students who I am honored to have worked with. Sarah Keithley, I owe so much to you. Thank you for wanting to borrow “my” microwave so many years ago. Thank you to Jim, Justin, Other

Justin (I'll let you guys settle that), Katharine, Erin, Alicia, Indu, Farith, Gustavo, Anne, Aurore, Ellison, Amanda, Hector, Savanna. You all made this much easier than it would have been alone. I am always amazed by your insights and intellect. Again, there isn't enough space here to write what I actually feel, nor do I even have the words. They should have sent a poet. To those I left out, I am sorry. This could have been an equal number of just pages of names. To my friends who weren't in the program: James, Nathan, Elisa.

And lastly to my family. Travis, Will, Sarah, and Mary and to all of my Parents, Thank you. I could have done with less "When are you going to finish" phone calls, but I know it was out of love. Thank you. You have heard me at my worst and celebrated with me at my best. Thank you for bearing with me.

This wasn't easy, but it was worth it. Thank you all for every little bit of encouragement and belief you put in to me.

A molecular biological model describing silver nanoparticle mechanism of toxicity and associated antibiotic resistance

Bryant Allson Chambers, Ph.D.

The University of Texas at Austin, 2018

Supervisor: Mary Jo Kirisits

Control of microbial growth is key to proper function of engineered systems and human health. Combating biological contamination in engineered processes is complicated due to the limited number of materials that are both able to impede microbial growth and are benign with respect to human and environmental health. Silver nanoparticles (AgNPs) have emerged as a novel biocide, reducing biological fouling in consumer goods and health care materials. Their almost ubiquitous usage is primarily due to their microbial cytotoxicity, limited human toxicity, and their ability to be incorporated into a wide variety of materials. The use of AgNPs is not without challenges; microbial toxicity varies by exposure methodology, and studies have shown that AgNPs have the potential to disrupt engineered biological processes either as nanoparticles or through the dissolution of aqueous silver ($Ag_{(aq)}$). The use of AgNPs is further complicated by their mechanisms of action; there is significant overlap of their biological targets with the targets of antibiotics. Thus, antibiotic resistance might result from AgNP exposure through the processes of co- and cross-resistance, in which one chemical selects for microbial resistance to a second (unrelated) chemical. In this work, the impact of AgNP aggregation and dissolution on toxicity to *Escherichia coli* was examined. Data indicate that conditions promoting high fractal dimension promote greater toxicity and induce an oxidative stress

response. Subsequent studies on the opportunistic human pathogen *Pseudomonas aeruginosa* were directed at elucidating the mechanisms of action of AgNPs and the microbial response. Transcriptomic and proteomic studies focused on defining a model of bacterial AgNP interaction and isolated mechanisms of toxicity of AgNPs. Further these data provided the first evidence of AgNP exposure resulting in antibiotic resistance through the expression of multidrug efflux pumps. Transcriptomic data indicated that the stress response systems activated as a result of AgNP exposure were localized to the periplasm while the stress response systems activated as a result of $Ag_{(aq)}$ exposure were localized to the cytoplasm, which supports a surface attachment model of bacterial AgNP interaction distinct from that of $Ag_{(aq)}$. Transcriptomic studies revealed that key antibiotic resistance systems, including *mexGHI* and *mexPQ,* were stimulated by AgNP exposure. *P. aeruginosa* cells that were pre-exposed to a sublethal concentration of AgNPs demonstrated increased resistance in subsequent antibiotic challenges, demonstrating that antibiotic resistance can be induced by AgNPs. The findings of this study are an important contribution to our understanding of the impacts of co- and cross-resistance induced by AgNP exposure and will ultimately help inform decisions related to human and environmental health.

Table of Contents

List of Tables

List of Figures

1. Introduction

1.1.1 Motivation

The modern urban landscape is changing quickly to meet the needs of growing populations. Smart materials with increased strength-to-cost ratios, advanced energy-saving capabilities, and self-disinfecting properties are now in mainstream use and are improving the quality of life for many people (Nel et al. 2009; Jung et al. 2011; Berge et al. 2013; Knetsch et al. 2011). Many of these modern materials derive their novel properties from the inclusion of metal- and nonmetal-core nanoparticles (Y. Li et al. 2006; Simon-deckers et al. 2009; Rai et al. 2012; X. Chen et al. 2008; Dastjerdi et al. 2010; 2010). Carbon nanotubes and iron-core nanoparticles can be used to increase the strength of concrete and steel (Reibold et al. 2006; Manzur et al. 2016; Horszczaruk et al. 2017); indium tin oxide and cadmium selenide nanoparticles increase the electrical efficiency of modern electronics (Peng et al. 1997; Mryasov et al. 2001); silver nanoparticles (AgNPs) and copper nanoparticles confer bacterial inactivation capabilities to clothing (Chatterjee et al. 2014; Simoncic et al. 2015), medical devices (Li et al. 2006; H. Y. Lee et al. 2007; Deredjian et al. 2011;), and water treatment processes (Sheng et al. 2011). While these advanced material traits are desirable, the eventual release of the nanoparticles to the environment might have negative consequences (Alvarez et al. 2009; Nowack 2010).

AgNPs have sparked considerable scientific interest owing to their toxicity to a wide range of bacteria (Sondi et al. 2004; Elechiguerra et al. 2005; Morones et al. 2005; Hwang et al. 2008;; Suresh et al. 2010; Musee et al. 201; Arnaout et al. 2012; Markowska et al. 2013;) and higher aquatic life (Miao et a/l. 2009; Laban et al. 2010; Julia Fabrega et al. 2011; Römer et al. 2011;). The database for the Project on Emerging Nanomaterials showed that the category of “products containing AgNPs” had the most substantial growth

among all monitored categories over the past 12 years, adding 500 new products since 2007 (Vance et al. 2015). The inclusion of AgNPs in many consumer goods is disconcerting because of the potential unintended disruption of bacterial processes in engineered and natural systems. For instance, the shedding of particulate and aqueous silver ($Ag_{(aq)}$) from clothing into wash water (Benn et al. 2008) indicates that there is potential for entry of these nanomaterials into the built environment and subsequently into natural ecosystems. Additionally, a study examining a theoretical release of AgNPs (Liang et al. 2010) into a wastewater treatment plant found the potential to disrupt activated sludge processes temporarily. Described as follows, the potential for AgNPs to disrupt bacterial processes in engineered and natural systems is supported by empirical evidence from bench-scale studies. Biofilms and bacterial flocs from wastewater treatment plants showed sensitivity to AgNPs, with biomass loss after exposure (Sheng et al. 2011; Hendren et al. 2013). Drinking water nitrification was inhibited when bacteria were exposed to a shock load of AgNPs (Choi et al. 2009). The microbiome in landfill composting processes was altered by AgNP exposure (Gitipour et al. 2013). AgNPs altered the microbiome of natural estuarine sediments (Bradford et al. 2009). To limit the unintended impacts of AgNPs, we must first understand the physical and chemical mechanisms that control the antimicrobial activity of AgNPs as well as the molecular-level response of bacteria to AgNPs.

1.1.2 Defining the Problem

The fate and transport of AgNPs in the environment depend on aggregation and dissolution (Baalousha et al. 2013; Römer et al. 2011; X. Li et al. 2012; Deonarine et al. 2011) as well as on their interactions with humic substances (Hurt, et al. 2010; Sonshine, et al. 2010; Hendren et al. 2013). In turn, these same processes might impact the bacterial toxicity of AgNPs. For instance, the bacterial toxicity of AgNPs is altered by pH and the

presence natural organic matter (Fabrega et al. 2009), which likely is a result of changes in aggregate morphology. The availability of complexing ligands also can alter the toxicity of AgNPs; sulfide, which is a very strong ligand for silver, dramatically reduces the bacterial toxicity of AgNPs (Levard et al. 2012a; 2012b). Interestingly, chloride, also a complexing ligand of silver, might cause the formation of a solid AgCl shell around AgNPs, thereby altering the observed aggregation state (Li et al. 2010; 2012) and limiting AgNP toxicity. Ionic strength affects AgNP aggregation, which in turn, impacts toxicity (Fabrega et al. 2009; Fabrega et al. 2011). Overall, solution chemistry has significant potential to affect the fate, transport, and bacterial toxicity of AgNPs.

Two distinct models describing the interaction of AgNPs with bacteria have been proposed in the literature. The first model attributes the toxicity of AgNPs to the production of Ag^+ (outside the cell) from oxidized nanoparticles (Pratsinis et al. 2010; Xiu et al. 2012). The second model requires contact between AgNPs and the bacterial surface; when AgNPs bind to the bacterial surface, they have the potential to release concentrated $Ag_{(aq)}$ into the outer membrane and periplasmic space (Morones et al. 2005;; X. Yang et al. 2012; Long et al. 2017). Since both models involve AgNP dissolution, they are both impacted by solution chemistry (e.g., ionic strength and availability of organic and inorganic ligands).

In the first model (focused on $Ag_{(aq)}$), the mechanisms of action of AgNPs by which the cell is harmed include protein oxidation, reactive oxygen species generation (ROS), DNA alteration, and potentially membrane disruption (Nies 1999; Silver 2003). In the second model (focused on AgNPs at the bacterial surface), the mechanisms of action of AgNPs include membrane disruption, lipid peroxidation via ROS, and protein oxidation (Nies 1999; Sondi et al. 2004; Elechiguerra et al. 2005; Choi et al. 2008). While the mechanisms of action overlap between the two models, only the second model directly considers the role of the particulate form with respect to bacterial toxicity.

Some of these mechanisms of action for AgNPs are shared with antibiotics and dissolved metals. The overlap of AgNP mechanisms of action with antibiotics suggest that bacterial adaptation to resist AgNP toxicity might also give rise to antibiotic resistance. Many antibiotics, such as penicillin and polymyxin (i.e., cationic polypeptides), affect the cellular envelope and lead to cell lysis (De Lencastre et al. 1999; Papp-Wallace et al. 2011). Quinolone and aminoglycoside antibiotics target DNA replication and increase protein misfolding, respectively (Giuliodori et al. 2007; Storz et al. 2011). Metals have the potential to promote the formation of hydrogen peroxide (H_2O_2) through a bis-glutathione intermediate, cause membrane disruption, and promote protein oxidation (Nies 1999; Nies 2003; Giles et al. 2003). Each of these routes of cytotoxicity is tightly linked to a particular stress response, which is a biochemical pathway that repairs cellular damage. For example, envelope damage is linked to *cpx*, *psp*, and *rcs* stress response pathways; DNA damage is linked to *lex* and *sos* stress response pathways; misfolded proteins are linked to *cpx* and *deg* stress response pathways (Ron 2006; Storz et al. 2011). While it has long been known that antibiotics activate such stress response systems (Markowska et al. 2014), recent evidence demonstrates that AgNPs also activate stress response systems, such as the sigma-S stress response system (Radzig et al. 2013). Thus, while AgNPs (via $Ag_{(aq)}$ production or surface interaction with cells), antibiotics, and dissolved metals represent different classes of stressors, their overlapping mechanisms of action (protein oxidation, ROS generation, DNA alteration, and potential membrane disruption) suggest that they have the potential to elicit similar stress responses in bacteria.

Bacteria can develop resistance (i.e., the ability to grow in the presence of a stressor) through general or specific stress response systems (Baker-Austin et al. 2006). These systems are the first line of defense in overcoming detrimental cellular conditions and offering protection to bacteria (Storz et al. 2000, 2011). General stress response

systems often encompass a high level of genetic regulation and react to a change in a gross characteristic (e.g., ionic strength or temperature) (Akbar et al. 2001; Coenye 2010). Specific stress response systems are smaller in scope and respond to specific signals (e.g., a specific metal, ROS) (Mols et al. 2011; Cabiscol et al. 2000). It is currently unknown whether the different classes of stressors under consideration in this dissertation (i.e., AgNPs, antibiotics, and dissolved metals) activate general and/or specific stress response networks in such a way that bacteria exposed to one class of stressor gain increased resistance to another. This selective process leads to co- and cross-resistance. Co-resistance is the condition in which two separate resistant determinants are on a shared genetic element and are selected for together; cross-resistance is the condition in which one resistant determinant protects against both stressors and is selected for simultaneously.

It is the overall goal of this dissertation to understand the basis for stress and toxicity to environmentally relevant Gram-negative bacteria (*Escherichia coli* and *Pseudomonas aeruginosa*) in the presence of AgNPs. The model of interaction between AgNPs and bacteria (i.e., (1) production of $Ag_{(aq)}$ outside the cell or (2) attachment of AgNPs to the cell surface) must be delineated to determine if the particulate form plays an important role in stressing the cells. Additionally, to support strategies for limiting the spread of antibiotic resistance in bacteria, the potential link between AgNP usage and antibiotic resistance must be examined. As such, the specific objectives of this research are as follows:

1. Characterize the effect of solution chemistry, including chloride concentration and ionic strength, on AgNP morphology, dissolution, and toxicity to bacteria.
2. Build a biomolecular model that describes how AgNPs interact with bacteria.

3. Build a biomolecular model that describes the potential for $Ag_{(aq)}$ and AgNPs to induce co- and cross-resistance to antibiotics.
4. Evaluate AgNP cross-resistance to a series of eight antibiotics.

1.1.3 Research Approach

Aligned to each of the above objectives, four research tasks were designed.

1. **Impact of exposure medium on bacterial nano-toxicity** The purpose of this task was to determine how the solution chemistry of biological media used to establish the bacterial toxicity of AgNPs impacts the morphology and dissolution of the AgNPs. The physical and chemical characteristics of thiomalic-acid-coated AgNPs were characterized in nine chemically distinct solutions (i.e., at a range of ionic strengths and chloride concentrations). Under these conditions, AgNPs were assessed for aggregation rate, dissolution propensity, and aggregate structure (fractal dimension). These physical characteristics were then linked to toxicity by exposing *E. coli* to AgNPs in the nine solutions. These data were used to select the solution chemistry for subsequent tasks so that AgNP stability was maintained.
2. **Molecular biological evidence for a surface attachment model of silver nanoparticle toxicity** The purpose of this task was to describe the model of interaction between AgNPs and bacteria (i.e., (1) production of $Ag_{(aq)}$ outside the cell or (2) attachment of AgNPs to the cell surface) via a transcriptomic approach. AgNPs and $Ag_{(aq)}$ were dosed to *P. aeruginosa* at sublethal levels. These cultures and a no-Ag control culture were interrogated with a transcriptomic analysis. Using data from key stress response systems, a

biomolecular model was built to describe how AgNPs interact with bacterial cells.

3. **Antibiotic resistance is stimulated by silver and silver nanoparticles.** The purpose of this task was to evaluate the activation of gene clusters involved in antibiotic stress response as a result of exposure to AgNPs or $Ag_{(aq)}$ via transcriptomic and proteomic approaches. AgNPs and $Ag_{(aq)}$ were dosed to *P. aeruginosa* at sublethal levels. These cultures and a no-Ag control culture were interrogated with transcriptomic and proteomic analyses. Using data from key antibiotic resistance genes, namely those encoding resistance nodulation division (RND) multi-drug efflux pumps, a biomolecular model was built to describe co- and cross-resistance among AgNP, $Ag_{(aq)}$, and antibiotics in bacteria.
4. **A study of silver-nanoparticle-induced resistance to antibiotics.** The purpose of this task was to expand the theoretical basis of AgNP-antibiotic co- and cross-resistance described in Task 3 by assessing the development of adaptive resistance to antibiotics in *P. aeruginosa.* Resistance to antibiotics was stimulated via exposure to a growth-limiting dosage of AgNPs in *P. aeruginosa.* Following this exposure and quenching of AgNPs, bacteria were exposed to one of a suite of eight antibiotics to determine if pre-exposure to AgNPs can induce antibiotic resistance. Further, a series of RND efflux pump over-expression and deletion mutants were exposed to AgNPs and $Ag_{(aq)}$ to evaluate their participation in the mitigation of efflux pumps in AgNP and $Ag_{(aq)}$ stress.

1.1.4 Dissertation structure

Chapter 2 provides an overview of the relevant literature. The mechanisms of action of antibiotics as compared to the two proposed models of AgNPs interaction and associated mechanisms of AgNP toxicity are reviewed. The potential influence of the physical and chemical attributes of AgNPs on their bacterial toxicity are discussed. The chapter then goes on to examine the potential link between antibiotic resistance and metal exposure as well as the mechanisms by which antibiotic resistance might be induced via metal exposure (a topic that has mostly been discussed conceptually to-date). Finally, the chapter outlines the bioinformatic techniques that could be applied to separate the effects of AgNPs from $Ag_{(aq)}$ on bacteria.

Chapters 3-6 present experimental methodology as well as results and their environmental implications. Each chapter was based on a manuscript prepared for submission to a journal. Chapter 3 (published) discusses the effects of chloride concentration and ionic strength on AgNP morphology, dissolution, and bacterial toxicity. The work links toxicity to stress induction, specifically discussing the expression of *katE*, a catalase gene, in response to AgNP exposure. Chapter 4 proposes a biomolecular model of AgNP interaction with *P. aeruginosa*, as derived from transcriptomic data of stress response genes. This work fuses the two existing models of interaction in the literature into a universal model, thereby explaining results obtained in previous studies. Results from this study provide a clear evidence of AgNP-cell-surface attachment, and differential action of intact AgNPs versus $Ag_{(aq)}$. Chapter 5 follows with evidence of induction of antibiotic resistance genes after sublethal AgNP and $Ag_{(aq)}$ exposure. Results from this chapter are the first evidence of AgNP-induced antibiotic resistance and are among the first data to directly illustrate the selection of antibiotic resistance through metal exposure. The chapter proposes a model of bacterial antibiotic resistance derived from surface and oxidative

stress. Chapter 6 provides evidence that AgNPs actually induces cross-resistance to some antibiotics in *P. aeruginosa*, and the role of RND efflux pumps in mitigating stress due to AgNP exposure is highlighted.

Chapter 7 concludes the dissertation by summarizing the major research findings and presenting opportunities for future work. It is followed by appendices and references to literature cited.

2. Literature Review

2.1 PROBLEM

2.1.1 Potential for nanoparticle-induced antibiotic resistance

Antibiotic resistance, the ability for a microorganism to grow in the presence of an antibiotic (defined as chemical compounds, naturally occurring or engineered, that are administered to an organism for a health benefit), is estimated to cost households in the United States over $35 billion dollars (US 2008) each year (Alliance for the Prudent Use of Antibiotics 2010). In this work, the term antibiotic resistance includes both adaptive antibiotic resistance, which is due to temporal expression of genes related to the mitigation of antibiotic stress (Fernandez 2010; Storz 2012), and mutative antibiotic resistance, which is due to hereditable changes in genes related to the mitigation of antibiotic stress (Galhardo et al. 2007). Experiments conducted in this work make no distinction between the two processes, and both processes could be occurring simultaneously.

Infections due to antibiotic-resistant organisms significantly increase the length of hospital stays (by 5-13 days) and, in some cases increase mortality, thereby greatly increasing societal costs (Alliance for the Prudent Use of Antibiotics 2010; Cosgrove et al. 2012; CDC 2013). Compounding these issues is a decline in the development of new antibiotics (Idsa 2004), which limits treatment options to fight many bacterial infections. Numerous strategies have been proposed to combat antibiotic resistance through new drug design (Norrby et al. 2005; Finch et al. 2006; Leung et al. 2011), but stewardship programs can be a means by which to effectively use existing antibiotics (Owens 2008; Lee et al. 2013). Recent evidence suggests that the development of antibiotic resistance involves complex interactions between bacterial stress response systems and antibiotics (Keith Poole 2012b; 2014), but the aforementioned antibiotic stewardship strategies do not

explicitly consider the role of bacterial stress response systems. Further, stress response systems are not only stimulated by antibiotics but also by other biocides (defined as chemical compounds that are detrimental to life), such as metals, reactive oxygen species (ROS), and physical stressors (Storz et al. 2000; Ron 2006). The interaction between biocides and stress response systems might lead to the development of co- and cross-resistance; in such scenarios, secondary biocides can promote resistance to a primary biocide (Baker-Austin et al. 2006), and physiological adaptive resistance can develop as a result of transient changes in gene expression related to stress mitigation (Breidenstein et al. 2008; Raja et al. 2008). Thus, the selective pressures promoting antibiotic resistance in the environment might be due not only to antibiotic usage but also to the interaction of other biocides with microbial stress response systems.

Several key studies have now linked the occurrence of antibiotic resistance to metals. For example, in a purely environmental context, copper, nickel, and chromium have been linked to the occurrence of antibiotic resistance genes. In engineered systems such as landfills (Wu et al. 2015) and drinking water treatment systems (Calomiris et al. 1984), the occurrence of the heavy metals copper and iron were correlated with the presence of antibiotic-resistant bacteria. Moreover, the presence of antibiotics as waste in a landfill did not, by themselves, correlate with the occurrence of antibiotic resistance genes; rather, heavy metals also needed to be present (Wu et al. 2015).

Silver nanoparticles (AgNPs) are an emerging environmental contaminant (Mueller et al. 2008) and biocide that are commonly incorporated into consumer goods. AgNPs are known to release aqueous silver (Chambers et al. 2014; Z.-M. Xiu et al. 2011b), are thought to promote the formation of extracellular ROS (Xia et al. 2008; Choi et al. 2008), and are known to cause physical stress to cells (S. Liu et al. 2009); all of these stresses can activate formal stress responses in bacteria (Ron 2006; Storz et al. 2000). Given that bacterial stress

response might overlap with antibiotic resistance pathways (discussed next), it is imperative that the environmental community examines the possibility of the co- and cross-resistance mechanisms by which AgNPs might induce antibiotic resistance.

2.1.2 Bacterial antibiotic resistance and bacterial stress response

Antibiotic resistance describes the ability of a microorganism to grow in the presence of an antibiotic. Classically, antibiotic resistance is achieved through four mechanisms: antibiotic target alteration, antibiotic inactivation, antibiotic sequestration, and antibiotic efflux (Hawkey 1998; Mazel et al. 1999; Walsh 2000; Kumar et al. 2005; Lin et al. 2015). Antibiotic resistance also might be due to adaptive responses, such as the transient expression of genes that mitigate the antibiotic's impact (Harrison et al. 2007). Recent work provides evidence of the role that adaptive stress response can play in mutative resistance; transcriptomic stress can cause mutational pressure on actively transcribed genes and lead to modification of regulator and coding regions (Jinks-Robertson et al. 2014). Thus, continued expression of genes required for transient stress response can lead to mutations in those genes, which, in turn, can lead to increased resistance.

Current research indicates that the aforementioned antibiotic resistance mechanisms are fundamentally controlled by bacterial stress response systems (De Lencastre et al. 1999; Storz et al. 2000; Poole 2012b; Markowska et al. 2014). For example, increase in an adaptive ROS stress response indirectly increased resistance to the aminoglycoside class of antibiotics through expression of a specific antibiotic stress response directing multidrug efflux pump expression in *Pseudomonas aeruginosa* (Dwyer et al. 2009; C. H. Lau et al. 2014); here, the underlying mechanism is co-regulation. At

longer time scales, an example of mutationally driven antibiotic resistance has been observed in *Escherichia coli;* here, activation of ROS stress response systems might induce the salt overly sensitive (SOS) response, which can increase mutation rates (Moore et al. 2017). Given that regions of active transcription are prone to more replicative error (Jinks-Robertson et al. 2014), antibiotic stress response systems that are actively undergoing transcription would have a higher likelihood of mutation; thus, this could result in an improved response to an antibiotic insult.

2.1.3 Defining stress

Bacterial stress can be described as a challenge to a bacterium's normal homeostasis under typical environmental conditions (Wassarman et al. 2011). Stress responses might occur as a part of normal active growth, during a no-growth phase, in addition to when an actual stressor is acting to disrupt normal cellular function (e.g., metabolism, protein synthesis, replication, membrane integrity) (Ron 2006; Storz et al. 2000). The current study focuses on stress response when a stressor is disrupting essential cellular functions.

Bacterial stress response systems are protein/DNA/RNA elements that act in concert to mitigate cellular harm. Often called a regulatory network, sensory elements activate major response regulators, which initiate multiple downstream effectors. The activating element is typically a transcriptional regulator that modulates expression of one or more genes to alleviate the result of a stressor (Storz et al. 2000) often by means of a two-component system (Stock et al. 2000; Kohanski et al. 2008; Eckweiler et al. 2012). For instance, a two-component (Figure 2.1) system acting in this way consists of a receptor protein that can sense a harmful molecule or damaged cellular component. As a result of this sensing, a change in some property of the receptor ultimately leads to the activation of

a response cascade that reduces the impact of the stressor. The receptor also might activate a master regulatory element such as a transcription factor, which can facilitate transcription of genes downstream of recognized promoters, thereby increasing the expression of multiple response elements tied to the same stressor. Recent research indicates that additional regulation of stress response also takes place at the level of RNA modification and RNA regulation, thereby providing even more regulation than previously known (Storz et al. 2000; Ron 2006; Wassarman et al. 2011; Balasubramanian et al. 2014).

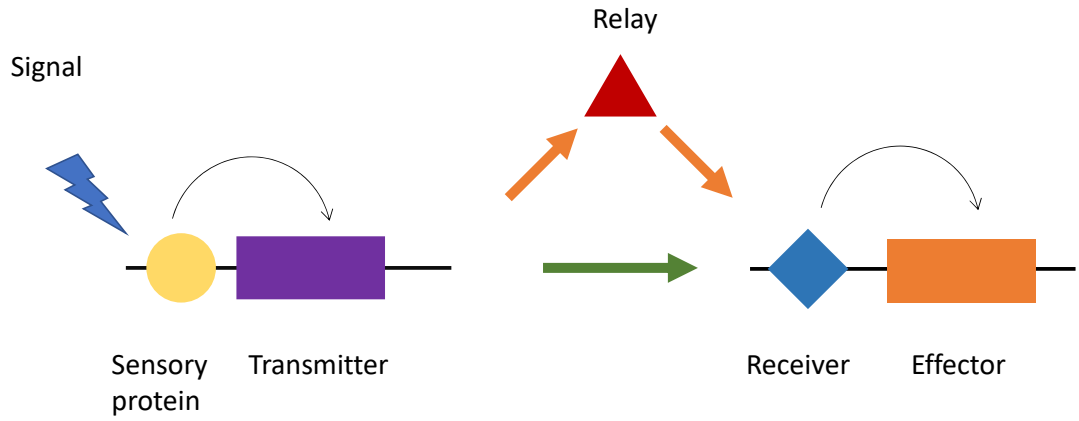

Figure 2.1. **Two-component sensory system.** This example of a two-component sensory system has two possible transmission mechanisms. In the first mechanism (green line) the input enters through a sensory protein and then goes to a transmitter that activates a receiver through phosphorylation; the receiver then activates some output effector. In the second mechanism (blue lines), the system uses a diffusible secondary relay to carry the signal to the receiver-output effector.

2.1.4 Description of common bacterial stress response systems

Stress response systems abound in bacteria and are often under complex control. Stress response systems include specific stress responses for particular categories of stressors (e.g., envelope stress, oxidative stress, oxygen deprivation, and osmotic stress) and result in the production of specific gene products to mitigate stressor effects (Storz et

al. 2000; 2011). Stress response systems also include more generalized stress responses that are activated by aggregate conditions (e.g., starvation, growth phase) and result in changes to morphology (e.g., biofilm or envelope construction and cell shape), growth rate, and mutagenesis rate (Storz et al. 2000; 2011). Overlap occurs among specific and general stress response systems. For example, *cpx* is a stress response regulator primarily activating DegP, a protease-chaperone system to degrade misfolded membrane proteins as part of the envelope stress response (Sawa et al. 2010). *cpx* induction also is stimulated by basic pH stress and general stress response morphological changes that are controlled by other regulators (Mileykovskaya et al. 1997; Danese et al. 1998; De Wulf et al. 2000; Otto et al. 2002; Lee et al. 2004; Fleischer et al. 2007). With respect to antibiotics, a stress response can occur during exposure to a specific antibiotic; for example, penicillins can be inactivated by β-lactamases or can be removed from the cell by efflux pumps (Livermore 1995). In addition to specific antibiotic stress responses, general stress responses can occur when cells are exposed to antibiotics; these general stress responses might act to change the permeability of a cell and its metabolic rates, without acting on the specific antibiotic itself (Li et al. 1994; Kumar et al. 2005; Ron 2006; Piddock 2006; Storz et al. 2011; Fernández et al. 2011; Poole 2004; 2012a; 2014). The stress response due to exposure to a specific antibiotic is often associated with that antibiotic's particular mechanism of action.

2.1.5 Defining antibiotics

Colloquially, the term "antibiotics" includes synthetic and natural compounds that are categorized as follows: tetracyclines, aminoglycosides, cationic polypeptides, β-lactams, quinolones, macrolides, and sulfonamides. These antibiotics utilize a variety of routes to elicit cytotoxicity. β-lactams and cationic polypeptides affect the cellular

envelope, leading to eventual cell lysis. Quinolones target DNA replication. Tetracyclines and aminoglycosides impair protein folding, while macrolides impair protein synthesis. Sulfonamides are metabolic disruptors, inhibiting folate biosynthesis. Many of these mechanisms of action are tightly linked to a stress response: envelope stress is linked to *cpx*, *psp*, and *rcs* pathways; DNA replication stress is linked to *lex* and *sos* pathways; and protein misfolding is linked to *cpx* and *deg* pathways (Ron 2006; Storz et al. 2011). Each of these pathways consists of a series of stress-mitigating proteins for a particular stressor. A particular stressor might induce the components of the same stress response pathways as compared to another stressor (e.g., envelope stress and protein misfolding both induce *cpx*), or a particular stressor might utilize a unique stress response pathway; this depends on the particular stressor and the extent of stress. The following section summarizes stress response systems relevant to the current study and discusses how they impact antibiotic resistance. The subsequent discussion will address how particular stress systems that primarily are associated with antibiotic resistance also might be activated by an alternative stressor, such as a nanomaterial.

2.1.6 Summary of important bacterial stress response systems relevant to the current study

2.1.7 Envelope stress response

Envelope stress to bacteria is a common environmental stress (Ron 2006; Storz et al. 2011) that can primarily be induced by environmental characteristics such as pH and temperature but also can be induced by exposure to particular stressors such as antibiotics and surfactants (Laubacher et al. 2008; Raivio et al. 2013). Activation of the envelope stress response limits the effect of many different harmful compounds and conditions (Rowley et al. 2006). Four major envelope stress response systems are known in Gram-

negative bacteria: extra-cytoplasmic function (a sigma factor), *cpxRA, baeRS*, and the phage shock response system (Rowley et al. 2006; Storz et al 2000; De Wulf et al. 2000; Poole 2012a; Poole 2014). These systems respond to a wide variety of stressors including heat shock, oxidative stress, ethanol, detergents, osmotic stress, biofilm formation, stationary phase, and growth-based stress (Rowley et al. 2006). For instance, *cpx* expression is altered by changes in the cellular envelope's physiology due to lipoprotein and protein damage and also due to virulence gene expression (Mileykovskaya et al. 1997; Danese et al. 1998; Fleischer et al. 2007). More than 100 genes are controlled under the regulation of envelope stress activation, some with unknown function (Piddock 2006; Raivio et al. 2013). A variety of responses can be activated, such as the excretion of new lipid material or the expression of efflux pumps (Otto et al. 2002; Potvin et al. 2008).

2.1.8 Oxidative stress response

Oxidative stress to bacteria is caused by ROS. ROS is a term describing the radical and non-radical variants of oxygen containing chemical species such as the hydroxyl radical and hydrogen peroxide (Thannickal et al. 2000; Finkel 2001; Apel et al. 2004). These reactive species act on the cellular envelope and other essential components of the bacterial cell and can cause cell death (Cabiscol et al. 2000; Apel et al. 2004; Fraud et al. 2011). Electron-poor radical species gain electrons to become stable, often causing the degradation of the lipid membrane, disruption of metabolic processes, protein damage, and, in some cases, DNA damage that might result in mutagenesis (Thannickal et al. 2000; Finkel 2001; Apel et al. 2004; Stark 2005).

In addition to being formed as a result of solution chemistry or generated by an abiotic catalyst such as a metal (Stohs et al. 1995; Nies 2003), ROS are formed as byproducts of aerobic metabolism (D'Autréaux et al. 2007) and might play a regulatory

role in prokaryotic cells (Cabiscol et al. 2000; Finkel 2001). Thus, numerous stress response and regulatory systems exist in bacteria to limit the harmful effects of ROS, as reviewed by Imlay (2008). A summary of these ROS stress response regulators is provided in Table 2.1, as adapted from Storz (2011). It is important to note that many of these response regulators are activated by thiol/disulfide sensory systems, all of which can likely be oxidized through Ag^{+} redox reactions with thiols (Toh et al. 2014).

All listed regulatory systems result in the expression of dismutases, catalases, and reductases, among other stress response pathways, that mitigate one or more ROS species directly. While hotly debated, the direct role of ROS stress response in antibiotic resistance seems to be limited; however, ROS stress responses likely increase mutagenesis and recruit other systems such as multidrug export pumps (reviewed later), both of which lead to antibiotic resistance (Kohanski et al. 2007; Kohanski, Dwyer, et al. 2010; Fraud et al. 2011; Poole 2014).

Table 2.1 Common ROS bacterial stress response regulators, adopted from Storz (2011)

System	Redox-active Center
SoxR	[2Fe-2S]
PqrR	[Fe-S]
OxyR	Cysteine
PerR	Histidine-coordinated Fe^{2+}
OhrR	Cysteine
RsrA	Cysteine
Spx	Cysteine

2.1.9 Dissolved metal stress response

In bacteria, metal stress response systems are common and include seven major families and many specialized subfamilies (Storz et al. 2011). Often these systems are

specific for a given metal, but some substrate flexibility exists (e.g., Ars senses both tin and arsenic in *E. coli)* (Storz et al. 2011; Giedroc et al. 2007). These sensors and response elements often increase the expression of metal efflux pumps (Nies 2003; Hu et al. 2007; Harrison et al. 2007; Chacón et al. 2014). Metal stress is tightly linked to antibiotic resistance. In many cases, separate antibiotic resistance and metal resistance genes are linked on the same genetic element (e.g., on the same plasmid or under the control of the same promoter), and selective pressure acts to retain both distinct elements despite separate function in a form of resistance termed "co-resistance" (Baker-Austin et al. 2006; Harrison et al. 2007). Additionally, some gene products can respond to both an antibiotic and a metal; here, pressure from the antibiotic or the metal causes selection for the same gene product in a form of resistance termed as "cross-resistance" (Baker-Austin et al. 2006; Harrison et al. 2007). In this situation, for example, a particular export system could pump out a metal and an antibiotic. Zinc, copper and imipenem (a carbapenem antibiotic) resistance have been linked to a co-resistance mechanism in *P. aeruginosa* (Caille et al. 2007). Imipenem resistance occurs through suppression of the OprD outer membrane porin, a channel through which imipenem enters the cell. Suppression of OprD is co-regulated by increased expression of *czcRS, copAB,* and *mexTEF* and causes increased resistance to carbapenem antibiotics. Zinc and copper activate the *copAB* and *czcRS* circuits, which then increase resistance to imipenem through down-regulation of the porin. Bacterial resistance to both metals and antibiotics is quite common in environmental samples and often occurs in wastewater and other waste streams. For example, power plant ash settling basins selected for antibiotic resistant microbial communities likely due to metals found in the ash (Baker-Austin et al. 2006; Stepanauskas et al. 2006), and pig fecal waste streams contained bacteria harboring a single gene conferring resistance to both copper and macrolide antibiotics (Séverine et al. 2002; Hasman et al. 2002). As with

oxidative and envelope stress, metals also activate multidrug efflux systems (Harrison et al. 2005; Baker-Austin et al. 2006;; Hu et al. 2007). Multidrug efflux pumps can confer broad spectrum antibiotic resistance and are integrated into many regulatory systems (Tseng et al. 1999; Alvarez-Ortega et al. 2013). The evidence for overlap between the expression of multidrug efflux systems and metal stress response demands investigation of co-and cross- antibiotic resistance derived from $Ag_{(aq)}$ and AgNP exposure.

2.1.10 Resistance nodulation division multidrug efflux pumps are shared between particular stress response systems

Of particular interest in the current study is a class of efflux pumps known as resistance nodulation division (RND) pumps, which are commonly co-regulated by many specific stress response systems (e.g., osmotic stress, metal stress, envelope stress). RND pumps are one of many different categories of efflux pumps found in Gram-negative bacteria, where they function not only to remove antibiotics but also to expel other types of molecules, such as lipids and signaling molecules (Tseng et al. 1999; Schweizer 2003; Piddock 2006; Poole 2008; Alvarez-Ortega et al. 2013). RND pumps are tripartite systems that are composed of an inner-membrane component, a linker, and an outer-membrane component (Piddock 2006; Tseng et al. 1999). In Gram-negative bacteria, and specifically in *P. aeruginosa*, there are four common RND pumps: MexAB, MexCD, MexEF, and MexXY (Poole 2001). These efflux systems can be activated by a range of stressors including membrane stress, growth-based stress, morphological/growth strategy (biofilm) stress, redox stress, and metal stress (Storz et al. 2011; Piddock 2006; Poole 2012a; Alvarez-Ortega et al. 2013; Tseng et al. 1999; Poole 2008, 2001; C. H. Lau et al. 2014; Poole 2012b; Fraud et al. 2008; Grkovic et al. 2001) and can export a wide array of

antibiotics. The inner membrane region often determines drug export specificity, but other components can influence the efflux rates (Tseng et al. 1999).

Efflux pump substrates range from complex antibiotics and organic compounds to metals (Blanco et al. 2016). Exposure to heavy metals is a common activator of a wide array of export pump families (Tseng et al. 1999; Nies 1999; Ramos et al. 2002). Interestingly, homologies between the metal export system CzcABC and RND efflux pumps might indicate potential export of metals (Co^+, Zn^+, Cd^+) by RND pumps (Legatzki et al. 2003; Hu et al. 2007), which, as mentioned above, are a class of pumps primarily associated with antibiotic export in the literature. Of the Mex families, groups AB and CD are the most highly characterized in terms of substrate specificity, while the substrate specificities of other Mex groups (JK, EF, PQ, and XY) have been less studied.

2.1.11 The link between metal-core nanoparticles and stress response systems

2.1.12 Silver nanoparticles are included in materials to limit biological growth

Metal-core nanoparticles are increasingly incorporated into materials, including solar panels (Mor et al. 2006; Wildgoose et al. 2006; Kamat 2007; Macak et al. 2007) and textiles (Dastjerdi et al. 2010; Maillard et al. 2013; Simoncic et al. 2015). They also are utilized in environmental (Anyaogu et al. 2008; J. Kim et al. 2010; Kang et al. 2012; Knetsch et al. 2011) and medical (Murthy 2007; Kumari et al. 2010; Chaloupka et al. 2010; Musee et al. 2011; Sun et al. 2014) applications. A primary benefit of metal-core nanoparticles in textile, environmental, and medical applications is their biocidal activity (Qi et al. 2005; Panáček et al. 2006; Luoma 2008; Julia Fabrega et al. 2011). Among many nanoparticles, AgNPs are most commonly used as antimicrobial and antifouling agents (Luoma 2008; Musee et al. 2011; Julia Fabrega et al. 2011; Dror-ehre et al. 2010; Maynard

2007). While advantageous at the outset, continued use of AgNPs over time might lead to the development of antibiotic resistance; for instance, AgNPs might stimulate stress response systems that provide resistance to antibiotics by activating regulatory elements that protect against shared mechanisms of action for antibiotics and AgNPs.

2.1.13 Mechanisms of action of silver nanoparticles and the potential link to stress response systems

The mechanisms of action by which AgNPs elicit a toxic effect on bacteria have been studied extensively. Literature supports the mechanism of AgNP toxicity to cause cellular envelope disruption, protein misfolding and ROS production, and metal dissolution (O. Choi et al. 2010, 2009; Xiu et al. 2011b; Pratsinis et al. 2010; Fabrega et al. 2011; Levard et al. 2013; Chambers et al. 2014). Interestingly, these mechanisms of action overlap with the mechanisms of action of antibiotics including aminoglycosides and quinolones. As follows, the proposed mechanisms of action of AgNPs are linked to the stress categories discussed earlier in this chapter (envelope and protein misfolding (2.1.6), oxidative (2.1.7), and metal (2.1.8) stress). While other stress response systems also are likely stimulated by exposure to AgNPs, the current work focuses on those associated with cellular envelope, oxidative, and metal stress because they are linked to increased expression of RND-type efflux pumps.

With respect to the mechanism of action related to cell envelope disruption, AgNPs have been demonstrated to cause cell wall pitting and membrane disruption (Feng et al. 2000; Sondi et al. 2004; Morones et al. 2005; Choi et al. 2008;). Additionally, the Ag^{+} that is released due to AgNP corrosion (Pratsinis et al. 2010; Xiu et al. 2011a; Levard et al. 2012b; Chambers et al. 2014) can lead to the formation of silver-protein adducts (Wigginton et al. 2010) at the bacterial surface. Thus, AgNPs should induce the envelope stress response. As such, induction of the envelope response is coordinated with expression

of the RND efflux pump MexAB, through the regulator CpxR, which sense misfolding proteins at the envelope (Tian et al. 2016). Envelope stress is linked to protein misfolding; stressors sensing membrane damage also sense oxidation damage to protein, likely caused by ROS generation in the periplasm. Additional misfolding sensors like AmgR can detect both at the bacterial surface and in the cytoplasm. Induction of the AmgR systems can activate RND efflux pumps MexAB, CD and XY (Lau et al. 2015).

With respect to the mechanism of action related to ROS production, AgNPs are linked to the formation of intracellular and extracellular ROS (Hu 2008; Carlson et al. 2008; Li et al. 2013). ROS can lead to lipid peroxidation (Stohs et al. 1995). Thus, AgNPs should induce the oxidative stress response, which should induce the expression of multidrug efflux pumps through the regulator MexR, an oxidative stress-sensing regulator of RND efflux pumps MexAB, MuxABC and MexXY (Adewoye et al. 2002; H. Chen et al. 2008; Mima et al. 2009). This would likely increase efflux of aminoglycoside and quinolone antibiotics (Poole 2001; Storz et al. 2011; Fraud et al. 2011 Lau et al. 2014).

Bacteria such as *P. aeruginosa* have metal sensory systems that can detect Cu^{2+} ions (Baker-Austin et al. 2006; Nagy 2010). Metal ions are known to activate many RND efflux pumps as well as some envelope sensory systems in this Gram-negative bacterium (Poole 2001; Baker-Austin et al. 2006; Teitzel et al. 2003; Harrison et al. 2007; Poole 2012b). Evidence exists linking metal stress response systems to RND efflux pumps in *P. aeruginosa*; for example, exposure to imipenem increases the expression of RND efflux pump components, causing decreased sensitivity of *P. aeruginosa* to not only imipenem but also chloramphenicol, quinolones, trimethoprim, Zn, Cd, and Co (Caille et al. 2007). Metal stress response should increase expression of RND efflux pumps MexAB, MexEF, and MuxABC (Caille et al. 2007; Mima et al. 2009) and increase resistance to quinolones and aminoglycosides.

2.1.14 Sublethal priming of antibiotic resistance genes

At a sublethal concentration (i.e., not high enough to cause cell death), AgNPs can supply selective pressure to activate one or more stress response systems, thereby "priming" a bacterium to survive exposure to not only this primary stressor but also to survive exposure to secondary stressors that are mitigated by the same stress response system. During this priming phase, transcription and translation of stress mitigation systems is adjusted, and cellular machinery is readied; thus, exposure to a primary stressor prepares the microorganism to mitigate exposure to a secondary stressor. In this context, it might be possible that exposure to a sublethal AgNP concentration would give a microorganism an increased capacity to export antibiotics. Recent data showed that a multidrug-resistant mutant of *E. coli*, with constitutively expressed resistance systems for ampicillin, streptomycin, and nalidixic acid, had much greater tolerance to AgNPs than did wild-type *E. coli* (Chambers et al. 2016, unpublished). While resistance to ampicillin and streptomycin is linked to specific mechanisms that act only on those antibiotics (Szczepanowski et al. 2005; Lau et al. 2015), resistance to nalidixic acid is linked to overproduction of RND pump MexAB (Poole et al. 1993). This provides preliminary evidence that the expression of RND efflux pumps can mitigate the toxicity of AgNPs to bacteria. As such, exposure to sublethal doses of AgNPs might activate RND efflux stress response systems and initiate antibiotic resistance in *P. aeruginosa.*

3. Impact of exposure medium on bacterial nano-toxicity[1]

This chapter addresses Task 1. Characterize the effect of solution chemistry, including chloride concentration and ionic strength, on AgNP morphology, dissolution, and toxicity to bacteria.

3.1 BACKGROUND

Many studies have evaluated the toxicity of silver nanoparticles (AgNPs) using a variety of exposure assays and exposure media (Musee et al. 2011; Morones et al. 2005; Sondi et al. 2004; Z.-M. Xiu et al. 2011a; O. Choi and Hu 2008; Bae et al. 2010; W. K. Jung et al. 2008). As a result, the mechanism of AgNP toxicity has been largely obfuscated by the influence of these varied exposure conditions (S. W. Kim et al. 2011; Levard et al. 2012b; Z.-M. Xiu et al. 2011a). Exposure media differ by ionic strength and chemical composition. Ionic strength can affect the aggregation of charged AgNPs (J Fabrega et al. 2009; Julia Fabrega et al. 2011; X. Li et al. 2012). Chemical composition of the medium has a complex interaction with AgNPs, where ligands such as chloride and sulfide might participate in surface reactions and thereby influence the chemical and physical properties

[1] The work presented in this chapter is published: Chambers, B. A., Afrooz A. R. M. N., Bae S., Aich N., Katz, L. E., Saleh N. B., Kirisits, M. J. Effects of Chloride and Ionic Strength on Physical Morphology, Dissolution, and Bacterial Toxicity of Silver Nanoparticles. *Environmental Science and Technology*. 2014 48 (1) 761-769. DOI: 10.1021/es403969x. I provided the primary intellectual design and conducted the majority of the experiments. A. R. M. N. Afrooz and N. Aich were Ph.D. students under the supervision of Dr. Saleh and assisted with AgNP physical characterization. S. Bae was a postdoctoral researcher under the supervision of Dr. Kirisits and assisted with molecular biological assays. L. Katz is a faculty member at the University of Texas at Austin and provided insight on chemical experiment design. N. B. Saleh is a faculty member at the University of Texas at Austin and provided insight on AgNP physical characterization. M. J. Kirisits is my doctoral advisor and provided direction on experimental design, data interpretation, and manuscript preparation.

of the AgNPs (e.g., dissolution, reactivity, aggregation) (Z.-M. Xiu et al. 2011a). Generally, the bacterial toxicity of AgNPs is thought to be due to AgNP dissolution in bulk solution (i.e., production of metal ions), envelope stress (e.g., envelope pitting, disruption of the electron transport chain), and intracellular stress (e.g., disruption of DNA replication and metabolic processes) (Sondi et al. 2004; Morones et al. 2005; Z.-M. Xiu et al. 2011b; O. Choi et al. 2009). Given that the chemistry of a nanoparticle's aqueous environment can influence its ability to initiate such processes, it is likely that choice of exposure medium will impact nanoparticle toxicity to bacteria. Knowledge of a selected exposure medium's effect on AgNP toxicity will allow the conduction of robust studies to query the mechanisms of action for AgNP against bacteria.

3.2 MATERIALS AND METHODS

AgNPs were synthesized utilizing a method modified from that described in Chen et al. (1999). Briefly, a well-mixed solution of 5 mL $AgNO_3$ (2 mM) was mixed with an equal volume of thiomalic acid (5.3 mM) and reduced drop-wise using freshly prepared $NaBH_4$ (79.3 mM) until the solution turned dark brown (~20 drops). The reaction was quenched using 30 mL acetone. AgNPs were sedimented by centrifugation (Avanti JE, Beckman Coulter, Pasadena, CA) at 10,000 x g for 50 min at 20˚C. AgNPs were resuspended in distilled deionized (DDI) water that had been adjusted to pH 9.0 with 5 N NaOH.

Characterizing the dependence of AgNP aggregation, dissolution, and morphology on exposure solution chemistry was accomplished by separately varying ionic strength (using $NaNO_3$) and chloride concentration (using KCl and NaCl) in the exposure solutions used to resuspend the AgNPs. Chloride concentration and ionic strength vary greatly

among the exposure solutions used in biological toxicity studies with AgNPs in the literature. Three tiers of ionic strength were evaluated in this task: ~8 mM (typical ionic strength of freshwater), ~40 mM (typical ionic strength of biological media), and ~150 mM (typical ionic strength of phosphate-buffered saline); these ionic strength values cover the range used in biological AgNP toxicity studies in the literature. At each ionic strength, up to four chloride concentrations were tested (0-140 mM). These exposure solutions are summarized in Table **3.1**, where a two-component nomenclature is utilized. The first component designates the ionic strength, where Lμ, Mμ, and Hμ represent ~8 mM, ~40 mM and ~150 mM ionic strength, respectively. The second component designates the chloride concentration in mM; thus, Hμ140 is an exposure solution with ~150 mM ionic strength and 140 mM chloride. AgNPs were resuspended in each of the exposure solutions shown in Table **3.1** for up to 5 hours at 30˚C, statically and in the dark, similar to the conditions of a typical biological exposure assay (described in the *Biological Characterization* subsection 3.1.4). After this incubation, AgNPs were examined using the techniques described in the following section.

Table 3.1. Composition of Exposure Solutions

Sample	high ionic strength				medium ionic strength			low ionic strength	
Parameter	Hμ140	Hμ32	Hμ2.7	Hμ0	Mμ31	Mμ2.7	Mμ0	Lμ2.7	Lμ0
pH	7.4	7.4	7.4	7.4	7.4	7.4	7.4	7.4	7.4
ionic strength (mM)	152.6	154.0	154.0	153.8	40.3	40.4	40.1	8.3	8.3
chloride (mM)	139.7	31.6	2.7	--	30.9	2.7	--	2.7	--

3.2.1 Physical and Chemical Characterization

The size of the as-synthesized AgNPs (before suspension in an exposure solution) was characterized using transmission electron microscopy (TEM) (Tecnai Spirit, FEI, Hillsboro, OR). Samples were dropped onto carbon-coated copper grids and air-dried for 10−20 min before analysis. Images were analyzed using ImageJ (National Institutes of Health, Bethesda, MD, http://imagej.nih.gov/ij), and statistical analyses were performed in Excel (Microsoft Corp., Redmond, WA).

AgNP dissolution was measured in all exposure solutions, except Lμ2.7. AgNPs were resuspended in 3.4 mL of each exposure solution at a final concentration of 1 mg/L and incubated statically in the dark. Samples were taken at 10 min and 1, 3, and 5 h and immediately centrifuged using an Amicon Ultra-4 3-kDa centrifugal filter at 7500 x g for 30 min, thereby separating $Ag_{(aq)}$ from undissolved AgNPs. Each permeate was analyzed using ion coupled plasma optical emission spectroscopy (ICP-OES; λ = 328.4 nm) after being acidified to 2% with nitric acid. Additionally, the concentration of $Ag_{(aq)}$ in the AgNP stock (from AgNP dissolution or unreacted Ag^+ from AgNP synthesis) was measured. Here, the AgNP stock (1 mL) was placed in dialysis tubing (3.5 kDa, Spectrum Laboratories, Rancho Dominguez, CA) and dialyzed for 14 h, changing the dialysate once at 6 h. Samples were acidified and analyzed by ICP-OES.

The aggregate structure of AgNPs in the exposure solutions was assessed. Light scattering measurements were conducted on an ALV-CGS/3 goniometer system (ALV-GmbH, Langen, Germany). Static light scattering (SLS) measurements were performed to describe the aggregate structure (i.e., fractal dimension) of the AgNPs. The SLS protocol is described in detail in Khan et al. (2013). Samples were prepared by resuspending AgNPs in 2 mL of each previously described exposure solution to a final concentration of 25 mg/L.

Samples were then sonicated for 15 min in a bath sonicator and filtered using a 0.45-µm nylon syringe filter. Angle-dependent scattering was collected from 12.5˚ to 80˚ at 0.5˚ increments for 0, 1, 3, and 5 h time points. Data were plotted as scattering intensity profiles, and fractal dimension was computed from log-log profiles of scatter intensity and wave vectors.

3.2.2 Biological Characterization

The biological significance of resuspending AgNPs in these exposure solutions was assayed by testing tolerance (the survival of a bacterium in the presence of a biocide) using a traditional tolerance assay. The tolerance of *Escherichia coli* MG4, a K12 strain, to AgNPs or $Ag_{(aq)}$ (dosed as $AgNO_3$) in the exposure solutions was tested by triplicate analyses of two biological replicates. *E. coli* was grown in a chemostat with a 12-h hydraulic detention time in Minimal Davis (MD) medium [in 1 L: 1 g $(NH_4)_2SO_4$, 7 g K_2HPO4, 2 g KH_2PO_4, 0.5 g sodium citrate, 0.1 g $MgSO_4$, 1 g glucose, pH 7.2]; after a steady state concentration of cells had been reached in the reactor, an aliquot of planktonic cells was removed and washed in the appropriate exposure solution. In a 96-well microtiter plate, each exposure solution was dosed with AgNPs or Ag(aq) to a final concentration of 0−1 mg/L Ag and inoculated with washed E. coli cells to a final concentration of ~107 colony-forming units per milliliter (CFU/mL). The plate was incubated statically for 5 h at 30 °C in the dark, and the viable cells remaining were enumerated in triplicate on Lysogeny Broth (Lennox) agar.

3.2.3 Oxidative stress response due to AgNP exposure

The expression of *katE* was examined to understand the role of oxidative stress in AgNP toxicity. *E. coli* grown in batch in MD medium were pelleted, and washed in Lµ0.

Washed cells were then added to a sample of AgNPs at 200 µg/L in Lµ0, Mµ31, or Hµ0 at an initial concentration of 3×10^7 CFU/mL. The suspensions were incubated in the dark for 5 h with shaking at 30 °C. An aliquot was taken for enumeration by viable plate counts on Lysogeny Broth (Lennox) agar, and the remaining cells were pelleted for RNA extraction. RNA was extracted in duplicate from each suspension and pooled, and complementary DNA (cDNA) was synthesized in duplicate reactions and pooled for analysis. Real-time, quantitative polymerase chain reaction (qPCR) primers targeting a 190-bp *katE* fragment were designed using Primer3 software40 and *E. coli* K-12 substrain MG1655, which has a sequenced genome. qPCR was run on each cDNA sample in triplicate. A *katE* standard curve was constructed using genomic DNA from *E. coli* MG4 (10^1−10^7 gene copies/reaction).

3.3 KEY FINDINGS

3.3.1 Characterization of Synthesized AgNPs

After synthesis, AgNPs resuspended in pH 9 DDI were characterized. TEM analysis showed spherical particles with an exponential distribution and average diameter of 2.9 nm (Figure 3.1), in close agreement with the 2.2-nm diameter described in the original synthesis (S. Chen et al. 1999). A typical batch of AgNPs contained 220 mg/L total silver, of which 7-9 µg/L was residual $Ag_{(aq)}$. Thus, when the AgNP stock was diluted for bacterial tolerance studies (to ≤ 1 mg/L), the residual $Ag_{(aq)}$ concentration was orders of magnitude below lethal levels.

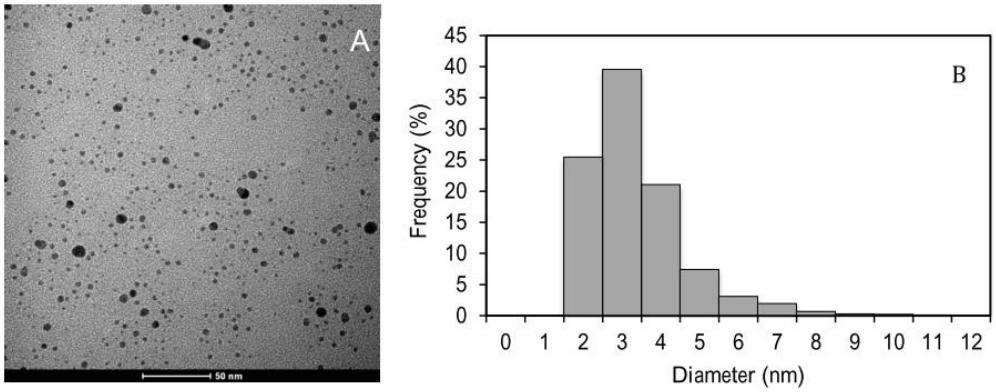

Figure 3.1. **Characterization of synthesized AgNPs resuspended in pH 9 DDI**. (A) Representative TEM micrograph; (B) histogram of measured particle diameters from three TEM images. Reprinted with permission from (Chambers, Bryant a., A. R M Nabiul Afrooz, Sungwoo Bae, Nirupam Aich, Lynn Katz, Navid B. Saleh, and Mary Jo Kirisits. 2014. "Effects of Chloride and Ionic Strength on Physical Morphology, Dissolution, and Bacterial Toxicity of Silver Nanoparticles." Environmental Science and Technology 48 (1): 761–69. doi:10.1021/es403969x.). Copyright (2018) American Chemical Society

3.3.2 Physical Characterization of AgNPs in Exposure Solutions

Dissolution

The release of $Ag_{(aq)}$ due to the dissolution of AgNPs under different ionic strength and chloride conditions was examined (Figure 3.2). The release of $Ag_{(aq)}$ from AgNPs is dependent upon oxidation (Levard et al. 2013; Z.-M. Xiu et al. 2011b), and $Ag_{(aq)}$ was detected in the exposure solutions dosed with AgNPs. In the absence of chloride, ionic strength only slightly impacted the initial release (at 10 min) of $Ag_{(aq)}$ from AgNPs (Figure 3.2 inset). However, for a constant ionic strength, the initial release of $Ag_{(aq)}$ from AgNPs was strongly affected by the presence of chloride in the exposure solution (Figure 3.2 inset). These data are consistent with previous literature findings that show rapid AgNP dissolution (Levard et al. 2013; X. Li et al. 2012). We continued to monitor $Ag_{(aq)}$ over 5 h, which corresponds to the timeframe of our tolerance studies and only saw continued AgNP dissolution at the highest chloride concentration (Hμ140, Figure 3.2). This is consistent with previous studies that have suggested that chloride might act catalytically in

the dissolution of AgNPs (Mulvaney et al. 1991; Kapoor 1998). Thus, our data indicate that chloride concentration is more important than ionic strength in driving AgNP dissolution.

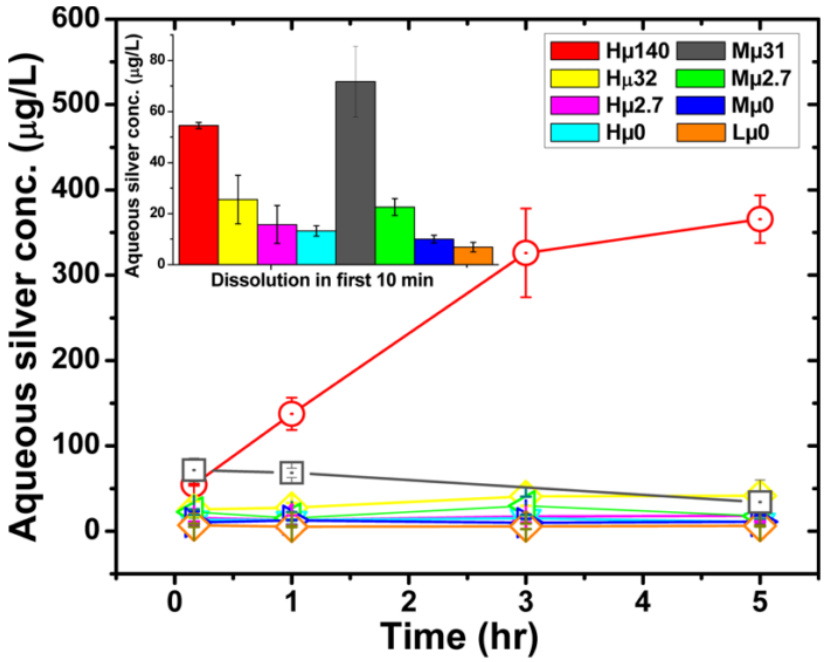

Figure 3.2. **Dissolution of AgNPs (dosed at 1 mg/L) over time as a function of ionic strength and chloride concentration.** Inset highlights the release of $Ag_{(aq)}$ after 10 min. Data points are the average of triplicate experiments, and error bars show one standard deviation. Reprinted with permission from (Chambers, Bryant a., A. R M Nabiul Afrooz, Sungwoo Bae, Nirupam Aich, Lynn Katz, Navid B. Saleh, and Mary Jo Kirisits. 2014. "Effects of Chloride and Ionic Strength on Physical Morphology, Dissolution, and Bacterial Toxicity of Silver Nanoparticles." Environmental Science and Technology 48 (1): 761–69. doi:10.1021/es403969x.). Copyright (2018) American Chemical Society

3.3.3 Aggregate Structure

Aggregate structure under different ionic strength and chloride conditions was examined via SLS (Figure 3.3). For a constant chloride concentration (0 mM), the fractal dimension (D_f) decreased with increasing ionic strength (Figure 3.3a). This observation is

consistent with classical electrostatic screening-induced fractal formation of colloids, as observed previously (Khan et al. 2013). Higher ionic strength reduces the electrostatic potential making particle-particle interactions more favorable and resulted in lower D_f (i.e., a more fractal structure in Hμ0 as compared to a more densely packed aggregate in Lμ0). On the other hand, at constant ionic strength (~40 mM), increased chloride concentrations showed increased D_f (Figure 3.3b). This shift in structure toward a more compact form in the presence of chloride supports the bridging of AgNPs via silver chloride ($AgCl^0_{(s)}$) formation. A similar observation of $AgCl^0_{(s)}$-induced bridging of AgNPs has been observed previously (X. Li et al. 2012) using TEM.

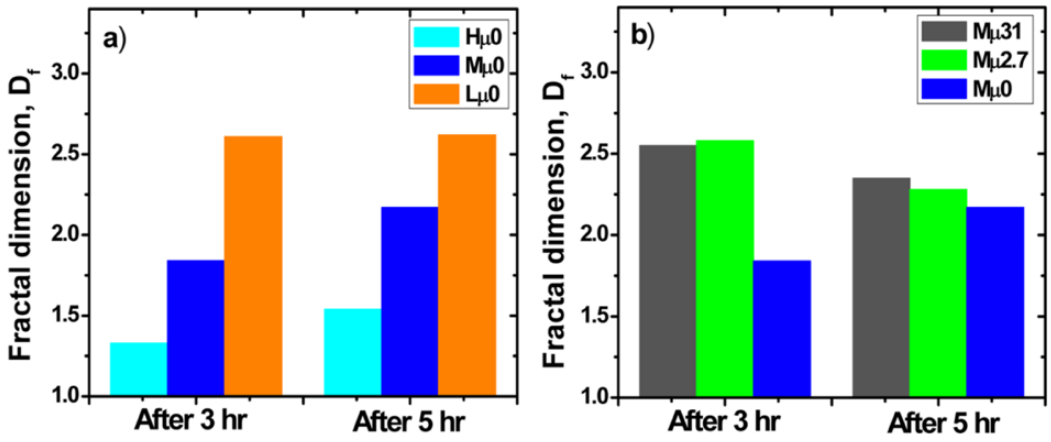

Figure 3.3. **Fractal dimension of AgNPs as a function of (a) ionic strength and (b) chloride concentration.** Reprinted with permission from (Chambers, Bryant a., A. R M Nabiul Afrooz, Sungwoo Bae, Nirupam Aich, Lynn Katz, Navid B. Saleh, and Mary Jo Kirisits. 2014. "Effects of Chloride and Ionic Strength on Physical Morphology, Dissolution, and Bacterial Toxicity of Silver Nanoparticles." Environmental Science and Technology 48 (1): 761–69. doi:10.1021/es403969x.). Copyright (2018) American Chemical Society

Biological Characterization of *E. coli* exposed to AgNPs and $Ag_{(aq)}$

Impact of Ionic Strength and Chloride on Bacterial Tolerance to AgNPs

As demonstrated above, the chemistry of the exposure solution impacts AgNP stability. Next, we examined the tolerance of *E. coli* to AgNPs in the nine exposure solutions; selected results are shown herein. Figure 3.4 demonstrates the tolerance of *E. coli* to AgNPs as a function of ionic strength at a constant chloride concentration (0 mM). At higher AgNP concentrations (greater than 50 µg/L), *E. coli* survival is less than 10%. At lower AgNP concentrations (15.6 and 31.2 µg/L), *E. coli* has the lowest tolerance to AgNPs under the highest ionic strength condition (Hµ0). This is likely due to one or more of the following reasons. (1) Hµ0 induces higher AgNP dissolution as compared to lower ionic strength exposure solutions (e.g., 15.3 and 5.6 µg/L $Ag_{(aq)}$ measured in the bulk solution after a 3-h exposure of AgNPs to Hµ0 and Lµ0, respectively, Figure 3.2), and Ag^+ is biocidal to bacteria (Ratte 1999; W. K. Jung et al. 2008; Z.-M. Xiu et al. 2011b). (2) Hµ0 causes the most compression of the electric double layer, which would facilitate closer proximity of cells to AgNPs. (3) Hµ0 induces a different aggregate structure as compared to lower ionic strengths. At higher ionic strengths, AgNPs were found to form more fractal structures (lower D_f) as compared to more densely packed structures at lower ionic strengths (Figure 3.3a), which leads to more available surface area for interaction with bacteria at higher ionic strengths. Close interaction of bacteria with AgNPs could facilitate the delivery of Ag^+ to the cells as the AgNPs dissolve, resulting in reduced tolerance of *E. coli* to AgNPs at higher ionic strengths.

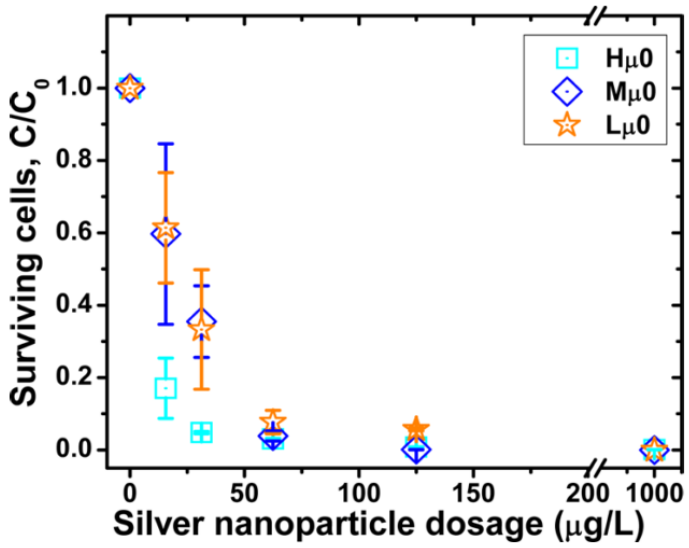

Figure 3.4**. Impact of ionic strength on the tolerance of *E. coli* to AgNPs. Surviving cells are shown as a function of AgNP dose.** Data are averages of triplicate tolerance assays of biological duplicates, and error bars represent one standard deviation. Reprinted with permission from (Chambers, Bryant a., A. R M Nabiul Afrooz, Sungwoo Bae, Nirupam Aich, Lynn Katz, Navid B. Saleh, and Mary Jo Kirisits. 2014. "Effects of Chloride and Ionic Strength on Physical Morphology, Dissolution, and Bacterial Toxicity of Silver Nanoparticles." Environmental Science and Technology 48 (1): 761–69. doi:10.1021/es403969x.). Copyright (2018) American Chemical Society

Figure 3.5a demonstrates the tolerance of *E. coli* to AgNP exposure as a function of chloride concentration at constant ionic strength (~40 mM). *E. coli* has the highest tolerance to AgNPs under the highest chloride condition shown (Mμ31).

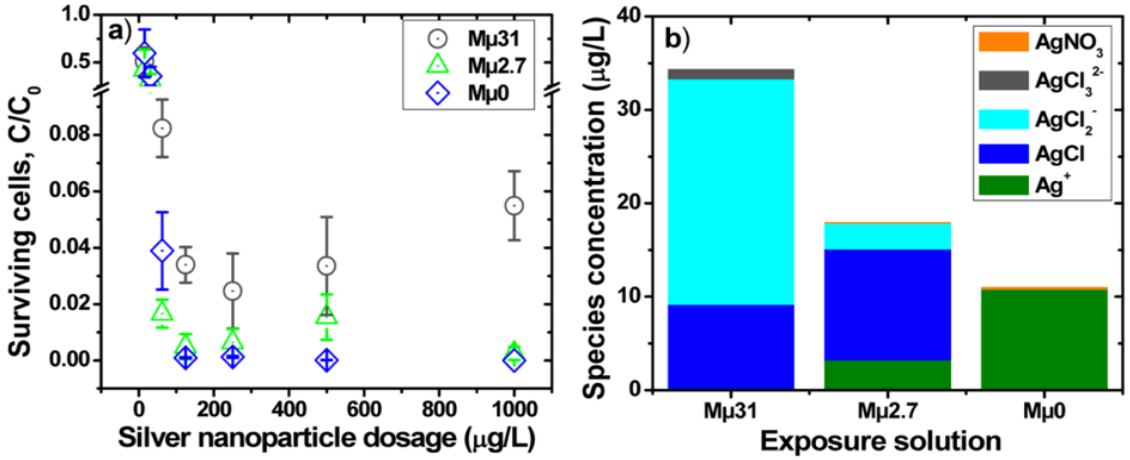

Figure 3.5.**Impact of chloride on tolerance of *E. coli* to AgNPs**. (a) Surviving cells as a function of AgNP dose; (b) theoretical equilibrium $AgCl_x^{(x-1)-}$ speciation of $Ag_{(aq)}$ produced 5 h after 1 mg/L AgNPs were dosed to a particular exposure solution, where $Ag_{(aq)}$ for each exposure solution is as shown in Figure 3.2. Cell data are the averages of triplicate tolerance assays of biological duplicates, and error bars represent one standard deviation. Reprinted with permission from (Chambers, Bryant a., A. R M Nabiul Afrooz, Sungwoo Bae, Nirupam Aich, Lynn Katz, Navid B. Saleh, and Mary Jo Kirisits. 2014. "Effects of Chloride and Ionic Strength on Physical Morphology, Dissolution, and Bacterial Toxicity of Silver Nanoparticles." Environmental Science and Technology 48 (1): 761–69. doi:10.1021/es403969x.). Copyright (2018) American Chemical Society

This is likely due to one or both of the following reasons. (1) Higher chloride concentrations result in more AgNP dissolution (Figure 3.2), but they also produce lower concentrations of Ag^+ and the neutral species $AgCl^0_{(aq)}$ (compare Mμ31 to Mμ2.7 in Figure 3.5b). While some work has proposed that only the total concentration of aqueous $AgCl_x^{(x-1)-}$, rather than its speciation, controls the overall toxicity to *E. coli* (Levard et al. 2013), our work makes the claim that $AgCl_x^{(x-1)-}$ speciation matters. The tolerance of *E. coli* to $Ag_{(aq)}$ increases as the charge on the dominant $AgCl_x^{(x-1)-}$ species decreases (e.g., greater tolerance results when $AgCl^{2-}$ is the dominant species as compared to when Ag^+ is the dominant species; Figure 3.5b). However, given the values of the $AgCl_x^{(x-1)-}$ stability constants, it is not possible to isolate the toxicity impact of each individual $AgCl_x^{(x-1)-}$ species. (2)

Chloride induces changes in AgNP aggregate structure. When chloride is low or absent (Mμ2.7 and Mμ0, respectively), AgNPs form more fractal structures (Figure 3.3b). This leads to higher available surface area for interaction with bacteria, likely facilitating the delivery of $Ag_{(aq)}$ to the cells as the AgNPs dissolve, resulting in reduced tolerance of *E. coli* to AgNPs at lower chloride concentrations. Our results are in contrast with an earlier study (Levard et al. 2013) that showed reduced tolerance of *E. coli* to AgNPs in the presence of higher chloride concentrations, but those results are likely confounded by simultaneous changes in ionic strength and chloride concentration.

3.3.4 Stress response induction

The induction of a key oxidation stress response gene was investigated to characterize the role of oxidative stress in AgNP toxicity and the cellular response to AgNP stress. *katE* encodes a cytoplasmic catalase that catalyzes the transformation of hydrogen peroxide, H_2O_2, to water and molecular oxygen to mitigate reactive oxygen species (ROS) stress (Loewen et al. 1985; Schellhorn 1995). AgNP toxicity has been linked to ROS production (O. Choi and Hu 2008; He et al. 2012; Long et al. 2017), and $Ag_{(aq)}$ has long been known to participate in Fenton reactions that generate ROS *in situ* (D. H. Nies 1999). Therefore, *katE* expression was used as a proxy of ROS-induced AgNP stress. As compared to the control (absence of AgNPs), the greatest increase in *katE* expression in the presence of AgNPs was observed in the Hμ0 exposure solution (Figure 3.6). *E. coli* exposed to AgNPs in exposure solution Mμ31 also showed a substantial increase in *katE* expression as compared to the control, but *E. coli* exposed to AgNPs in exposure solution Lμ0 did not demonstrate increased *katE* expression as compared to the control. The greatest induction of *katE* in *E. coli* exposed to AgNPs (relative to the control) in Hμ0 is

consistent with the lowest *E. coli* survival after exposure to AgNPs in that exposure solution (Figure 3.4), Overall, these data support the idea that ROS play a role in AgNP toxicity.

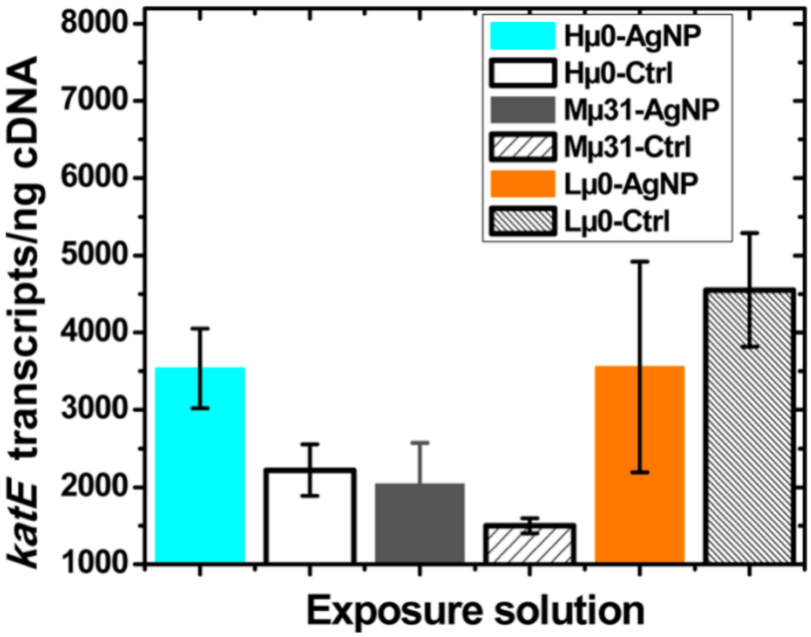

Figure 3.6 ***katE* expression in *E. coli*.** Transcript copy number was measured for cells exposed to different ionic strength and chloride conditions in the presence and absence (control) of AgNPs. Data represent triplicate qPCR reactions from duplicate biological experiments; error bars represent one standard deviation. Reprinted with permission from (Chambers, Bryant a., A. R M Nabiul Afrooz, Sungwoo Bae, Nirupam Aich, Lynn Katz, Navid B. Saleh, and Mary Jo Kirisits. 2014. "Effects of Chloride and Ionic Strength on Physical Morphology, Dissolution, and Bacterial Toxicity of Silver Nanoparticles." Environmental Science and Technology 48 (1): 761–69. doi:10.1021/es403969x.). Copyright (2018) American Chemical Society

3.3.5 Summary

Chloride- and ionic-strength-mediated changes in the physical morphology, dissolution, and bacterial toxicity of AgNPs were evaluated comprehensively. The findings separate the impact of ionic strength from that of chloride concentration and are illustrated schematically in Figure 3.7. As ionic strength was increased, AgNP aggregation likewise

increased (such that the hydrodynamic radius [HR] increased), fractal dimension (D_f) strongly decreased (providing increased available surface relative to suspensions with higher D_f), and the release of $Ag_{(aq)}$ increased. With increased Ag^+ in solution and the absence of chloride, *E. coli* demonstrated reduced tolerance to AgNP exposure (i.e., toxicity increased) under higher ionic strength conditions. As chloride concentration was increased, aggregates were formed (HR increased); relatedly, D_f increased. Furthermore, AgNP dissolution strongly increased at increased chloride conditions, but the dominant, theoretical, equilibrium aqueous silver species shift to negatively charged $AgCl_x^{(x-1)-}$ species, which appeared to be less toxic to *E. coli* than were neutral or positively charged aqueous silver species. Thus, *E. coli* demonstrated increased tolerance to AgNP exposure under higher chloride conditions (i.e., toxicity decreased). Overall, this work indicates that the environmental impacts of AgNPs must be evaluated under relevant and well-defined water chemistry conditions.

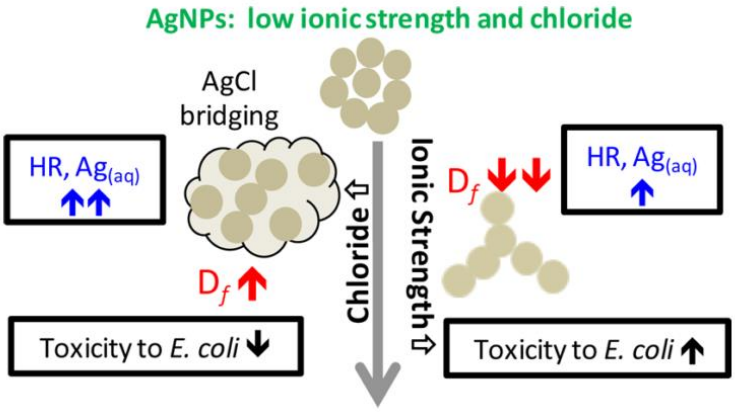

Figure 3.7. **Summary of the effects of chloride concentration and ionic strength on physical morphology, dissolution, and bacterial toxicity of AgNPs**
Reprinted with permission from (Chambers, Bryant a., A. R M Nabiul Afrooz, Sungwoo Bae, Nirupam Aich, Lynn Katz, Navid B. Saleh, and Mary Jo Kirisits. 2014. "Effects of Chloride and Ionic Strength on Physical Morphology, Dissolution, and Bacterial Toxicity of Silver Nanoparticles." Environmental Science and Technology 48 (1): 761–69. doi:10.1021/es403969x.). Copyright (2018) American Chemical Society

This work informs the model of bacterial-AgNP interaction that will be evaluated in Chapter 4. The potential for metal-ion-based toxicity (i.e., due to AgNP dissolution), cell-envelope disruption (i.e., decreased D_f for AgNPs at high ionic strength implies greater potential for nanoparticle-cell interaction), and ROS stress (i.e., increased catalase expression in the presence of AgNPs under some exposure solution conditions) suggests that metal, envelope, and oxidative stress response systems could be activated in bacteria exposed to AgNPs.

4. Molecular biological evidence for a surface attachment model of silver nanoparticle toxicity

This chapter addresses Task 2. Build a biomolecular model that describes how AgNPs interact with bacteria.

4.1 INTRODUCTION

The model of interaction of silver nanoparticles (AgNPs) with bacteria has been hotly debated during the past ten years. Proposed mechanisms have ranged from quantum tunneling and rapid lipid peroxidation to aqueous silver release ($Ag_{(aq)}$) due to AgNP corrosion (Nel 2007). Knowledge of an interaction model would inform nanoparticle design and synthesis, thereby facilitating the development of engineered nanoparticles tailored to a specific purpose. Further, such knowledge would inform risk management strategies to help limit negative environmental impacts. Establishing a comprehensive model of AgNP toxicity to bacteria has been difficult. For example, variations in exposure media (e.g., type and concentration of ligands, ionic strength) and particle capping agents have sometimes yielded confounding toxicity results among studies. The presence of molecular oxygen (O_2) can destabilize the outer shell of a nanoparticle promoting a dissolution model (Xiu et al. 2011b) while investigations focusing on capping agent length have found that nanoparticle-specific effects can persist (Long et al. 2017), making it difficult to construct a consistent model of interaction between AgNPs and bacteria.

Dissolution, complexation, and aggregation are competing processes that impact nanoparticle stability, and they also have the potential to impact AgNP toxicity. Sulfide, sulfate, and chloride can impact the dissolution of AgNPs and speciation of $Ag_{(aq)}$, which will directly influence toxicity to bacteria. For example, high ratios of Cl^- to $Ag_{(aq)}$ (from

dissolution of AgNPs) tend to cause the formation of negatively charged $AgCl_x^{(x-1)-}$ complexes, where such negatively charged species tend to have decreased toxicity to bacteria as compared to the toxicity of neutral or positively charged $AgCl_x^{(x-1)-}$ species (Chambers et al. 2014). Additionally, complexation of sulfur species with dissolved $Ag_{(aq)}$ implicates the same ligand and dissolution interaction processes occurring with exposed Ag atoms on the surface of the AgNPs. This surface complexation can reduce AgNP bacterial toxicity (Levard et al. 2012a). O_2 promotes redox processes that weaken the outer atomic metal shell of the nanoparticle and causes the release of toxic Ag^+, but O_2 eventually leads to the conversion of toxic Ag^+ to nontoxic $AgO_{(aq)}$ (Xiu et al. 2011b). In addition to being a ligand, chloride can impact the aggregation of AgNPs, where the morphology and chemistry of the aggregates will influence their toxicity to bacteria. For instance, while chloride can promote AgNP dissolution (Chambers et al. 2014), chloride also causes AgNPs to form compact aggregates with non-toxic shells (Li et al. 2010, 2012). In many cases, the processes of dissolution, complexation, and aggregation take place simultaneously (Pratsinis et al. 2010 Levard et al. 2012b; Xiu et al. 2012; Chambers et al. 2014) such that AgNP toxicity can simultaneously impacted by dissolution, complexation, and aggregation. Overall, the dominant mechanisms of AgNP toxicity to bacteria is highly dependent on the chemical environment of the AgNPs.

The understanding of AgNP toxicity in the literature falls under two major models of interaction between AgNPs and bacteria: (1) the surface attachment model of bacterial-AgNP interaction, which includes nanoparticle-specific effects (Nel et al. 2009; Levard et al. 2012b); and (2) the nanoparticle-dissolution model of bacterial-AgNP interaction (Xiu et al. 2012). Research on the surface model of bacterial-AgNP interaction (i.e., the impact of intact AgNP as opposed to dissolved $Ag_{(aq)}$) has focused on the size and shape (Morones et al. 2005; Pratsinis et al. 2010; Simon-Deckers 2009) and capping agent (Yang et al.

2011; El Badawy et al. 2011; Long et al. 2017) of AgNPs. Several researchers have found that AgNPs above a critical size threshold (~5-10 nm) have reduced toxicity to bacteria as compared to that of an equivalent dose of $Ag_{aq)}$ (Choi 2008; Pratsinis et al. 2010;). Many researchers have suggested that this disparity is due to surface complexation by ligands in the medium used for the toxicity assay (Julia Fabrega et al. 2009; Laban et al. 2010; Meyer et al. 2010; Yin et al. 2011) resulting in an incapacitated particle that has no outward facing reactive surface. Oxidation of surface proteins in the cell envelope occurs during AgNP exposure as well, reinforcing the existence of surface contact between AgNPs and bacteria (Lok et al. 2006). Additionally, electron microscopy indicates binding of AgNPs to bacterial membranes (Sondi et al. 2004; Morones et al. 2005). Research supporting a nanoparticle-dissolution model of bacterial-AgNP interaction has focused on the release of $Ag_{(aq)}$ species via the dissolution of AgNPs. Here, studies have shown that the toxicity of AgNPs to bacteria is the same as the toxicity of an equivalent $Ag_{(aq)}$ dose (Pratsinis et al. 2010; Ho et al. 2010; Xiu et al. 2012;). Although $Ag_{(aq)}$ from the dissolution of AgNPs seems to be an important factor in AgNP toxicity, the length of the polymer coating the AgNP surface directly impacts toxicity by controlling the amount of $Ag_{(aq)}$ released (Long et al. 2017). The researchers hypothesize that the polymer coating length also might affect binding of AgNP to bacteria.

Parsing out the contribution of surface attachment of AgNPs versus a dissolved species as the model of interaction between AgNPs and bacteria has been difficult. Some approaches use complex synthesis methods to produce AgNPs with chemically distinct dissolution behaviors (Pratsinis et al. 2010; Long et al. 2017). Other approaches examine the role of the dissolved species in toxicity by either removing or stimulating the release of $Ag_{(aq)}$ with complexation (Ho et al. 2010; Xiu et al. 2012). Both of these are particle-centric frameworks that do not explicitly consider the bacterial response. Hybrid particle- and

bacterial-centric frameworks have been limited to measuring bacterially produced reactive oxygen species (ROS), which are a signal for bacterial stress, utilizing diffusible reporter chemicals (Choi 2008; Park et al. 2009) or imaging the interaction of AgNPs with cells (Sondi et al. 2004; Morones et al. 2005). Both approaches do not directly interrogate bacterial responses. In the current work, we take a completely bacterial-centric viewpoint and query the bacterial stress response to AgNPs. Bacterial stress response systems, which are biomolecular stress mitigation pathways, are tightly controlled at the transcriptional level and are differentially expressed according to specific stresses (Storz et al. 2011). Metal stress response systems are tightly coupled to specific stress inputs (e.g., the *merAB* mercury response system in *E. coli).* Heavy metal stress response systems can be localized to specific regions in a cell (Nies 2003; Storz et al. 2011), thereby providing a direct lens to differentiate the localization of AgNP stress and potentially isolating it from the effects of $Ag_{(aq)}$. Transcriptomics will be useful for characterizing the stress response of bacteria to AgNPs, such that a consistent model of interaction between AgNPs and bacteria can be formulated. In this study, *Pseudomonas aeruginosa* was exposed to citrate-capped AgNPs or $Ag_{(aq)}$, and the transcriptomic responses to these stressors were measured relative to a no-Ag control. In particular, the expression of four key metal stress and ROS response systems (*copAB, katABEN, czcABCRS,* and *muxABC)* were used to propose a model of interaction between AgNPs and bacteria, distinct from the model of interaction between $Ag_{(aq)}$ and bacteria. These data provide a unique view of how a bacterium differentiates between stress due to a metal-core nanoparticle and stress due to an aqueous metal.

4.2 SUMMARY OF INITIAL HYPOTHESES

The experiments performed in this chapter sought to delineate the model of interaction between AgNPs and bacteria by testing two hypotheses (Figure 4.1). The first

hypothesis is that AgNPs caused toxicity to bacteria through a surface-attachment model of interaction. Physiochemical data in Chapter 3 supported this model. For example, under conditions where AgNPs had a lower fractal dimension, bacteria showed increased susceptibility to AgNPs (Figure 3.4) and increased *katE* expression(Figure 3.6). These data indicate that AgNP surface attachment to cells might result in ROS formation, contributing to cell death. Hypothesis 2 is that the nanoparticle-dissolution model of interaction in which AgNPs dissolute to release Ag^+ in solution; the Ag^+ then speciated and elicits a toxic effect (e.g., ROS and protein oxidation) on bacteria. Ion speciation, primarily toward positively charged Ag^+ was previously found to promote toxicity (Figure 3.2), and these data support the nanoparticle-dissolution model. In this chapter, a transcriptomic approach was utilized, and the location of the stress responses were used to test the hypotheses. If bacteria respond differently to AgNPs than $Ag_{(aq)}$, then a different transcriptional pattern will be observed in response to these two stressors; however, if the nanoparticle-dissolution model takesprimacy, no substantial differences in transcriptomic patterns should be evident between AgNPs and $Ag_{(aq)}$.

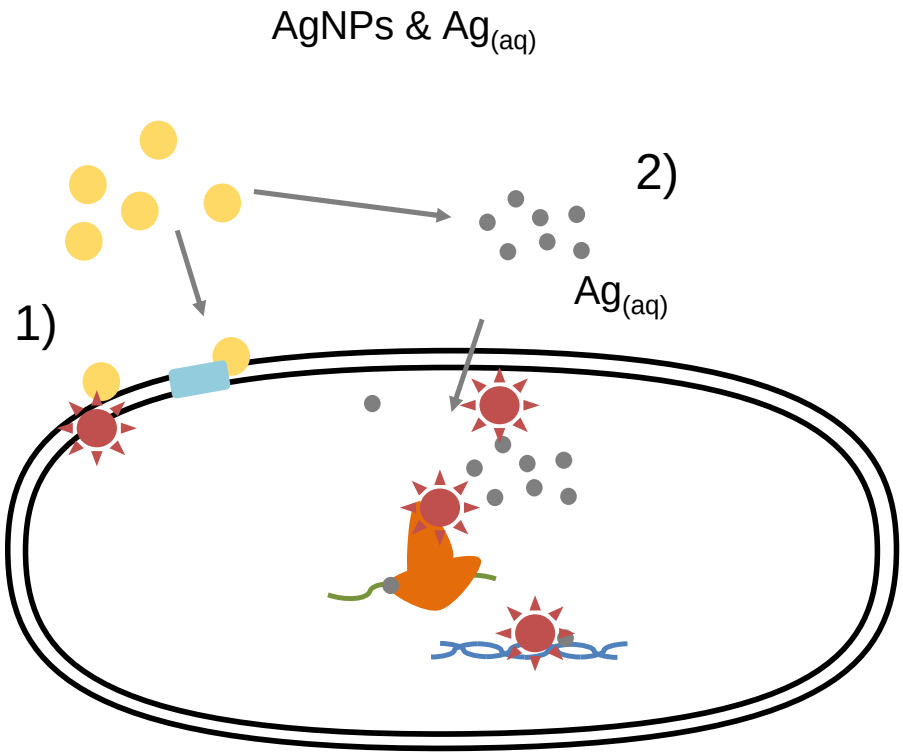

Figure 4.1 **Potential models of bacterial-AgNP interaction**. Two potential models of interaction: 1) surface-attachment model, wherein AgNPs disrupt the bacterial surface and produce ROS and 2) nanoparticle-dissolution model, wherein AgNPs release $Ag_{(aq)}$, which causes metal and ROS toxicity to the cell.

4.3 Materials and Methods

The molecular effects of AgNPs and $Ag_{(aq)}$ were studied with a transcriptomic approach, providing a systems-level view. A hierarchical network analysis was performed to group and isolate differentially expressed stress response pathways. The transcriptomic analysis yielded a substantial quantity of data that required a statistical evalution. As follows, detailed procedures are provided for all of these methods.

4.3.1 $Ag_{(aq)}$ and AgNPs

AgNPs used in this study were purchased from nanoComposix (San Diego, CA). AgNPs were capped with citrate and were 10 nm in diameter; the stock solution was 0.2 mg/mL and were stored in 2 mM sodium citrate solution. Stock solutions were kept in the dark and refrigerated until use. $Ag_{(aq)}$ stocks were made at 100 mg/L from $AgNO_3$ (Fisher, Waltham, MA). $Ag_{(aq)}$ was stored at 4 ˚C in the dark in ultra pure water, partially acidified at 2% v/v with HNO_3 (Fisher, Waltham MA). Fresh $Ag_{(aq)}$ was made monthly to limit oxidation of $Ag_{(aq)}$ into $Ag_2O_{(aq)}$.

4.3.2 Bacteria

The model organism *P. aeruginosa* PAO1 was used for the determination of sublethal AgNP and $Ag_{(aq)}$ concentrations and for the transcriptomic experiments. *P. aeruginosa* PAO1 with a *lasB::gfp* reporter fusion (described previously in Kirisits et al. 2005) was used in quorum sensing (QS) experiments. Freezer stocks of the strains were stored at -80 ˚C in a 75:25 (v/v) mixture of Luria Bertani (0.5 g/L NaCl; LB) broth and glycerol.

4.3.3 Media

LB broth (Fisher Scientific; Waltham, MA) was used to culture inocula and prepare freezer stocks of bacteria. LB agar (15 g/L agar) was used to streak the freezer stocks and to conduct viable plate counts. Minimal Salt Vitamin Glucose (MSVG) medium was used for continuous-culture of bacteria in chemostats. MSVG (for 1L) consists of 1 g $(NH_4)_2SO_4$, 0.06 g $MgSO_4 \cdot 7H_2O$, 0.06 g $CaCl_2$, 0.02 g KH_2PO_4, 0.03 g $Na_2HPO_4 \cdot 7H_2O$, 2.383 g 2-[4-(2-hydroxyethly)piperazin-1-yl]ethanesulfonic acid (HEPES), 1 mL of 10 mM $FeSO_4$, 1 mL of 1000× vitamin stock solution [per liter: 20 mg biotin, 20 mg folic acid, 50 mg thiamine HCl, 50 mg D-calcium pantothenate, 1 mg vitamin B12, 50 mg

riboflavin, 50 mg nicotinic acid, 100 mg pyridoxine HCl, and 50 mg p-aminobenzoic acid], and 0.220 mL of 20 g/L glucose solution). Minimal Davis (MD) medium was used during stress induction experiments because it promoted the formation of low fractal dimension aggregates, which were associated with the expression of the stress response gene *katE* (Chambers et al. 2014). MD medium (for 1 L) consists of 1 g $(NH_4)_2SO_4$, 7 g K_2HPO4, 2 g KH_2PO_4, 0.5 g sodium citrate, 0.1 g $MgSO_4$, 1 g glucose, pH 7.2. Glucose and vitamin stock solutions were sterilized using a 0.220-µm polyethersulfone (PES) bottle-top filter (Corning; Corning, NY); all other bacterial growth media were sterilized using an autoclave. MSVG medium was stored for a maximum of 3 weeks to avoid precipitation of HEPES. Ionic strength of all media used in this study was approximately 40 mM; this was chosen because it balanced AgNP toxicity with AgNP stability (Figure 3.4).

4.3.4 Chemostat

A chemostat was used for continuous-culture of the bacteria, which provided a consistent inoculum for the following experiment. All such experiments contained a control to confirm that the inoculum (taken from the chemostat) met the target concentration. In the chemostat, fresh influent medium was pumped from a reservoir (1.8-L capacity) to the bacterial growth chamber (0.2-L capacity; Figure 4.2). A bubble-break was installed to prevent bacteria in the growth chamber from moving into the medium reservoir. Chemostats were operated at a flow rate of 0.183 mL/min, producing a hydraulic detention time of 18.2 h.

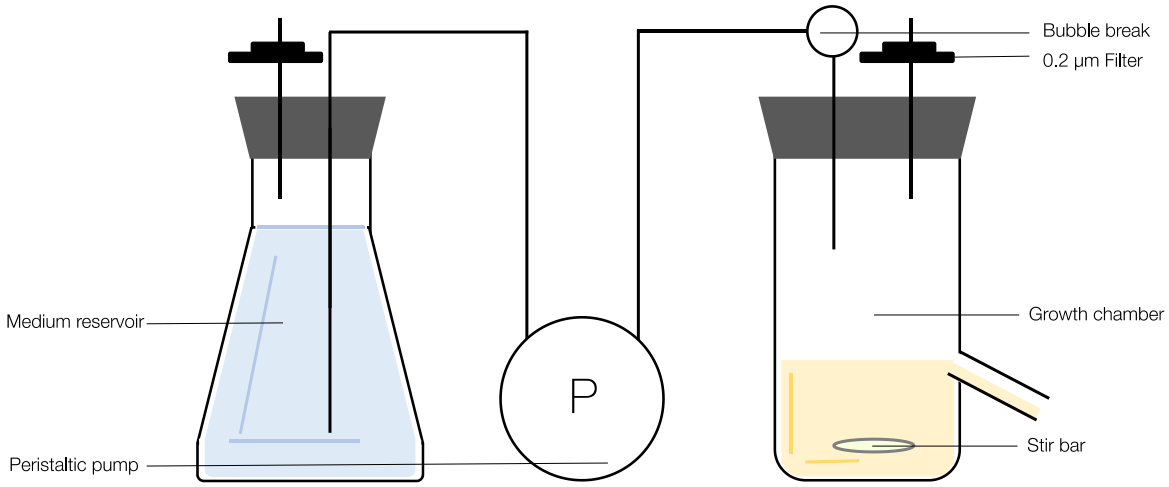

Figure 4.2: **Schematic of Chemostat.** The chemostat is composed of a reservoir to feed fresh influent medium and a growth chamber.

The preparation of the chemostat was completed over five days. On day one, fresh *P. aeruginosa* was struck on LB agar medium from freezer stock and incubated at 35 ˚C overnight. On day two, the chemostat was washed, autoclaved, and filled with fresh MSVG medium; the chemostat was allowed to run for one day prior to inoculation to ensure no contamination; the growth chamber was stirred on a stir plate at 225 RPM and ambient temperature (approximately 22.2 ˚C degrees). A single colony of *P. aeruginosa* was retrieved with a sterile loop hook from the streak plate and stirred into 5 mL of LB broth in a culture tube. The inoculum was incubated for 15 h at 35 ˚C and shaken at 200 RPM. On day three, the chemostat was inoculated with 1 mL of the liquid culture and operated in batch mode for 24 h. On day 4, flow was initiated in the chemostat; at the end of day 5, an aliquot from the chemostat was used for viable plate counts. The target cell density was 5 x 10^7 colony forming units (CFU)/mL, and actual concentrations ranged from 4 to 6 x 10^7 CFU/mL; precision in the bacterial concentration was necessary for experimental

consistency. Bacteria grown in the chemostat were used to inoculate trascriptomic experiments.

4.3.5 Viable plate counts

Viable plate counts for *P. aeruginosa* were conducted using the spot-plate technique (Figure 4.3). Briefly, the sample to be enumerated was sonicated in a bath sonicator (Bathsonic 3510; Fisher; Waltham, MA) for 10 min and vortexed gently for 15 s. Ten-fold serial dilutions were conducted using MD medium in a microtiter plate. Dilutions (10^0 – 10^{-7}) were plated in triplicate with 10-µL spots on LB agar plates using a multichannel pipettor. The plates were incubated at 35 ˚C, and colonies were counted after 20 h. A target of 10-40 CFU/spot was used to choose which dilution to count. The number of cells in the original sample was calculated according to Equation 4.1, where D is the dilution factor.

Equation 4.1 $$\frac{colonies}{0.01\,mL} \cdot D = \frac{CFU}{mL}$$

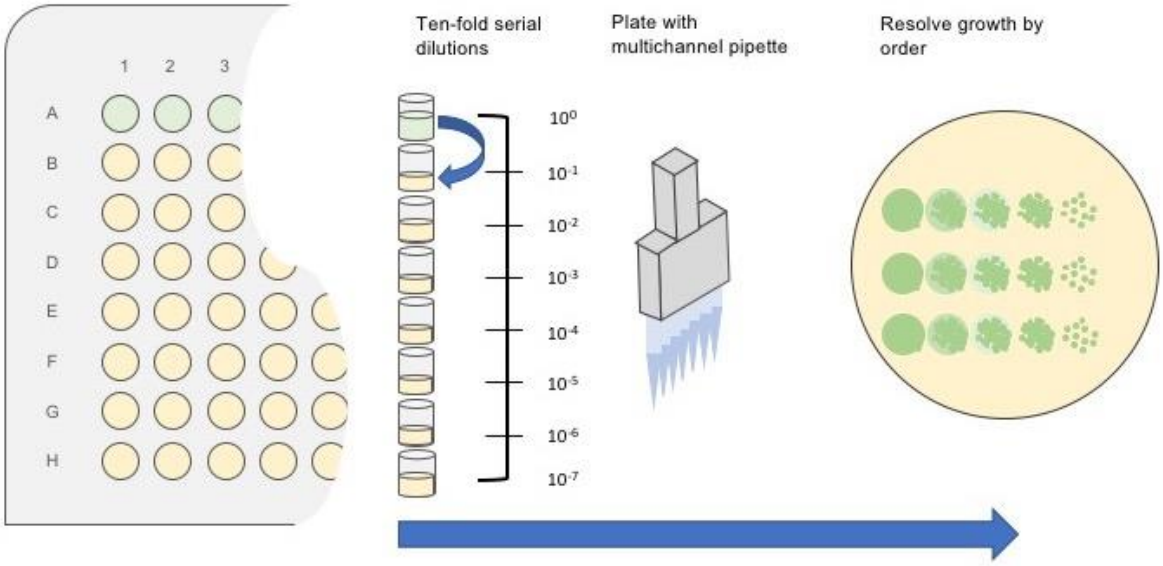

Figure 4.3: **Spot-plate method**. This method was used to enumerate viable bacteria from a well-dispersed liquid culture. An aliquot of the sample to be interrogated was loaded (90 µL; green) into the top row of the microtiter plate; all subsequent rows were filled with 90 µL of sterile diluent. Serial dilutions were performed by mixing 10 µL from each well in row A to row B, followed by mixing via aspiration with the pipette. Ten-fold serial dilutions were continued to the extent desired in subsequent rows. Then, a multichannel pipettor was used to place a 10-µL spot for each dilution of interest on an agar plate. After incubation, CFU were counted for spots that contain 10-40 CFU, and CFU/mL of the original sample was calculated.

4.3.6 Determination of sublethal AgNP and $Ag_{(aq)}$ concentrations

Sublethal concentrations of AgNPs and $Ag_{(aq)}$ were determined for *P. aeruginosa*, such that the bacteria would be stressed but not inactivated in substantial numbers (> 99% survival). To determine these concentrations, toxicity experiments were performed as follows. Two technical replicates of six biological replicates were performed for each stressor (AgNP and $Ag_{(aq)}$) and the no-Ag control (no stressor). To each 50-mL, AgNPs (final concentrations = 7, 3.5, 1.75, 0.88, 0.44, 0.22, 0.11 and 0 µg/L as Ag) or $Ag_{(aq)}$ (dosed from $AgNO_3$, final concentrations = 1.2, 0.6, 0.3, 0.16, 0.08, 0.04 and 0 µg/L as Ag) were

added. No stressor was added to the no-Ag control. The cultures were inverted five times and incubated at 35˚C for 30 min. Then, 2.6 µg/L of sodium thiosulfate was added to all cultures (including the no-Ag control) to quench the action of silver, followed by spot-plate counts. Sodium thiosulfate was the chosen quenching agent because cysteine (common silver quenching agent used in the literature) resulted in lower-purity RNA (lower A_{260}/A_{280} ratio).

4.3.7 Quorum sensing induction

QS describes the process by which some bacteria (including *P. aeruginosa*) regulate gene expression based on cell concentration, and it is considered to be a global gene regulation system. Therefore, to isolate the transcriptomic impact of AgNPs or $Ag_{(aq)}$, the bacterial concentration in those experiments must be below that required to induce QS. To verify that QS was not induced in the cultures used for transcriptomics, *P. aeruginosa* PAO1 with a *lasB::gfp* reporter fusion was cultured in the chemostat described in the section 4.1.6. After reaching steady state, cell concentration was measured with the spot-plate method, and QS induction was queried with fluorescence microscopy and spectroscopy. As a control where QS was induced, *P. aeruginosa* PAO1 *lasB::gfp* was grown overnight on an LB agar plate and in LB broth. A 1-mL aliquot was removed from the chemostat and the batch control culture, centrifuged at 5000 RCF for 6 min, and resuspended in phosphate buffered saline (PBS); the centrifugation and resuspension in PBS was repeated a second time. The resuspended cells were examined on a Nikon (Tokyo, Japan) 80i epifluorescence microscope equipped with a FITC filter (excitation at 480 nm and emission of 508 nm), and images were captured with the Nikon Elements© software. Aliquots of washed cells from the chemostat and batch control culture were transferred to a microtiter plate, and relative fluorescence units (RFU) and optical density at 600 nm

(OD_{600}) were measured using a Synergy HT-I plate reader (BioTek; Winooski, VT). The sensitivity for fluorescence measurements was set at 120. The ratio of fluorescence to OD_{600} indicating no induction of QS genes had been previously identified as $< 10^5$ (Kirisits et al. 2005).

4.3.8 Batch culture exposure of *P. aeruginosa* for transcriptomic analyses

Batch cultures were prepared for transcriptomic studies. To a 250-mL culture flask, 100 mL of MD medium and 1.5 mL of *P. aeruginosa* PAO1 chemostat culture were added; typically, 6-9 flasks were inoculated at once. The cultures were incubated for 7-9 h at 35 ˚C with shaking. Cultures were checked periodically for OD_{600} in a Synergy HT-I plate reader (BioTek; Winooski, VT). Upon reaching an OD_{600} of 0.047-0.054, corresponding to a bacterial density of 1 x 10^7 CFU/mL at which no QS induction was observed, the cultures were composited in a sterile 1-L bottle. Then, a 50-mL aliquot of the composite sample was transferred to a sterile 50-mL polypropylene tube. A sublethal concentration of AgNPs or $Ag_{(aq)}$ was added to each 50 mL sample. A no-Ag control was run in parallel. The cells were incubated at 35 ˚C temp 30 min.

4.3.9 Harvesting bacteria for transcriptomic analysis

After quenching the cultures from section 4.1.10 with 2 µg/L sodium thiosulfate, the cultures were filtered using 0.22-µm Millipore© (Billerica, MA) PVDF Durapore® filters and a Millipore (Billerica, MA) 1225 vacuum sampling manifold, which was sterilized with ethanol prior to sample processing. After the liquid fraction of each sample was removed, the vacuum was paused, and 2 mL of RNAlater (Qiagen; Germantown, MD) was applied. The RNAlater was allowed to slowly percolate under minimal vacuum; this technique was suggested during discussions with manufacturer. Filters were removed from

the manifold with sterile tweezers and were placed in 2-mL, RNase-free conical tubes. The filters were stored at -80 ˚C for at least 24 h before further processing.

4.3.10 RNA extraction protocol

Prior to RNA extraction, all working surfaces and equipment involved in the extraction procedure were wiped with RNaseZAP! (ThermoFisher; Waltham, MA). The filter tubes (containing cells and filters) were removed from the -80 ˚C freezer and thawed on ice for 20 min. RNA extraction was performed with the Qiagen RNeasy kit (Qiagen; Germantown, MD). Minor changes were made to the manufacturer's protocol to facilitate RNA extraction from the filter surface, and the changes are summarized as follows: A 100-µL aliquot of 15 mg/mL lysozyme in TE buffer (10 mM Tris-Cl, 1 mM EDTA, pH 8.0) was added directly to the thawed filter tubes. These tubes were placed on a vortexer with a multi-tube adaptor and vortexed at a setting of 10 for 10 min. The tubes were attached horizontally to the vortexer with the filter on the underside of its tube, such that lysozyme was in constant contact with the filter surface. Following lysozyme incubation, the tubes were placed on ice for 5 min. A 350-µL aliquot of buffer RLT from the RNeasy kit was added to the filter tubes and vortexed at a setting of 7 for 10 s. After a 10-s centrifugation step at 5000 RCF to separate the liquid from the filter, the RLT/lysozyme mixture was transferred to a 2-mL, gasket-sealed bead-beating tube (Fisher Scientific; Waltham, MA). Bead lysis matrix (30-40 mg of lysis matrix "E" beads) was added to each tube (MP Biomedicals; Santa Ana, CA). The tubes were processed in a FastPrep©-25 Classic® homogenizer (MP Biomedicals; Santa Ana, CA) for 3 x 50 s, with 5 min on ice between homogenization steps. The tubes were centrifuged at 17000 RCF and briefly rested on ice until the supernatant was transferred to a new RNase-free tube. A 220-µL aliquot of pure,

undenatured ethanol was added to the supernatant. The tube was inverted/flicked five times, and then all liquid was transferred to a Qiagen RNeasy kit (Germantown, MD) quick spin column. From here, the manufacturer's RNeasy mini protocol for bacterial samples was followed. At the final step of the protocol, purified RNA was eluted with 20 µL of RNase-free water, and the eluate was passed through the column a second time to increase yield. RNA was quantified on a NanoDrop (ThermoFisher; Waltham, MA), and an A_{260}/A_{280} ratio of 1.8-2.2 was targeted. RNA quality was assessed by gel electrophoresis. RNA was stored at -80 ˚C until it was submitted to the University of Texas at Austin Genome Sequencing and Analysis Facility for further processing and sequencing. There, rRNA was removed using the Ribo-Zero rRNA Removal Kit for bacteria (Illumina; San Diego, CA). Library construction was completed using the Illumina TruSeq Stranded total RNA (Illumina; San Diego, CA), and sequencing was performed on a MiSeq 2000 (Illumina; San Diego, CA) using 250-bp, paired-end reads. Quality was assessed with a Bioanalyzer 2100 (Agilent; Santa Clara, CA) after RNA extraction and ribosome removal.

Sequence analysis

RNA sequence read quality was evaluated with fastQC (Bioinformatics). Transcriptome assembly was completed using the BowTie analysis pipeline (Langmead et al. 2012) and linked to the annotated *P. aeruginosa* genome (Stover et al. 2000). DESeq2 in R was used for mapping analysis. Normalization was used to correct for library size and RNA composition bias such that the counts in a sample with a lower number of counts would be adjusted upwards to match a sample with a greater number of counts. For each gene, normalization was performed by calculating the geometric mean of counts for that gene across all tested samples (e.g., AgNP exposed, $Ag_{(aq)}$ exposed and un-exposed controls) and dividing the counts for that gene in a particular sample by the mean across

all to create a size factor for each gene in the genome used to normalize the counts for each sample. Further analysis was conducted with Matlab (Mathworks; Niatic, MA) using the bioinformatics toolbox® and the artificial intelligence and machine learning toolbox®. The sequence fragments were aligned to a reference genome (Wurtzel et al. 2012) in Bow Tie 1.2.2. Log_2-fold expression (Equation 4.2) was calculated for the average of six replicates in each condition referenced against the no-Ag control. Statistical analysis was performed in Excel using an ANOVA to find significant differences between the expression of genes exposed to $Ag_{(aq)}$, AgNPs and the no-Ag control. A 95% confidence interval was used to establish significance. Principal component analysis (PCA) was completed in MATLAB. Log_2fold transcriptomic data for $Ag_{(aq)}$ and AgNP (relative to the no-Ag control) were reduced to a variance matrix. The minimum variance of the first two principal components was plotted. A hierarchical model was then applied to these data, which clustered the data into eight groups. The model used a top-down sort. Gene names were mapped onto the points so that the implication of the clusters could be analyzed.

Equation 4.2. $\log_2 Fold\ Expression = \log_2 \frac{A}{B}$

Where:

A is the experimental condition (transcript count for a particular gene with AgNP or $Ag_{(aq)}$ exposure)

B is the reference condition (transcript count for a particular gene in the no-Ag control)

4.4 Results and Discussion

4.4.1 Physical characteristics of AgNPs used in this study

AgNPs used in this work were suspended in MD medium at an ionic strength of 40 mM approximately equivalent to the Mμ0 exposure solution described in Table 3.1. This condition stabilizes the particles and minimizes their dissolution as compared to media with higher ionic strength (140 mM) and/or destabilizing ligands (e.g., chloride) (Chambers et al. 2014, Chapter 3). Dissolution of AgNPs at a 1 mg/L concentration measured in Chapter 3 at conditions similar to those used in this study resulted in a 13 μg/L release of total $Ag_{(aq)}$, which was statistically indistinguishable from the release of 10 μg/L Ag^+ in the Lμ0 exposure solution (Table 2.1) The particles were completely stable over 5 h. Further, exposure in a medium ionic strength buffer promoted the formation of branched fractal aggregates (Figure 3.3) that had a constant aggregate diameter (data not shown) over the duration of the experiment. Formation of the branched aggregate increased AgNP toxicity (Figure 3.4) as compared to less branched aggregates (Lμ0) and increased the expression of the stress response system *katE* (Figure 3.6). In summary, the medium ionic strength condition utilized in this chapter promoted conditions that preserved nanocharacteristics of the AgNPs.

Furthermore, $Ag_{(aq)}$ that was released from AgNPs under the conditions utilized in this chapter was likely present primarily in the Ag^{+} form due to limited ligand availability. Therefore, under the chemistry conditions chosen in this chapter, the biological response to AgNPs was likely attributable primarily to the nanoparticle form rather than the $Ag_{(aq)}$ form. Additionally, the sublethal AgNP and $Ag_{(aq)}$ concentrations chosen for this chapter would not stimulate transcription of global stress response systems like RpoS, which would indicate overloading of the bacterial stress response.

4.4.2 Quorum sensing induction

To ensure that the transcriptomic response of *P. aeruginosa* to AgNPs and $Ag_{(aq)}$ were not confounded by QS induction, a quorum-sensing reporter strain (*P. aeruginosa* PAO1 *lasB::gfp)* was grown under the same culture conditions as the experimental strain, *P. aeruginosa* PAO1, in the chemostat. The green fluorescent protein (GFP) was highly expressed by the reporter strain grown overnight on an LB agar plate (Figure 4.4A and B). When grown to a density of 10^7 CFU/mL, which was the bacterial concentration at which RNA was harvested in the transcriptomic experiments, the reporter strain showed little GFP expression (Figure 4.4C and D). It was concluded that QS was not induced under the culturing conditions of this study, and the transcriptomes produced during exposure to AgNPs and $Ag_{(aq)}$ were not impacted by QS. This is critical because previous studies have shown that expression of some antibiotic resistance genes, specifically multidrug efflux pumps MexAB and CD, to be regulated through QS (Maseda et al. 2004; Aeschlimann 2003). All chemostat aliquots were verified to have RFU/OD_{600} ratio less than 10^5.

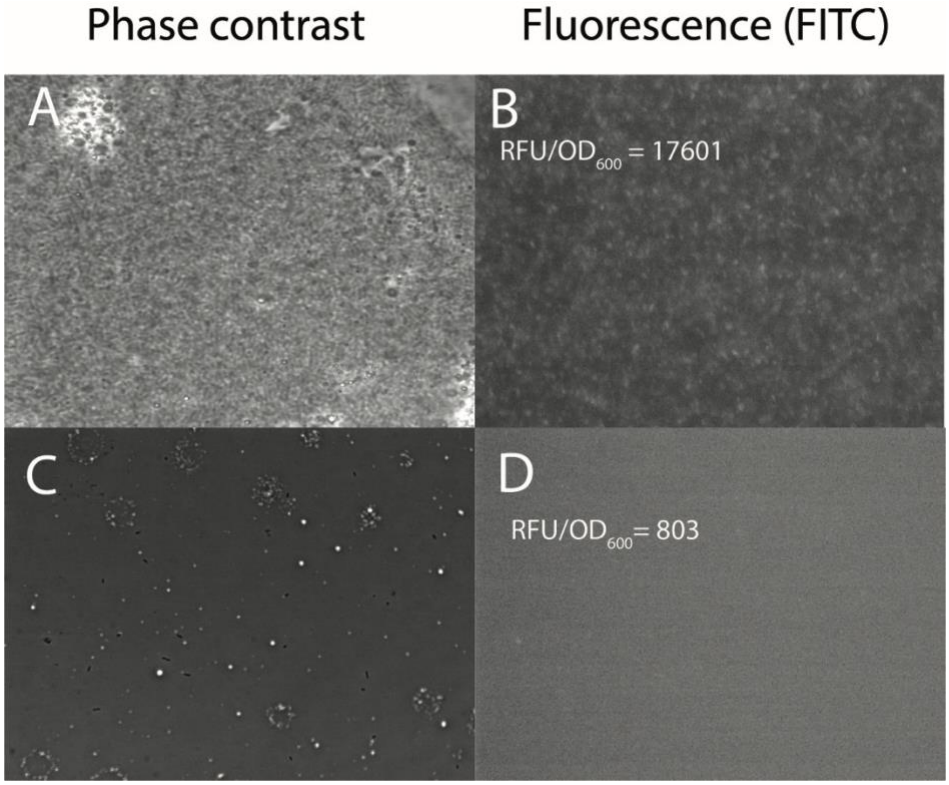

Figure 4.4. **Induction of quorum sensing genes.** Phase-contrast (A, C) and epifluorescence (B, D) micrographs of reporter strain *P. aeruginosa* PAO1 *lasB::gfp* grown overnight to produce visible colonies on LB agar (A-B) and to a density of 10^7 CFU/mL, the concentration at which cell were harvested for RNA extraction (C-D). Cells were washed twice in phosphate buffered saline prior to imaging. Fluorescence was observed using a FITC filter cube (480ex/520em). While quorum sensing was induced in the overnight agar culture, as expected, quorum sensing was not induced in the chemostat culture. The ratio of the fluorescence to the OD is given in overlaid text; the ratio was below QS induction for cells grown at a density of 1 x 10^7 CFU/mL.

4.4.3 Determination of sublethal $Ag_{(aq)}$ and AgNP concentrations

Sublethal concentrations, which stress the cells without causing substantial decreases in viable plate counts, were determined for AgNPs and $Ag_{(aq)}$. The sublethal concentration was defined as the concentration at which bacteria survival was 99% survival using a plate count assay. The sublethal concentrations were 0.08 µg/L for $Ag_{(aq)}$ (Figure 4.5A), and 1 µg/L for AgNPs (Figure 4.5B). Subsequent transcriptomic experiments were

conducted at these defined sublethal exposure concentrations, where the use of sublethal concentrations allowed the recovery of sufficient RNA for downstream analysis.

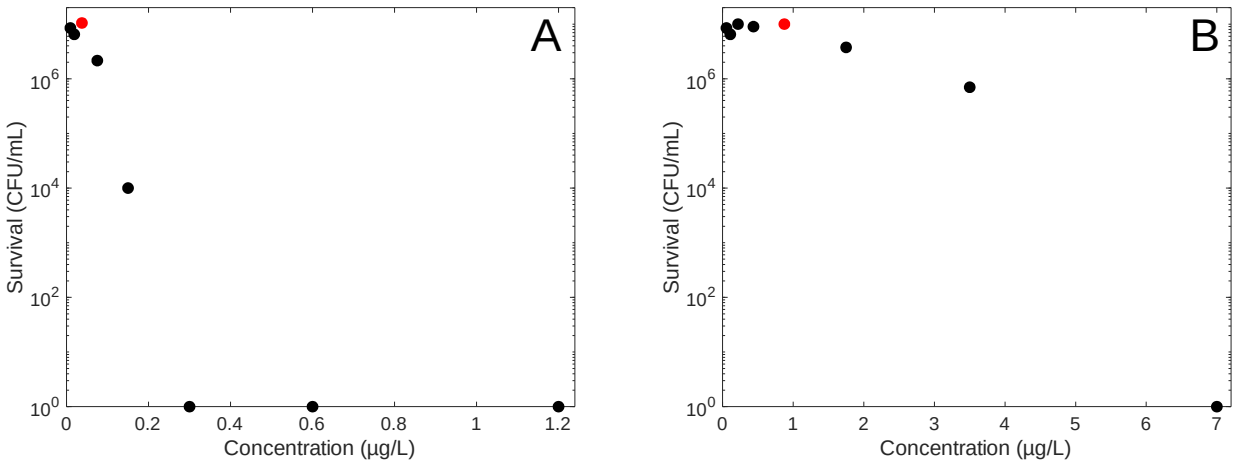

Figure 4.5. **Determination of sublethal $Ag_{(aq)}$ and AgNP concentrations.** *P. aeruginosa* PAO1 was grown in a chemostat in MSVG at 10^7 CFU/mL. Cells were washed and exposed to stressors (A) $Ag_{(aq)}$ and (B) AgNPs for 30 min, followed by quenching with sodium thiosulfate. Bacteria were enumerated via the spot-plate technique. Data points represent average of biological duplicates. Red dots indicate the chosen sublethal concentration.

4.4.4 Principal component analysis of $Ag_{(aq)}$ and AgNP action against *P. aeruginosa*

Dissimilarity between the $Ag_{(aq)}$ and AgNP transcriptomes was evaluated through principal component analysis (PCA). This approach groups data by minimizing the variance between genes; genes with similar variance should group and could potentially be part of similar stress response systems or concerted biochemical pathways. A hierarchical model can then be applied to group genes into unique clusters that might have a linked function or biochemical pathway regulation. After the data were reduced to their principal components, a hierarchical model was applied to the principal component data set (Figure

4.6). PCA analysis with the applied hierarchical model confirmed that the majority of the data clusters together (cluster 4, Figure 4.6) indicating that majority of the genes are expressed similarly between cells that were exposed to sublethal concentrations of $Ag_{(aq)}$ or AgNPs. This result was expected given that many studies hypothesize that the toxicity of AgNPs is primarily due to the release of $Ag_{(aq)}$ (Xiu et al. 2011b; Levard et al. 2012b; Chambers et al. 2014).

Key differences between the $Ag_{(aq)}$ and AgNP transcriptomes were found in the expression of stress response pathways and were evident from the cluster analysis (Figure 4.6), particularly in clusters 2, 3, and 5, which contained small subset of genes associated with metal efflux pumps. These genes are specifically related to metal stress response and bacterial envelope stress response. Genes associated with resistance nodulation division (RND) efflux pumps and P-type ATPase export systems occurred in cluster 5; however, many of these systems also mapped to the shared cluster 4 and cluster 2. These stress response systems included the multi-metal stress response systems, *muxABC,* and the copper stress response system, *copAB,* indicating that some metal stress response pathways might be differentially expressed. Also found in cluster 2 was a bacterial envelope stress response system primarily associated with of repair disulfide bond formation, *dsbA* and *dsbB*. These gene products repair oxidative damaged sulfur-crosslinking of inner membrane proteins and are essential for virulence (Ha et al. 2003; Shouldice et al. 2011). This clustering implicates a differential mechanism between the interaction of *P. aeruginosa* with $Ag_{(aq)}$ and AgNPs. The expression of these systems is explored in detail to build a model of bacterial interaction of $Ag_{(aq)}$ and AgNPs in the following discussion.

The impact of $Ag_{(aq)}$ versus AgNPs on bacteria has been investigated in numerous studies (Pratsinis et al. 2010; Z.-M. Xiu et al. 2011b; Levard et al. 2012b; Chambers et al. 2014), but the results have been mixed. While the impact of AgNPs on bacteria is largely

believed to derive from $Ag_{(aq)}$ produced from AgNP dissolution (Pratsinis et al. 2010; Z.-M. Xiu et al. 2011b, 2012), other studies have shown some effects on bacteria from the AgNPs themselves (Sondi et al. 2004; Morones et al. 2005; C. Lok et al. 2006). Metal and oxidative stress response system clustering might indicate differential cellular response to $Ag_{(aq)}$ and AgNP. To this end, several key metal stress and oxidative stress response systems (the copper system *copAB*, the oxidative stress system *katAB* and *katE*, and the multi-metal efflux systems *czcABC* and *muxABC*) were used to build a model of interaction of $Ag_{(aq)}$ and AgNPs with *P. aeruginosa*.

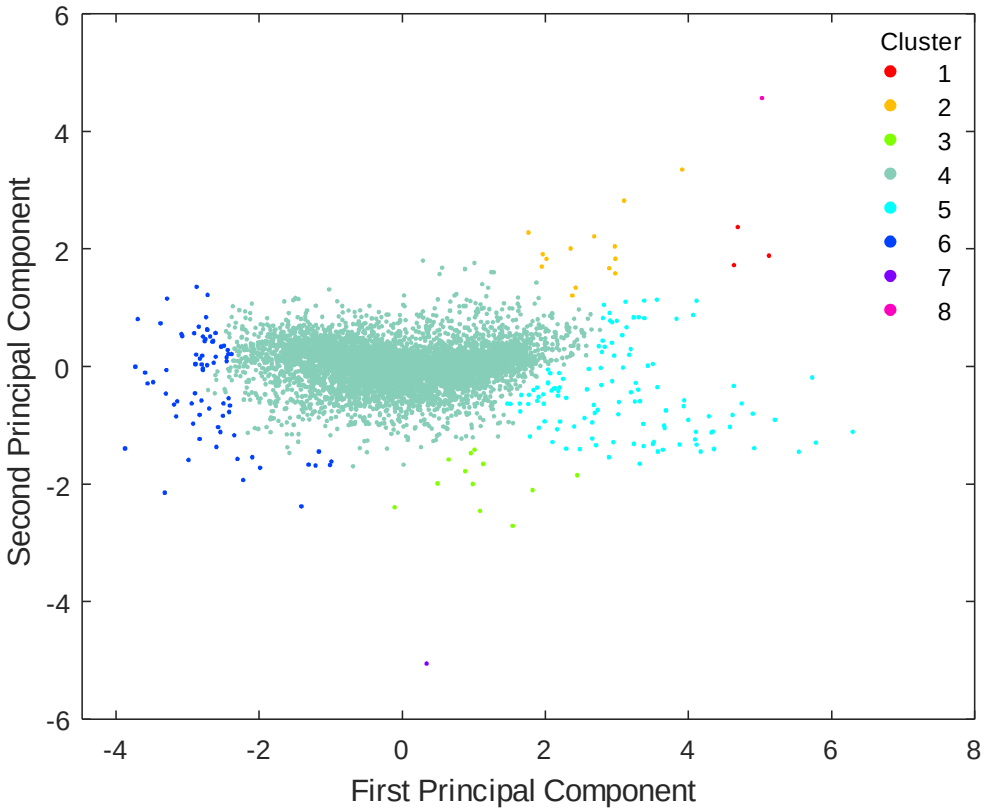

Figure 4.6. **PCA analysis with hierarchical clustering of the transcriptomes.** Log_2 expression of genes resulting from $Ag_{(aq)}$ and AgNP exposure relative to a no-Ag control were plotted along the first and second principal components. The first two components explain 98% of the variance between the data sets. Clusters were defined using the cluster algorithm in Matlab.

4.4.1 General stress induction

It should be noted that no induction of global stress response regulators was observed in the transcriptomic analyses; specifically induction of RpoS, the global stress response regulator indicating a general cell wide stress condition (Storz 2012), was not observed. Rather, bacteria were exhibiting active transcription of stress systems to overcome the stress.

4.4.2 Localization of $Ag_{(aq)}$ and AgNPs

Copper and oxidative stress response to AgNPs

The differential expression of two stress response systems, the copper stress response system (*copABCRS*) and members of the oxidative stress response systems, catalases (*katABEN*), are illustrated in Figure 4.7. As compared to the no-Ag control, *P. aeruginosa* exposed to AgNPs demonstrated a significant increase in the transcription of genes for copper monooxygenase (*copA*), a copper export pump (*copB*), and a porin channel (*oprC*) that sequesters copper; exposure to $Ag_{(aq)}$ did not cause an increase in their transcription relative to the control. Copper toxicity typically results from hydrogen peroxide generation derived from membrane bound copper, potentially disrupting cytochromes or generated through Fenton chemistry (Rodruigez- Montelongo et al. 1993; Nies 1999;). The oxidative stress associated with silver is similar to that of copper, where both are thought to form complexes with proteins and to form peroxide (Nies 1999; Gadd et al. 1977). AgNPs also have been found to generate hydrogen peroxide after first

releasing Ag^+ in solution (He et al. 2012), again illustrating potential overlap with copper chemistry and the generation of hydrogen peroxide. Further evidence of overlapping chemistry can been found in copper stress response systems; copper stress mitigation enzymes CueO and CusABC in *Escherichia coli* have been shown to have substrate flexibility for $Ag_{(aq)}$ (Silver 2003; Nies 2003). Induction of *copA and copB* by AgNPs (Figure 4.7) is the first evidence that the *copABC* system in *P. aeruginosa* responds to $Ag_{(aq)}$, a response system derived from the CueO-oxygenase-like enzyme CopA. Substrate flexibility for Ag^+ in the Cu^+ or Cu^{2+} active sites in copper response systems such as *copRS* are likely the cause induction of copper stress response systems by silver. A similar response of a copper system responding to silver stress was observed with the *E. coli cusRS* copper response system (Yamamoto et al. 2005; Simon Silver 2003).. The porin-encoding gene *oprC* also has been linked to copper stress mitigation; it is theorized the channel does not import copper but binds it a regulatory fashion, potentially sequestering it (Yoneyama et al. 1996). Overall, the induction of copper stress response genes with gene products localized in the periplasm shows a concerted effort by *P. aeruginosa* to mitigate the impact of AgNPs, specifically their release of $Ag_{(aq)}$ and production of hydrogen peroxide.

The similarities of silver and copper chemistry have been covered in previous reviews (Nies 2003; Nies 2010). Copper resistance systems in *E. coli* can mitigate silver stress (Macomber et al. 2009; Gudipaty et al. 2012); it is thought that this substrate flexibility is derived from the similarity of copper and silver chemistry (both group 11 elements) and their similar ionic sizes (95 pm and 110 pm for Cu (I) and Ag (I) respectively. Ag^+ has a higher affinity for sulfur than copper, and, on a molar basis, is more toxic than copper (Nies 2003). It is possible that complexed species of silver would likely not have the same toxicity as the free ion, Ag^+. Ag likely binds to glutathione in bacterial cells and

as a result reduces its likelihood of export (Nies 2003); the same would likely be true for other $Ag_{(aq)}$ – ligand complexes, (e.g., chloride, sulfide, sulfate).

P. aeruginosa contains four catalases localized to different cellular regions; KatA and B are localized to the periplasm and KatE and N are cytoplasmic. Catalases facilitate the conversion of hydrogen peroxide to water (Schellhorn 1995). As compared to the no-Ag control, *P. aeruginosa* exposed to AgNPs demonstrated a statistically significant increase in the transcription of *katA* and *katB* ($p < 0.05$) and a slight increase in the transcription of *katE* and *katN* (Figure 4.7); exposure to $Ag_{(aq)}$ did not significantly increase their transcription relative to the control. Thus, these data support the generation of hydrogen peroxide, a form of ROS, in bacteria exposed to AgNPs, which is similar to the findings of He et al. (2012). While KatA and KatB are localized to the periplasm, KatE and KatN are located in the cytoplasm (Figure 4.8). This suggests that surface-induced hydrogen peroxide stress could propagate into the cytoplasm.

The localization of these response elements in the cell leads to the proposed molecular model presented in Figure 4.8, which illustrates the mechanism of action for a sublethal dosage of AgNPs. Attachment of AgNP to the surface of the bacterial cell likely results in AgNP dissolution given the availability destabilizing ligands and release of Ag^+ into the periplasm and subsequent formation of hydrogen peroxide by cytochrome stress. Consistent with the linkage between copper stress response systems and mitigation of $Ag_{(aq)}$ stress in *E. coli*, $Ag_{(aq)}$ in the periplasm likely activates *copA* and *copB* response elements to detoxify $Ag_{(aq)}$. Further, induction of both *katA* and *katB* limits the action of hydrogen peroxide produced by Ag^+ from AgNP dissolution. Of interest is that these enzymes all are located in the periplasm, and those with cytoplasmic paralogues show only slight induction in the presence of AgNPs.

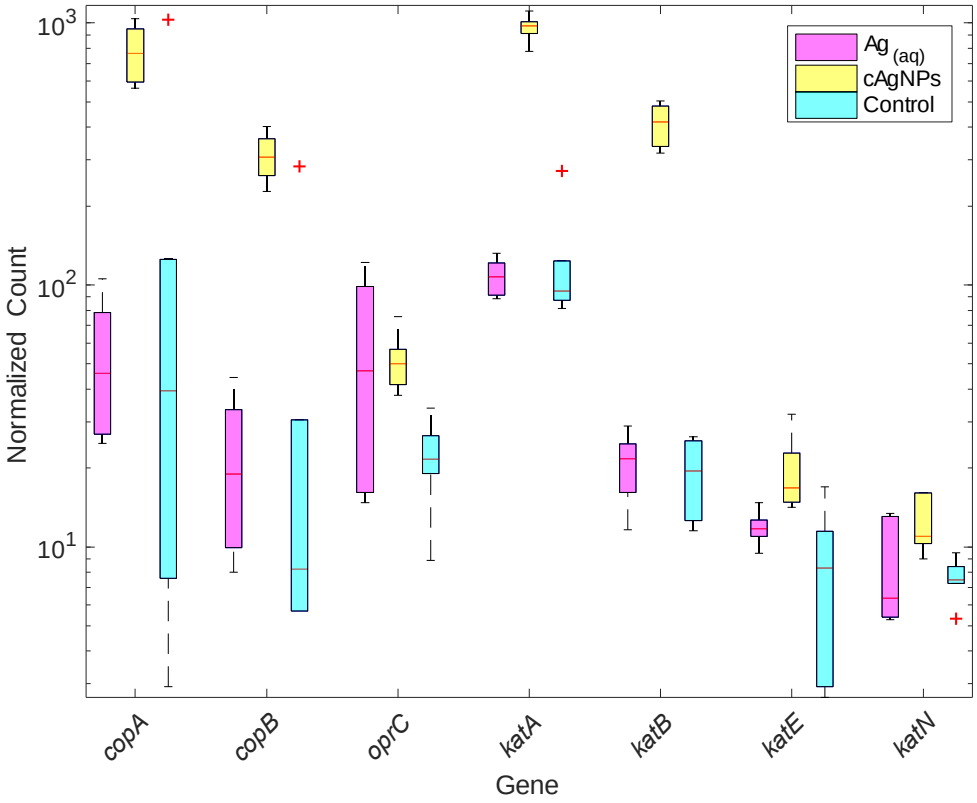

Figure 4.7. **Induction of copper stress response genes and ROS stress response genes in the presence of $Ag_{(aq)}$ or AgNPs and in a no-Ag control.** Transcriptomic analysis of *P. aeruginosa* exposed to sublethal dosage of $Ag_{aq)}$ and AgNPs for the copper stress mitigation pathway *copABC* and ROS stress response genes *katABEN* (encoding catalases). Data represent the normalized counts of six biological replicates for each condition. Box plots represent median values with quartiles, and results were normalized for total counts across each sample group.

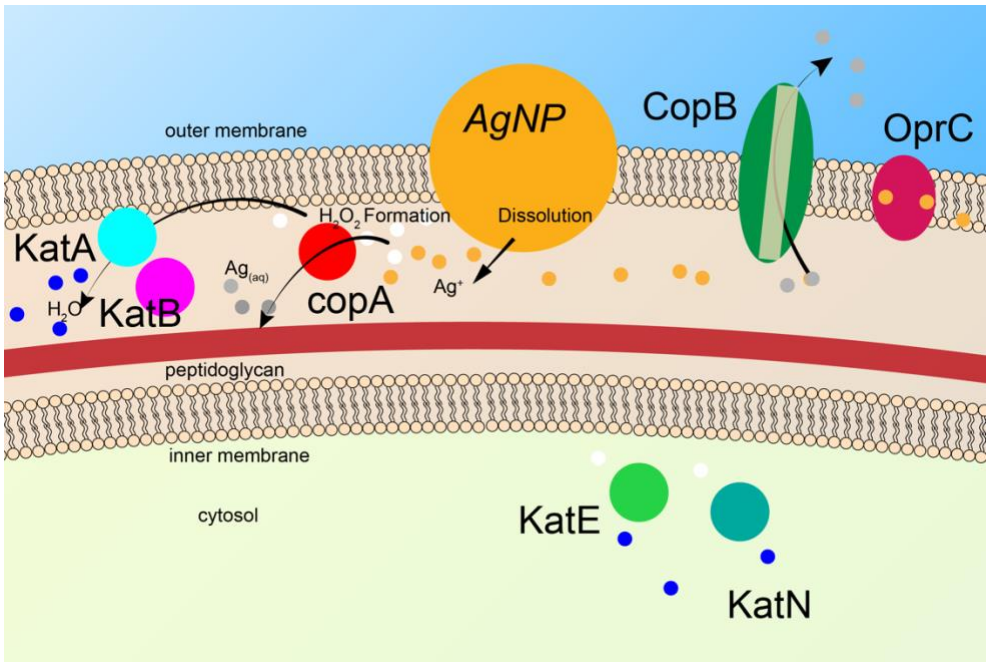

Figure 4.8 **Proposed molecular model of AgNP interaction, as supported by transcriptomic data from *P. aeruginosa*.** Attachment of AgNPs to the outer membrane is followed by AgNP dissolution and production of Ag^+. Dissolution likely occurs in the periplasm as evidenced by significantly increased transcription of periplasmic stress response genes *copA*, *copB*, *katA* and *katB*. CopA, a periplasmically localized monooxygenase, produces hydrogen peroxide in response to the presence of Ag^+,. Excess hydrogen peroxide is then reduced to water via expression of *katA* and *katB*. $Ag_{(aq)}$ can then be exported through the divalent metal export system CopB. Cytoplasmically localized catalases KatE and KatN show slight upregulation in the presence of AgNPs.

Multimetal resistance cluster czcABC is stimulated by AgNPs and $Ag_{(aq)}$

The transcriptomic data was used to evaluate induction of the *czcABC* system, a metal stress response system whose gene products act within the periplasm and the cytoplasm, by *P. aeruginosa* in the presence of AgNP or $Ag_{(aq)}$. The periplasmic and intracellular function of the CzcABC system present a unique lens to examine AgNP and $Ag_{(aq)}$ stress. The recently characterized pump system CzcABC is a classical tripartite RND efflux pump; CzcA occurs along the cytoplasmic membrane, CzcB is a channel in the

periplasm, and CzcC is an outer membrane factor (D. Nies 2003; Tseng et al. 1999; Perron et al. 2004; Vaccaro et al. 2016). Interestingly, a fourth component has been discovered, CzcI, which has the ability to feed stressors from the periplasm directly into channel CzcB. Evidence for this fourth component exists in many *Pseudomonas* spp., but this component is not uniformly distributed across the genus (Vaccaro et al. 2016). A simple BLAST-based search using the *Pseudomonas stutzeri czcI* sequence found no orthologs in *P. aeruginosa* PAO1*;* however, additional evidence supports open channel loading of efflux substrate directly from the periplasm. A periplasmic inlet for efflux pump substrates likely exists and explains the operation of this pump in the absence of a periplasmic binding protein, like CzcI (Legatzki et al. 2003; Benz 2006). Furthermore, binding sites for metals have been found to exist on the periplasmic side of the pump inlet, CzcA, indicating a second mechanism for periplasmic metal efflux in the absence of a substrate shuttle like CzcI (Benz 2006). Thus, the RND efflux pump CzcABC is a metal export pump capable of alleviating metal stress in the cytoplasm and the periplasm, and as such, could potentially highlight a differential action of AgNPs and $Ag_{(aq)}$.

As compared to the no-Ag control, *P. aeruginosa* exposed to AgNPs or $Ag_{(aq)}$ demonstrated increased transcription of all pump components (*czcABC*) and response system elements (*czcRS*) (Figure 4.9). AgNPs induced greater changes in expression of CzcABC than did $Ag_{(aq)}$, but $Ag_{(aq)}$ still induced a substantial change in the expression of response regulators CzcRS and outer and periplasmic components *czcC* and *czcB*. A molecular model of the activity of the *czcABCRS* system is provided in Figure 4.10. The induction of the system by AgNPs provides additional support for the surface-attachment model of bacterial-AgNP interaction but also links $Ag_{(aq)}$ stress to either the periplasm or the intracellular environment. Export processes through the inner membrane factor, CzcA, also explain the activation of the system under $Ag_{(aq)}$ stress. The binding of $Ag_{(aq)}$ to the

small molecule glutathione, an intercellular oxidation limiting molecule, might inhibit the export of $Ag_{(aq)}$ from the periplasm through the export system, CzcABC, similar to copper (Nies 1999; Legatzki et al. 2003). As such, the limited activation of the CzcABC system during $Ag_{(aq)}$ stress may result from competitive binding of $Ag_{(aq)}$ with ligands in the cytoplasm.

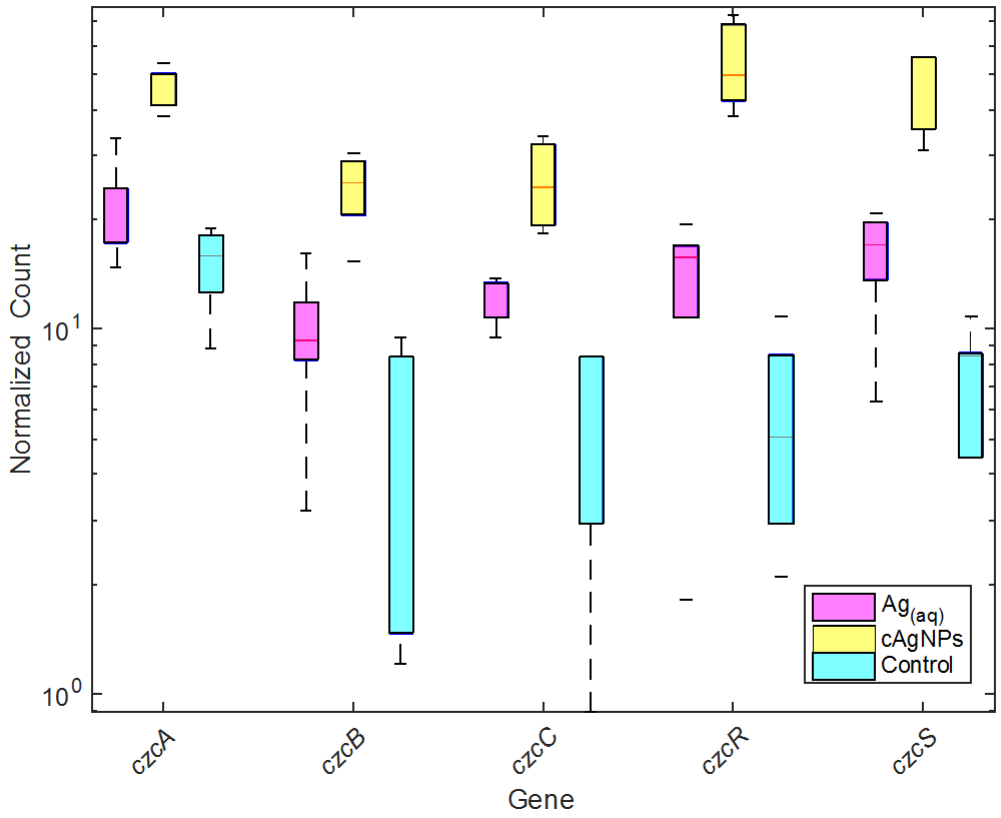

Figure 4.9. **Induction of the multimetal efflux gene cluster *czcABCRS* in the presence of $Ag_{(aq)}$ or AgNPs and in a no-Ag control.** Transcriptomic analysis of *P. aeruginosa* exposed to sublethal dosage of $Ag_{(aq)}$ and AgNPs for the multimetal efflux pump CzcABC (encoding a tripartite pump) and response system CzcRS. Data represent the normalized counts of 6 biological replicates for each condition. Box plots represent median values with quartiles and samples were normalized for total counts across each sample group.

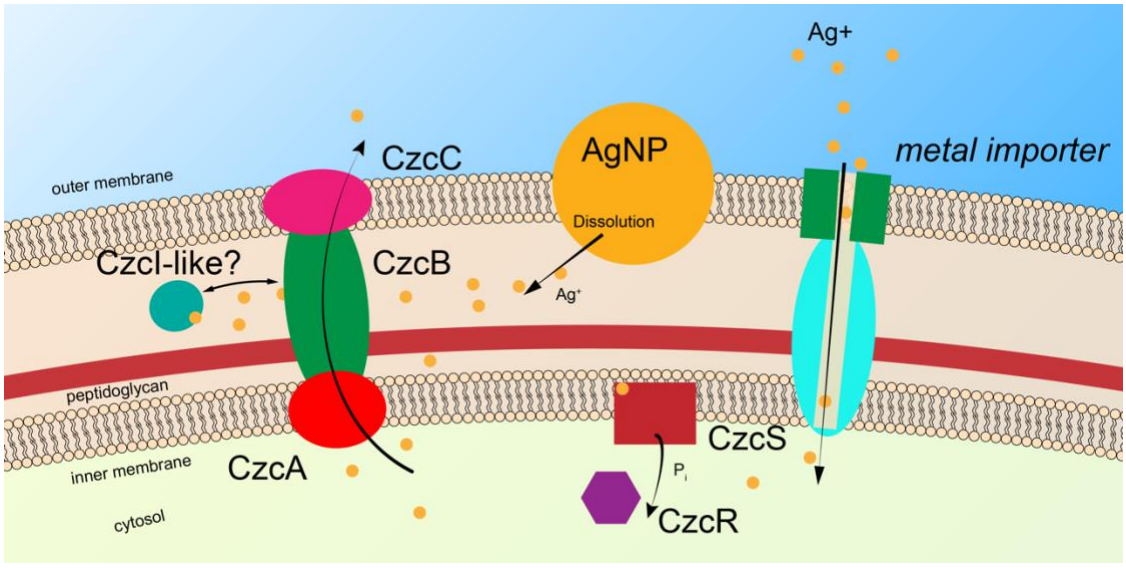

Figure 4.10. **Proposed molecular model for $Ag_{(aq)}$ and AgNP stress mitigation by the *czcABC* system.** Attachment of AgNPs to the outer membrane is followed by subsequent dissolution of Ag^+. At low doses, AgNP stress is likely localized to the periplasm while $Ag_{(aq)}$ can enter the cytoplasm through metal importers. Action of Czc is directed both intracellularly and in the periplasm. Because the feed of the pump faces the cytoplasm, stress due to $Ag_{(aq)}$ in the cytoplasm can be mitigated. Recent work, however, suggests that an additional loading mechanism exists the periplasmic space with an independently regulated shuttle providing a mechanism for the induction of *czcABC* in the presence of periplasmically acting AgNPs.

The transcription of muxABC, encoding a cytoplasmically fed asymmetric pump, is induced by $Ag_{(aq)}$ but not by AgNPs

MuxABC is a tripartite system, similar to CzcABC, where MuxA is the internal-facing cytoplasmic membrane factor, MuxB is a periplasm-spanning channel, and MuxC is an outer membrane factor (Mima et al. 2009). MuxABC is unique in its structural arrangement compared to the other 11 RND efflux pumps in *P. aeruginosa*. The *muxABC* components are arranged asymmetrically such that no periplasmic loading is possible (Li et al. 2007, 2016). Regulation of this system has been linked to the action of CpxRS, which also regulates *mexABC* expression (Tian et al. 2016); however, a complete understanding of the regulation of *muxABC* regulation has not yet been obtained.

As compared to the no-Ag control, *P. aeruginosa* exposed to $Ag_{(aq)}$ demonstrated a statistically significant increase in the transcription of *muxABC* Figure 4.11); exposure to AgNPs did not cause an increase in *muxABC* transcription relative to the no-Ag control. These data support a model in which $Ag_{(aq)}$ toxicity is exerted in the cytoplasm but has minimal effect in the periplasmic space (Figure 4.12). In this model, AgNP dissolution should have no impact on *muxABC* transcription because its stress would be confined to the periplasm. Regulation of *muxABC* expression is coupled to a diffusible cytoplasmic response regulator, CpxS (Winsor et al. 2016), which could respond to $Ag_{(aq)}$ species inside the cell. $Ag_{(aq)}$ ions are imported through metal import channels (Ferguson et al. 2004), typically spanning the periplasm and directly into the cytoplasmic space. Uncharacterized structurally in *P aeruginosa*, MuxABC is most similar to the *E. coli* and *Salmonella enterica* RND pump MdtABC (Li et al. 2016). The MdtABC system has recently been linked to zinc and copper stress mitigation (Nishino et al. 2007), and, as such, MuxABC also is likely involved in metal mitigation. Shown earlier, copper and silver chemistries overlap and the specificity of a copper-exporting pump might coincide with silver export. Overall, the model of interaction proposes that the mitigation of $Ag_{(aq)}$ stress is directed from the cytoplasm (Figure 4.12), whereas the mitigation of AgNPs is directed from the periplasm (Figure 4.8 and Figure 4.10.)

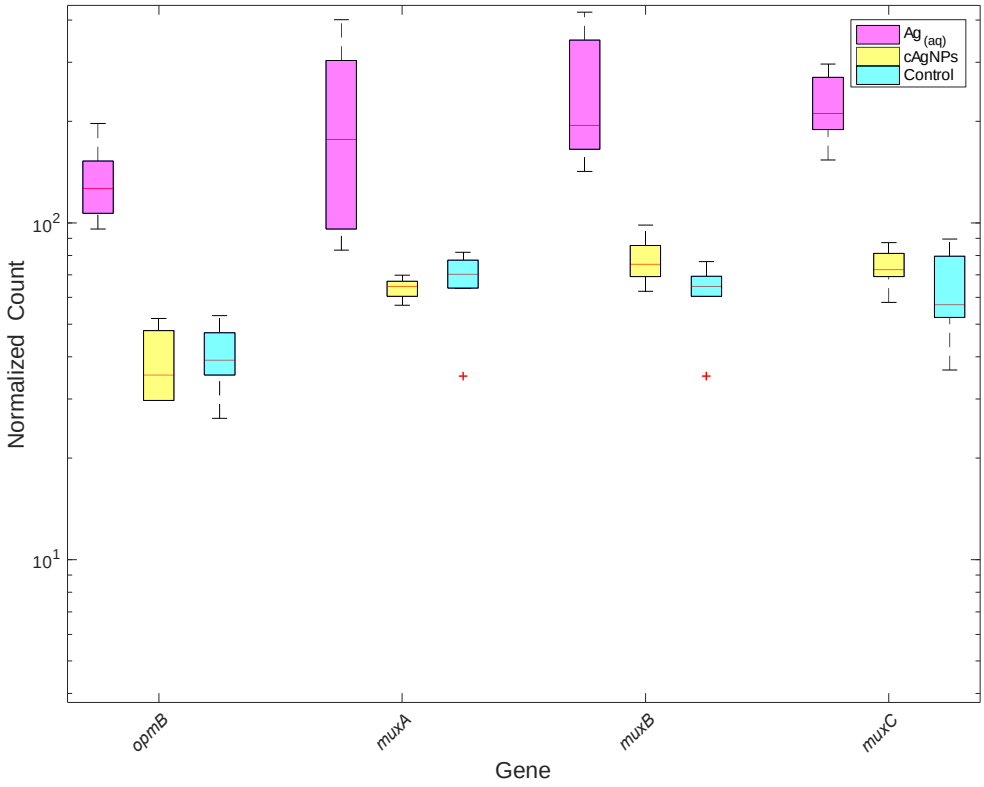

Figure 4.11. **Induction of RND multimetal efflux gene cluster *muxABC* in the presence of $Ag_{(aq)}$ or AgNPs and in a no-Ag control.** Transcriptomic analysis of *P. aeruginosa* exposed to sublethal dosage of $Ag_{(aq)}$ and AgNPs for the multimetal efflux pump MuxABC (encoding a tripartite pump) Data represent the normalized counts of 6 biological replicates for each condition. Box plots represent median values with quartiles and samples were normalized for total counts across each sample group. "+" indicates outlier.

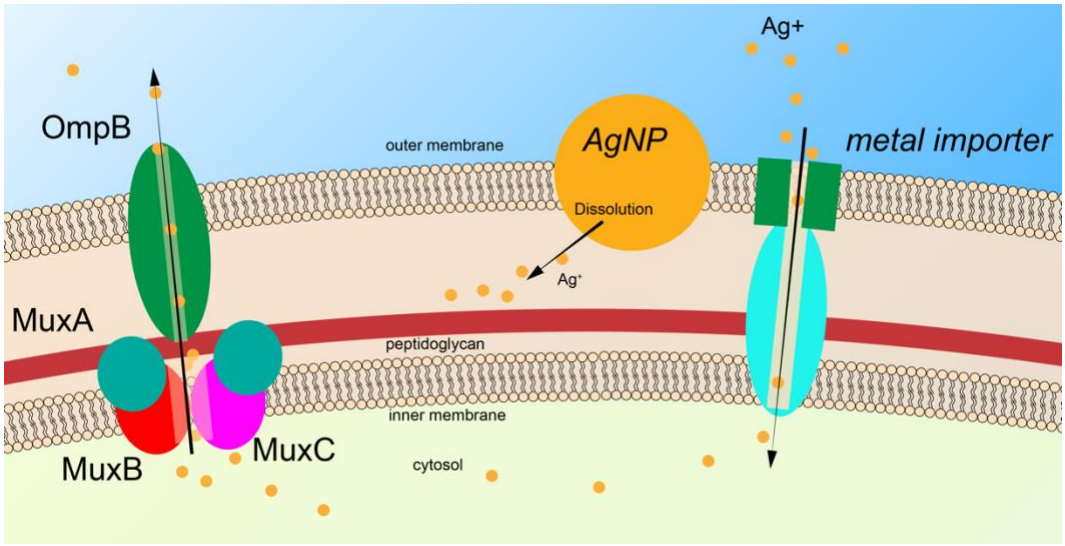

Figure 4.12. **Proposed molecular model for mitigation of $Ag_{aq)}$ and AgNP stress by the MuxABC system.** $Ag_{(aq)}$ enters the cell through cationic metal import systems, which delivers silver ions directly to the cytoplasm. In general, ions that are not needed are exported immediately. *muxABC's* regulation is unknown, but it likely relates to *cpxRS*. The structure of MuxABC is asymmetric such that export is only available from the cytoplasm. Thus cytoplasmic stress due to $Ag_{(aq)}$ is alleviated directly from the cytoplasm. Therefore, in a surface-attachment model of AgNP stress, AgNP stress is localized to the periplasm and no mitigation of AgNP stress is possible with the MuxABC system.

4.5 Conclusion and Summary

The two hypotheses examined in this chapter were evaluated using a molecular approach centered on the expression of bacterial stress response systems. The localization of stress response systems during AgNP exposure were focused on the periplasm, suggesting a surface-attachment model of interaction for AgNPs and bacteria. That is, under the water chemistry conditions tested here, the surface-attachment model of interaction was correct, and the nanoparticle-dissolution model of interaction was incorrect. In particular, a periplasmically located P-type ATPase efflux pump (encoded by *copB*) and associated copper monooxygenase (encoded by *copA*) as well as coupled porin and binding protein (encoded by *oprC*) and catalase enzymes (encoded by *katA* and *katB*)

were primarily induced by AgNPs and were periplasmically localized (Figure 4.7). The transcriptomic profiles suggest that AgNP toxicity is promoted by ion release in the periplasm and subsequent formation of H_2O_2. Additional data suggested that a periplasmically located intracellular-facing RND cation efflux pump (encoded by *czcABC*) exported metal stressors from the periplasm and that AgNP stress was directed in the periplasm (Figure 4.9). $Ag_{(aq)}$ stress was localized intracellularly; the expression of an intracellular cytoplasmic export pump, *muxABC*, was stimulated only by $Ag_{(aq)}$. Analysis of the location of these systems and their respective actions informed a proposed model of interaction of AgNPs and bacteria that is consistent with reported observations of the impact of AgNPs on bacteria (Long et al. 2017; El Badawy et al. 2011; O. Choi et al. 2010). A summary of the overall model of interaction is provided in Figure 4.13. AgNPs were found to act periplasmically, and $Ag_{(aq)}$ primarily induced intracellular export systems. Thus, under the tested water chemistry conditions, AgNP toxicity is derived from the interaction of the AgNPs and the bacteria surface at sublethal doses.

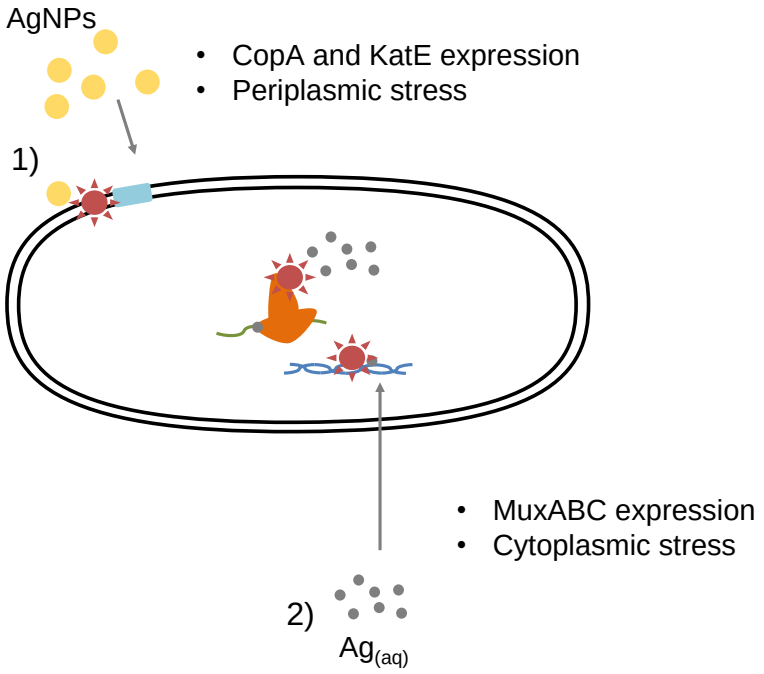

Figure 4.13 Model of interaction summary under the tested water chemistry conditions. AgNPs were found to act periplasmically. $Ag_{(aq)}$ activated more intracellular stress response systems. The results show that toxicity of AgNP is directly relatable to interactions between AgNPs and the bacterial envelope/periplasmic space.

A comprehensive model of nanoparticle toxicity is therefore dependent on selected surface capping agent (Asharani et al. 2008; El Badawy et al. 2011; Long et al. 2017), solution composition, particle stability (Kvítek et al. 2008; Römer et al. 2011; Li et al. 2012; Chambers et al. 2014), and particle surface oxidation (Mulvaney et al. 1991; Z.-M. Xiu et al. 2011b), all of which influence the likelihood of surface attachment of AgNPs to a bacterium. If the persisting conditions select for particle stability without significant dissolution of $Ag_{(aq)}$, the mechanism of interaction will follow a pathway for particle attachment to a bacterium. Following the attachment, a particle will interact with the outer membrane and periplasmic space and disrupt cellular metabolic processes, membrane integrity, and protein folding (Sondi 2004; Morones et al. 2005; Lok et al. 2006; Lok et al.

2007; Long et al. 2017). In the event that the particles undergo rapid aggregation, toxicity is likely negligible; however, if dissolution occurs as a function of solution chemistry, the mechanism of toxicity will be $Ag_{(aq)}$-mediated, as reported by several studies (Pratsinis et al. 2010; Z.-M. Xiu et al. 2012).

The interaction of AgNPs with bacteria is affected by AgNP aggregation, dissolution, and the surface features of the bacteria (Fabrega et al. 2009; Römer et al. 2011; Chambers et al. 2014). Contributing further still are the available stress response systems that can mitigate the effect of nanotoxicity. Bacteria harboring extensive metal stress response systems (*e.g., Metalodurans* spp., *Pseudomonas* spp.*)* will adapt by expressing oxidases and export systems dependent on the pathway of AgNP toxicity (D. Nies 2003) while those without would die. Metal toxicity systems function in the absence of oxygen, and the formation of reactive nitrogen species can induce the expression of stress response systems (D. H. Nies 1999; Hassan et al. 1999; Perron et al. 2004) perhaps explaining limited AgNP toxicity under anaerobic stress (Xiu et al. 2011b, 2012; Miller et al. 2013). Furthermore, presence of ROS or reactive nitrogen species can induce stress response systems that extend beyond that of metal or surface stress response; rather, the AgNPs used in this study induced numerous antibiotic resistance gene clusters (e.g., *mexABC, muxABC)*

With clear evidence supporting a surface-attachment model of interaction, future nanoparticle design should consider target organism and the stress response systems harbored by that organism. Balancing surface features (e.g., capping agent, zeta potential) alongside bacterial physiology (e.g., characteristic surface carbohydrates, surface proteins) as well as activation of metal stress responses and bulk solution characteristics will lead to effective, targeted killing of bacterial cells. Still further exists the possibility of using surface attachment as a means to deliver cancer therapeutics.

5. Antibiotic resistance is stimulated and maintained by aqueous silver and silver nanoparticles

This chapter addresses Task 3. Build a biomolecular model that describes the potential for $Ag_{(aq)}$ and AgNPs to induce co- and cross-resistance to antibiotics.

.

5.1 INTRODUCTION

Silver nanoparticles (AgNPs) are increasingly included in consumer products. AgNPs are the fastest growing category in the database for the Project on Emerging Nanotechnologies, adding more than 500 products in the preceding 10 years (Vance et al. 2015). The integration of AgNPs into products ranging from toys to athletic clothing to medical equipment (Ji et al. 2007; Anyaogu et al. 2008; Chaloupka et al. 2010; Dastjerdi et al. 2010; Musee et al. 2011; Maillard et al. 2013) is largely a function of AgNP toxicity to microorganisms (Sondi et al. 2004; Morones et al. 2005). Since AgNPs can easily be incorporated into a variety of materials, including plastics and fabrics, they represent a flexible material for controlling fouling (Murthy 2007; Dastjerdi et al. 2010; Vance et al. 2015).

Two models of interaction have been proposed to describe the impact of AgNPs on cells: (1) the dissolution of AgNPs to produce toxic aqueous silver ($Ag_{(aq)}$) in bulk solution (Xiu et al. 2011b; 2012) and (2) the attachment of AgNPs directly to the bacterial cell envelope (Sondi 2004; Morones et al. 2005;; Long et al. 2017; Chapter 4 of this work). In both cases, AgNPs exert toxicity to the bacterium through multiple mechanisms of action that directly compromise bacterial cell integrity, enzymatic function, and replicative

processes. The attachment of AgNPs to the surface of a bacterium causes lipid peroxidation and generation of H_2O_2, resulting in stress in the periplasm and at the cytoplasmic membrane (Sondi et al. 2004; Morones et al. 2005; Lok et al. 2008; Ho et al. 2010; He et al. 2012;). $Ag_{(aq)}$ transported into the cell through porins or metal influx pumps causes proteins to misfold through the oxidation of sulfur-containing amino acid residues (Lok et al. 2006; Lok et al. 2007; Wigginton et al. 2010). Intracellular $Ag_{(aq)}$ has been linked to DNA replication and transcription disruption through the formation of DNA and RNA adducts (Silver et al. 1999; Arakawa et al. 2001). The mechanisms of action of AgNPs and $Ag_{(aq)}$ that target the bacterial surface, protein folding, and DNA replication overlap very closely with the mechanisms of action of many antibiotics; this overlap might indicate the potential development of antibiotic resistance (i.e., the ability of an organism to grow in the presence of an antibiotic) due to AgNP and $Ag_{(aq)}$ exposure.

Antibiotics are divided into groups based on their mechanism of action. Aminoglycosides target ribosomes and cause protein misfolding during translation, which disrupts the function of the protein (Lee et al. 2009). Cationic polypeptides and β-lactams target the bacterial envelope, thereby compromising cellular integrity and eventually leading to lysis (Waxman et al. 1983; De Lencastre et al. 1999). Quinolones target DNA replication and render a cell incapable of producing daughter cells (Giuliodori et al. 2007). To mitigate the effect of antibiotics, bacteria possess a variety of stress response systems (reviewed in Storz et al. 2011).

Stress response systems are coupled to regulators that sense changes in the homeostasis of a bacterium, as signaled by small molecules (e.g., peroxide species; Cabiscol et al. 2000; Storz et al. 2000; Cardenal-Muñoz et al. 2013); these regulators activate stress response systems. Some stress response regulators can directly detect antibiotic presence. For example, the penicillin response system responds only to the

presence of ß-lactams (Farra et al. 2008). However, more often, stress response regulators detect non-specific molecules (e.g., H_2O_2, metals). A stress response can result in the production of enzymes that modify the structure of the antibiotic (Livermore 1995) or the production of efflux pumps, which act to export a wide range of stressors including metals and antibiotics (Schweizer 2003; Kumar et al. 2005; Baker-Austin et al. 2006; Storz et al. 2011). A key group of efflux pumps is the resistance nodulation and division (RND) family. RND pumps are a tripartite system that span the cytoplasmic membrane, periplasmic space, and outer membrane, comprised of many homologs that reduce stress from metals, antibiotics, and organic compounds (Alvarez-Ortega et al. 2013; Tseng et al. 1999; Anes et al. 2015). The existence of a broad range of bacterial stress response system regulators suggests that multiple stressors could induce the same stress response system, which could ultimately lead to increased resistance to a stressor. Co- and cross-resistance describe the situation in which the resistance of a cell to a primary stressor is stimulated by the cell's exposure to a secondary stressor. When a shared genetic element (e.g., a plasmid) is involved, this is termed co-resistance; co-resistance to imipenem has been observed in *Pseudomonas aeruginosa* after exposure to copper, cadmium, and zinc (Caille et al. 2007). When a gene product with the ability to mitigate both stressors is involved, this is termed cross-resistance (Baker-Austin et al. 2006; Edward Raja et al. 2008).

Given the overlap among the mechanisms of action of AgNPs, $Ag_{(aq)}$, and antibiotics, it is plausible that the bacterial stress response elicited by exposure to AgNPs or $Ag_{(aq)}$ could result in increased bacterial resistance to antibiotics. Antibiotic resistance, where antibiotics lose their effectiveness for treating infections, is a $38 billion (US 2007) human health problem (US CDC 2013). Recently, rates of new antibiotic discovery have fallen while the frequency of occurrence of antibiotic-resistant bacterial strains has risen (World Health Organization 2011). Understanding the potential for co- and cross-

resistance to antibiotics derived from bacterial exposure to AgNP or $Ag_{(aq)}$ could help to limit further expansion of antibiotic resistance. In this study, a transcriptomic and proteomic approach was utilized to examine the induction of RND efflux pumps (a general stress response) and specific antibiotic resistance systems in *P. aeruginosa* exposed to AgNPs or $Ag_{(aq)}$. Additionally, to examine the potential for long-term mutagenesis derived from exposure to AgNP or $Ag_{(aq)}$, the induction of DNA repair systems was evaluated.

5.2 SUMMARY OF INITIAL HYPOTHESES

A series of hypotheses describing potential antibiotic responses resulting from exposure to AgNPs or $Ag_{(aq)}$ was derived from the model of bacterial-AgNP interaction and the model of bacterial-$Ag_{(aq)}$ interaction discussed in Chapter 4. The first series of hypotheses derived from the model of bacterial-AgNP interaction. AgNP stress was localized in the periplasm and resulted production of the ROS H_2O_2 (Figure 4.8). These data suggest the hypothesis that the antibiotic resistance stimulated by AgNP exposure might be limited to antibiotics acting at the bacterial envelope (e.g., penicillins and polymyxins). The production of ROS in the periplasm due to AgNP exposure also might activate resistance to antibiotics that produce ROS stress (e.g., aminoglycosides). The second series of hypotheses focused on the model of bacterial-$Ag_{(aq)}$ interaction. These hypotheses focused on the intracellular action of $Ag_{(aq)}$ (Figure 4.12). This hypothesis is that $Ag_{(aq)}$ acts intracellularly (Figure 4.9 and Figure 4.11) and might induce resistance to antibiotics that cause protein misfolding (e.g., macrolides, aminoglycosides) and those that impact DNA replication (e.g., ciprofloxacin). A summary of these hypotheses is provided in Figure 5.1.

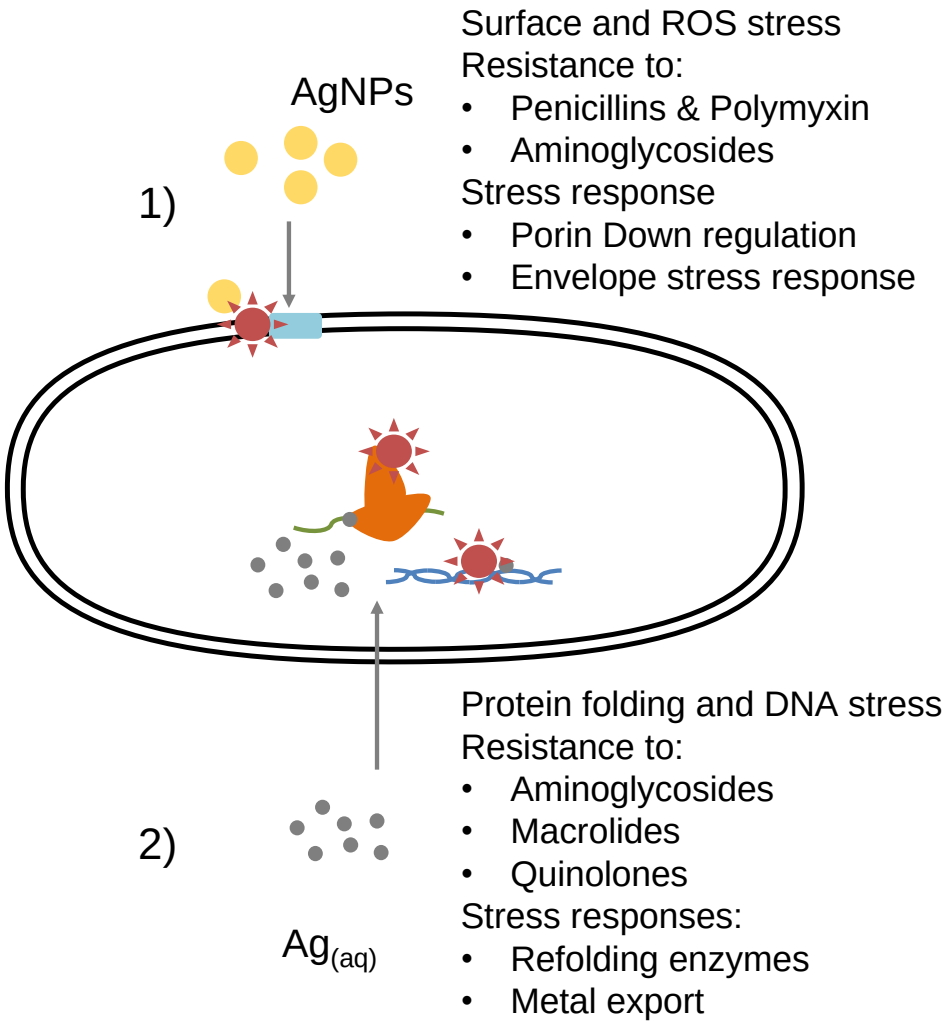

Figure 5.1 **Potential antibiotic resistance derived from model of interaction between bacteria and 1) AgNPs or 2) $Ag_{(aq)}$.** Under the tested water chemistry conditions, AgNPs were found to elicit toxicity through a surface-attachment model and disrupt periplasmic function while $Ag_{(aq)}$ acted intracellularly.

5.3 Materials and Methods

The molecular effects of AgNPs and $Ag_{(aq)}$ on the Gram-negative opportunistic human pathogen *P. aeruginosa* were studied with transcriptomic and proteomic

approaches, thereby providing a systems-level view. A hierarchical network analysis was performed to group and identify differentially expressed stress response pathways. Both approaches yielded a substantial quantity of data was evaluated statistically. As follows, detailed procedures are provided for all of these methods.

5.3.1 $Ag_{(aq)}$ and AgNPs

AgNPs used in this study were purchased from nanoComposix (San Diego, CA). AgNPs were capped with citrate and were 10 nm in diameter; the stock solution was 0.2 mg/mL and were stored in 2 mM sodium citrate. Stock solutions were kept in the dark and refrigerated until use. $Ag_{(aq)}$ stocks were made at 100 mg/L from $AgNO_3$ (Fisher, Waltham, MA). $Ag_{(aq)}$ was stored at 4 ˚C in the dark in ultrapure water, acidified at 2% v/v with HNO_3 (Fisher, Waltham MA).

5.3.2 Bacteria

The model organism *P. aeruginosa* PAO1 was used in the study. *P. aeruginosa* PAO1 *lasB::gfp*, described previously in Kirisits et al. (2005), was used to evaluate quorum sensing (QS) induction. Both strains were stored at -80˚C in a mixture (75:25 v/v) of Luria Bertani (0.5 g/L NaCl; LB) broth and glycerol.

5.3.3 Media

LB broth (Fisher Scientific; Waltham, MA) was used to culture inocula and prepare freezer stocks of bacteria. LB agar (15 g/L agar) was used to streak the freezer stocks and to conduct viable plate counts. Minimal Salt Vitamin Glucose (MSVG) medium was used for continuous-culture of bacteria in chemostats. MSVG (for 1L) consists of 1 g $(NH_4)_2SO_4$, 0.06 g $MgSO_4 \cdot 7H_2O$, 0.06 g $CaCl_2$, 0.02 g KH_2PO_4, 0.03 g $Na_2HPO_4 \cdot 7H_2O$, 2.383 g 2-[4-(2-hydroxyethly)piperazin-1-yl]ethanesulfonic acid (HEPES), 1 mL of 10 mM $FeSO_4$, 1 mL of 1000× vitamin stock solution [per liter: 20 mg biotin, 20 mg folic

acid, 50 mg thiamine HCl, 50 mg D-calcium pantothenate, 1 mg vitamin B12, 50 mg riboflavin, 50 mg nicotinic acid, 100 mg pyridoxine HCl, and 50 mg p-aminobenzoic acid], and 0.220 mL of 20 g/L glucose solution). Minimal Davis (MD) medium was used during stress induction experiments because it promoted the formation of low fractal dimension aggregates, which were associated with the expression of the stress response gene *katE* (Chambers et al. 2014). MD medium (for 1 L) consists of 1 g $(NH_4)_2SO_4$, 7 g K_2HPO4, 2 g KH_2PO_4, 0.5 g sodium citrate, 0.1 g $MgSO_4$, 1 g glucose, pH 7.2. Glucose and vitamin stock solutions were sterilized using a 0.220-µm polyethersulfone (PES) bottle-top filter (Corning; Corning, NY); all other bacterial growth media were sterilized using an autoclave. MSVG medium was stored for a maximum of 3 weeks to avoid precipitation of HEPES. Ionic strength of all media used in this study was approximately 40 mM; this was chosen because it balanced AgNP toxicity with AgNP stability (Figure 3.4).

5.3.4 Chemostat

A chemostat was used for continuous-culture of *P. aeruginosa*. Fresh influent medium was pumped from a reservoir (1.8-L capacity) to the bacterial growth chamber (0.2-L capacity;

Figure 4.2). A bubble-break prevented bacteria in the growth chamber from contaminating the reservoir. The chemostat was operated at a flow rate of 0.183 mL/min, producing an 18.2-h hydraulic detention time.

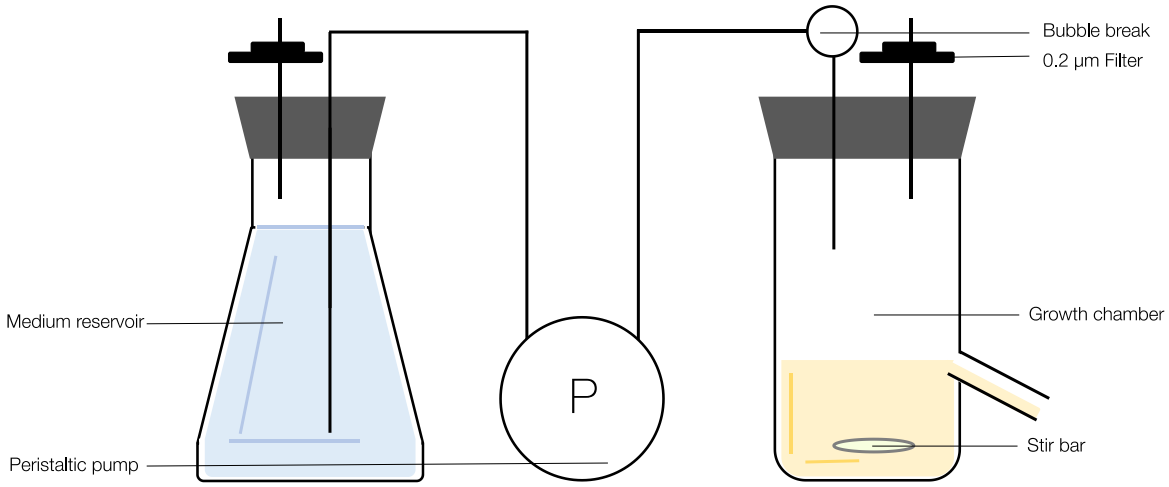

Figure 5.2: **Schematic of Chemostat**. Fresh influent medium is pumped from the reservoir to the growth chamber.

The preparation of the chemostat was completed over five days. On day one, *P. aeruginosa* freezer stock was struck on LB agar medium and incubated at 35˚C overnight. On day two, the chemostat was autoclaved and filled with fresh MSVG medium; the growth chamber was stirred on a stir plate at 225 RPM and ambient temperature (~22 ˚C). A test tube of LB broth was inoculated with single colony of *P. aeruginosa* from the streak plate. The inoculum was incubated overnight with shaking at 35˚C. On day three, after microscopic confirmation that the media in the chemostat was sterile, the chemostat was inoculated with 1 mL of the liquid culture and operated in batch mode for 24 h. On day 4, flow was initiated in the chemostat. At the end of day 5, an aliquot from the chemostat was used for viable plate counts. The target cell density in the chemostat was 5 x 10^7 colony-forming units (CFU)/mL, and actual concentrations ranged from 4 to 6 x 10^7 CFU/mL. *P. aeruginosa* PAO1 *lasB::gfp* grown in the chemostat was used to inoculate

batch experiments to examine QS (see section 0), and *P. aeruginosa* PAO1 grown in the chemostat was used to inoculate batch experiments for stress induction (see section 5.4.4).

5.3.5 Viable plate counts

Viable plate counts for *P. aeruginosa* were conducted using a spot-plate technique (Figure 4.3). Briefly, the sample to be enumerated was sonicated in a bath sonicator (Bathsonic 3510; Fisher; Waltham, MA) for 10 min and vortexed gently for 15 s. Ten-fold serial dilutions were prepared in MD medium in a microtiter plate and plated in triplicate (10-µL spots) on LB agar plates. The plates were incubated overnight at 35˚C. A target of 10-40 CFU/spot was used to choose which dilution to count. The bacterial concentration in the original sample was calculated according to Equation 5.1, where D is the dilution factor (1/dilution).

$$\text{Equation 5.1 } \frac{colonies}{0.01\,mL} \cdot D = \frac{CFU}{mL}$$

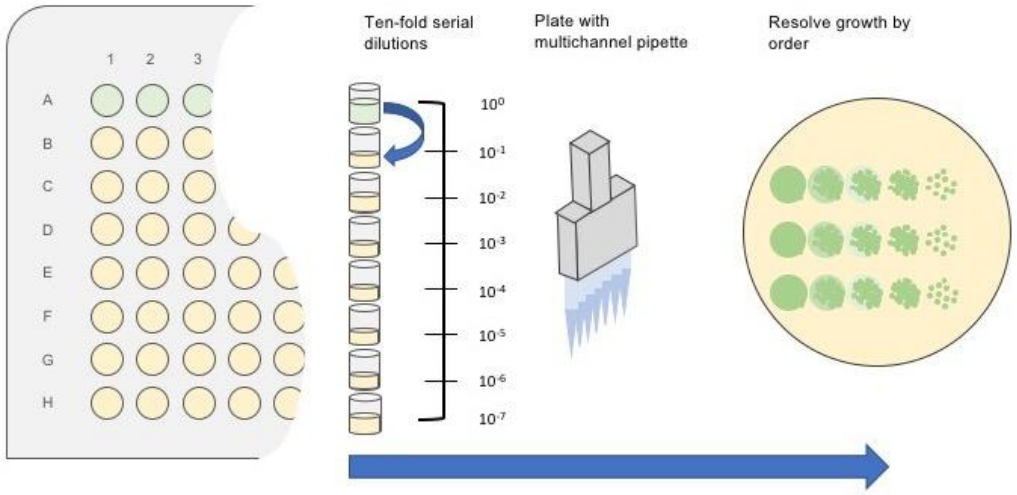

Figure 5.3: **Spot-plate method for viable plate counts.** This method was used to enumerate viable bacteria from a well-dispersed liquid culture. An aliquot of the sample to be interrogated was loaded (90 µL; green) into the top row of the microtiter plate; all subsequent rows were filled with 90 µL of sterile diluent. Serial dilutions were performed by mixing 10 µL from each well in row A to row B, followed by mixing via aspiration with the pipette. Ten-fold serial dilutions were continued to the extent desired in subsequent rows. Then, a multichannel pipettor was used to place a 10-µL spot for each dilution of interest on an agar plate. After incubation, CFU were counted for spots that contained 10-40 CFU, and CFU/mL of each original sample was calculated.

5.3.6 Quorum sensing induction

QS describes the process by which some bacteria (including *P. aeruginosa*) regulate gene expression based on cell density, and it is considered to be a global gene regulation system. Therefore, to isolate the transcriptomic and proteomic impact of exposure to AgNPs or $Ag_{(aq)}$, the bacterial concentration in those experiments must be below that required to induce QS. To verify that QS was not induced in the cultures used for transcriptomics and proteomics, *P. aeruginosa* PAO1 with a *lasB::gfp* reporter fusion was cultured in the chemostat (5.3.4). After reaching steady state, cell concentration was measured with the spot-plate method, and QS induction was queried with fluorescence microscopy and spectroscopy. As a control where QS was induced, *P. aeruginosa* PAO1

lasB::gfp was grown overnight on an LB agar plate and in LB broth. A 1-mL aliquot was removed from the chemostat and a full scrape with a loop hook was taken from the LB agar plate and suspended in phosphate buffered saline. Both aliquots were centrifuged at 5000 x g for 6 min and resuspended in phosphate buffered saline (PBS); the centrifugation and resuspension in PBS were repeated a second time. The resuspended cells were examined on a Nikon (Tokyo, Japan) 80i epifluorescence microscope equipped with a FITC filter (excitation at 480 nm and emission at 508 nm), and images were captured with the Nikon Elements© software. Aliquots of washed cells from the chemostat and batch control culture were transferred to a microtiter plate, and relative fluorescence units (RFU) and optical density at 600 nm (OD_{600}) were measured using a Synergy HT-I plate reader with a 485/20 nm excitation and a 530/25 nm emission filter combo (BioTek; Winooski, VT). The sensitivity for fluorescence measurements was set to 120 (no units).

5.3.7 Preparation of batch cultures for stress induction of *P. aeruginosa* with AgNPs and $Ag_{(aq)}$ for use in transcriptomic and proteomic analyses

To a 250-mL culture flask, 100 mL of MD medium and 1.5 mL of *P. aeruginosa* PAO1 chemostat culture were added; typically, 6-9 flasks were inoculated at once. The cultures were incubated for 7-9 hours at 35 ˚C with shaking. Cultures were checked periodically for OD_{600} in a Synergy HT-I plate reader (BioTek; Winooski, VT). Once reaching an OD_{600} of 0.047-0.054, corresponding to a bacterial density of $1x10^7$ CFU/mL, the cultures were composited in a sterile 1-L bottle. Then, a 50-mL aliquot of the composite sample was transferred to a sterile 50-mL polypropylene tube for exposure to AgNPs, $Ag_{(aq)}$ or no exposure control.

5.3.8 Determination of sublethal AgNP and $Ag_{(aq)}$ concentrations

To induce stress without killing substantial numbers of bacteria, sublethal concentrations of AgNPs and $Ag_{(aq)}$ were determined. To 50-mL composite cultures of *P. aeruginosa* in MD described in the previous section, AgNPs and $Ag_{(aq)}$ were dosed to obtain a range of final concentrations. In parallel, a no-Ag control was prepared. The cultures were inverted five times and incubated with shaking at 200 rpm at 35˚C for 30 min. Then, sodium thiosulfate (2.6 µg/L [final concentration]) was added to all cultures to quench the silver toxicity. Spot-plate counts were performed to confirm measure toxicity. Duplicate biological replicates were prepared for each condition and plated in triplicate technical replicates. Sodium thiosulfate was utilized because cysteine (commonly used quenching agent for silver in the literature) resulted in lower A_{260}/A_{280} ratios after RNA. Two technical replicates of six biological replicates were performed for each stressor (AgNP and $Ag_{(aq)}$) and the no-Ag control. The sublethal concentration was defined as the highest concentration of stressor that showed 99% cell survival.

5.3.9 Harvesting bacteria for transcriptomic analysis

Cells were prepared as described section 5.3.7 and exposed to sublethal doses of $Ag_{(aq)}$ and AgNPs as described in section 5.3.8. After quenching with sodium thiosulfate (2.6 µg/L [final concentration]), the cultures were filtered using 0.22-µm Millipore PVDF Durapore® filters and a Millipore 1225 vacuum sampling manifold (Billerica, MA), which was sterilized with ethanol prior to sample processing. After the liquid fraction of each sample was removed, the vacuum was paused, and 2 mL of RNAlater (Qiagen; Germantown, MD) was applied. The RNAlater was allowed to slowly percolate under minimal vacuum, as suggested by Qiagen technical support. Filters were removed from the

manifold with sterile tweezers and placed in 2-mL, RNase-free conical tubes. The filters were stored at -80˚C for at least 24 hours before further processing.

5.3.10 RNA extraction protocol

Prior to RNA extraction, all working surfaces and equipment involved in the extraction procedure were wiped with RNaseZAP! (ThermoFisher; Waltham, MA). The conical tubes (containing cells and filters) were removed from the -80˚C freezer and thawed on ice for 20 min. RNA extraction was performed with the Qiagen RNeasy kit (Qiagen; Germantown, MD). Minor changes were made to the manufacturer's protocol to facilitate RNA extraction from the filter surface, and the changes are summarized as follows. A 100-µL aliquot of 15 mg/mL lysozyme in TE buffer (10 mM Tris-Cl, 1 mM EDTA, pH 8.0) was added directly to the thawed filter tubes. These tubes were placed on a vortexer with a multi-tube adaptor and vortexed at a setting of 10 for 10 min. The tubes were attached horizontally to the vortexer with the filter on the underside of its tube, such that lysozyme was in constant contact with the filter surface. Following lysozyme incubation, the tubes were placed on ice for 5 min. A 350-µL aliquot of buffer RLT from the RNeasy kit was added to the filter tubes and vortexed at a setting of 7 for 10 s. After a 10-s 5000 x g centrifugation step to separate the liquid from the filter, the RLT/lysozyme mixture was transferred to a 2-mL, gasket-sealed bead-beating tube (Fisher Scientific; Waltham, MA). A 30- to 40-mg aliquot of lysis matrix "E" beads (MP Biomedicals; Santa Ana, CA) was added to each tube. The tubes were processed in a FastPrep©-25 Classic® homogenizer (MP Biomedicals; Santa Ana, CA) for 3 x 50 s, with 5 min on ice between homogenization steps. The tubes were centrifuged at 17000 x g and briefly rested on ice until the supernatant was transferred to a new RNase-free tube. A 220-µL aliquot of pure, undenatured ethanol was added to the supernatant. The tube was inverted/flicked five times, and then all liquid

was transferred to a quick spin column from the Qiagen RNeasy kit (Germantown, MD). From here, the manufacturer's RNeasy mini protocol for bacterial samples was followed. At the final step of the protocol, purified RNA was eluted with 20 µL of RNase-free water, and the eluate was passed through the column a second time to increase yield. RNA was quantified on a NanoDrop (ThermoFisher; Waltham, MA), and an A_{260}/A_{280} ratio of 1.8-2.2 was targeted. RNA quality was assessed by gel electrophoresis. RNA was stored at -80˚C until it was submitted to the University of Texas at Austin Genomic Sequencing and Analysis Facility for further processing and sequencing. There, rRNA was removed using the Ribo-Zero rRNA Removal Kit for Bacteria (Illumina; San Diego, CA). Library construction was completed using the Illumina TruSeq Stranded total RNA kit (Illumina; San Diego, CA), and sequencing was performed on a MiSeq 2000 (Illumina; San Diego, CA) using 250-bp, paired-end reads. Quality was assessed with a Bioanalyzer 2100 (Agilent; Santa Clara, CA) after RNA extraction and rRNA removal.

RNA sequence analysis

RNA sequence read quality was evaluated with fastQC (Andrews 2010). Transcriptome assembly was completed using the BowTie analysis pipeline (Langmead et al. 2012) and linked to the annotated *P. aeruginosa* genome (Stover et al. 2000). Further analysis was conducted with Matlab (Mathworks; Niatic, MA) using the bioinformatics toolbox® and the artificial intelligence and machine learning toolbox®. The sequence fragments were aligned to a reference genome (Wurtzel et al. 2012) in Bow Tie 1.2.2. Log_2-fold expression (Equation 4.2) was calculated for the average of six replicates in each condition referenced against the no-Ag control. Statistical analysis was performed in Excel using an ANOVA to find significant differences between the expression of genes exposed to $Ag_{(aq)}$, AgNPs and the no-Ag control. A 95% confidence interval was used to establish

significance. Principal component analysis (PCA) was completed in MATLAB. Log_2fold transcriptomic data for $Ag_{(aq)}$ and AgNP (relative to the no-Ag control) were reduced to a variance matrix. The minimum variance of the first two principal components was plotted. A hierarchical model was then applied to these data, which clustered the data into eight groups. The model used a top-down sort. Gene names were mapped onto the points so that the implication of the clusters could be analyzed.

Equation 5.2. $\log_2 Fold\ Expression = \log_2 \frac{A}{B}$

Where:

A is the experimental condition

B is the no-Ag control

5.3.11 Harvesting bacteria for proteomic analysis

Cells were prepared as described section 5.3.7 and exposed to sublethal doses of $Ag_{(aq)}$ and AgNPs as described in section 5.3.8. Proteomic samples were harvested centrifugally in 50-mL conical tubes. Cells were pelleted first in a bucket rotor centrifuge (Allegra X-15R and GH-3.8A bucket rotor; Beckman Coulter; Indianapolis, IN). Centrifugation was performed at 980 x g for 15 min at 20˚C, where slow acceleration and deceleration were used to aid pelleting. Next, all supernatant, except the final 2 mL, was carefully withdrawn from liquid surface of the tube with an electric 50-mL transfer pipet. The remaining 2 mL, including the pellet, were resuspended by 5-10 gentle finger taps to the tube. The resuspended pellet was transferred to a 2-mL microfuge tube and spun at 7000 x g for 15 min at 4˚C in a benchtop microfuge (Fisher; Waltham, MA). This two-step centrifugation process, and particularly the low temperature of the second centrifugation step, ensured high cell yield and formation of a firm pellet. Finally, the supernatant was

removed, and pellets were frozen in liquid nitrogen immediately. These samples were stored at -80˚C until protein extraction.

Protein extraction and sample preparation for proteomic analysis

For the harvested bacterial samples described in the previous section, protein was typically extracted for ten samples at a time. The samples were removed from the -80˚C freezer and thawed to 4˚C on ice. Lysis buffer was prepared fresh before each protein extraction. For 1 mL of lysis buffer (8 M urea, 30 mM NaCl, 5 mM $CaCl_2$, 50 mM Tris-HCL) 1 µL protease inhibitor cocktail [ThermoFisher; Waltham, MA]) was added. After 1 mL of lysis buffer was added to each sample, the samples were vortexed vigorously. Lysis was performed in four freeze-thaw cycles. Samples were frozen for 2 min in liquid nitrogen and then placed above a compacted bed of ice in a sample rack in an ice bucket at 25 ˚C such that air could circulate during the thaw while maintaining the samples at 4 ˚C. Thawed samples from the last cycle were centrifuged at 17,000 x g, and the supernatant of each sample was transferred to a fresh 2-mL microfuge tube.

Protein concentration was determined with a Bradford assay kit (Fisher Scientific; Waltham, MA), prior to storage of extracted samples. A protein concentration greater than 100 µg/mL was targeted to ensure sufficient material for proteomic analysis. The procedure suggested by the manufacturer was modified as follows. The Bradford reagent was equilibrated to 25˚C in the dark. A 344.6-µL aliquot of this reagent was mixed with 15.4 µL of extracted protein and allowed to react for 10 min at 25˚C in the dark. From this point forward, the manufacturer's standard protocol was followed. Protein concentration was determined by absorbance at 546 nm using a Synergy HT-I (BioTek; Winooski, VT) microtiter plate reader. A standard curve (0, 10, 100 and 250 µg/L) was prepared with

bovine serum albumin (Sigma Aldrich; St. Louis, MO). Protein extracts were stored for 2 months at -20˚C.

All protein extracts were processed for mass spectrometry peptide characterization at the same time. Samples were thawed on ice, and an aliquot of each sample was transferred into a fresh tube containing approximately 100 µg total protein. For every 100 µL of lysate used, 5 µL of dithiothreitol (DTT; 100 mM stock) was added. The overall mixture was incubated for an hour in the dark. Following incubation, 3.5 µL of iodoacetamide (IAA, 500 mM) was added for every 100 µL of lysate to alkylate the sample. Urea was diluted to 1.5 M with Buffer T (50 mM Tris, and 5 mM $CaCl_2$ buffered at pH of 8) following alkylation to achieve a final urea concentration of 1.5 M, and protein lysate was digested overnight (15 h) at 37˚C with trypsin (MassSpec Gold; Promega, Madison, WI). The digestion was quenched with 50 µL 0.1% formic acid and frozen at -80 ˚C until submission to the Proteomics Facility at the University of Texas at Austin.

The remainder of the preparation was conducted at the core. Briefly, samples were desalted with Ziptips™ (EMD Millipore, Temecula, California) and freeze-dried. Samples were analyzed with a quad-orbital-trap-matrix-assisted-laser-desorption ionization (MALDI)-mass spectrum analyzer (Thermo Orbitrap Fusion hybrid-mass-spectrometer with quadrupole linear ion traps and orbitrap detectors; ThermoFisher Scientific; Waltham, MA); the instrument was coupled with an Ultimate 3000 RSLCnano for nanoflow ultra high-pressure liquid chromatography separation.

Analysis

The peptide data were analyzed using Proteome Discoverer 2.0 (ThermoFisher Scientific), MASCOT (MatrixScience, Boston, MA) and X!tandem database search algorithms on the Stampede Supercomputer at the University of Texas Advanced

Computing Center. Peptide identification was performed with Skyline (McCross Labs). Protein counts were output and analyzed using the Matlab bioinformatics toolbox®.

5.4 Results and Discussion

5.4.1 Physical characteristics of AgNPs used in this study

AgNPs used in this work were suspended in MD medium at an ionic strength of 40 mM approximately equivalent to the Mμ0 exposure solution described in Table 3.1. This condition stabilizes the particles and minimizes their dissolution as compared to media with higher ionic strength (140 mM) and/or destabilizing ligands (e.g., chloride) (Chambers et al. 2014, Chapter 3). Dissolution of AgNPs at a 1 mg/L concentration measured in Chapter 3 at conditions similar to those used in this study resulted in a 13 μg/L release of total $Ag_{(aq)}$, which was statistically indistinguishable from the release of 10 μg/L Ag^+ in the Lμ0 exposure solution (Table 2.1) The particles were completely stable over 5 h. Further, exposure in a medium ionic strength buffer promoted the formation of branched fractal aggregates (Figure 3.3) that had a constant aggregate diameter (data not shown) over the duration of the experiment. Formation of the branched aggregate increased AgNP toxicity (Figure 3.4) as compared to less branched aggregates (Lμ0) and increased the expression of the stress response system *katE* (Figure 3.6). In summary, the medium ionic strength condition utilized in this chapter promoted conditions that preserved nanocharacteristics of the AgNPs.

Furthermore, $Ag_{(aq)}$ that was released from AgNPs under the conditions utilized in this chapter was likely present primarily in the Ag^+ form due to limited ligand availability. Therefore, under the chemistry conditions chosen in this chapter, the biological response to AgNPs was likely attributable primarily to the nanoparticle form rather than the $Ag_{(aq)}$ form. Additionally, the sublethal AgNP and $Ag_{(aq)}$ concentrations chosen for this chapter

would not stimulate transcription of global stress response systems like RpoS, which would indicate overloading of the bacterial stress response.

5.4.2 Quorum sensing controlled gene induction

As discussed in Chapter 4, QS was not induced in *P. aeruginosa* at the cell concentration used in the stress induction experiments (1 x 10^7 CFU/mL) (Figure 4.4). Therefore, QS did not confound the interpretation of the transcriptomic and proteomic data from the stress induction experiments.

5.4.3 Determination of sublethal $Ag_{(aq)}$ and AgNP concentrations

As discussed in Chapter 4, the sublethal doses of $Ag_{(aq)}$ and AgNPs were determined for subsequent use in the stress induction experiments. The sublethal dose is 0.08 µg/L for $Ag_{(aq)}$ (Figure 4.5) and 1 µg/L for AgNPs (Figure 4.5).

5.4.4 Transcriptomic analysis of *P. aeruginosa* exposed to $Ag_{(aq)}$ or AgNPs

The expression of antibiotic stress response systems was examined for *P. aeruginosa* exposed to $Ag_{(aq)}$ or AgNPs relative to the no-Ag control. The overall patterns of gene expression were highly similar between bacteria exposed to $Ag_{(aq)}$ and bacteria exposed to AgNPs (Figure 5.4). This result was expected given that the mechanisms of action of $Ag_{(aq)}$ and AgNPs overlap. In particular, both $Ag_{(aq)}$ and AgNPs are linked to mechanisms of action that disrupt protein folding, cell envelope integrity, and DNA replication (Nies 1999; Morones et al. 2005; Lok et al. 2007). However, some key differences between the response of cells exposed to $Ag_{(aq)}$ and cells exposed to AgNPs exist. As shown in Chapter 4, the expression of specific metal toxicity pathways, namely copper mitigation pathways (Figure 4.5) and the metal efflux system *czcABC* (Figure 4.7) were induced by AgNPs, and expression of metal efflux system *muxABC* was induced by

$Ag_{(aq)}$. These data suggest that AgNP stress was localized to the cellular surface and that $Ag_{(aq)}$ stress was localized to the cytoplasm.

Induction of stress response systems related to antibiotics showed similarity between AgNP and $Ag_{(aq)}$ exposure. Bacteria exposed to $Ag_{(aq)}$ and AgNPs showed increased expression of RND multidrug efflux genes as compared to the no-Ag control (Figure 5.4). The overall expression of RND efflux genes was greater in AgNP-exposed bacteria as compared to $Ag_{(aq)}$-exposed bacteria. DNA repair responses were down-regulated (Figure 5.4) for both stressors relative to the no-Ag control. This might indicate that metal-directed stress has the potential to limit DNA repair; this could increase mutagenicity because exposed bases are under higher stress during transcription (Jinks-Robertson et al. 2014). In total, both $Ag_{(aq)}$ and AgNPs cause similar expression patterns, which links their mechanistic behavior. Using the hierarchical model of $Ag_{(aq)}$ and AgNP gene induction, key RND efflux stress response pathways were examined in detail, using their expression to build a potential unifying model of metal-induced antibiotic resistance.

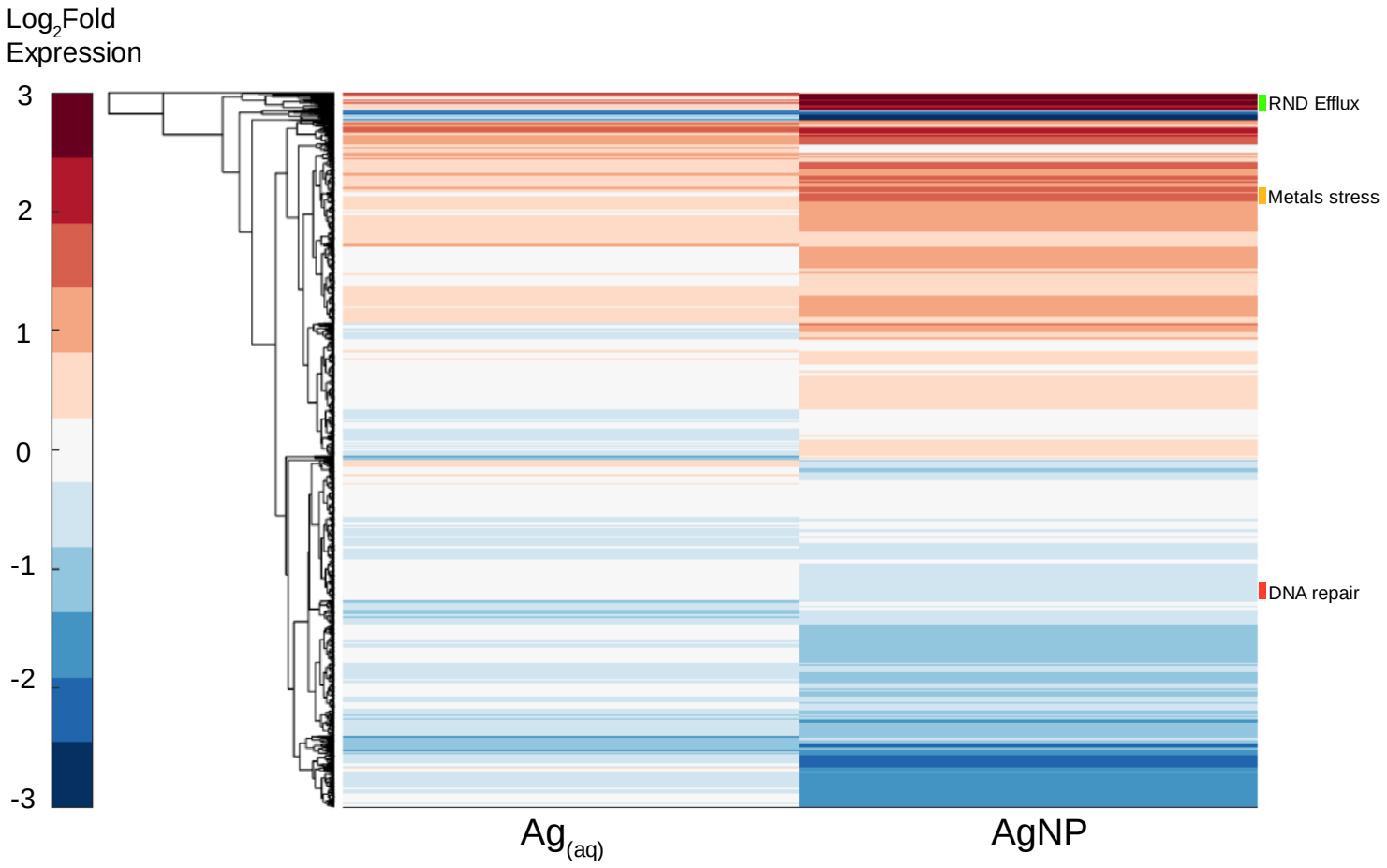

Figure 5.4. **Hierarchical cluster analysis of *P. aeruginosa* transcriptomic response to $Ag_{(aq)}$ and AgNPs**. *Log_2 transform of normalized transcript counts relative to no-Ag control transcript counts are presented. Regions of interest are denoted to the right of the figure. Transcriptomes are the average of six biological replicates.*

5.4.5 General Stress induction

It should be noted that no induction of global stress response regulators was observed in the transcriptomic analyses; specifically induction of RpoS, the global stress response regulator indicating a general cell wide stress condition (Storz 2012), was not observed. Rather, bacteria were exhibiting active transcription of stress systems to overcome the stress.

Transcription of RND efflux pumps is induced by $Ag_{(aq)}$ and AgNPs

As compared to the no-Ag control, exposure of *P. aeruginosa* to $Ag_{(aq)}$ or AgNPs was found to significantly increase the expression of antibiotic efflux genes and a subset of specific antibiotic resistance genes. The efflux systems were often of the RND efflux pump family, which is a diverse group of efflux pumps found in Bacteria and Archaea. Pumps of the RND family, typically classified as multidrug efflux pumps (MEPs; e.g., *mex*, *mux*) in *Pseudomonas*, export a range of targets including metals, polycyclic aromatic compounds, and antibiotics (Tseng et al. 1999; ; Piddock 2006; Alvarez-Ortega et al. 2013). It is therefore likely that regulatory systems controlling the expression of MEPs in *P. aeruginosa* are activated by metals (Baker-Austin et al. 2006) and the chemical species (e.g., ROS) associated with their toxicity (D. Nies 2003).

$Ag_{(aq)}$ induces expression of three RND efflux pumps of the* mex *family

Three multidrug efflux systems, capable of exporting a range of antibiotics, were induced by exposure to a sublethal dosage (0.08 µg/L) of $Ag_{(aq)}$ (Figure 5.5), MexAB, MexXY, and MuxABC. Antibiotic targets of the *mexAB* system include quinolones, macrolides, and tetracyclines. The second system, *mexXY* is most closely associated with aminoglycoside resistance but also is linked to quinolone resistance (Poole et al. 1993; Masuda et al. 2000; Yoneda et al. 2005). The induction of these two systems due to

exposure to $Ag_{(aq)}$ might prime *P. aeruginosa* for resistance to these specific antibiotics. Interestingly, the regulation of these two systems is not directed by antibiotics alone. Rather, several small molecules and other chemicals affect their expression, including acyl-homoserine lactones (e.g., QS signals) (Maseda et al. 2004) and oxidants (e.g., H_2O_2) (H. Chen et al. 2008). Thus, a diverse array of chemicals exerts control over the *mexAB* and *mexXY* systems, and, in particular, the data in Figure 5.5 suggest that *mexAB* and *mexXY* are linked to metal stress mitigation.

Central in the regulation of *mexAB* is the oxidation-sensing *mexR* (H. Chen et al. 2008). The increased expression of *mexAB* by $Ag_{(aq)}$ can be explained through two potential mechanisms. First, $Ag_{(aq)}$ oxidation of exposed cysteine residues within outward-facing alpha helices of the regulatory protein MexR could block DNA interactions of MexR and stop negative regulation of MexAB (Jacob et al. 2003; McNeil et al. 2015). The oxidation of exposed cysteine residues by $Ag_{(aq)}$ could occur directly through an SN_2 pathway resulting in a silver-cysteine adduct (Giles et al. 2003; Jacob et al. 2003; Lok et al. 2007) or indirectly through the potential formation of a thiolate species after which rearrangement and formation of a disulfide bond occurs (Giles et al. 2003). In both cases the negative regulator, MexR, would now be incapable of binding DNA, and thus, increased expression of *mexAB* would be expected. Second, $Ag_{(aq)}$ can react with glutathione and stimulate the generation of peroxide through a bisglutathione intermediate (Nies 1999; Kachur et al. 1998); subsequent interaction of this peroxide with sensory protein MexR, a negative *mexAB* regulator (H. Chen et al. 2008), can increase expression of *mexAB* by promoting an inactive conformation of MexR (D'Autréaux et al. 2007; Chen et al. 2008; Alvarez-Ortega et al. 2013)

The *mexXY* system is induced in *P. aeruginosa* by exposure to $Ag_{(aq)}$ (Figure 5.5B). The *mexXY* system has previously been linked to cytoplasmic membrane stress and the

activation of protein misfolding regulators. Induction of the *mexXY* multidrug efflux system is linked to two regulatory systems, *amgRS* and *armZ/mexZ*, both of which detect misfolded proteins at the cytoplasmic membrane (Hay et al. 2013; Lau et al. 2015). Relatedly, $Ag_{(aq)}$ has the potential to interact with exposed cysteine groups in proteins to form adducts, which can lead to protein misfolding and loss of function (Nies 1999; Kittler et al. 2010; Lok et al. 2007). Transcriptional analysis showed the impact of $Ag_{(aq)}$ on the inner face of the cytoplasmic membrane (Chapter 4) where metabolic enzymes are located. Metal stress, including silver, causing protein misfolding could occur with key metabolic enzymes located near the cytoplasmic membrane and cause a short circuiting of energy production in the cell (Nies 1999; Giedroc et al. 2007; Storz et al. 2011;). In agreement with this model is the expression of an inner face of the cytoplasmic membrane/periplasmic misfolding repair system *dsbAB* (disulfide-bridge repair) capable of repairing incorrectly crosslinked proteins (Łasica et al. 2007). Interestingly, the expression of additional stress response systems is co-regulated by members of the Dsb family and Mgr, of which *mexR* is a member (Cardenal-Muñoz et al. 2013). Expression of *dsbA* and *dsbB* was increased under $Ag_{(aq)}$ stress (data not shown), highlighting a potential co-regulatory network that might exist between the expression of *mexXY* and *mexAB*. Additionally, the regulator MexZ, is part of the TetR family of regulators, which are known to bind copper; thus, similar to the MexR silver adduct formation mechanism, $Ag_{(aq)}$ also might interrupt *mexZ* DNA binding.

Lastly, the expression of *muxABC*, which encodes an MEP, was increased in response to a sublethal $Ag_{(aq)}$ dosage (Figure 5.5C); AgNPs also induced the expression of *muxABC* but not to the same degree as did $Ag_{(aq)}$. *muxABC* is linked to the efflux of quinolones in addition to some aminoglycosides and tetracyclines (Mima et al. 2009; Li et al. 2016). The induction of *muxABC* has recently been linked to *cxpR* and *nalD*, which both

are regulators of the *mexAB* system (Tian et al. 2016). Of the two regulators, *nalD* is included in the TetR family of regulators (Morita et al. 2006); similar to *mexZ*, it could potentially undergo modification and binding by $Ag_{(aq)}$ through oxidation of cysteine groups (Cuthbertson et al. 2013), changing is ability to bind DNA and therefore its regulation of the *mux* and *mexAB* operons. The second potential regulator of the *mux* system, CpxR, is a cell envelope stress response system similar to *amgRS*. *cpxR* is linked to misfolded protein stress (Storz et al. 2000; Wassarman et al. 2011; Raivio et al. 2013) and is located in the cytoplasm of *P. aeruginosa* (Winsor et al. 2016). The expression of *cpxR* has been directly linked to copper-stimulated induction and to imipenem resistance (Perron et al. 2004; Caille et al. 2007). Activation of this same response system by $Ag_{(aq)}$ is possible given the overlapping chemistry of copper and silver (Nies 1999). Thus, all of the major MEP systems induced by $Ag_{(aq)}$ share a common pattern: they have one component of a modifiable TetR family regulator, and have overlapping response with the *mexAB* system.

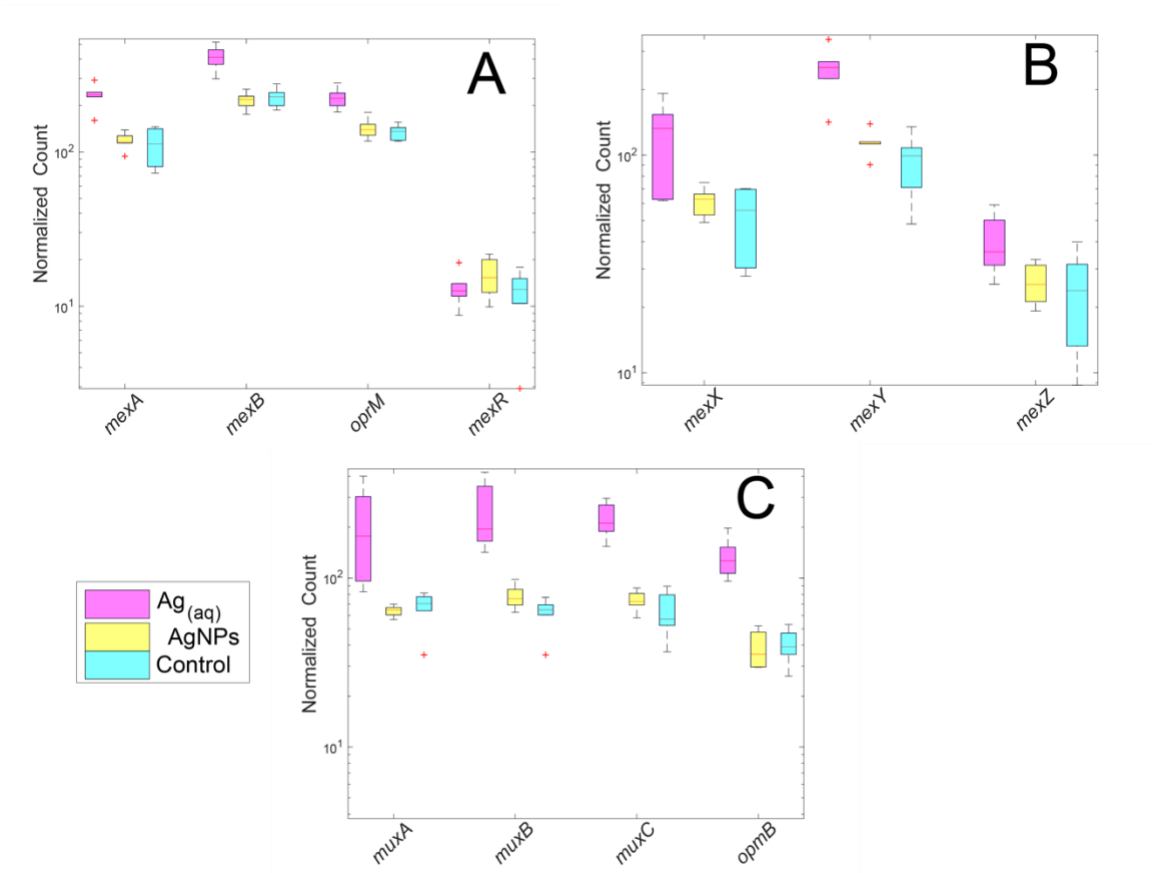

Figure 5.5. **Normalized transcription counts of selected MEPs in *P. aeruginosa*.** Genes encoding three RND MEPs showed increased transcription after 30 min of exposure to $Ag_{(aq)}$ at a sublethal (0.08 µg/L) dosage: a) *mexAB* and related genes) *mexXY and regulator mexZ* c) *muxABC* and related genes. Data are the average of six biological replicates, and boxplots represent the median and first quartile.

5.4.6 AgNPs induce two RND efflux pumps

AgNPs, though made of silver, likely impact *P. aeruginosa* through a different model of interaction than does $Ag_{(aq)}$ (Chapter 4). While $Ag_{(aq)}$ enters the cytoplasm and tends to elicit an intracellular response, AgNPs are more localized to the cell surface (Sondi et al. 2004; Morones et al. 2005; Julia Fabrega et al. 2009) and exert stress in the periplasm and at the cytoplasmic membrane (Chapter 4). This cell envelope stress is similar to the

action of antibiotics acting at the cell envelope might induce the expression of MEPs and thereby increase antibiotic resistance (Tseng et al. 1999; Baker-Austin et al. 2006; Alvarez-Ortega et al. 2013). Exposure of *P. aeruginosa* to AgNPs was found to increase expression of two antibiotic resistance MEP systems: *mexGHI* and *mexPQ* (Figure 5.6A and B, respectively). Both systems are relatively uncharacterized, but it is known that both of them efflux macrolides, quinolones, and some aminoglycosides (Li et al. 2004; Li et al. 2016). Interestingly, both systems are linked to metal stress response, with *mexGHI* being associated with vanadium stress mitigation (Séverine et al. 2002) and *mexPQ* with copper stress mitigation (Thaden et al. 2010). AgNPs periplasmic stress is caused by metal dissolution (Figure 4.6); this connects the mechanism of action of AgNPs to antibiotic resistance through overlap with metal stress regulators. It is thought that the *mexPQ* system is regulated by a CueR homolog in *P. aeruginosa.* (Thaden et al. 2010), which uses a sulfur-oxidation based sensory system (Macomber et al. 2009; Dupont et al. 2011) that is similar to peroxide sensory systems in MexR. The presence of a sulfur-oxidation based sensory system is further evidence that antibiotic and metal stress systems are generally connected via oxidation regulation.

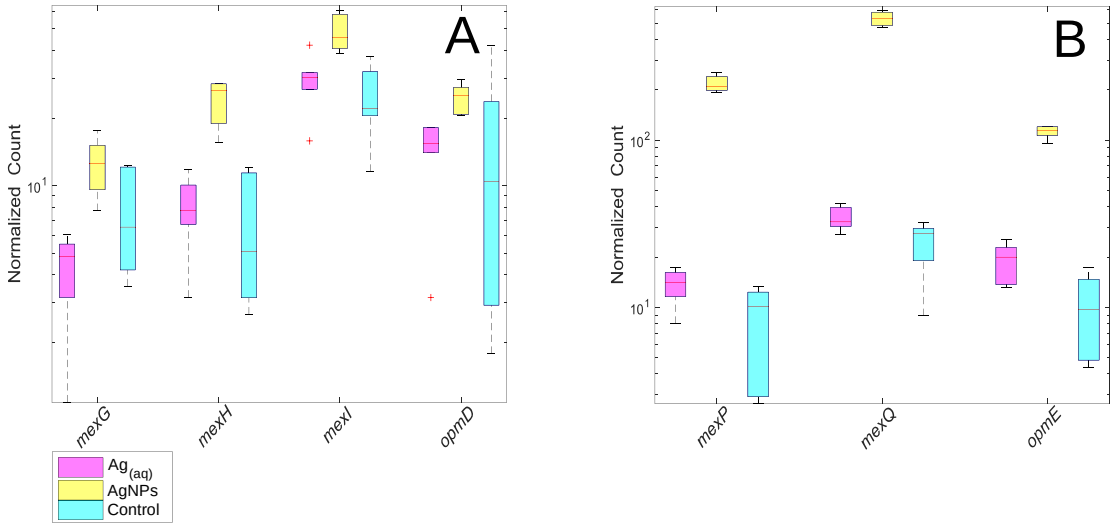

Figure 5.6. **Normalized transcription counts of selected MEPs in *P. aeruginosa*.** Two RND MEPs responding with increased transcription after 30 min of exposure to AgNPs at a sublethal (1 µg/L) dosage: a) *mexGHI* and related genes b) *mexPQ* and related genes. Data are the average of six biological replicates, and boxplots represent the median and first quartile.

In addition to inducing the expression of general stress response systems like MEPs, sublethal exposure to AgNPs and $Ag_{(aq)}$ also was linked to increases in transcription of two specific antibiotic resistance systems (Figure 5.7). Expression of the RND efflux system *triABC* was induced only by exposure to sublethal concentrations of AgNPs (Figure 5.7A). This system includes a more recently identified RND efflux pump in *P. aeruginosa* that responds almost entirely to triclosan stress and is therefore categorized as a specific antibiotic stress responder, despite being linked to the detergent sodium dodecyl sulfate (SDS; Mima et al. 2007; Castranova et al. 2016). Induction of this system mitigates outer membrane and periplasmic stress, which corroborates the surface-attachment model of interaction between AgNPs and bacteria as proposed in Chapter 4.

In addition, a newly discovered aminoglycoside response system regulated by the sensory system *amgRS* was induced by $Ag_{(aq)}$ and AgNP exposure (Figure 5.7B). The

amgRS system detects surface stress through reduced porin expression and misfolded proteins (Krahn et al. 2012; Lau et al. 2013; C. H. F. Lau et al. 2015). This links directly to the expression of the generalized stress response system *mexXY* (Figure 5.5C), which co-regulates the *amgRS*-associated stress response system (Lau et al. 2015). Again, this supports a model where AgNP and antibiotic stress is generalized by global stress regulators sensing membrane disruption and oxidative stress. This broad response allows a cell to defend against antibiotics and metal stress simultaneously.

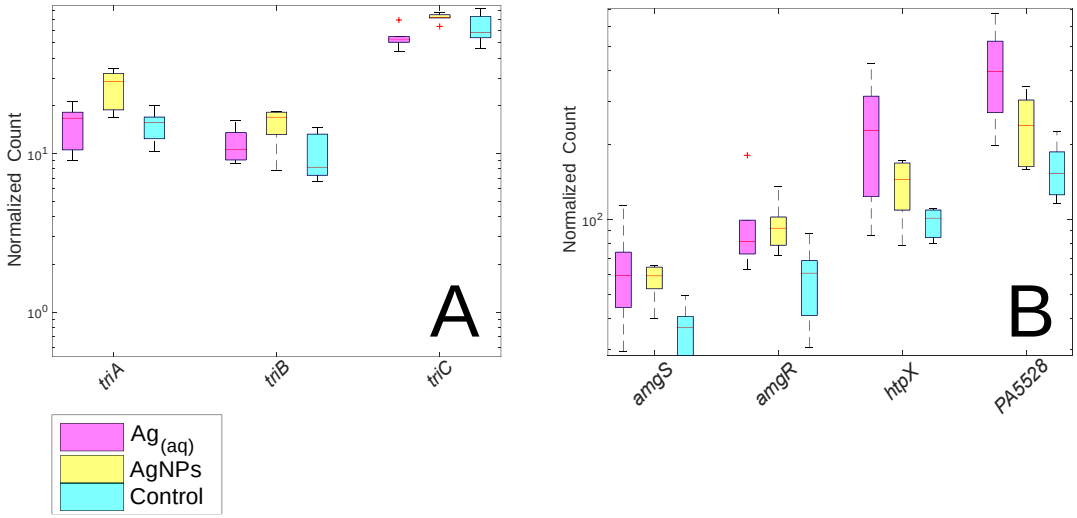

Figure 5.7. **Normalized transcription counts of selected specific antibiotic resistance genes in *P. aeruginosa*.** Antibiotic resistance genes respond with increased transcription after 30 min of exposure to AgNPs and $Ag_{(aq)}$ at a sublethal (0.08 µg/L) dosage: a) the triclosan resistance RND pump, *triABC* b) the aminoglycoside response system, sensory system *amgRS* with effector genes *htpX* and PA5528. Data are the average of six biological replicates, and boxplots represent the median and first quartile.

5.4.7 AgNPs and $Ag_{(aq)}$ results in peptide synthesis of key antibiotic resistance determinants

Proteomic studies often do not correlate well with transcriptomic data (Maier et al. 2009; Taniguchi et al. 2011). Transcriptomic data are a representation of what possible regulatory decisions are in process, but the majority of transcripts are never made into

protein. Therefore, proteomic data more closely represent the enzymatic capabilities of the cell. Consistent with transcriptomic analysis (Figure 5.5, Figure 5.6, Figure 5.7), proteomic analysis of *P. aeruginosa's* response to sublethal dosages of $Ag_{(aq)}$ or AgNPs showed that cells increased their translation of antibiotic resistance proteins (Figure 5.8). For example, outer-membrane porins OprD and OprB (Wylie et al. 1995; X. Z. Li et al. 1997) were downregulated due to $Ag_{(aq)}$ and AgNP stress (Figure 5.8), likely decreasing the flux of metal and antibiotic stressors into the cell (Wylie et al. 1995; Perron et al. 2004). Porins are associated with the influx of antibiotics into bacterial cells, and their down-regulation represents a significant action to decrease antibiotic susceptibility (Wylie et al. 1995; Delcour 2009). In addition to this general response, the translation of four particular antibiotic resistance proteins was evident from proteomic analysis, discussed as follows.

Production of the aminoglycoside stress response sensor AmgR was significantly increased in the presence of $Ag_{(aq)}$ and AgNPs. This maps well to the transcriptomic results related to AmgR-regulated pathways, *mexAB (*Figure 5.5A), *mexXY (*Figure 5.5B), and the *amgRS* response gene group (Figure 5.7). In similar fashion, production of MexA was substantially increased in the presence of $Ag_{(aq)}$, confirming that these two independent drug efflux systems are upregulated. Additionally, the production of penicillin-binding protein B (Waxman et al. 1983; Farra et al. 2008) was increased in the presence of $Ag_{(aq)}$ stress, and the production of the polymyxin response protein ArnA (Williams et al. 2005) was increased as a result of both $Ag_{(aq)}$ and AgNP stress. Taken together, these data illustrate that AgNPs and $Ag_{(aq)}$ stimulate the synthesis of proteins related to antibiotic resistance, though it is unknown if these proteins are in an active state.

In total, proteomic data confirm portions of the biomolecular model developed via transcriptomic analysis. The up-regulation and translation of key antibiotic resistance systems including the major regulator AmgRS (as well as the MexAB system), the up-

regulation and translation of specific antibiotic resistance stress response system ArnA, and the decreased translation of porins illustrate that the bacteria are attempting to export stressors, targeting a specific stress response linked to membrane stress, and generally decreasing the influx of stressors. A summary of the antibiotic stress response systems induced by exposure to AgNPs or $Ag_{(aq)}$ is given in Figure 5.9. The lack of discovery of additional systems involved in the response to AgNPs and $Ag_{(aq)}$ in the proteomic data set (as compared to the transcriptomic data set) is likely a result of increased noise in proteomic studies because the mass spectrum analysis used to generate the proteomic data is more limited as compared to the capabilities of RNAseq (Sidoli et al. 2017). However, the proteomic data provide additional evidence of cross-resistance between $Ag_{(aq)}$/AgNPs and antibiotics in *P. aeruginosa*.

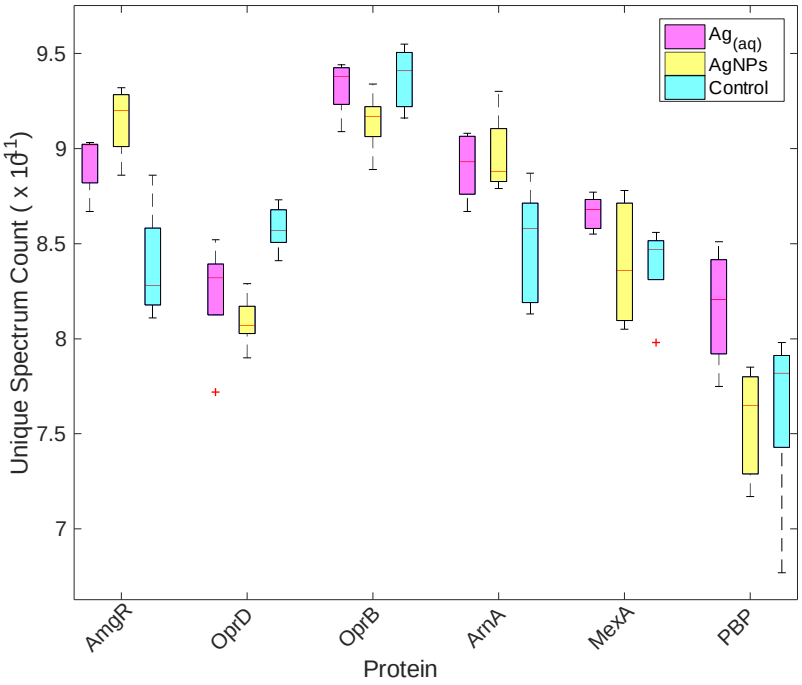

Figure 5.8. **Total unique spectrum counts of antibiotic resistance gene clusters in *P. aeruginosa*.** Production of antibiotic resistance proteins increases after 30 min of exposure to $Ag_{(aq)}$ and AgNPs at a sublethal (0.08 and 1 µg/L, respectively) dosage. Data are the average of five biological replicates, and boxplots represent the median and first quartile.

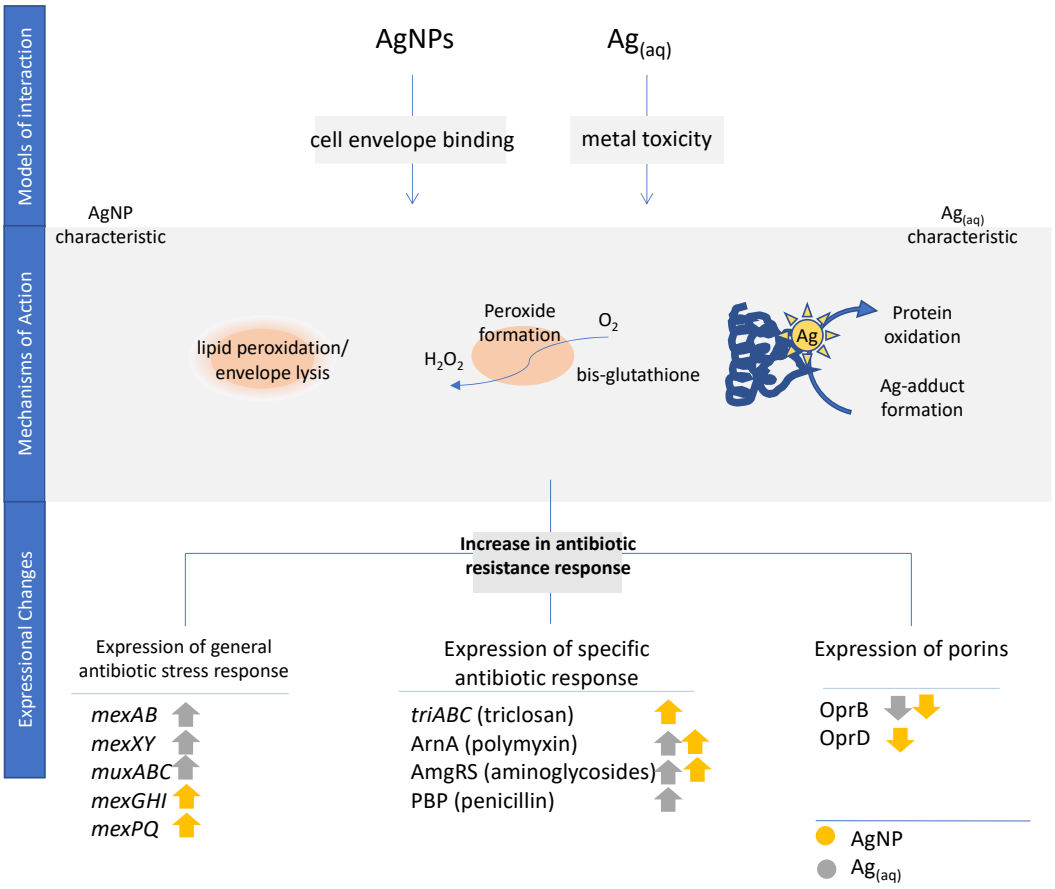

Figure 5.9 **Summary of antibiotic resistance systems induced by exposure to $Ag_{(aq)}$ or AgNPs.** The model of interaction between $Ag_{(aq)}$ or AgNPs and bacteria and the major mechanisms of toxicity of $Ag_{(aq)}$ and AgNPs toward bacteria are provided. The mechanisms of $Ag_{(aq)}$ toxicity overlap with those of AgNPs (e.g., oxidative stress, misfolding); while th ey are representative of $Ag_{(aq)}$ toxicity, they might also indicate toxicity of intact AgNPs.

5.4.8 DNA repair systems are down-regulated in response to $Ag_{(aq)}$ and AgNP stress, likely increasing mutational frequency and adaptability to stress

DNA repair systems limit the extent to which mutations accumulate in organisms as a result of errors in DNA replication. Two major DNA repair systems are down-regulated due AgNP exposure: the recombination repair system Rec (A Kuzminov 1999), and the mismatch repair system Mut (Marinus 2012) (Figure 5.10). Both systems act to

preserve the fidelity of DNA during periods of replication. The Rec system excises incorrect bases from the new strand, using the old strand as a template and has the potential to integrate DNA from an additional strand (Kuzminov 1999). The Rec system is a multicomponent DNA repair system that has more than 18 components including constituents A-R, some of which are duplicates (such as the exonuclease components RecJ and F) while others are essential parts of the main system and participate in bridging and linking damaged DNA (Andrei Kuzminov 1994; A Kuzminov 1999); not all parts are necessary during a given repair, but all Rec proteins are part of the complete Rec repair system. The Mut system fills gaps in DNA using methylated strands to identify the older, correct, parent strand. Several genes showed differential expression after AgNP treatment as compared to the no-Ag control. Four genes in the Rec system were down-regulated as a result of AgNP stress, but $Ag_{(aq)}$ stress produced no major changes in *rec* transcription. AgNP exposure also down-regulated the expression of two genes in the Mut stress response system. There is evidence that under sublethal stress conditions, mutational stress response systems, specifically Mut, are downregulated to increase mutational frequency (Andersson et al. 2014). Both of these systems were down-regulated as a result of AgNP stress, potentially as a result of energy losses due to electron transport chain malfunction deriving from periplasmic stress (Chapter 4); loss of energy might put the cell in a weakened state incapable of replicating DNA immediately. In some cases, when cells are under higher stress, they can also increase mutational rates as a means of creating an offspring with a genetic advantage as a means of increasing survival (Galhardo et al. 2007). The reduced expression of mutational repair might indicate a shift in bacterial survival strategy during AgNP stress, leading to increased mutational frequency from which higher variability and therefore increased survivability might derive (Galhardo et al. 2007; Moore et al. 2017).

Evolutionary selection is traditionally thought to act linearly through direct pressure on a specific trait. At some time, an event occurs allowing only those organisms with the best characteristics to overcome and survive a new stress, thereby resulting in natural selection (Darwin 1859). These changes occur as a result of genetic mutation and interaction with selective pressures in the environment (Dawkins 1968). While the premise is still very much true, the process is more complicated; it has recently been discovered that regions undergoing active transcription are more prone to mutation than are regions of DNA that are not transcriptionally active (Poveda et al. 2010; Jinks-Robertson et al. 2014). This increased mutational frequency is caused by the presence of transcriptional equipment in regions of active DNA transcription, where the transcriptional equipment forces exposed bases into a harsher chemical environment resulting from stressor exposures. Selective pressure might be focused on causing mutations in non-coding regions more frequently (Knibbe et al. 2007) meaning that changes in regulation rather than changes in functionality of the gene products are sufficient to develop bacterial tolerance or resistance to the selective pressure. Thus, given the down-regulation of DNA repair mechanisms in *P. aeruginosa* exposed to $Ag_{(aq)}$ or AgNPs (Figure 5.10) and the increased transcription of MEPs described above, the emergence of increasingly antibiotic-resistant *P. aeruginosa* is possible.

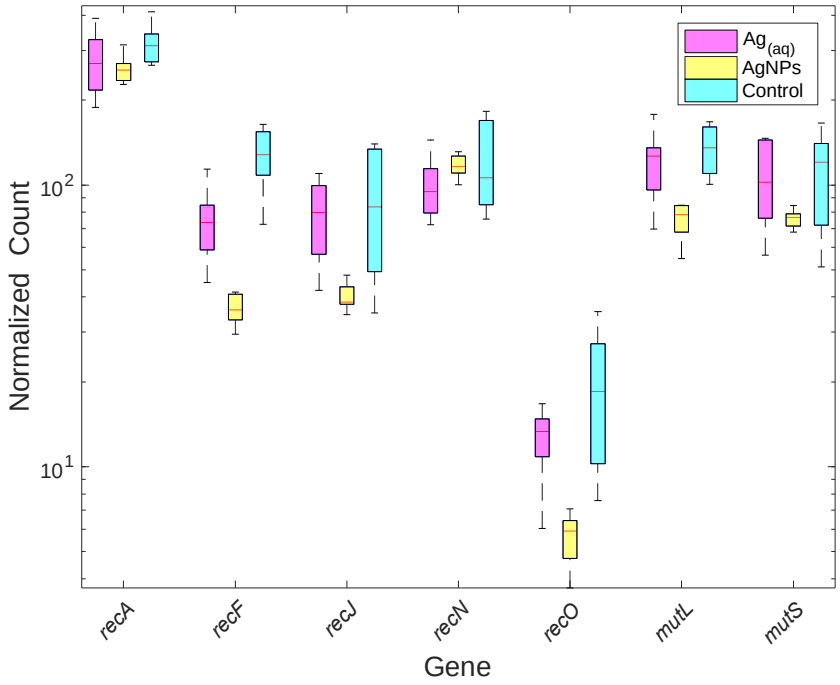

Figure 5.10. **Normalized transcription counts of DNA repair gene clusters *recA-O and associated genes* and *mutLS* in *P. aeruginosa*.** Transcriptional response was measured after 30 min of exposure to $Ag_{(aq)}$ and AgNPs at a sublethal (0.08 and 1 µg/L, respectively) dosage. Data are the average of six biological replicates, and boxplots represent the median and first quartile.

5.5 Conclusion and Summary

Two series of hypotheses were investigated in Chapter 5 regarding the potential for antibiotic resistance as a result of exposure to $Ag_{(aq)}$ or AgNPs. The first series of hypotheses focused on the potential for antibiotic resistance to develop from stress induced by bacterial-AgNP interaction and the associated ROS and periplasmic stress (Figure 4.8). This series of hypotheses focused on antibiotics that acted on the bacterial envelope (e.g., penicillins and polymyxin) and produced ROS by-products (e.g., aminoglycosides). However, the data did not support increased resistance to antibiotics acting on the bacterial envelope. Interestingly, the data did illustrate that resistance to antibiotics acting on the

bacteria envelope was greater in bacteria exposed to $Ag_{(aq)}$ (Figure 5.8) Exposure to AgNPs increased potential antibiotic resistance to three classes of antibiotics including aminoglycosides, macrolides, and quinolones through expression MEPs MexPQ and GHI (Figure 5.6). Aminoglycoside resistance is directed by ROS generation, confirming part of the mechanism observed in Chapter 3. AgNPs unexpectedly decreased expression of DNA repair systems RecA-R and MutLS (Figure 5.10), which has the potential to increase mutagenic processes. Porin expression also was down-regulated (Figure 5.8) potentially decreasing influx of antibiotics associated with OmpD. The second series of hypotheses examined the potential for antibiotic resistance to develop after exposure to $Ag_{(aq)}$ derived from cytoplasmic stresses such as protein misfolding stress and DNA stress (Figure 5.1). Bacterial exposure to $Ag_{(aq)}$ increased potential antibiotic resistance to five classes of drugs including aminoglycosides, macrolides, quinolones, tetracyclines, and penicillins (Figure 5.5 and Figure 5.8). Resistance to these antibiotics was stimulated through induction of regulators AmgR and oxidative sensing stress response system MexR. Interestingly, resistance to penicillins was stimulated by exposure to $Ag_{(aq)}$ (Figure 5.8), which was predicted to result from AgNP periplasmic stress (Figure 5.1 and Figure 4.7) but not predicted to result from $Ag_{(aq)}$ stress. Another interesting result was that DNA stress was observed with AgNP exposure but not $Ag_{(aq)}$ exposure. A summary of these results is shown in Figure 5.11.

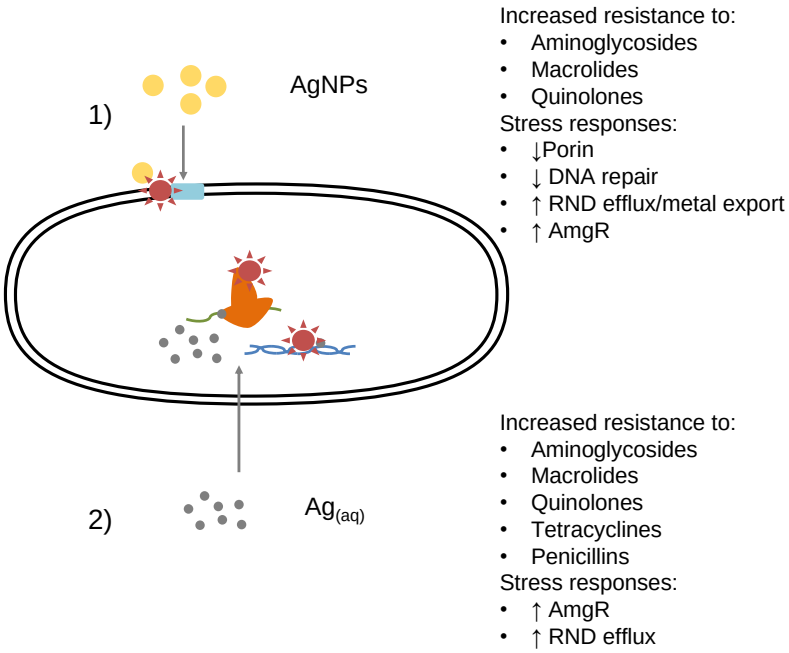

Figure 5.11 **Summary of potential antibiotic resistance resulting from exposure to 1) AgNPs and 2) $Ag_{(aq)}$ relative to the no-Ag control.**

A general pattern emerged across all interrogated systems (e.g., MexAB, MexXY, MexGH, MexPQ): all stimulated gene clusters had regulators that were linked to one of two methods of cross-resistance: (1) bacterial envelope disruption detected by protein misfolding (e.g., *mexAB, mexXY, muxABC, mexGHI, mexPQ)* or (2) oxidation of exposed cysteine residues in oxidation-sensing proteins of the MgrR and TetR families (e.g., *mexAB, mexGHI, mexEFG)*. In the first method of cross-resistance, membrane stress from AgNPs or disrupted proteins forming adducts to $Ag_{(aq)}$ both activate protein misfolding pathways. Detection of malformed proteins is then transduced by AmgR, which elicits stress responses that result in efflux of molecules associated with disruption of protein folding (i.e., aminoglycosides). In this study, heavy metal oxidation of proteins could cause disruption of protein folding, thereby stimulating sensory system AmgR that directs antibiotic resistance. The second method of cross-resistance is oxidation of cysteine

residues in key proteins. The oxidation of cysteine residues in detectors of the MgrR family might derive from surface stress, metal oxidation, or adduct formation. This action is worrisome because a basic local alignment search for Mgr and TetR orthologues in the *P. aeruginosa* genome indicated that 13 stress response system regulators of these families are linked to antibiotic resistance. Through either method of cross-resistance, the action of $Ag_{(aq)}$ and AgNPs have the potential to activate many systems overlapping with antibiotic stress response, potentially increasing antibiotic resistance.

Treatment processes and antibiotic stewardship must undergo reform. Treatment processes should consider increased removal of metals and AgNPs before waters and waste come into contact with biological processes. In the health-care setting, stewardship programs must use a comprehensive framework to limit the interaction of antibiotics with treatment $Ag_{(aq)}$ and AgNP coated surfaces and bandages chosen to treat patients. Efforts in this regard would reduce the potential stimulation of antibiotic resistance by $Ag_{(aq)}$ or AgNPs.

6. Silver nanoparticle-induced resistance to antibiotics

6.1 INTRODUCTION

Silver nanoparticles (AgNPs) are increasingly used in consumer and healthcare products to control microbial growth (Maynard 2007; Vance et al. 2015). AgNPs were found to leach from textiles into wash water (Benn et al. 2008) and to accumulate in wastewater solids (Levard et al. 2012b) with close contact to bacteria. This contact would likely expose bacteria to AgNPs in the range of 0.5 µg/L (Hendren et al. 2013), which has been shown to induce stress responses in bacteria (Chapters 4 and 5). Recent studies suggest that there are two potential models of interaction for AgNPs and bacteria: (1) a surface attachment model of interaction in which AgNPs bind to the cellular envelope releasing $Ag_{(aq)}$ into the periplasm (Sondi et al. 2004; Morones et al. 2005; Lok et al. 2006) or (2) a dissolution mechanism of interaction in which AgNPs in bulk suspension release $Ag_{(aq)}$ via a dissolution (Morones et al. 2005; Pratsinis et al. 2010; Xiu et al. 2012; Long et al. 2017). In both cases, AgNPs cause toxicity through a variety of mechanisms of action including protein oxidation (Lok et al. 2006), loss of cell envelope integrity (Stohs et al. 1995; Sondi et al. 2004; Barani et al. 2011), and DNA adduct formation (Arakawa et al. 2001), all of which are similar to the mechanisms of action of heavy metals, specifically $Ag_{(aq)}$ (Nies 1999; Nies 2003).

Exposure to heavy metals, including silver, are thought to elicit increased antibiotic resistance, which represents the ability of a bacterium to grow in the presence of an antibiotic (Baker-Austin et al. 2006). Metals have been found in hospital effluents. For example, copper (Cu), lead (Pb), cadmium (Cd), and zinc (Zn) were found at concentrations of 213, 281, 2.6 and 1434.4 mg/kg, respectively, in sediment deposited in hospital outlet pipes; moreover, the presence of these toxic metals correlated to the presence of antibiotic resistance genes in local microbial communities ($r > 0.72$, $p<0.001$)

(Laffite et al. 2016). Evidence of the link between metals and antibiotic resistance extends beyond hospital settings. A study in a Chinese landfill demonstrated that increased antibiotic resistance gene copy number correlated to the presence of heavy metals, particularly Cd and Cr ($r > 0.85$, $p<0.05$), but the presence of antibiotic resistance genes did not correlate to the presence of antibiotics (Wu et al. 2015). Similar results were found in an ecological setting, where tetracycline resistance genes in soil correlated closely with the presence of copper (Knapp et al. 2011).

Metals have been linked to increases in multidrug efflux pump (MEP) expression and antibiotic resistance in a process known as physiological adaptation. In Chapter 5, *Pseudomonas aeruginosa* exposed to $Ag_{(aq)}$ or AgNPs showed increased expression of five multidrug efflux systems; bacteria exposed to $Ag_{(aq)}$ showed increased expression of *mexAB, mexXY, and muxABC* (Figure 5.5), and bacteria exposed to AgNPs showed increased expression of *mexGHI* and *mexPQ* (Figure 5.6). Exposure to Cu, Cd, and Zn promoted resistance to the antibiotics imipenem and ofloxacin by restricting the expression of *oprD*, which encodes a porin (Perron et al. 2004; Caille et al. 2007) in *P. aeruginosa*. In addition to pumps, specific antibiotic response genes can mitigate metal stress. The newly characterized gene *tcrB*, a Cpx-like metal stress response gene in *Enterococcus faecium*, promoted resistance to copper while also promoting resistance to several macrolide antibiotics (Hasman et al. 2002). A genetic element such as a plasmid can harbor separate resistance genes for metals and antibiotics, and the presence of the plasmid would confer both types of resistance. Many such multidrug resistant plasmids harbor both antibiotic resistance genes and metal resistance genes (Baker-Austin et al. 2006). For example, a plasmid cured from a *Salmonella* strain in manganese-contaminated sediments showed resistance to ten antibiotics and five heavy metals including Cr, Cd, Ni, As, and Pb (Ghosh et al. 2000). All of these data indicate that metal exposure can increase antibiotic resistance

in bacteria. However, it is not known if AgNPs, which have mechanisms of action derived from their corrosion, can cause antibiotic resistance in bacteria.

This research seeks to evaluate the impact of pre-exposing bacteria to environmentally relevant concentrations of AgNPs to determine its potential to increase antibiotic resistance. Here, *P. aeruginosa* was exposed to low concentrations of AgNPs (4 µg/L) causing a growth limitation and subsequently were grown in the presence of antibiotics to assess a growth advantage or disadvantage. Additionally, a series of *P. aeruginosa* MEP mutants were exposed to $Ag_{(aq)}$ or AgNPs to evaluate the potential link between antibiotic efflux pump expression and silver resistance.

6.2 SUMMARY OF INITIAL HYPOTHESES

The central hypothesis investigated in Chapter 6 determines if the potential AgNP and $Ag_{(aq)}$ induced MEP expression evaluated in Chapter 5 can manifest as actual antibiotic resistance in *P. aeruginosa.* The model of bacterial-AgNP interaction determined in Chapter 4 indicated that AgNPs, under the tested water chemistry conditions, caused a toxic response through disruption of the periplasm (Figure 4.7) and generation of H_2O_2 (Figure 4.8). A summary of these mechanisms action can be found in Figure 7.1. These mechanisms might stimulate an antibiotic resistance response when they occur below a threshold at which significant toxicity occurs. This antibiotic resistance might occur as a result of transcriptional changes in the expression of antibiotic resistance gene products or over successive generations by mutational changes in the regulation of these resistance systems. In Chapter 5, AgNPs stimulated expression of MEPs MexGHI and MexPQ, which are associated with aminoglycoside antibiotic resistance (Figure 5.6). Thus, it is possible that pre-exposure to AgNPs might stimulate resistance to aminoglycosides through

expression of MEPs MexGHI and MexPQ. Additional periplasmic stress observed in Chapter 4 (Figure 4.8) might promote physiological changes in the bacterial envelope improving resistance to envelope-targeting antibiotics (e.g., penicillins and polymyxin B). Although increases in expression of resistance gene groups associated with surface-stress were not observed in Chapter 5, antibiotics with a surface mechanism of action are investigated here. Pathways providing resistance to aminoglycosides are linked to oxidative stress sensors as well (e.g., MexR and AmgR), which could provide resistance to a range of additional antibiotics. Decreases in DNA repair (Figure 5.10) might provide a mechanism by which resistance could develop further through mutagenesis in a form that is inherited through generations. These experiments will test if pre-exposure to a low toxicity dose might increase resistance. A summary of these hypotheses is provided in Figure 6.1.

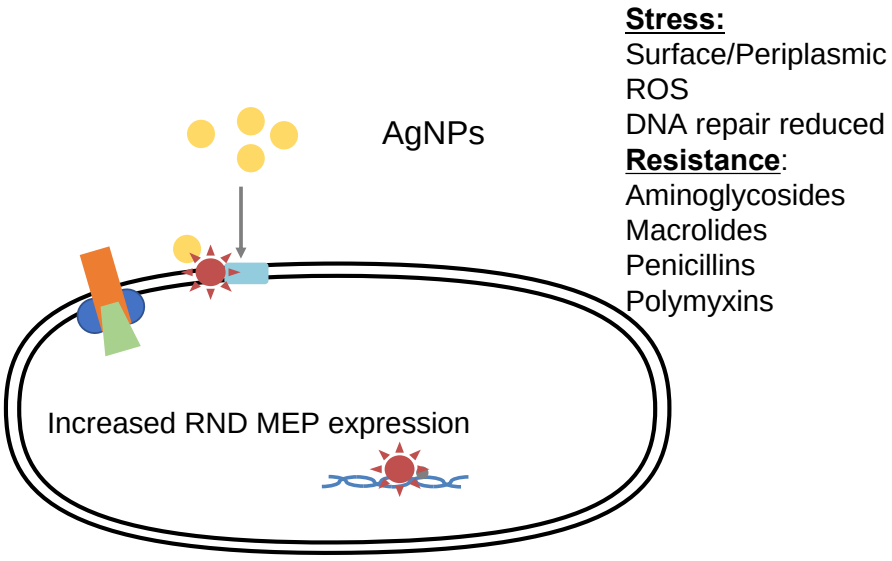

Figure 6.1 **Summary of potential antibiotic reistance mechanisms and antibiotic classes.**

6.3 MATERIALS AND METHODS

6.3.1 Nanoparticles

The AgNPs used in this research were manufactured by nanoComposix (San Diego, CA). Per the manufacturer, the AgNPs had an average metal core diameter of 9.9 nm (±1.9 nm) as measured by transmission electron microscopy (TEM) and a 14-nm hydrodynamic radius as measured by dynamic light scattering (DLS). The AgNPs were stored in a liquid suspension of 2 mM citrate at 4 ˚C.

6.3.2 Bacteria

Six strains of *P. aeruginosa* were used in this study. Freezer stocks were stored at -80 ˚C in a mixture of Luria Bertani (0.5 g/L NaCl; LB) broth and glycerol (75:25 v/v). *P. aeruginosa* PAO1 was used in the atibiotic resistance experiments. Five strains of *P. aeruginosa* PAO1 (generously provided by Keith Poole, Queen's University, Kingston, Ontario, Canada) were used in the genetic resistance experiments as follows: K767 was the parent strain from which all of the following mutants were derived; KP2 was a *mexAB* over-expression mutant, resistant to nalidixic acid; KP3 was a Δ*mexAB* mutant; KP4 was a *mexCDJ* over-expression mutant, resistant to norfloxacin; and KP5 was a Δ*mexCDJ* mutant. All mutants were transposon mutants.

6.3.3 Media

LB broth (Fisher Scientific; Waltham, MA) was used to culture inocula and prepare freezer stocks of bacteria. LB agar (15 g/L agar) was used to streak the freezer stocks and to conduct viable plate counts.

Minimal Salt Vitamin Glucose (MSVG) medium was used for continuous-culture of bacteria in a chemostat. MSVG (for 1L) consists of 1 g $(NH_4)_2SO_4$, 0.06 g $MgSO_4 \cdot 7H_2O$, 0.06 g $CaCl_2$, 0.02 g KH_2PO_4, 0.03 g $Na_2HPO_4 \cdot 7H_2O$, 2.383 g 2-[4-(2-hydroxyethly)piperazin-1-yl]ethanesulfonic acid (HEPES), 1 mL of 10 mM $FeSO_4$, 1 mL of 1000x vitamin solution [per liter: 20 mg biotin, 20 mg folic acid, 50 mg thiamine HCl, 50 mg D-calcium pantothenate, 1 mg vitamin B12, 50 mg riboflavin, 50 mg nicotinic acid, 100 mg pyridoxine HCl, and 50 mg p-aminobenzoic acid], and 0.220 mL of 20 g/L glucose solution). MSVG medium was stored for a maximum of 3 weeks to avoid precipitation of HEPES.

Minimal Davis (MD) medium was used during antibiotic resistance experiments to promote the formation of low fractal dimension aggregates. MD medium (for 1 L) consists of 1 g $(NH_4)_2SO_4$, 7 g K_2HPO4, 2 g KH_2PO_4, 0.5 g sodium citrate, 0.1 g $MgSO_4$, 1 g glucose, pH 7.2.

Mueller-Hinton (MH) broth was used during antibiotic resistance testing. MH broth (for 1 L) consists of 2 g beef infusion solids, 17.5 g casein hydrolysate, 1.5 g starch, pH 7.4.

The aforementioned glucose and vitamin stock solutions were sterilized using a 0.220-µm polyethersulfone (PES) bottle-top filter (Corning; Corning, NY). All other bacterial growth media components were sterilized with an autoclave.

6.3.4 Chemostat

A chemostat was used for continuous-culture of the bacteria used maintain a source of bacteria for inoculating the antibiotic stress induction samples. The chemostat was beneficial because it produced a consistent bacterial density. Further, all assays contained an internal control to verify that the target initial bacterial concentration was met. In the

chemostat, fresh influent medium was pumped from a reservoir (1.8-L capacity) to the bacterial growth chamber (0.2-L capacity;

Figure 4.2). A bubble-break was installed to prevent bacteria in the growth chamber from moving into the medium reservoir. Chemostats were operated at a flow rate of 0.183 mL/min producing a hydraulic detention time of 18.2 h.

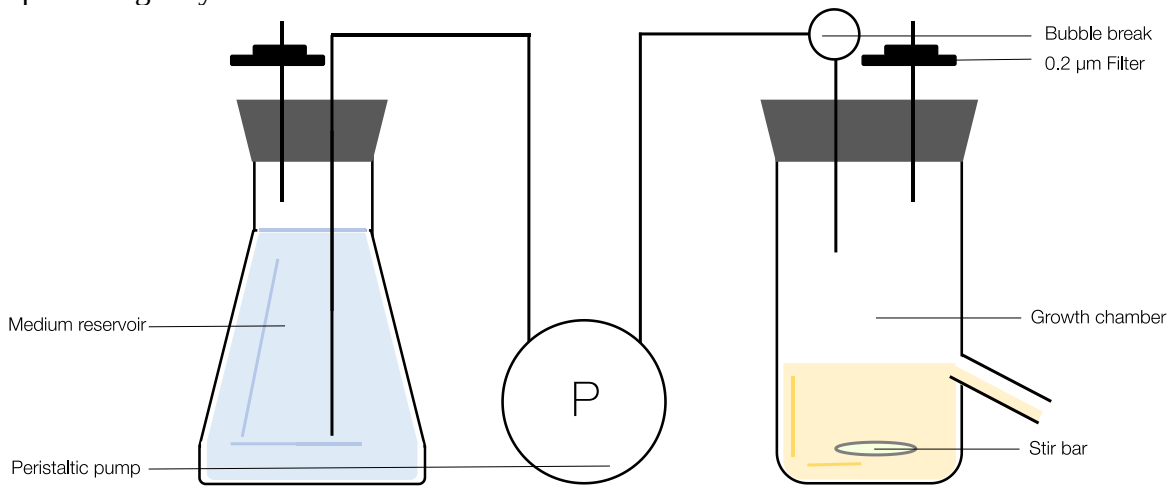

Figure 6.2: **Schematic of Chemostat**. The chemostat is composed of an influent medium reservoir and a growth chamber.

The preparation of the chemostat was completed over five days. On day one, fresh *P. aeruginosa* PAO1 was struck on LB agar medium from freezer stock and incubated at 35 ˚C overnight. On day two, the chemostat was washed, autoclaved, and filled with fresh MSVG medium; the chemostat was allowed to run for one day prior to inoculation to ensure no contamination; the growth chamber was stirred on a stir plate at 225 RPM and ambient temperature (approximately 22.2 ˚C degrees). A single colony of *P. aeruginosa* PAO1 was retrieved with a sterile loop hook from the streak plate and stirred into 5 mL of LB broth in a culture tube. The inoculum was incubated for 15 h at 35 ˚C and shaken at

200 RPM. On day three, the chemostat was inoculated with 1 mL of the liquid culture and operated in batch mode for 24 h. On day 4, flow was initiated in the chemostat; at the end of day 5, an aliquot from the chemostat was used for viable plate counts. The target cell density was 5 x 10^7 colony forming units (CFU)/mL, and actual concentrations ranged from 4 to 6 x 10^7 CFU/mL; precision in the bacterial concentration was necessary for experimental repeatability. Bacteria grown in the chemostat were used to inoculate AgNP pre-exposure experiments.

6.3.5 Viable plate counts

Viable plate counts for *P. aeruginosa* were conducted using a spot-plate technique (Figure 4.3). Briefly, the sample to be enumerated was sonicated in a bath sonicator (Bathsonic 3510; Fisher; Waltham, MA) for 10 min and vortexed gently for 15 s. Ten-fold serial dilutions were prepared in MD medium in a microtiter plate and plated in triplicate (10-µL spots) on LB agar plates. The plates were incubated overnight at 35˚C. A target of 10-40 CFU/spot was used to choose which dilution to count. The bacterial concentration in the original sample was calculated according to Equation 6.1, where D is the dilution factor (1/dilution).

Equation 6.1 $$\frac{colonies}{0.01\,mL} \cdot D = \frac{CFU}{mL}$$

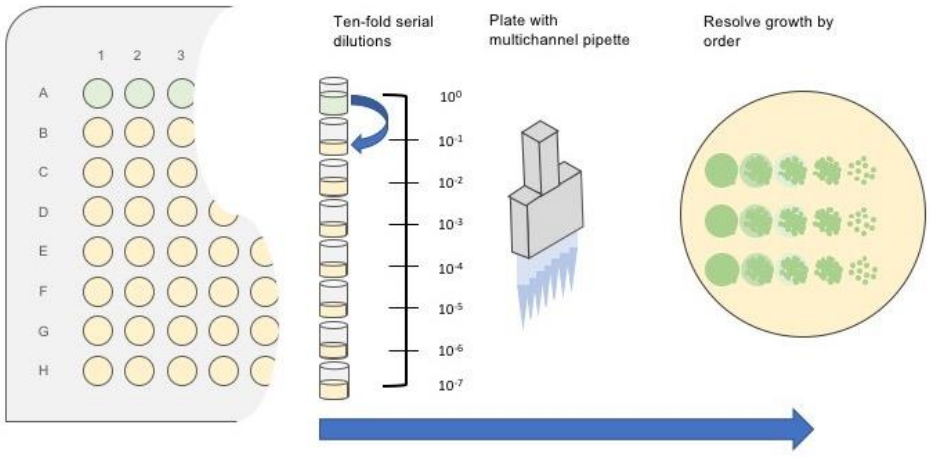

Figure 6.3: **Spot-plate method.** This method was used to enumerate viable bacteria from a well-dispersed liquid culture. An aliquot of the sample to be interrogated was loaded (90 µL; green) into the top row of the microtiter plate; all subsequent rows were filled with 90 µL of sterile diluent. Serial dilutions were performed by mixing 10 µL from each well in row A to row B, followed by mixing via aspiration with the pipette. Ten-fold serial dilutions were continued to the extent desired in subsequent rows. Then, a multichannel pipettor was used to place a 10-µL spot for each dilution of interest on an agar plate. After incubation, CFU were counted for spots that contained 10-40 CFU, and the CFU/mL of each original sample was calculated.

6.3.6 Stressor calibration

Growth-limiting dosages

A modified setup of the standard micro-broth minimum inhibitory concentration (MIC) assay was used to determine the biocidal concentrations of AgNPs and selected antibiotics. Experiments were conducted on the basis of growth in the presence of a stressor, such that the traditional definition of "minimum inhibitory dose", that is the concentration of stressor at which bacteria are no longer able to replicate, did not apply. As such, the term growth-limiting dose (GLD) was employed, defined as the condition under which presence of a stressor during growth limits the growth of an organism to a defined percentage of the growth of an unexposed control. The GLD_5 was defined as the

concentration of AgNPs at which the cells achieve 95% of the population density of the no-AgNP control after 9 hours of growth. This definition ensures that the bacteria are stressed but that the majority of them are able to overcome the AgNP insult. Similarly, GLD_{AB} (the GLD for an antibiotic) was defined as the concentration of antibiotic at which the cells achieve 45-70% of the population density of the no-antibiotic control by the end of a 20-h growth period.

6.3.7 AgNP GLD_5

The Clinical Laboratory Institute's standard micro-broth dilution method (Clinical Laboratory Institute 2012) was adapted for determination of the AgNP GLD_5 (Figure 6.4). To begin, a microtiter plate was loaded with 180 µL of MD medium in all wells except row A, which was loaded with 360 µL of MD medium. AgNPs were then dosed to row A at twice the desired final concentration (to account for volume addition when bacteria were inoculated to the assay). Starting with row A, one-half the volume of each well (180 µL) was transferred to the next row (B) and mixed by aspiration with a pipette, resulting in a 2-fold dilution of the AgNPs; this process was repeated successively through row G, after which 180 µL was removed from G and discarded. No AgNPs were added to the last row (H), which served as the no-AgNP control. Then, 142 µL of fresh MD medium and 38 µL of sonicated *P. aeruginosa* PAO1 cells (from the chemostat) were added to all rows and mixed by aspiration with a pipette. Thus, the desired AgNP concentration was achieved in each row at an initial cell concentration of 5×10^5 CFU/mL. The plate was incubated in a plate reader (Synergy HTI; BioTek, Winooski, VT) at 35 ˚C for 10 h. During this time, optical density at 600 nm (OD_{600}) was measured every 20 min following 5 sec of "medium" intensity shaking. The plate was covered to minimize evaporative losses, and the

absorbance reading was taken through the bottom of the plate. Results were exported to Excel®, and the results of eight technical replicates were averaged. The GLD_5 was determined as the concentration at which the cells achieve 95% of the population density of the no-AgNP control after 9 hours of growth. The GLD_5 of AgNPs were averaged as the total of six technical replicates from triplicate biological replicates; the GLD_5 survival was calculated by interpolating between the control and lowest category of AgNPs tested.

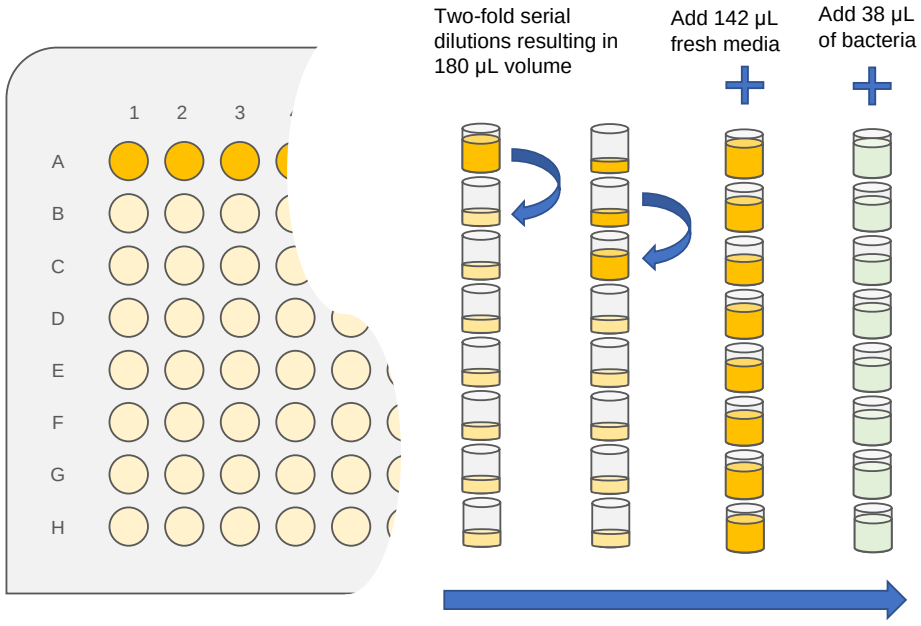

Figure 6.4. **Determining GLDs for AgNP and antibiotics**. All wells first were loaded with 180 µL of appropriate medium except for row A, which contained 360 µL. Stressors (AgNPs or antibiotics) were then dosed at 2x of the final target concentration. The solution was mixed well and 2-fold serial dilutions were prepared in rows A-G; row H was reserved for controls (no antibiotic or AgNP exposure). Following antibiotic or AgNP addition, 142 µL of fresh medium and 38 µL of bacterial cells were added to each well. Growth was measured for 20 h via absorbance at 600 nm in a plate reader.

Optical density correlation to colony-forming units at the GLD_5

At the AgNP GLD_5, the growth curve as measured by OD_{600} was correlated to CFU/mL. Here, the approach described in the previous section was modified somewhat. Specifically, microtiter plates were loaded with PAO1 at 5 x 10^5 CFU/mL and the AgNP GLD_5 concentration. OD_{600} was measured every 20 min; starting at 3 h, 90-µL aliquots were manually retrieved from duplicate wells every 20 min for plate counts. After a well was manually sampled, this well was no longer used for absorbance measurements. The 90-µL aliquots were used for spot plate counts. A correlation was prepared for OD_{600} and CFU/mL. The time of incubation to reach approximately 10^7 CFU/mL (early log phase) was noted, and this time was used in subsequent experiments as the point at which to harvest AgNP-exposed bacteria for pre-exposure assays.

Antibiotic GLD determination

GLD_{AB} was found for selected antibiotics using a similar approach as that for determining GLD_5 for AgNPs (Figure 6.4). Briefly, a microtiter plate was loaded with 180 µL of MH medium in all wells except row A, which was loaded with 360 µL of MH medium. Antibiotics were dosed to row A at twice the target final concentration. Starting with row A, one-half the volume of each well (180 µL) was transferred to the next row (B) and mixed by aspiration with a pipette, resulting in a 2-fold dilution of the AgNPs; this process was repeated successively through row G, and the last 180 µL was discarded. No antibiotics were transferred to the last row (H), which served as the no-antibiotic control. Then, 142 µL of fresh MD medium and 38 µL of sonicated *P. aeruginosa* PAO1 cells (from the chemostat) were added to all rows and mixed by aspiration with a pipette. Thus, the desired antibiotic concentration was achieved in each row at an initial cell concentration of 5 x 10^5 CFU/mL. The plate was incubated in a plate reader (Synergy HT-I; BioTek, Winooski, VT) at 35 ˚C for 20 h. During this time, OD_{600} was measured every 20 min

following 5 sec of "medium" intensity shaking. The plate was covered to minimize evaporative losses, and the absorbance reading was taken through the bottom of the plate. Results were exported to Excel®, and the results of two biological replicates, each with three technical replicates, were averaged. Eight antibiotics were evaluated, representing six cellular targets (Table 6.1). The GLD_{AB} was determined as the concentration at which the antibiotic exposed organism achieved ~55%-65% of the growth of the organism grown in the absence of that stressor at mid-log phase (approximately 15 h). Concentrations were interpolated to calculate the specific concentration to be used. GLD_{AB} values were averaged as the total of three technical replicates from three biological replicates.

Table 6.1. Summary of antibiotics used in study

Antibiotic	Category	Target
Carbenicillin	β-lactam	peptidoglycan
Cefamandole	β-lactam	penicillin-binding protein
Kanamycin	aminoglycoside	30S ribosomal subunit
Lincomycin	lincosamide	50S ribosomal subunit
Nalidixic Acid	quinolone	DNA gyrase
Novobiocin	quinolone-like	DNA gyrase
Ofloxacin	fluoroquinolone	DNA gyrase
Polymyxin B	cationic polypeptide	cell membrane

6.3.8 Passivation of AgNPs

Three chemical agents (L-cysteine, sodium thiosulfate, and citrate) for passivation of AgNPs were evaluated for their effectiveness to eliminate the biocidal action of AgNPs. This was done using a growth-based assay in which a 5 x 10^5 CFU/mL inoculum was challenged with AgNPs at the GLD_5. Passivation agents were applied at a mass concentration equivalent to the GLD_5 and 2x the GLD_5. In addition to passivated samples, three controls were evaluated. The first was a stressor negative and passivator negative control, which showed normal growth in the absence of a passivator. The second was passivator negative and stressor positive, to evaluate toxicity of the stressor. The third was a passivator positive and stressor negative control to evaluate the effect of the passivator

on bacteria. Passivation agents were chosen because of their ability to chelate Ag^+ and to form covalent bonds to Ag^+ via a S-Ag bond; all passivation agents used in this study have been investigated in previous studies (Bae et al. 2010) Passivation agents were dosed at a 1:1 or 2:1 ratio of passivation agent to AgNPs, 4 and 8 µg/L respectively as performed in Bae et al. (2010).

6.3.9 Antibiotic resistance testing

Antibiotic resistance studies were conducted by exposing *P. aeruginosa* PAO1 to the GLD_5 of AgNPs followed by subsequent exposure to the GLD_{AB} of a selected antibiotic to evaluate changes in antibiotic resistance resulting from previous AgNP exposure (called "pre-exposure" and "antibiotic resistance" plates, respectively, in Figure 6.5). Antibiotic resistance studies were conducted as follows.

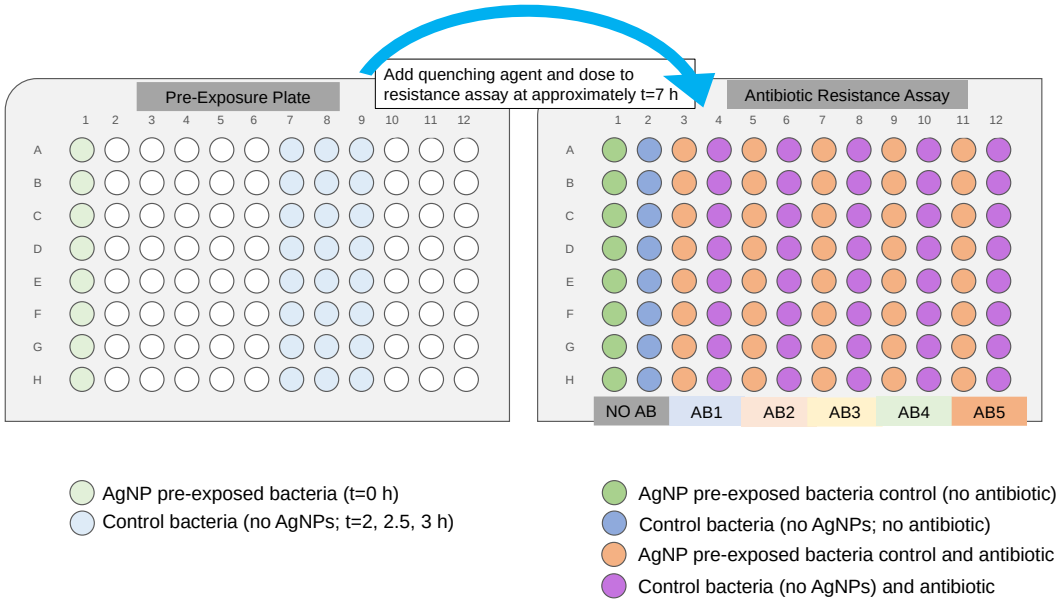

Figure 6.5. **Antibiotic resistance experiments.** *P. aeruginosa* PAO1 was grown in the presence of GLD_5 of AgNPs for 7 h or in the absence of AgNPs for 5 h. These bacteria were then used to inoculate an antibiotic resistance assay to evaluate whether pre-exposure to AgNPs could induce a growth advantage or disadvantage in *P. aeruginosa* in the presence of antibiotics.

An aliquot of *P. aeruginosa* PAO1 was removed from the chemostat (5×10^6 CFU/mL), bath-sonicated for 15 min, and vortexed. For AgNP-exposure experiments, these cells were inoculated into fresh MD medium containing the GLD_5 of AgNPs at a final concentration of 5×10^5 CFU/mL. For control experiments (where cells were not exposed to AgNPs), the cells were inoculated into fresh MD medium in the same microtiter plate as the AgNP-exposed cells, but this occurred 2, 2.5, and 3 h after bacteria were inoculated for AgNP exposure. The purpose of this lag was to ensure that the control and AgNP-exposed bacteria reached the same concentration (OD_{600} of 0.091 or 5×10^7 CFU/mL) at the same time. OD_{600} was monitored for 7 h to determine when the bacterial concentration reached this target. At that point, the control and AgNP-exposed bacteria

were mixed with 4 µg/L L-cysteine to passivate the AgNPs and transferred to the antibiotic resistance plate (Figure 6.5).

In the antibiotic resistance assay, eight technical replicates of at least triplicate biological replicates were performed for each antibiotic. Tests were conducted in pairs, such that one set of eight technical replicates with AgNP-exposed cells was run in parallel with one set of eight technical replicates with control cells (not exposed to AgNPs) during the same biological replicate. Additionally, a no-antibiotic control was run with AgNP-exposed bacteria and control bacteria (not exposed to AgNPs) to demonstrate that both sets of cells met the target initial bacterial concentration of 5×10^5 CFU/mL (acceptable range, 4×10^5 - 6×10^5). For the results of an experiment to be accepted, the passivated no-AgNP control cells and passivated AgNP-exposed cells had to grow at the same rate, ensuring that each group was loaded with the same inoculum density with no growth difference during the antibiotic challenge.

The antibiotic resistance assays (Figure 6.5) were set-up in a microtiter plate. All wells were first loaded with 356.4 µL of MD medium; an aliquot of medium was then withdrawn to allow for antibiotics to be added to each column except for the first two, which were reserved for the no-antibiotic controls. The remaining columns were dosed with an antibiotic at its respective GLD_{AB}, which are summarized as follows: carbenicillin (8 µg/mL), nalidixic acid (140 µg/mL), kanamycin (1.5 µg/mL), cefamandole (500 µg/mL), ofloxacin (4.5 µg/mL) polymyxin B (0.08 µg/mL), lincomycin (400 µg/mL), chloramphenicol (32 µg/mL), and novobiocin (8.26 µg/mL). Antibiotic stocks were prepared at sufficiently high concentrations so that only 2-10 µL of each stock was added to each well (0.6-2% of the total well volume). As shown in Figure 6.5, each pair of columns targeted a particular antibiotic; one column was inoculated with control *P. aeruginosa* (no pre-exposure to AgNPs), and the other column was inoculated with *P.*

aeruginosa that had been pre-exposed to AgNPs. This plate was immediately transferred to the plate reader, and OD_{600} was measured every 20 min for 20 h with "medium" intensity shaking before each read at 30 ˚C. AgNP pre-exposure experiments were composed of 8 technical replicates across 2-3 biological replicates. Standard deviation was calculated across all biological replicates. Data were exported to Excel® for analysis.

6.3.10 Mutant resistance experiments

Bacteria preparation

The genetic elements contributing to antibiotic resistance were examined using a series of genetically engineered *P. aeruginosa* mutants (deletion or over-expression mutations related to multidrug-export pumps). Exposure studies were used to evaluate the resistance of the mutants to AgNP and $Ag_{(aq)}$ relative to the resistance of the parent strain. Micro-broth experiments were inoculated from freezer cultures prepared in LB broth. Cultures of K767, and KP2-5 (*mexAB, mexCDJ* and *mexXY* mutants create by transposon mutagenisis) were inoculated to 50 mL of LB broth in baffled 250-mL culture flasks and grown for 17 h at 35 ˚C with shaking. Triplicate spot plates were performed to measure bacterial concentration at the end of the culturing.

Calibration of parent strain K767

AgNP and $Ag_{(aq)}$ resistance testing was conducted in microtiter plates, and the growth of mutant strains was compared to the growth of parent strain K767. The GLD_{50}, the dose of stressor reducing growth of stressor-exposed cells to 50% of that of cells not exposed to the stressor, was determined for K767. An aliquot (180 µL) of MD medium was added to all wells of a microtiter plate except row A, which was loaded with 360 µL, less the volume of AgNP or Ag stock at twice the desired concentration. Starting with row

A, one-half the volume of each well (180 µL) was transferred to the next row (B) and mixed by aspiration with a pipette, resulting in a 2-fold dilution of the AgNP or $Ag_{(aq)}$; this process was repeated successively through row G. No AgNPs or $Ag_{(aq)}$ were transferred to the last row (H), which served as the controls without AgNPs or aqueous $Ag_{(aq)}$. The actual AgNP concentration was still twice the desired concentration. An additional 142 µL of fresh MD medium was added to all wells followed by 10 µL of thawed K767 freezer stock, diluted to 5 x 10^6 CFU/mL; thus all wells were inoculated to a final concentration of 5 x 10^5 CFU/mL. As previously stated, the GLD_{50} concentration of AgNPs and $Ag_{(aq)}$ was defined as the concentration resulting in 50% reduction in ultimate growth as compared to a no-Ag control.

Genetic basis for $Ag_{(aq)}$ and AgNP resistance

All mutant strains were subsequently challenged with $Ag_{(aq)}$ or AgNPs at a concentration of stressor causing growth to be limited to 50% of the unchallenged parent strain, K767. All inocula were diluted to the same initial density from freezer stock of each at densities determined from plate counts and inoculated directly into an AgNP or $Ag_{(aq)}$ resistance assay. Microtiter plates were prepared by adding 360 µL of MH medium less the volume required to produce a final concentration of 5 µg/L of AgNPs or 1.1 µg/L of $Ag_{(aq)}$ (stock prepared such that no greater than 20 µL were added), and 10 µL of thawed bacterial freezer stock diluted to 5 x 10^6 CFU/mL. This resistance assay plate was immediately transferred to the plate reader, and OD_{600} was measured every 20 min for 30 h at 35 ˚C with "medium" intensity shaking before each read.

6.4 RESULTS AND DISCUSSION

6.4.1 Physical characteristics of AgNPs used in this study

AgNPs used in this work were suspended in MD medium at an ionic strength of 40 mM, approximately equivalent to the Mμ0 exposure solution described in Table 3.1. This condition stabilizes the particles and minimizes their dissolution as compared to media with higher ionic strength (140 mM) and/or destabilizing ligands (e.g., chloride) (Chambers et al. 2014, Chapter 3). Dissolution of AgNPs at a 1 mg/L concentration measured in Chapter 3 at conditions similar to those used in this study resulted in a 13 μg/L release of total $Ag_{(aq)}$, which was statistically indistinguishable from the release of 10 μg/L Ag^+ in the Lμ0 exposure solution (Table 2.1) The particles were completely stable over 5 h. Further, exposure in a medium ionic strength buffer promoted the formation of branched fractal aggregates (Figure 3.3) that had a constant aggregate diameter (data not shown) over the duration of the experiment. Formation of branched aggregates increased AgNP toxicity (Figure 3.4) as compared to less branched aggregates (Lμ0) and increased the expression of the stress response system *katE* (Figure 3.6). In summary, the medium ionic strength condition utilized in this chapter promoted conditions that preserved nanocharacteristics of the AgNPs. Therefore, under the chemistry conditions chosen in this chapter, the biological response to AgNPs was likely attributable primarily to the nanoparticle form rather than the $Ag_{(aq)}$ form.

6.4.2 AgNP GLD_5 determination

The GLD_5 of AgNPs for *P. aeruginosa* PAO1 was 4 μg/L (Figure 6.6). GLD_5 concentrations were comparable to sublethal (i.e., non-biocidal) concentrations found to

induce biofilm formation (10.8 µg/L; Yang 2015) and approach the theoretical range of AgNP concentrations found in wastewater treatment plant solids (0.35 µg/L; Hendren et al. 2013). As such, the GLD_5 is relevant to environmental engineered systems. Furthermore, previous studies have observed changes in stress response gene expression at sub-MIC antibiotic dosages (Andersson et al. 2014), which suggests that the GLD_5 values used in the current study are likely causing changes in stress response system expression to grow in the presence of the AgNPs.

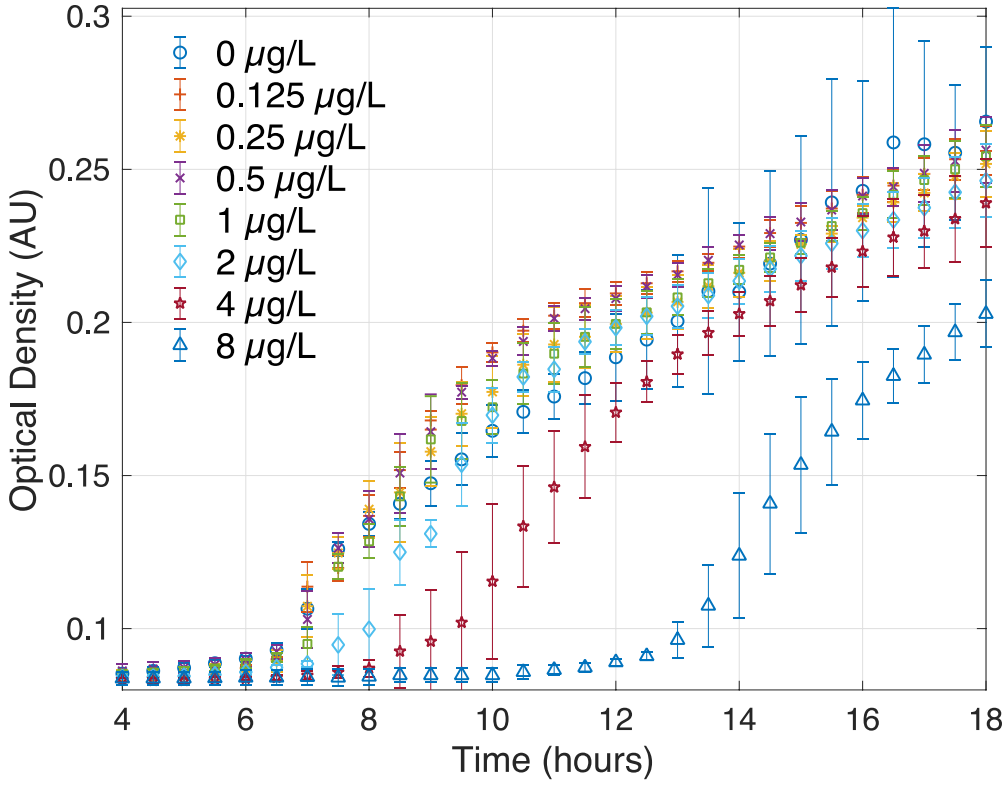

Figure 6.6. **Determination of GLD_5 of AgNPs for *P. aeruginosa* PAO1.** Eight technical replicates for each of two biological replicates were averaged for each tested AgNP concentration. The observed GLD_5 was 4 µg/L of AgNPs at 7 h after inoculation.

6.4.3 Passivation of AgNPs

Both L-cysteine and sodium thiosulfate were found to be effective at a 1:1 ratio (Figure 6.7A and B), reducing the biocidal effect of the AgNPs such that growth in passivated AgNP conditions (+ AgNPs; +passivation agent) matched growth in the control (-AgNP; -passivation agent). Cysteine (commonly used as a passivator in the literature) was used in these studies because of its relative low cost. Citrate did not reduce the antimicrobial activity of AgNPs (Figure 6.7C). Rather, the presence of citrate as a passivating agent actually exacerbated AgNP toxicity. It is possible that the added citrate destabilized the AgNP cap and promoted dissolution of AgNPs through a ligand-promoted mechanism (Misra et al. 2012).

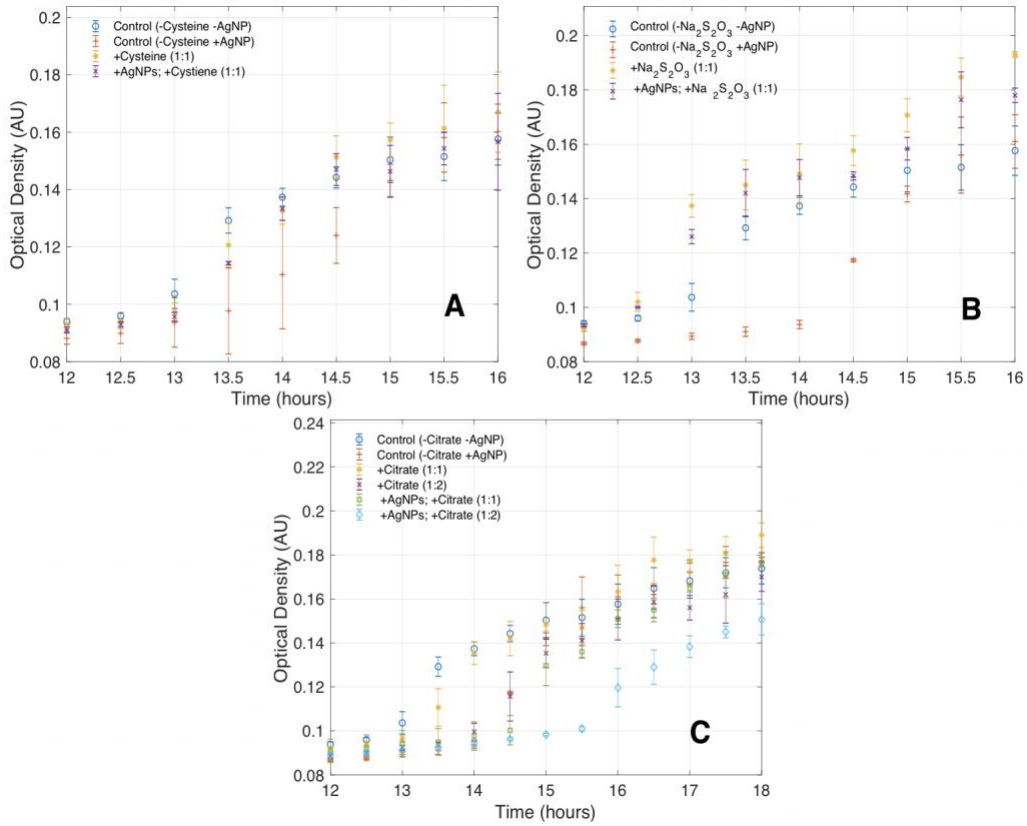

Figure 6.7. **Passivation of AgNPs.** AgNPs were passivated to eliminate biocidal activity. Three passivation agents were tested: A) L-cysteine B) sodium thiosulfate, and C) citrate. Three controls were conducted for all passivation agents. A primary control (o) containing no passivation agent and no AgNPs (passivator negative) was employed to characterize baseline growth. A biocidal control (+) indicated the contribution of toxicity at the GLD_5 of AgNPs. A passivation control (*) was used to characterize any changes in growth contributed by the passivation agent. Lastly, AgNPs were combined with a passivating agent under experimental conditions to evaluate mitigation of the biocidal action of AgNPs. Passivation agents and AgNPs were dosed at the beginning of the assay at a mass ratio of 1:1 or 2:1 of passivation agent to AgNP concentration (4 µg/L). A 5 x 10^5 CFU/mL inoculum was dosed to the assay.

6.4.4 Antibiotic GLD determination

The antibiotic GLD (GLD_{AB}) was defined as the concentration of antibiotic that reduced growth of *P. aeruginosa* PAO1 to ~55-65% of the no-antibiotic control as

measured by absorbance. The objective of these experiments was to find a range of antibiotic concentrations at which bacterial growth was impacted, so that the impact of antibiotics in this concentration range could be tested on cells pre-exposed to AgNPs. Thus, growth advantages or disadvantages due to pre-exposure to AgNPs would be evident in antibiotic resistance testing.

The GLD_{AB} was evaluated for eight compounds representing six antibiotic classes: aminoglycosides, ß-lactams, cationic-polypeptides, fluoroquinolones, lincomycin, and quinolones (Figure 6.8). Carbenicillin, cefamandole, and polymyxin B act at the cell envelope (wall and membrane). Kanamycin and lincomycin act on ribosomes. Nalidixic acid, novobiocin, and ofloxacin act on DNA gyrase. No general pattern of GLD_{AB} was observed for antibiotics included in this study. This is likely because of the diverse range of chemical structure and toxicological activity of the antibiotics. The values of GLD_{AB} are summarized in Table 6.2.

Table 6.2 Summary of antibiotic GLD_{AB}

Target/Drug	**GLD_{AB}**	**Reduction of Control (AgNP un-exposed) Growth**
Envelope-Targeting Antibiotics		
Carbenicillin	8 µg/mL	54%
Cefamandole	500 µg/mL	55%
Polymyxin B	0.08 µg/mL	51%
Ribosome-Targeting Antibiotics		
Kanamycin	1.5 µg/mL	48%
Lincomycin	400 µg/mL	51%
Replication-Targeting Antibiotics		
Nalidixic Acid	140 µg/mL	43%
Novobiocin	4.5 µg/mL	51%
Ofloxacin	8.26 µg/mL	43%

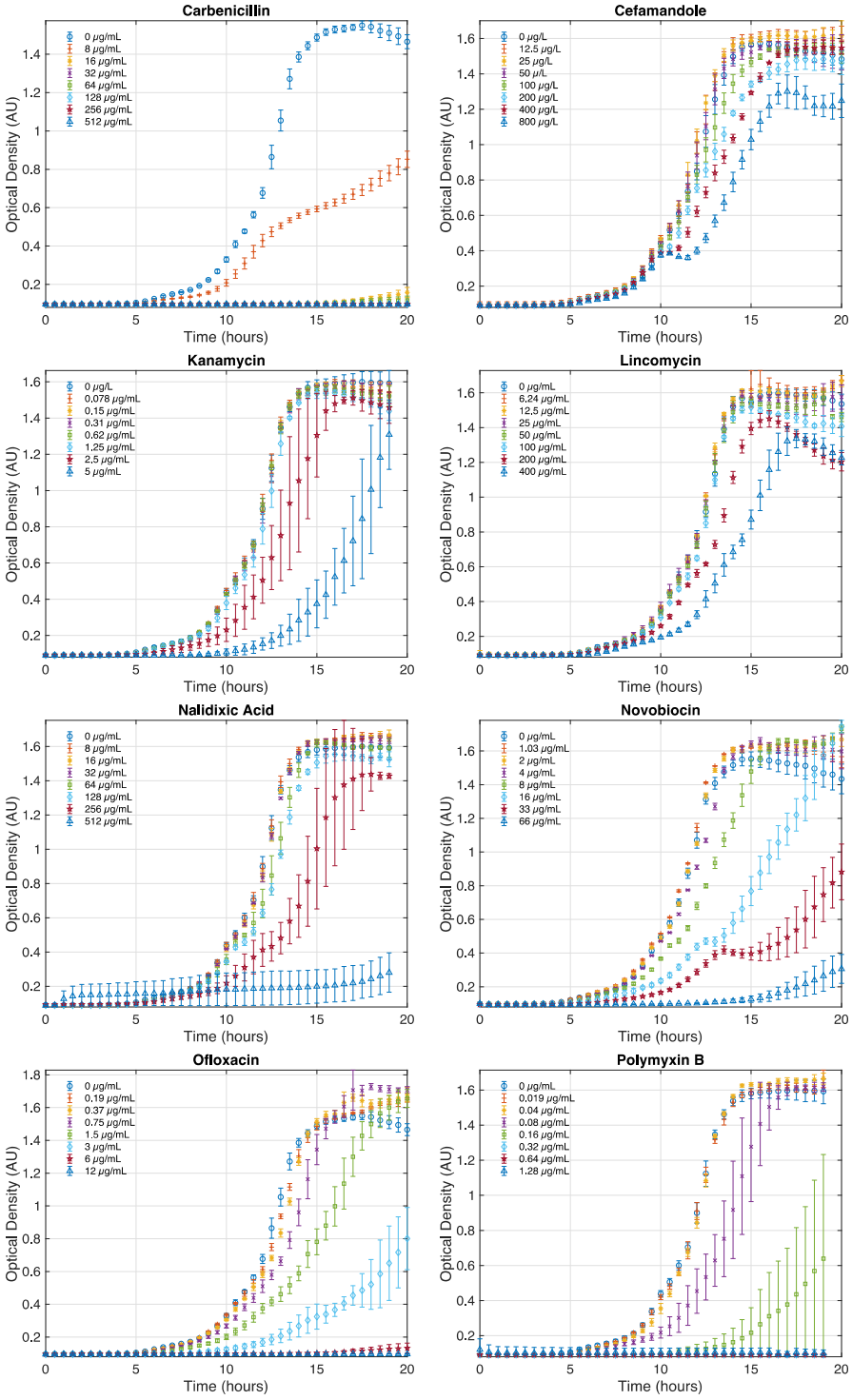

(Caption on following page)

Figure 6.8. **GLD_{AB} for eight antibiotics used to assess Antibiotic resistance potential of AgNPs.** Antibiotics were dosed to micro-broth assays in which antibiotics were added to MH medium and diluted two-fold for each of the seven tested concentrations in addition to a no-antibiotic-control. *P. aeruginosa* PAO1 was inoculated to each well at an initial density of 5 x 10^5 CFU/mL. The GLD for each antibiotic was characterized as the concentration of antibiotic that limited bacterial growth to 50% of the no-antibiotic control. Data are the average of four technical replicates for biological duplicates.

6.4.5 Antibiotic resistance testing

Antibiotic resistance was assayed using a two-step growth-based procedure. *P. aeruginosa* PAO1 was exposed to AgNPs for seven hours and then subsequently exposed to antibiotics to assay changes in susceptibility. Resistance was characterized as a result of increased doubling times and early entry into log-phase growth as compared to a no-AgNP control.

Bacteria were first exposed to the AgNP GLD_5 (5 µg/L). Pre-exposed and control bacteria (not exposed to AgNPs) were then challenged with antibiotics following AgNP passivation with L-cysteine at a 1:1 ratio. Both the control cells (without AgNP exposure) and cells pre-exposed to AgNPs were treated with L-cysteine. OD_{600} and plate counts (CFU/mL) were correlated to ensure that the inocula for the antibiotic resistance assays were exactly the same (Figure 6.9). An OD of 0.091 AU was found to correlate to a density of approximately 5 x 10^7 CFU/mL. This OD_{600} was equivalent to early log-phase growth and therefore used to inoculate the antibiotic resistance assay. The pre-exposure phase was monitored closely to ensure that cell density did not exceed the critical OD_{600} of 0.091 AU. A lag of approximately 2 h separated the inoculation of bacteria pre-exposed to AgNPs and inoculation of control bacteria (cells without AgNP exposure) to the pre-exposure plate (Figure 6.5) to ensure both sets of samples reached the critical OD_{600} simultaneously.

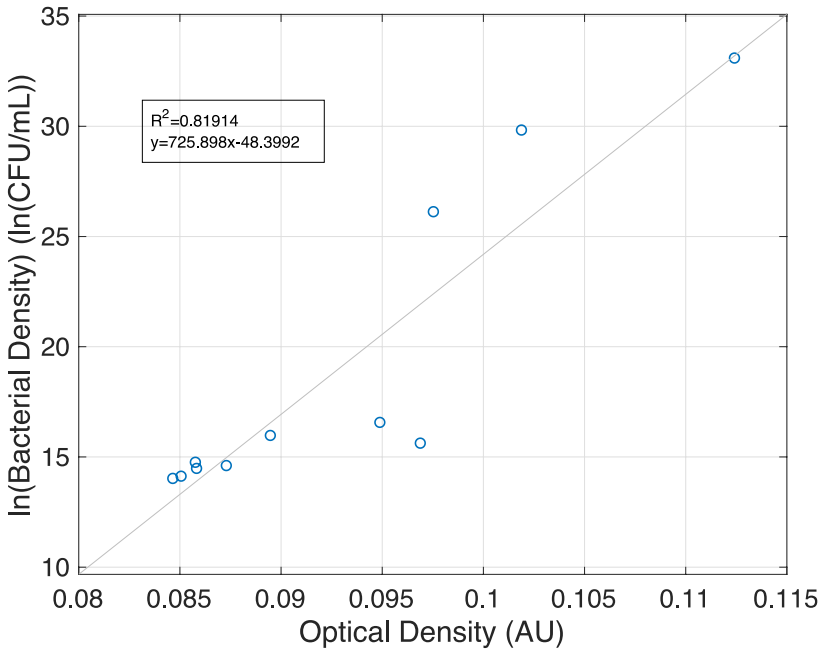

Figure 6.9. **Correlation of OD_{600} to CFU/mL for *P. aeruginosa* PAO1.** Cells were grown for 10 h at 35 ˚C, and OD_{600} was measured at 20-min intervals. At each measurement, wells were sacrificed and plated in triplicate for two biological replicates.

The final quality control experiment performed on antibiotic resistance experiments evaluated the growth of two control samples. A negative control (bacteria not exposed to AgNPs) was grown in MH medium without antibiotics and a positive control (with cells pre-exposed to AgNPs) was grown in MH medium without antibiotics. Pre-exposed bacteria and bacteria that had not been exposed to AgNPs were dosed to the antibiotic resistance assay at 5 x 10^5 CFU/mL. For a resistance assay to pass quality control, the positive control and the negative control had to show exactly the same growth curve. Specifically, the controls had to enter log-phase growth simultaneously to ensure that the bacterial densities were the same between the two samples at a particular time. Additionally, negative and positive controls were required to reach stationary phase faster

than did the bacteria in experiments dosed with antibiotics. An example of a quality control experiment is provided inFigure 6.10. In addition to quality control using growth curves, inoculum density was confirmed through plate counts of the negative and positive control wells of the antibiotic resistance assay. The target bacterial concentration was 5 x 10^5 CFU/mL.

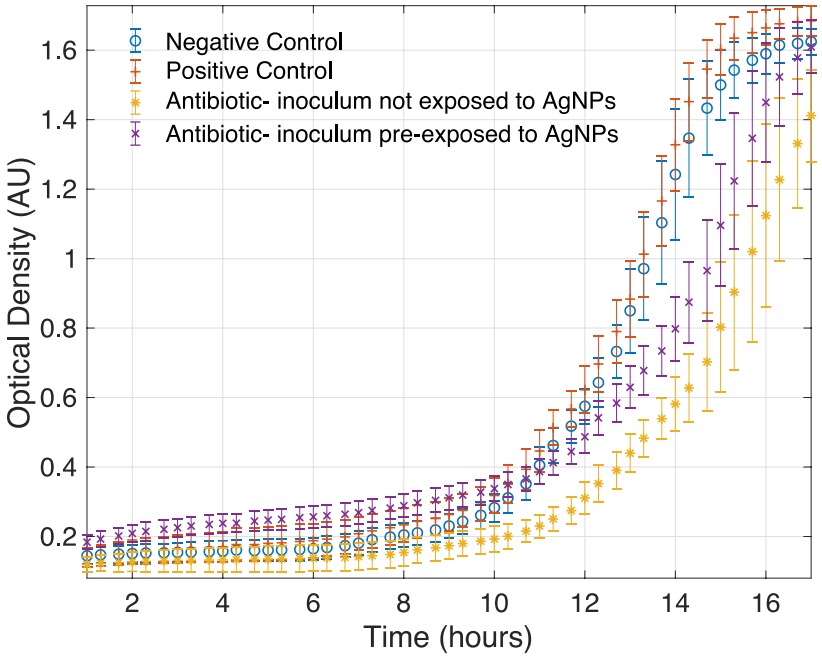

Figure 6.10. **Quality control experiment for antibiotic resistance assay**. Two controls were run in tandem with antibiotic resistance assays. A negative control (o) was grown without AgNP pre-exposure and in the absence of antibiotics. A positive control (+) was grown with AgNP pre-exposure and in the absence of antibiotics. Also shown are two experimental samples: bacteria not previously exposed to AgNPs but challenged with nalidixic acid (*); bacteria pre-exposed to AgNPs and subsequently challenged with nalidixic acid (x). A separate aliquot of either the negative control (cells not pre-exposed to AgNP) or the positive control (cells exposed to AgNP) were added to respective samples at the same time and at the same theoretical bacterial concentration. Upon addition to the antibiotic resistance assay, cells were grown in MH medium. The positive and negative controls were compared to experimental samples of each antibiotic tested in the assay to ensure equivalent inoculum concentrations were added following the pre-exposure phase because each inoculum (pre-exposed/ control) was taken from a different source.

6.4.6 AgNP-induced antibiotic resistance

Changes in resistance of *P. aeruginosa* as a result of pre-exposure to AgNPs were observed for three antibiotics, as determined by differences in doubling time: carbenicillin, kanamycin, and nalidixic acid (Figure 6.11). Bacteria exposed to carbenicillin showed an increase in antibiotic susceptibility as a result of AgNP pre-exposure. The doubling-time of the AgNP-exposed cells relative to the control cells was 20% longer during the antibiotic resistance assay. This might be explained by membrane and wall pitting from the stress of localization of AgNPs on the surface of bacteria (Sondi et al. 2004). Carbenicillin is a ß-lactam antibiotic that targets peptidoglycan in the cell wall and causes dividing cells to burst as a result of compromised crosslinking and reduced wall integrity (Butler et al. 2017). It is possible that AgNP-compromised cell walls were more easily impacted by carbenicillin to provide a growth advantage for control bacteria.

Bacteria pre-exposed to AgNPs showed an increase in resistance to kanamycin (Figure 6.11-kanamycin) and nalidixic acid (Figure 6.11-nalidixic acid). Doubling-times during mid-log growth for AgNP GLD_5 antibiotic exposed bacteria decreased after to pre-exposure to AgNPs by 21% and 9.5% for kanamycin and nalidixic acid, respectively. Both kanamycin and nalidixic acid are mitigated by MEPs MexAB and MexXY. Carbenicillin is not mitigated by MexXY; its export is attributable to MexAB (Masuda et al. 2000).

The reduced doubling times observed for bacteria pre-exposed to AgNPs as compared to bacteria not exposed to AgNPs indicate that bacteria shifted their growth strategy to one that was more suited to mitigate antibiotic stress. This reduction of doubling times is evidence that AgNPs have the potential to stimulate antibiotic resistance. Radical changes must be undertaken in how we approach antibiotic stewardship both in and out of the health care setting. Stewardship programs should consider the environment in which antibiotics are being utilized. For instance, if an AgNP-coated catheter is employed,

patients should not receive an antibiotic like nalidixic acid given the potential for the development of resistance at the catheter insertion site. Further a comprehensive understanding of mixed wasting of antibiotics and AgNP-coated materials in landfills should be incorporated into stewardship programs. Patients might submit expired antibiotics to a collection group for destruction.

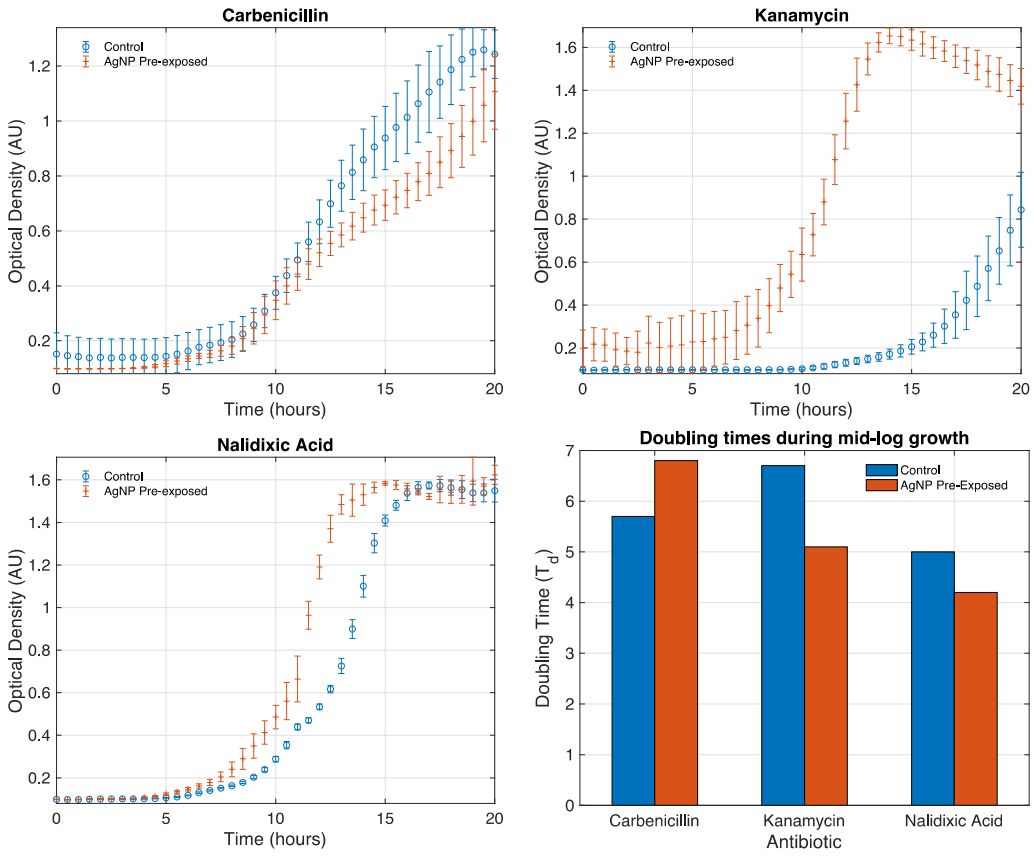

Figure 6.11. **Impact of pre-exposure to AgNPs on antibiotic resistance**. A separate aliquot of each control, either negative (no AgNP pre-exposure) or positive (AgNP pre-exposed) *P. aeruginosa* PAO1, was challenged in an antibiotic resistance assay. Bacteria were grown in MH medium. Data are the averages of eight technical replicates for biological duplicates. Doubling times of bacterial growth were calculated in mid-log using R.

Among the eight antibiotics included in the resistance assay, *P. aeruginosa* showed no change in resistance to five of them (Figure 6.12); for two, the export is not attributable to MexAB export (polymyxin B, novobiocin) (Masuda et al. 2000). Lincomycin, cefamandole, and ofloxacin resistance was attributable to common export systems MexAB, CD, and XY, with ofloxacin having the greatest-fold increase as a result of over-expression of the respective gene clusters. Both the MexAB and XY systems were slightly upregulated by exposure to AgNPs and $Ag_{(aq)}$ (Figure 6.12).

Growth in the presence of cefamandole showed no initial AgNP pre-exposure advantage; however, a trend of early maximum growth (at 15 h) was seen in all cefamandole replicates. This might indicate that the small benefit of increased export was competing with the negative effect of AgNP surface attachment. That is, there was an apparent survival benefit of pre-exposure through an export mechanism, but residual AgNPs attached to the surface might have inflicted damage that cefamandole could exploit. This is supported by the observed atypical growth curve.

Lincomycin showed only minor export attributable across all export systems (Masuda et al. 2000) such that any modification of porin or export pump transcription might have limited effect on lincomycin activity. Of the antibiotics showing no change in resistance, ofloxacin had the greatest attribution of resistance derived from efflux pump transcription. This is the only antibiotic that did not follow trends that could be explained by MEP expression, suggesting additional mechanisms might exist that could limit the effect of ofloxacin under the conditions tested.

Interestingly, polymyxin B, which is a cationic polypeptide targeting the outer membrane of the bacterial envelope (Fernandez et al. 2010), did not show a decrease in toxicity, similar to carbenicillin. Carbenicillin, a ß-lactam acting at the peptidoglycan layer in the periplasm is distinctly different than the outer membrane action of polymyxin B.

Stress from AgNP exposure was localized to the periplasm (Figure 4.8) where the peptidoglycan layer exists. The differential toxicological response to the two antibiotics, carbenicillin and polymyxin B also supports the hypothesis of localization of AgNP stress in the periplasm; it also suggests why AgNP pre-exposure stress carryover could cause a decrease in resistance to carbenicillin but have no effect on polymyxin B.

In total, three antibiotics with decreased sensitivity as a result of pre-exposure of cells to AgNPs showed some attributable relation to MexAB export, and three antibiotics without decreased sensitivity showed no relationship. Thus, it is likely that MexAB was a factor in decreased susceptibility to antibiotics through a potential efflux mechanism. MexAB might have also played a role in mitigation of AgNP toxicity.

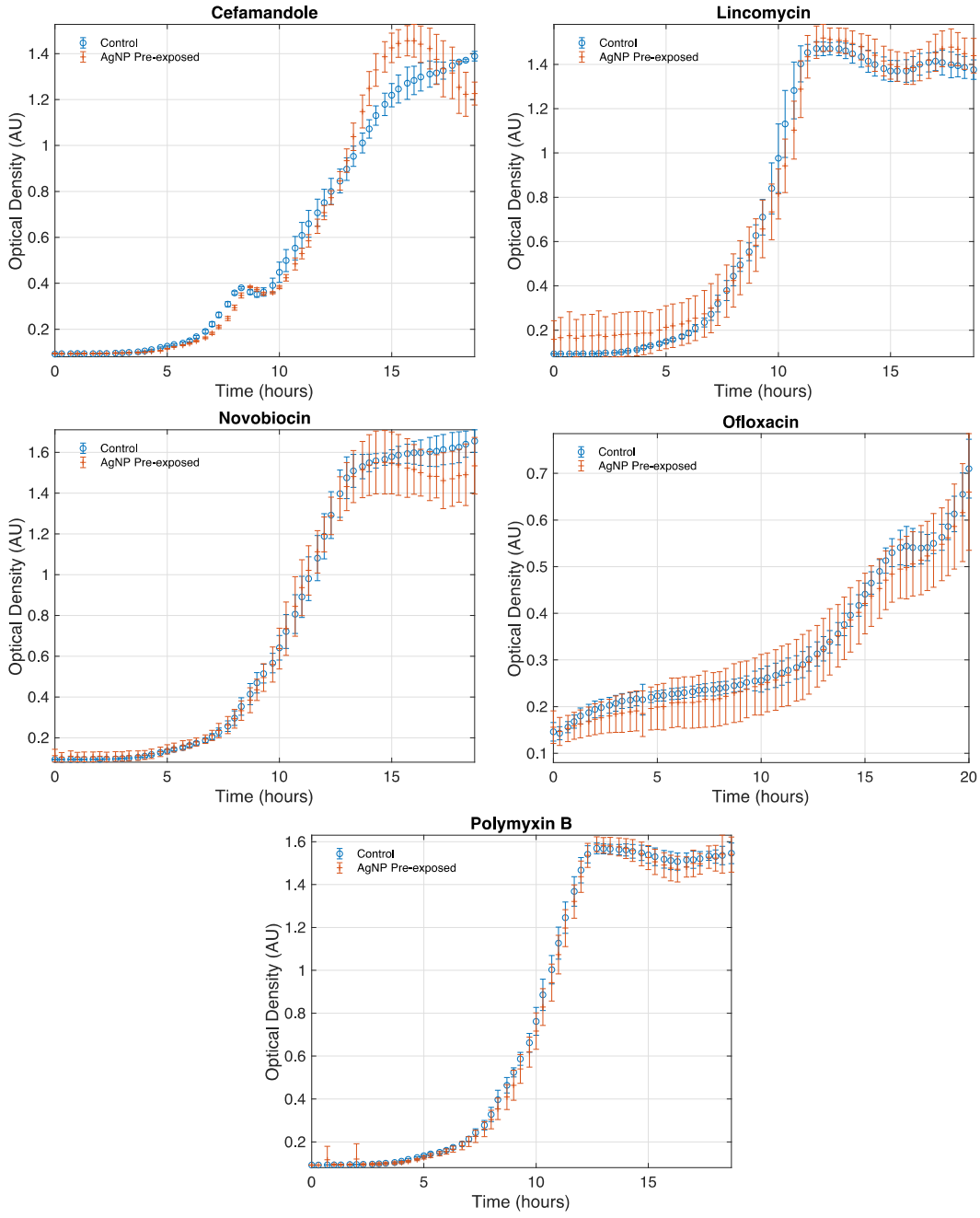

(caption on next page)

Figure 6.12. **Antibiotic exposed conditions with no change in resistance as a result of AgNP pre-exposure.** A separate aliquot of either negative (no AgNP pre-exposure) or positive (AgNP pre-exposed *P. aeruginosa* PAO1) controls were challenged in an antibiotic resistance assay. Bacteria were grown in MH medium. Data are the averages of eight technical replicates for biological duplicates. Doubling times of bacterial growth were calculated in mid-log using R.

6.4.7 Efflux pump mutants AgNP tolerance

The relationship between RND MEPs, specifically MexAB, CD and XY, and $Ag_{(aq)}$ and AgNP resistance was investigated. These experiments were conducted by exposing over-expressing pump mutants and deletion mutants to GLD_{50}, the dose of stressor reducing growth by 50% as compared to control cells (no AgNP exposure). The GLD_{50} for $Ag_{(aq)}$ was determined to be 1.1 µg/L $AgNO_3$ (Figure 6.13). The GLD_{50} AgNP, determined from the previously conducted GLD_5 study (Figure 6.6), was 5 µg/L.

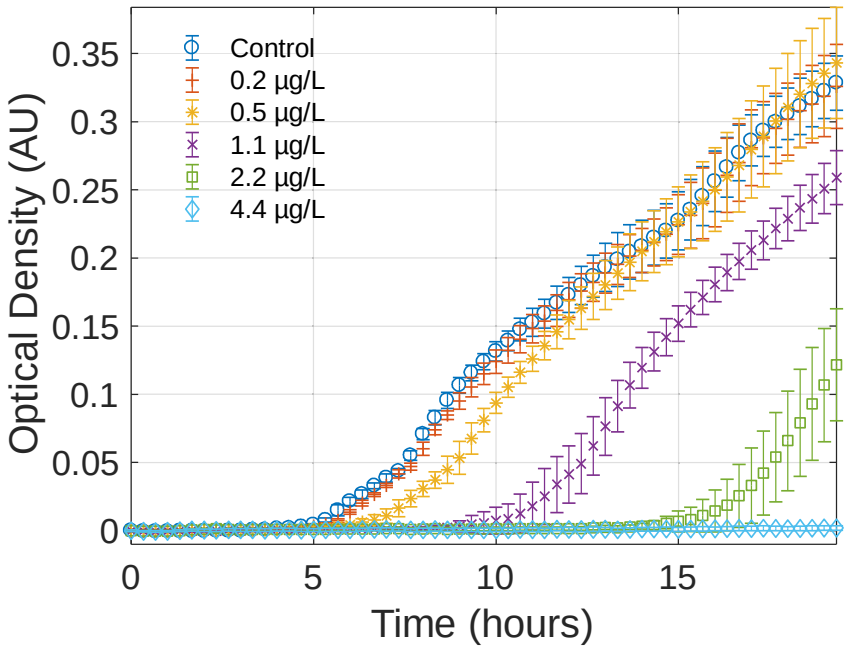

Figure 6.13 **$Ag_{(aq)}$ GLD_{50} determination.** *P. aeruginosa* PAO1 was exposed to $Ag_{(aq)}$ (0-4.4 µg/L) for 20 h. Eight technical replicates and two biological replicates were averaged for each data set. The observed GLD_5 was at 4 µg/L dosage of AgNPs. This occurred approximately 7 h after inoculation.

All mutant strains grew with the same advantage as compared to the parent strain (KP767) (Figure 6.14). These results suggest that overexpression of the *mexAB* and *mexXY* system alone is insufficient to increase resistance to AgNPs or $Ag_{(aq)}$ and that there is likely no pump metal export. Ag stress has been linked to MexAB with respect to *czcABC*. *P. aeruginosa* mutants isolated in a burn ward with high silver resistance harbored gene clusters linking silver resistance to a homologous protein of CzcCBA (Silver et al. 1999). It is possible that while constitutive expression of RND efflux pumps MexAB, CD, or XY can provide resistance to antibiotics, increased silver resistance could come from another cellular component. Further, the difference between the parent strain and mutants could derive from inherent resistance due to the transposon itself.

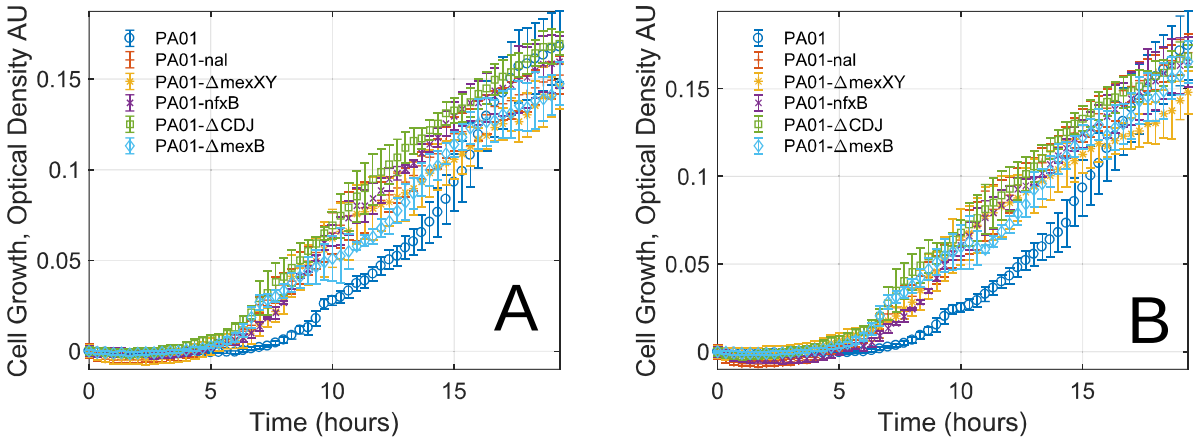

Figure 6.14. **Resistance of efflux-pump mutants to $Ag_{(aq)}$ and AgNPs**. *P. aeruginosa* efflux pump mutants were grown in MD medium for 30 h in the presence of (A) $Ag_{(aq)}$ or (B) AgNPs. Mutants were derived from wild type parent strain PAO1, K767. PAO1-nal constitutively expressed efflux pump MexXY; the corresponding knockout mutant, PAO1-Δ*mexXY*, was deficient in efflux pump MexXY. Mutant PAO1-nfxB constitutively expressed efflux pump MexCDJ and the corresponding knockout mutant, PAO1-Δ*mexCDJ*, was deficient in efflux pump MexCDJ.

6.5 Conclusions and Summary

The hypothesis of chapter 6 was *P. aeruginosa* pre-exposed to AgNPs will induce stress response systems leading to antibiotic resistance. This hypothesis is based on data presented in Chapters 4 and 5 that indicate the model of bacterial-AgNP interaction stimulates stress response systems in the periplasm and generates ROS (Figure 4.7), and that AgNPs induced the expression of several key antibiotic resistance systems associated with aminoglycoside, macrolide, and quinolone stress response (Figure 5.6). A summary of the interaction of these systems can be found in Figure 7.1, and a summary of all systems is included in Appendix A. The data observed in Chapter 6 validate this hypothesis, illustrating that AgNPs can cause stress that produces antibiotic resistance. Data indicated that AgNP stress was sufficient to induce antibiotic resistance to nalidixic acid and

kanamycin (Figure 6.11). Exposure to AgNPs resulted in greater susceptibility to carbenicillin (Figure 6.11) potentially resulting from increased periplasmic stress caused by AgNP exposure (Figure 4.8). No change in resistance was observed for five additional antibiotics. An overview of antibiotic resistance to selected antibiotic is summarized in Figure 6.15. Resistance might have been derived from expression of the RND efflux pumps, MexAB, MexXY, MexGHI, or other MEPs. AgNP stimulated production of cellular H_2O_2 could oxidize exposed cysteine groups on the MgrA family regulator, MexR, resulting in inhibition of negative regulatory control of Mex export systems controlling MexXY and MexAB (Adewoye et al. 2002). AgNP stimulation of MEP MexPQ (Figure 5.6) might have also contributed to the increased resistance given its associated export of quinolones like nalidixic acid.

Interestingly, decreased susceptibility as a result of bacterial pre-exposure to AgNPs was observed for an envelope-targeting antibiotic (i.e., carbenicillin). This unexpected result might indicate that export systems could not overcome surface stress cause by AgNP. A second cell envelope-targeting antibiotic, polymyxin B, which targets the outer membrane and affects endotoxin and lipid integrity, had no change in toxicity as a result of bacterial pre-exposure to AgNPs. This target is substantially different than the periplasmic location of action of carbenicillin, which supports the idea that AgNPs cause periplasmic stress (Figure 4.8). While the overall result of AgNP pre-exposure was not a pan-resistant bacterium, the evidence does support increased resistance to certain antibiotics resulting from AgNP pre-exposure. This is troubling in light of the increased use of AgNPs in consumer goods (Vance et al. 2015), particularly in the health care setting (Li et al. 2006; Lo et al. 2009).

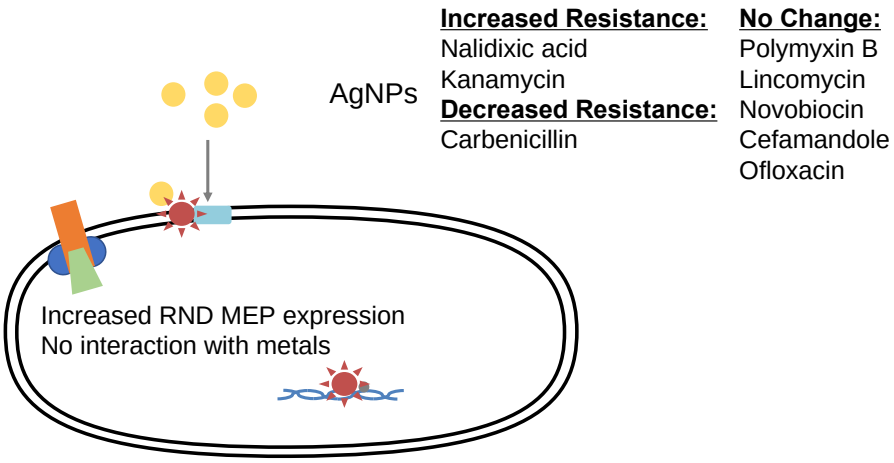

Figure 6.15 **Summary of antibiotic resistance derived from pre-exposure to AgNPs.** *P. aeruginosa* showed increased resistance to two antibiotics (e.g., nalidixic acid and kanamycin) while decreasing resistance to the envelope-targeting antibiotic carbenicillin. An additional envelope-targeting antibiotic polymyxin did not show any change in toxicity indicating that there might not have been significant surface stress under the tested conditions.

Resistance to kanamycin is not particularly worrisome because its usage was discontinued in humans due to side effects including cochlear damage (Tepper et al. 1980). Nalidixic acid, however, is used for treatment of urinary tract infections and dysentery in humans (Aventis 2008). Thus, the development of antibiotic resistance to nalidixic acid due to AgNP pre-exposure is potentially problematic. AgNPs and silver-coated catheters are now seeing increased use in hospitals (Roe et al. 2008). With antimicrobial-resistant, community-acquired urinary tract infections on the rise (Gupta et al. 2001), the placement of AgNP-coated structures near the site of infection might stimulate antibiotic resistance and limit treatment options.

Carbenicillin-challenged bacteria might have responded with increased susceptibility to antibiotics as result of accrued envelope damage resulting from AgNP pre-

exposure. This result is promising as it indicates that some antibiotic/nanoparticle combinations might improve treatment options. Further, it has been corroborated in a study finding that combinational AgNP – antibiotic treatment led to increased toxicity of bacteria and that the combination of AgNPs and antibiotics showed 80% more toxicity with tetracycline and enoxacin (Deng et al. 2016). In that study, combinatorial therapy was administered co-incidentally, (i.e., drugs and AgNPs were administered at the same time). When administration was co-incidental the two stressors compounded stress and resulted in higher toxicity (Singh et al. 2017). The focus of the current study did not specifically look at the effects of antibiotic binding to AgNPs for improved delivery. Coupling antibiotic dosing and AgNP pre-exposure to physiochemical AgNP attributes (e.g., such as the aggregation state, or fractal dimension (Chapter 3) could lead to strides in enhancing the toxicity of combinatorial AgNP-antibiotic treatments.

Decreased options for treatment have given rise to antibiotic stewardship plans, strategies for increasing the lifespan of exiting antibiotics by limiting the development of resistance (Owens 2008; Lee et al. 2013). Currently, these strategies do not incorporate the interaction of other materials in hospital settings nor do they extend to waste and water treatment strategies. Future plans should incorporate broader antibiotic and material interactions with stress response systems that possibly lead to co-and cross-resistance pathways like those found in this study. Alternative therapies may provide comparable outcomes with lower risk than small molecule target inactivation, the paradigm of current treatment strategies. Rapidly customizable treatment options such as micro RNA therapy could provide a path forward.

7. Conclusions and future work

7.1 SUMMARY

Silver nanoparticles (AgNPs) are finding widespread use in consumer goods, primarily because of their biocidal action (Sondi 2004; Vance et al. 2015). AgNPs are used to inhibit biological souring of clothing (Lee et al. 2007), prevent biofouling in engineered systems (Dror-ehre et al. 2010), and maintain sterility of surgical equipment in the health care setting (Li et al. 2006; Roe et al. 2008). Enhanced material function comes at a cost, however; AgNPs have the potential to enter wastewater systems and the environment (Benn et al. 2008), potentially disrupting biological systems (Liang et al. 2010). Understanding the mechanisms controlling the toxicity of AgNPs is key to limiting these environmental effects. The model of bacterial-AgNP interaction has been disputed, with two competing models in play. The first model of interaction holds that AgNP toxicity is a function of ionic silver (Ag^+) release and controlled by aqueous chemistry (Z.-M. Xiu et al. 2012); the second model of interaction proposes that AgNPs bind to the surface of bacteria and disrupt the cellular envelope (Long et al. 2017; Morones et al. 2005). Both models of interaction can exert mechanisms of action that cause protein oxidation, protein misfolding, and disrupt cellular envelope integrity. In all cases, the mechanisms of action of AgNPs (e.g., protein oxidation, protein misfolding stress, and cellular envelope disruption) are very similar to those of antibiotics, which are natural or synthetic compounds used to treat infections (Storz et al. 2011; Lin et al. 2015; Maillard et al. 2013). Antibiotic resistance can result from the expression of bacterial stress response systems (Li et al. 2007; Kohanski, DePristo, et al. 2010) and co- selective pressures, two stressors whose stress can be mitigated through either the same genetic pathway or protein (e.g., AgNPs and antibiotics) (Baker-Austin et al. 2006). Thus, interactions of AgNPs with

antibiotic stress response systems might give rise antibiotic resistance and must be investigated.

The objectives of this work were as follows:

1. Characterize the effect of solution chemistry, including chloride concentration and ionic strength, on AgNP morphology, dissolution, and toxicity to bacteria.
2. Build a biomolecular model that describes how AgNPs interact with bacteria.
3. Build a biomolecular model that describes the potential for $Ag_{(aq)}$ and AgNPs to induce co- and cross-resistance to antibiotics.
4. Evaluate AgNP cross-resistance to a series of eight antibiotics.

Efforts to characterize the impact of physical and chemical parameters on AgNP toxicity were completed in Chapter 3. The study was broken into three parts: morphology, toxicity, and stress response. Each part was evaluated with a focus on either the role of ionic strength or chloride. Morphology was studied by examining four particle characterization features: dissolution, surface plasmon resonance, aggregation, and fractal dimension. Aggregation was not significantly impacted by ionic strength, but it was increased in higher chloride media. An increase in ionic strength was found to dramatically decrease the fractal dimension of aggregates, driving aggregates from a fractal dimension of 0.5 in a 150 mM ionic strength solution to 2.4 in 40 mM ionic strength. Dissolution was greatest in the presence of media containing chloride. The greatest overall dissolution occurred in the Hμ140 (highest ionic strength, 140 mM chloride) medium. Dissolution also increased with higher ionic strength, but not as significantly as the case with higher chloride media. This indicates a possible ligand-promoted dissolution mechanism in the

destabilization of AgNPs within the first 10 minutes of medium exposure. Surface plasmons yielded the most stable peaks (λ = 394 nm) in low ionic strength and low chloride media, suggesting that the most stable particles were found in these conditions. Toxicity substantially increased in higher ionic strength media but decrease as the chloride concentration increased. Chloride might limit the toxicity of AgNPs through the formation of an AgCl shell around the particles and also through $Ag_{(aq)}$ coordination with Cl^-, which resulted in negatively charged complexes with a lower probability of migrating through the electric double layer. In total, chloride promoted the formation of large, non-toxic aggregates, while higher ionic strength increased toxicity by forming branched aggregates of semi-stable nanoparticles. This is likely caused by an increased probability of AgNP interactions with bacteria due to an increased aggregate surface area as compared to less branched aggregates. The relative activation of the stress response gene *katE,* encoding a catalase, was greatest in higher ionic strength media, confirming that the toxicity of AgNPs is greatest in medium ionic strength media without $Ag_{(aq)}$-scavenging ligands present.

Chapter 4 proposed a biomolecular model describing a surface-attachment mechanism for AgNPs that is substantially different from the activity of $Ag_{(aq)}$ for specific tested water chemistry conditions. AgNPs were exposed to bacteria in a 40 µM ionic strength solution. Four characteristic stress response systems were evaluated in the construction of this model: the periplasmically localized copper stress response pathway, CopAB, and reactive oxygen species response pathway, KatAB*;* the periplasmically and cytoplasmically localized stress response system, CzcABC*;* and the cytoplasmically localized drug and metal efflux system, MuxABC. Transcriptomic data indicated that the localization of the stress response system was crucial in determining in which of the two stressors, AgNPs or $Ag_{(aq)}$, activated that specific stress response system. AgNPs activated periplasmically localized stress response systems, specifically CopAB, and KatAB. Data

suggested that the copper stress response systems had sufficient substrate flexibility to respond to silver and quenching of peroxide stress was significantly higher in the periplasm by KatAB. Cytoplasmically localized KatD showed no differential activation btween $Ag_{(aq)}$ and AgNPs. Both AgNPs and $Ag_{(aq)}$ activated the metal stress response system, CzcABC; a unique export pump primarily loaded from the periplasm but also from the cytoplasm. Induction of CzcABC was roughly 0.5-log units greater with AgNPs than with $Ag_{(aq)}$; however, the pump would primarily have substrate loaded in the periplasm. The expression of the asymmetric cytoplasmically localized pump MuxABC was induced only in the presence of $Ag_{(aq)}$. Thus, the localization of AgNP-induced stress response systems tended to be in the periplasm, while $Ag_{(aq)}$ stress tended to be in the cytoplasm. These results support a surface-attachment model for AgNPs under the tested water chemistry conditions.

Chapter 5 examined the potential of AgNPs and $Ag_{(aq)}$ to induce antibiotic resistance gene clusters in *P. aeruginosa*. A bioinformatics approach was used to screen for expression of differentially expressed biochemical pathways after exposure to sublethal doses of AgNPs and $Ag_{(aq)}$ in a 40 µM ionic strength solution. A transcriptomic and proteomic approach was used in this study. The induction of a series of resistance nodulation division (RND) efflux pumps closely associated with multidrug resistant bacteria were examined through transcriptomics, and the translational output of these up-regulations also were examined. Additionally, the down-regulation of DNA repair systems was observed for both stressors. $Ag_{(aq)}$ increased the expression of genes encoding three multidrug efflux pump systems (MEPs): *mexAB, mexXY,* and *muxABC*. Each of these are associated with aminoglycoside antibiotic resistance, likely stimulated by an oxidation sensory system interaction with $Ag_{(aq)}$. AgNPs induced a differential set of genes encoding MEPs, *mexGHI* and the recently discovered *mexPQ,* which are associated with macrolide

and aminoglycoside resistance. AgNPs and $Ag_{(aq)}$ induce the expression of two specific stress response systems: the triclosan *triABC* system and the aminoglycoside *amgRS* and PA5528 system, respectively. This indicated that there was not only a broad antibiotic resistance response, but also that specific antibiotic systems were induced as well, directly linking AgNP and $Ag_{(aq)}$ stress to antibiotic resistance stress response systems. Proteomics data indicated that several systems, including MexABC, AmgRS, and penicillin binding protein B, were translated. Expression of DNA repair systems were decreased in the presence of AgNPs, signaling possible increases in mutation rates. This down regulation could lead to mutational resistance events.

Chapter 6 illustrates concretely with microbiological evidence that AgNPs can induce antibiotic resistance in *P. aeruginosa.* Antibiotic resistance genes were stimulated during a pre-exposure phase in which *P. aeruginosa* was challenged to grow in the presence of a 4 μg/L "growth-limiting dosage" of AgNPs, while a control group of bacteria was allowed to grow in the absence of AgNPs. After 5 hours of growth in the presence of AgNPs, the biocidal activity of AgNPs was quenched with cysteine, and bacteria were transferred to a second growth assay, during which they were challenged with antibiotics for 20+ hours. Eight antibiotics were chosen to examine the development of antibiotic resistance caused by AgNP pre-exposure. Three antibiotics, nalidixic acid, kanamycin, and carbenicillin, showed differential impacts on the growth of *P. aeruginosa* after pre-exposure to AgNPs. *P. aeruginosa* was more resistant to nalidixic acid and kanamycin, but less resistant to carbenicillin as compared to a culture of bacteria not pre-exposed to AgNPs. These studies indicate that AgNPs can cause antibiotic resistance. A summary of the interactions of $Ag_{(aq)}$ and AgNPs with bacteria and their potential to cause antibiotic resistance is provided in Figure 7.1. This figure traces the surface- attachment model of

interaction and subsequent mechanisms of action by which AgNPs can cause toxicity to bacteria. The figure also describes how bacterial stress response systems integrate this information and elicit an antibiotic resistance response following $Ag_{(aq)}$ and AgNP exposure.

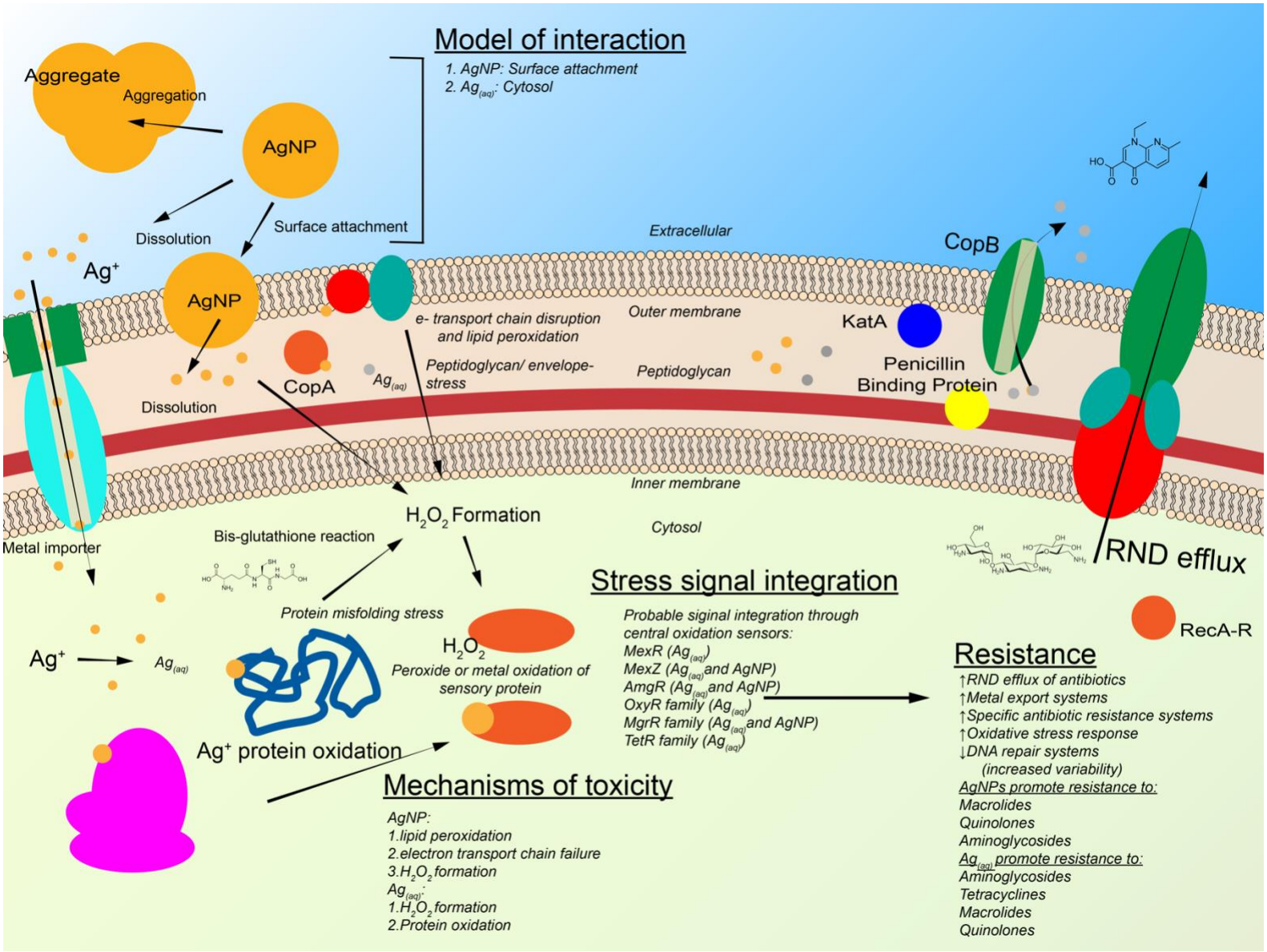
Model of interaction
1. AgNP: Surface attachment
2. Ag(aq): Cytosol
Aggregate
Aggregation
AgNP
Dissolution
Surface attachment
Ag+
AgNP
Extracellular
CopB
e- transport chain disruption and lipid peroxidation
Outer membrane
KatA
Peptidoglycan/ envelope-stress
Peptidoglycan
Penicillin Binding Protein
CopA
Ag(aq)
Dissolution
Inner membrane
H2O2 Formation
Cytosol
Metal importer
Bis-glutathione reaction
RND efflux
Stress signal integration
Protein misfolding stress
Probable siginal integration through central oxidation sensors:
MexR (Ag(aq))
MexZ (Ag(aq) and AgNP)
AmgR (Ag(aq) and AgNP)
OxyR family (Ag(aq))
MgrR family (Ag(aq) and AgNP)
TetR family (Ag(aq))
RecA-R
Ag+
Ag(aq)
H2O2
Peroxide or metal oxidation of sensory protein
Resistance
↑RND efflux of antibiotics
↑Metal export systems
↑Specific antibiotic resistance systems
↑Oxidative stress response
↓DNA repair systems
(increased variability)
AgNPs promote resistance to:
Macrolides
Quinolones
Aminoglycosides
Ag(aq) promote resistance to:
Aminoglycosides
Tetracyclines
Macrolides
Quinolones
Ag+ protein oxidation
Mechanisms of toxicity
AgNP:
1.lipid peroxidation
2.electron transport chain failure
3.H2O2 formation
Ag(aq):
1.H2O2 formation
2.Protein oxidation

Figure 7.1 **Summary of potential mechanisms of AgNP- and $Ag_{(aq)}$-directed formation of antibiotic resistance under tested water chemistry conditions**. AgNPs interact with the bacterial cell by means of a surface-attachment model of interaction. Here it is proposed that AgNPs partially dissolve into the periplasm and release high doses of Ag^+ into the periplasm. AgNPs can also corrode in solution and can release Ag^+ and $Ag_{(aq)}$ species into solution, which can elicit a toxic cellular response. AgNPs cause toxicity through a series of mechanisms of toxicity. These mechanisms are lipid peroxidation in the periplasm, ROS formation, and electron transport chain failure. $Ag_{(aq)}$ has the potential to oxidize proteins and form ROS species, namely, H_2O_2. All of these stress mechanism are likely integrated through a central set of stress response sensors responding to oxidation, either by metals or by H_2O_2. These sensors ultimately result in an antibiotic resistance response in the cell. AgNP-exposure increases expression of resistance gene clusder for resistance to macrolides, quinolones, and aminoglycosides, and $Ag_{(aq)}$-exposure increases expression of resistance gene clusters for resistance to aminoglycosides, tetracyclines, penicillins, macrolides, and quinolones.

7.2 IMPLICATIONS

This research has addressed several deficiencies of AgNP toxicology research, illustrating that bulk solution processes can have substantial impacts on AgNP toxicity. Bulk solution processes involving ligands can control the toxicity of AgNPs and affect their morphology. Morphological differences also impact and can direct AgNP toxicity. That the fractal dimension (i.e., the extent of aggregate branching) of AgNP aggregates can influence toxicity implicates a surface-attachment model wherein AgNPs must make contact with the surface of a cell to elicit a toxic response when conditions do not support rapid bulk dissolution. Additional transcriptomic data support this finding and illustrate that AgNPs likely cause periplasmic stress, while $Ag_{(aq)}$ tends to act through cytoplasmic toxicity mechanisms. These data imply that AgNP toxicity can be directed through surface modification of the nanoparticle. Particles designed to better interact with bacterial surface functional groups might have increased toxicity. If limitations to toxicity are sought, surface chelation molecules can be designed that either force dissolution or block particle access to bacteria could be beneficial.

The greatest implications of this work are related to antibiotic resistance. With clear evidence of the induction of antibiotic resistance and subsequent formation of antibiotic resistance, the inclusion of AgNPs in consumer goods should not go unregulated. Potential access to the environment and their inclusion in hospital settings indicates that AgNPs could be a source of risk in engineered and environmental systems. Further evidence of generalized antibiotic resistance mechanisms linking metal stress and oxidative stress to

the induction of antibiotic resistance are cause for concern; thus, waste treatment should seek to separate metal waste and biological treatment, unless directly necessary.

7.3 FUTURE WORK

The biomolecular model of bacterial AgNP interaction under tested water conditions indicates periplasmic stress response is clear evidence of a surface attachment mechanism of antibiotic resistance. With this, clearer data should be sought to illustrate this surface interaction in greater detail, possibly by examining the dissolution and speciation of AgNPs. Use of soft transmission x-ray microscopy (STXM), coupled with statistical analysis, can give information on the oxidation state of silver particulates near the periplasm in 20 nm resolution. Oxidation state changes in AgNPs and the precipitation of silver metal or silver oxide in the periplasm would provide clear evidence of an oxidative stress response derived from the monooxygenase CopA. Furthermore, these data could physically show the interactions of AgNPs at the surface.

In addition, the dynamics of the two bacterial AgNP interaction models, that is the dissolution model of interaction and the surface attachment model, could be reconciled into a single model of interaction. If experiments were conducted under AgNP-dissolution promoting conditions, $Ag_{(aq)}$ might overtake the action of AgNP surface-attachment and the genetic response of bacteria exposed to AgNPs should more closely mirror that of bacteria exposed to $Ag_{(aq)}$. Reverse transcription, real-time, quantitative polymerase chain reaction (RT-qPCR) examining the expression of *copAB, katAB, muxABC,* and *czcABC* genes in destabilizing conditions for AgNPs could be used to clearly illustrate when the bulk dissolution model overtakes the surface attachment model.

Antibiotic resistance data clearly indicated *P. aeruginosa* was able to adapt to AgNP and Ag stresses through expression of MEPs. Future work should focus on the regulation of these pumps and their activation of as a result of metal exposure. Oxidation sensing stress response regulators could be activated by oxidation by metal species or formation of metal adducts imparing DNA binding. Metal adducts with proteins or oxidized polypeptide chains should exist that provide evidence of which regulators, and thus, what antibiotics are susceptible to this action. Modern mass spectrum proteomics is now capable of measuring polypeptide oxidation and should be used to provide evidence of the activity of this mechanism.

The effect of physiochemical parameters (e.g., aggregation, fractal dimension, and dissolution) should be examined more closely with respect to the induction of antibiotic resistance gene clusters. RND efflux pumps might respond with greater upregulation under conditions promoting AgNP corrosion and release of Ag^{+}. Varying the exposure medium to either increase AgNP corrosion or increase AgNP aggregation would further elucidate the role of AgNPs in the development of antibiotic resistance. Further experiments should examine the role of metal ions in activation of antibiotic resistance gene clusters; variations in metals by either their softness (a term describing the acidity of the metal) or by metal ion radius could further implicate metals in the activation of antibiotic resistance genes and provide valuable information about the interaction of metals with stress response sensory active sites.

Further work should also focus on how to normalize the dosage of $Ag_{(aq)}$ and AgNP in the context of stress. In these experiments conducted as part of this dissertation, the dosage of the two stressors, $Ag_{(aq)}$ and AgNPs was normalized by chosing a condition at which 1% cell death occurred (sections 4.1.9 and 5.1.18). Cell death was used to establish sublethal dosages used to induce a stress response (section 4.2.5). A competing

normalization proceedure could induce stress normalized by total dosed silver. In such an experiment, a dosage of 1.5 µg/L of silver, roughly equally death at 50%, would challenge $Ag_{(aq)}$ and AgNP exposed cells with the same total amount of Ag so that equivalent silver amount of toxicant is used and the relative amount of stress induction could be queried. A series of key stress response systems (KatE, CopA, CzcABC, and MuxAB) could be investigated with a reverse transcription quantitative polymerase chain reaction, quantifying stress response induction by amount of total silver. This would ensure that the observed response is not a function of a dose but rather directly because of the model of interaction.

8. Appendix A. Summary of stress response system in this dissertation

Summary of key stress response system described in this dissertation

MexAB	RND efflux pump exporting aminoglycosides and quinolones
MexXY	RND efflux pump exporting aminoglycosides, tetracyclines, and quinolones
CzcABC	RND efflux pump exporting cadmium, copper, and zinc
MuxABC	RND efflux pump exporting metals, macrolides, and quinolones
MexGHI	RND efflux pump exporting vanadium, macrolides, and quinolones
MexPQ	RND efflux pump exporting copper, macrolides, and quinolones
CopAB	Copper stress system containing a copper monooxygenase and P-type APTase pump
KatABEN	Reactive oxygen species stress response system encoding catalases to convert peroxide to water
RecA-R	DNA repair system with single strand integration and backfill repair
MutLS	DNA repair system using methlyation repair
PBP	Penicillin binding protein
TriABC	RND efflux pump exporting triclosan

The following code should generate a heat map with an attached dendrogram as well as a principal component analysis with an applied hierarchical model superimposed. A superimposed neural net is also possible.

```
%AgNPval=importdata('control_v_AgNP.csv');
%AgVal=importdata('control_v_Aqueous_Ag.csv');
```

```
norm=importdata('Normailized_counts.csv');%imports the normalized data
set

mean_norm=ones(length(norm.data(:,1)),3);%creates a matrix of ones that
is the length of


for ix=1:length(norm.data(:,1))% feeds each of the subsets into the
matrix of ones that will be fed the averaged values
    mean_norm(ix,:)=[mean(norm.data(ix,1:6)), mean(norm.data(ix,7:12)),
mean(norm.data(ix,13:18))];
end

lognorm=ones(length(norm.data(:,1)),2); %creates a matrix of ones
(length of data x 2) that will be used to feed the control normalized
data

for ix=1:length(norm.data(:,1))%feeds the control normalized data into
the new matrix
    lognorm(ix,:)=[mean_norm(ix,3)/mean_norm(ix,1),
mean_norm(ix,2)/mean_norm(ix,1)];
end

log2norm=log2(lognorm);% takes the log2 of the data and produces the
working dataset
genenames=norm.textdata(2:length(norm.textdata(:,1)),2);%cell array of
gene names


%__----------------------UNCOMMENT HERE_________

% this will examine gene expression and gene name list and
%remove any non-number entries including inf
%-------------------------------------------
nanIndices=any(isnan(log2norm),2);
log2norm(nanIndices,:)=[];
genenames(nanIndices)=[];

infIndices=any(isinf(log2norm),2);
log2norm(infIndices,:)=[];
genenames(infIndices)=[];

%Ok... lets filter some more - this will filter by variance, entropy
and
%lowvalue ADD MORE TO THIS see
https://www.mathworks.com/help/bioinfo/examples/gene-expression-
profile-analysis.html
%EDIT THIS TO INCLUDE MORE!
mask=genevarfilter(log2norm);%will create a mask of genes with small
variance
```

```
log2smallvar=log2norm(mask,:);
genessmal=genenames(mask);

[mask, log2smallvar, genessmal] =
genelowvalfilter(log2smallvar,genessmal,'AbsVal',1.5);%cuts low
expression genes
%[mask, log2smallvar, genessmal] = geneentropyfilter(log2smallvar,
genessmal,'prctile',15);%cuts genes with low entropy

%-----------Clustergrams-EDIT TO FINISH-----------------
%this will eventually make several clustergrams one for all genes and
one
%for unfiltered genes.
map1=clustergram(log2norm,'RowLabels',genenames,'ColumnLabels',{'Ag_a_q
' 'cAgNP'},'Colormap',redbluecmap);% for all genes
%for filtered genes
map2=clustergram(log2smallvar,'RowLabels',genessmal,'ColumnLabels',{'Ag
_a_q' 'cAgNP'},'Colormap',redbluecmap);% for only those with large
differences genes


%------------PCA with neural net-------------------
%this operates on the whole data set



[pc, zscores, pcvars]=pca(log2norm);
figure
pcclusters = clusterdata(zscores(:,1:2),'maxclust',8,'linkage','av');
gscatter(zscores(:,1),zscores(:,2),pcclusters)
xlabel('First Principal Component');
ylabel('Second Principal Component');
title('Principal Component Scatter Plot with Colored Clusters');

P = zscores(:,1:2)';
net = newsom(P,[4 4]);

net = train(net,P);

distances = dist(P',net.IW{1}');
[d,cndx] = min(distances,[],2); % cndx contains the cluster index

figure
gscatter(P(1,:),P(2,:),cndx); legend off;
hold on
plotsom(net.iw{1,1},net.layers{1}.distances);
hold off

Small data set plotting
```

```
% %this operates on the small data set
% [pc, zscores, pcvars]=pca(log2smallvar);
% figure
% pcclusters = clusterdata(zscores(:,1:2),'maxclust',8,'linkage','av');
% gscatter(zscores(:,1),zscores(:,2),pcclusters)
% xlabel('First Principal Component');
% ylabel('Second Principal Component');
% title('Principal Component Scatter Plot with Colored  Clusters for
Small Variance');
%
% P = zscores(:,1:2)';
% net = newsom(P,[4 4]);
%
% net = train(net,P);
%
% distances = dist(P',net.IW{1}');
% [d,cndx] = min(distances,[],2); % cndx contains the cluster index
%
% figure
% gscatter(P(1,:),P(2,:),cndx); legend off;
% hold on
% plotsom(net.iw{1,1},net.layers{1}.distances);
% hold off
```

9. References

Centers for Disease Control and Prevention. 2013. “Antibiotic Resistance Threats in the United States, 2013; US CDC.” doi:CS239559-B.

Adewoye, Lateef, Ainsley Sutherland, Ramakrishnan Srikumar, and Keith Poole. 2002. “The MexR Repressor of the mexAB-oprM Multidrug Efflux Operon in *Pseudomonas aeruginosa*: Characterization of Mutations Compromising Activity.” *Journal of Bacteriology* 184 (15): 4308–12. doi:10.1128/JB.184.15.4308-4312.2002.

Aeschlimann, Jeffrey R. 2003. “The Role of Multidrug Efflux Pumps in the Antibiotic Resistance of *Pseudomonas aeruginosa* and Other Gram-Negative Bacteria.” *Pharmacotherapy* 23 (7): 916–24. doi:10.1592/phco.23.7.916.32722.

Ahkami, Amir H., Richard Allen White, Pubudu P. Handakumbura, and Christer Jansson. 2017. “Rhizosphere Engineering: Enhancing Sustainable Plant Ecosystem Productivity.” *Rhizosphere* 3 (April). Elsevier: 233–43. doi:10.1016/j.rhisph.2017.04.012.

Akbar, Samina, Tatiana a Gaidenko, Choong Min CM Choong M I N Kang, Mary O’ Reilly, Kevin M Devine, Chester W Price, and Choong Min CM Choong M I N Kang. 2001. “New Family of Regulators in the Environmental Signaling Pathway Which Activates the General Stress Transcription Factor sB of Bacillus Subtilis.” *Journal of Bacteriology* 183 (4): 1329–38. doi:10.1128/JB.183.4.1329.

Alliance for the Prudent Use of Antibiotics. 2010. “The Cost of Antibiotic Resistance to U. S. Families and the Health Care System.” http://www.tufts.edu/med/apua/consumers/personal_home_5_1451036133.pdf.

Alvarez-Ortega, Carolina, Jorge Olivares, and José L. Martínez. 2013. “RND Multidrug Efflux Pumps: What Are They Good For?” *Frontiers in Microbiology* 4 (February): 1–11. doi:10.3389/fmicb.2013.00007.

Alvarez, Pedro J J, Vicki Colvin, Jamie Lead, and Vicki Stone. 2009. “Research Priorities to Advance Eco-Responsible Nanotechnology.” *ACS Nano* 3 (7): 1616–19. doi:10.1021/nn9006835.

Andersson, Dan I., and Diarmaid Hughes. 2014. “Microbiological Effects of Sublethal Levels of Antibiotics.” *Nature Reviews Microbiology* 12 (7). Nature Publishing Group: 465–78. doi:10.1038/nrmicro3270.

Andrews, S. 2010. “FastQCL a Quality Control Tool for High Throughput Sequence Data. Available Online at: Http://www.bioinformatics.babraham.ac.uk/projects/fastqc.” http://www.bioinformatics.babraham.ac.uk/projects/fastqc/.

Anes, João, Matthew P. McCusker, Séamus Fanning, and Marta Martins. 2015. “The Ins and Outs of RND Efflux Pumps in Escherichia Coli.” *Frontiers in Microbiology* 6 (JUN): 1–14. doi:10.3389/fmicb.2015.00587.

Anyaogu, Kelechi C., Andrei V. Fedorov, and Douglas C. Neckers. 2008. “Synthesis, Characterization, and Antifouling Potential of Functionalized Copper Nanoparticles.” *Langmuir* 24 (8): 4340–46. doi:10.1021/la800102f.

Apel, Klaus, and Heribert Hirt. 2004. “Reactive Oxygen Species: Metabolism, Oxidative Stress, and Signal Transduction.” *Annual Review of Plant Biology* 55 (1): 373–99. doi:10.1146/annurev.arplant.55.031903.141701.

Arakawa, H, Jf Neault, and Ha Tajmir-Riahi. 2001. “Silver(I) Complexes with DNA and RNA Studied by Fourier Transform Infrared Spectroscopy and Capillary Electrophoresis.” *Biophys J* 81 (3): 1580–87. doi:10.1016/S0006-3495(01)75812-2.

Asharani, P V, Yi Lian Wu, Zhiyuan Gong, and Suresh Valiyaveettil. 2008. “Toxicity of Silver Nanoparticles in Zebrafish Models.” *Nanotechnology* 19 (25): 255102. doi:10.1088/0957-4484/19/25/255102.

Aventis. 2008. “USP Nalidixic Acid Dosage Guide.” *United States Pharmacopiea*, 3–12.

Baalousha, M, Y Nur, I Römer, M Tejamaya, and J R Lead. 2013. “Effect of Monovalent and Divalent Cations, Anions and Fulvic Acid on Aggregation of Citrate-Coated Silver Nanoparticles.” *The Science of the Total Environment* 454–455 (June). Elsevier B.V.: 119–31. doi:10.1016/j.scitotenv.2013.02.093.

Badawy, Amro M El, Rendahandi G Silva, Brian Morris, Kirk G Scheckel, Makram T Suidan, Thabet M Tolaymat, Amro M E L Badawy, et al. 2011. “Surface Charge-Dependent Toxicity of Silver Nanoparticles.” *Environmental Science & Technology* 45 (1): 283–87. doi:10.1021/es1034188.

Bae, Eunjoo, Hee-Jin Jin Park, Jeongjin Lee, Younghun Kim, Jeyong Yoon, Kwangsik Park, Kyunghee Choi, and Jongheop Yi. 2010. “Bacterial Cytotoxicity of the Silver Nanoparticle Related to Physicochemical Metrics and Agglomeration Properties.” *Environmental Toxicology and Chemistry* 29 (10): 2154–60. doi:10.1002/etc.278.

Baker-Austin, Craig, Meredith S Wright, Ramunas Stepanauskas, and J V McArthur. 2006. “Co-Selection of Antibiotic and Metal Resistance.” *Trends in Microbiology* 14 (4): 176–82. doi:10.1016/j.tim.2006.02.006.

Balasubramanian, Deepak, Hansi Kumari, Melita Jaric, Mitch Fernandez, Keith H. Turner, Simon L. Dove, Giri Narasimhan, Stephen Lory, and Kalai Mathee. 2014. “Deep Sequencing Analyses Expands the *Pseudomonas aeruginosa* AmpR Regulon to Include Small RNA-Mediated Regulation of Iron Acquisition, Heat Shock and Oxidative Stress Response.” *Nucleic Acids Research* 42 (2): 979–98. doi:10.1093/nar/gkt942.

Barani, Hossein, Majid Montazer, Nasrin Samadi, and Tayebeh Toliyat. 2011. “Nano Silver Entrapped in Phospholipids Membrane: Synthesis, Characteristics and Antibacterial Kinetics.” *Molecular Membrane Biology* 28 (4): 206–15. doi:10.3109/09687688.2011.565484.

Benn, Troy M., and Paul Westerhoff. 2008. “Nanoparticle Silver Released into Water from Commercially Available Sock Fabrics.” *Environmental Science & Technology* 42 (11): 4133–39. doi:10.1021/es7032718.

Benz, Roland. 2006. *Bacterial and Eukaryotic Porins*. Edited by Johm Wiley & Sons. 1st ed. New York, NY.

Blanco, Paula, Sara Hernando-Amado, Jose Reales-Calderon, Fernando Corona, Felipe Lira, Manuel Alcalde-Rico, Alejandra Bernardini, Maria Sanchez, and Jose Martinez. 2016. “Bacterial Multidrug Efflux Pumps: Much More Than Antibiotic

Resistance Determinants." *Microorganisms* 4 (1): 14. doi:10.3390/microorganisms4010014.
Bradford, Adam, Richard D Handy, James W Readman, Andrew Atfield, and Martin Mühling. 2009. "Impact of Silver Nanoparticle Contamination on the Genetic Diversity of Natural Bacterial Assemblages in Estuarine Sediments." *Environmental Science & Technology* 43 (12): 4530–36. http://www.ncbi.nlm.nih.gov/pubmed/19603673.
Breidenstein, Elena B M, Bhavjinder K. Khaira, Irith Wiegand, Joerg Overhage, and Robert E W Hancock. 2008. "Complex Ciprofloxacin Resistome Revealed by Screening a *Pseudomonas aeruginosa* Mutant Library for Altered Susceptibility." *Antimicrobial Agents and Chemotherapy* 52 (12): 4486–91. doi:10.1128/AAC.00222-08.
Butler, Kenneth, Arthur R English, and Verne A Ray. 2017. "Carbenicillin : Chemistry and Mode of Action Author (S): Kenneth Butler , Arthur R . English , Verne A . Ray and A . E . Timreck Source : The Journal of Infectious Diseases , Vol . 122 , Supplement . Symposium on Carbenicillin : A Clinical Profile (Sep" 122.
Cabiscol, Elisa, Jordi Tamarit, and Joaquim Ros. 2000. "Oxidative Stress in Bacteria and Protein Damage by Reactive Oxygen Species." *International Microbiology* 3 (1): 3–8. doi:10.2436/im.v3i1.9235.
Caille, Olivier, Claude Rossier, and Karl Perron. 2007. "A Copper-Activated Two-Component System Interacts with Zinc and Imipenem Resistance in *Pseudomonas aeruginosa*." *Journal of Bacteriology* 189 (13): 4561–68. doi:10.1128/JB.00095-07.
Calomiris, Jon J., John L. Armstrong, and Ramon J. Seidler. 1984. "Association of Metal Tolerance with Multiple Antibiotic Resistance of Bacteria Isolated from Drinking Water." *Applied and Environmental Microbiology* 47 (6): 1238–42.
Cardenal-Muñoz, Elena, and Francisco Ramos-Morales. 2013. "DsbA and MgrB Regulate steA Expression through the Two- Component System PhoQ/PhoP in Salmonella Enterica." *Journal of Bacteriology* 195 (10): 2368–78. doi:10.1128/JB.00110-13.
Carlson, C, S M Hussain, a M Schrand, L K. Braydich-Stolle, K L Hess, R L Jones, J J Schlager, et al. 2008. "Unique Cellular Interaction of Silver Nanoparticles: Size-Dependent Generation of Reactive Oxygen Species." *The Journal of Physical Chemistry B* 112 (43): 13608–19. doi:10.1021/jp712087m.
Castranova, Vincent, Bahman Asgharian, Phil Sayre, West Virginia, and North Carolina. 2016. "HHS Public Access" 98 (2): 1922–2013. doi:10.1080/10937404.2015.1051611.INHALATION.
Chacón, Kelly N, Tiffany D. Mealman, Megan M. McEvoy, Ninian J. Blackburn, K. N. Chacon, Tiffany D. Mealman, Megan M. McEvoy, and Ninian J. Blackburn. 2014. "Tracking Metal Ions through a Cu/Ag Efflux Pump Assigns the Functional Roles of the Periplasmic Proteins." *Proceedings of the National Academy of Sciences of the United States of America* 111 (43): 15373–78. doi:10.1073/pnas.1411475111.
Chaloupka, Karla, Yogeshkumar Malam, and Alexander M. Seifalian. 2010. "Nanosilver as a New Generation of Nanoproduct in Biomedical Applications." *Trends in*

Biotechnology 28 (11). Elsevier Ltd: 580–88. doi:10.1016/j.tibtech.2010.07.006.
Chambers, Bryant a., A. R M Nabiul Afrooz, Sungwoo Bae, Nirupam Aich, Lynn Katz, Navid B. Saleh, and Mary Jo Kirisits. 2014. "Effects of Chloride and Ionic Strength on Physical Morphology, Dissolution, and Bacterial Toxicity of Silver Nanoparticles." *Environmental Science and Technology* 48 (1): 761–69. doi:10.1021/es403969x.
Chatterjee, Arijit Kumar, Ruchira Chakraborty, and Tarakdas Basu. 2014. "Mechanism of Antibacterial Activity of Copper Nanoparticles." *Nanotechnology* 25 (13): 135101. doi:10.1088/0957-4484/25/13/135101.
Chen, Hao, Jie Hu, Peng R Chen, Lefu Lan, Zigang Li, Leslie M Hicks, Aaron R Dinner, and Chuan He. 2008. "The *Pseudomonas aeruginosa* Multidrug Efflux Regulator MexR Uses an Oxidation-Sensing Mechanism." *Proceedings of the National Academy of Sciences of the United States of America* 105 (36): 13586–91. doi:10.1073/pnas.0803391105.
Chen, Sihai, and Keisaku Kimura. 1999. "Water Soluble Silver Nanoparticles Functionalized with Thiolate." *Chemistry Letters* 28 (11). [Tokyo]: Chemical Society of Japan, 1972-: 1169–70. doi:10.1246/cl.1999.1169.
Chen, X., and H. J. Schluesener. 2008. "Nanosilver: A Nanoproduct in Medical Application." *Toxicology Letters* 176 (1): 1–12. doi:10.1016/j.toxlet.2007.10.004.
Choi, O K, and Z Q Hu. 2009. "Nitrification Inhibition by Silver Nanoparticles." *Water Science and Technology : A Journal of the International Association on Water Pollution Research* 59 (9): 1699–1702. doi:10.2166/wst.2009.205.
Choi, Okkyoung, Thomas E Clevenger, Baolin Deng, Rao Y Surampalli, Louis Ross, and Zhiqiang Hu. 2009. "Role of Sulfide and Ligand Strength in Controlling Nanosilver Toxicity." *Water Research* 43 (7). Elsevier Ltd: 1879–86. doi:10.1016/j.watres.2009.01.029.
Choi, Okkyoung, Kathy Kanjun Deng, Nam-Jung Jung Kim, Louis Ross, Rao Y. Surampalli, and Zhiqiang Hu. 2008. "The Inhibitory Effects of Silver Nanoparticles, Silver Ions, and Silver Chloride Colloids on Microbial Growth." *Water Research* 42 (12): 3066–74. doi:10.1016/j.watres.2008.02.021.
Choi, Okkyoung, and Zhiqiang Hu. 2008. "Size Dependent and Reactive Oxygen Species Related Nanosilver Toxicity to Nitrifying Bacteria." *Environmental Science & Technology* 42 (12): 4583–88. doi:10.1021/es703238h.
Choi, Okkyoung, Chang-Ping Ping Yu, G. Esteban Fernández, and Zhiqiang Hu. 2010. "Interactions of Nanosilver with Escherichia Coli Cells in Planktonic and Biofilm Cultures." *Water Research* 44 (20): 6095–6103. doi:10.1016/j.watres.2010.06.069.
Coenye, Tom. 2010. "Response of Sessile Cells to Stress: From Changes in Gene Expression to Phenotypic Adaptation." *FEMS Immunology and Medical Microbiology* 59 (3): 239–52. doi:10.1111/j.1574-695X.2010.00682.x.
Cosgrove, Sara E, Youlin Qi, Keith S Kaye, Adolf W Karchmer, and Yehuda Carmeli. 2012. "M ETHICILLIN R ESISTANCE IN S TAPHYLOCOCCUS AUREUS B ACTEREMIA ON P ATIENT O UTCOMES : M ORTALITY , L ENGTH OF S TAY , AND H OSPITAL C HARGES."

Cuthbertson, L., and J. R. Nodwell. 2013. "The TetR Family of Regulators." *Microbiology and Molecular Biology Reviews* 77 (3): 440–75. doi:10.1128/MMBR.00018-13.

D'Autréaux, Benoît, and Michel B Toledano. 2007. "ROS as Signalling Molecules: Mechanisms That Generate Specificity in ROS Homeostasis." *Nature Reviews Molecular Cell Biology* 8 (10): 813–24. doi:10.1038/nrm2256.

Danese, Paul N., and Thomas J. Silhavy. 1998. "CpxP, a Stress-Combative Member of the Cpx Regulon." *J. Bacteriol.* 180 (4): 831–39. http://jb.asm.org/cgi/content/long/180/4/831.

Darwin, Charles. 2004. *On the Origin of Species*. Barnes & Noble.

Dastjerdi, Roya, and Majid Montazer. 2010. "A Review on the Application of Inorganic Nano-Structured Materials in the Modification of Textiles: Focus on Anti-Microbial Properties." *Colloids and Surfaces B: Biointerfaces* 79 (1). Elsevier B.V.: 5–18. doi:10.1016/j.colsurfb.2010.03.029.

Delcour, Anne H. 2009. "Outer Membrane Permeability and Antibiotic Resistance." *Biochimica et Biophysica Acta* 1794 (5). Elsevier B.V.: 808–16. doi:10.1016/j.bbapap.2008.11.005.

Deng, Hua, Danielle McShan, Ying Zhang, Sudarson S. Sinha, Zikri Arslan, Paresh C. Ray, and Hongtao Yu. 2016. "Mechanistic Study of the Synergistic Antibacterial Activity of Combined Silver Nanoparticles and Common Antibiotics." *Environmental Science and Technology* 50 (16): 8840–48. doi:10.1021/acs.est.6b00998.

Deonarine, Amrika, Boris L T Lau, George R Aiken, Joseph N Ryan, and Heileen Hsu-Kim. 2011. "Effects of Humic Substances on Precipitation and Aggregation of Zinc Sulfide Nanoparticles." *Environmental Science & Technology* 45 (8): 3217–23. doi:10.1021/es1029798.

Deredjian, Am??lie Amélie, C??line Céline Colinon, Elisabeth Brothier, Sabine Favre-Bonté, Benoit Cournoyer, Sylvie Nazaret, Sabine Favre-Bont??, Benoit Cournoyer, and Sylvie Nazaret. 2011. "Antibiotic and Metal Resistance among Hospital and Outdoor Strains of *Pseudomonas aeruginosa*." *Research in Microbiology* 162 (7): 689–700. doi:10.1016/j.resmic.2011.06.007.

Dror-ehre, A, A Adin, G Markovich, and H Mamane. 2010. "Control of Biofilm Formation in Water Using Molecularly Capped Silver Nanoparticles." *Water Research* 44 (8). Elsevier Ltd: 2601–9. doi:10.1016/j.watres.2010.01.016.

Dupont, Christopher L, Gregor Grass, and Christopher Rensing. 2011. "Copper Toxicity and the Origin of Bacterial Resistance — New Insights and Applications †," 1–16. doi:10.1039/C1MT00107H.

Dwyer, Daniel J., Michael Kohanski, and James J. Collins. 2009. "Role of Reactive Oxygen Species in Antibiotic Action and Resistance." *Current Opinion in Microbiology* 12 (5): 482–89. doi:10.1016/j.mib.2009.06.018.

Eckweiler, Denitsa, Monika Schniederjans, Ariane Zimmermann, Vanessa Jensen, Maren Scharfe, Robert Geffers, Susanne Ha, et al. 2012. "The *Pseudomonas aeruginosa* Transcriptome in Planktonic Cultures and Static Biofilms Using Rna Sequencing."

PLoS ONE 7 (2). doi:10.1371/journal.pone.0031092.
Edward Raja, Chelliah, Sundaresan Sasikumar, and Govindan Sadasivam Selvam. 2008. "Adaptive and Cross Resistance to Cadmium (II) and Zinc (II) by *Pseudomonas aeruginosa* BC15." *Biologia* 63 (4): 461–65. doi:10.2478/s11756-008-0095-y.
Elechiguerra, Jose Luis, Justin L Burt, Jose R Morones, Alejandra Camacho-bragado, Xiaoxia Gao, Humberto H Lara, and Miguel Jose Yacaman. 2005. "Interaction of Silver Nanoparticles with HIV-1 Interaction of Silver Nanoparticles with HIV-1." doi:10.1186/1477-3155-3-6.
Fabrega, J, SR Fawcett, and JC Renshaw. 2009. "Silver Nanoparticle Impact on Bacterial Growth: Effect of pH, Concentration, and Organic Matter." *Science & Technology*, 7285–90. http://pubs.acs.org/doi/abs/10.1021/es803259g.
Fabrega, Julia, Shona R Fawcett, Joanna C Renshaw, and Jamie R Lead. 2009. "Silver Nanoparticle Impact on Bacterial Growth: Effect of pH, Concentration, and Organic Matter." *Environmental Science & Technology* 43 (19): 7285–90. http://www.ncbi.nlm.nih.gov/pubmed/19848135.
Fabrega, Julia, Samuel N Luoma, Charles R Tyler, Tamara S Galloway, and Jamie R Lead. 2011. "Silver Nanoparticles: Behaviour and Effects in the Aquatic Environment." *Environment International* 37 (2). Elsevier Ltd: 517–31. doi:10.1016/j.envint.2010.10.012.
Farra, Anna, Sohidul Islam, Annelie Strålfors, Mikael Sörberg, and Bengt Wretlind. 2008. "Role of Outer Membrane Protein OprD and Penicillin-Binding Proteins in Resistance of *Pseudomonas aeruginosa* to Imipenem and Meropenem." *International Journal of Antimicrobial Agents* 31 (5). Elsevier: 427–33. doi:10.1016/j.ijantimicag.2007.12.016.
Feng, Q. L., J. Wu, G. Q. Chen, F. Z. Cui, T. N. Kim, and J. O. Kim. 2000. "A Mechanistic Study of the Antibacterial Effect of Silver Ions on Escherichia Coli and Staphylococcus Aureus." *Journal of Biomedical Materials Research* 52 (4): 662–68. doi:10.1002/1097-4636(20001215)52:4<662::AID-JBM10>3.0.CO;2-3.
Ferguson, Andrew D., and Johann Deisenhofer. 2004. "Metal Import through Microbial Membranes." *Cell* 116 (1): 15–24. doi:10.1016/S0092-8674(03)01030-4.
Fernandez, L., W. James Gooderham, Manjeet Bains, Joseph B. McPhee, Irith Wiegand, Robert E. W. Hancock, Lucía Fernández, et al. 2010. "Adaptive Resistance to the 'Last Hope' Antibiotics Polymyxin B and Colistin in *Pseudomonas aeruginosa* Is Mediated by the Novel Two-Component Regulatory System ParR-ParS." *Antimicrobial Agents and Chemotherapy* 54 (8): 3372–82. doi:10.1128/AAC.00242-10.
Fernández, Lucía, Elena B.M. Breidenstein, and Robert E.W. Hancock. 2011. "Creeping Baselines and Adaptive Resistance to Antibiotics." *Drug Resistance Updates* 14 (1): 1–21. doi:10.1016/j.drup.2011.01.001.
Finch, R., and P. A. Hunter. 2006. "Antibiotic Resistance--Action to Promote New Technologies: Report of an EU Intergovernmental Conference Held in Birmingham, UK, 12-13 December 2005." *Journal of Antimicrobial Chemotherapy* 58 (Supplement 1): i3–22. doi:10.1093/jac/dkl373.

Finkel, Toren. 2001. “Reactive Oxygen Species and Signal Transduction.” *IUBMB Life* 52 (1–2): 3–6. doi:10.1080/15216540252774694.
Fleischer, Rebecca, Ralf Heermann, Kirsten Jung, and Sabine Hunke. 2007. “Purification, Reconstitution, and Characterization of the CpxRAP Envelope Stress System of Escherichia Coli.” *The Journal of Biological Chemistry* 282 (12): 8583–93. doi:10.1074/jbc.M605785200.
Fraud, Sebastien, Aaron J. Campigotto, Zhilin Chen, and Keith Poole. 2008. “MexCD-OprJ Multidrug Efflux System of *Pseudomonas aeruginosa*: Involvement in Chlorhexidine Resistance and Induction by Membrane-Damaging Agents Dependent upon the AlgU Stress Response Sigma Factor.” *Antimicrobial Agents and Chemotherapy* 52 (12): 4478–82. doi:10.1128/AAC.01072-08.
Fraud, Sebastien, and Keith Poole. 2011. “Oxidative Stress Induction of the MexXY Multidrug Efflux Genes and Promotion of Aminoglycoside Resistance Development in *Pseudomonas aeruginosa*.” *Antimicrobial Agents and Chemotherapy* 55 (3): 1068–74. doi:10.1128/AAC.01495-10.
Gadd, Geoffrey Michael. 2010. “Metals, Minerals and Microbes: Geomicrobiology and Bioremediation.” *Microbiology* 156 (3): 609–43. doi:10.1099/mic.0.037143-0.
Gadd, GM, and AJ Griffiths. 1977. “Microorganisms and Heavy Metal Toxicity.” *Microbial Ecology* 4: 303–17. http://link.springer.com/article/10.1007/BF02013274.
Galhardo, Rodrigo S, P J Hastings, and Susan M Rosenberg. 2007. “Mutation as a Stress Response and the Regulation of Evolvability.” *Critical Reviews in Biochemistry and Molecular Biology* 42 (5): 399–435. doi:10.1080/10409230701648502.Mutation.
Ghosh, Anjali, Amarika Singh, P. W. Ramteke, and V. P. Singh. 2000. “Characterization of Large Plasmids Encoding Resistance to Toxic Heavy Metals in Salmonella Abortus Equi.” *Biochemical and Biophysical Research Communications* 272 (1): 6–11. doi:10.1006/bbrc.2000.2727.
Giedroc, David P, and Alphonse I Arunkumar. 2007. “Metal Sensor Proteins: Nature’s Metalloregulated Allosteric Switches.” *Dalton Transactions (Cambridge, England : 2003)*, no. 29: 3107–20. doi:10.1039/b706769k.
Giles, Niroshini M., Arron B Watts, Gregory I. Giles, Finoa H. Fry, Jinnifer A. Littlechild, and Claus Jacob. 2003. “Metal and Redox Modulation of Cysteine Protein Function.” *Chemistry & Biology* 10: 677–93. doi:10.1016/S1074-5521(03)00174-1.
Gitipour, Alireza, Amro El Badawy, Mahendranath Arambewela, Bradley Miller, Kirk G Scheckel, W Thiel, Michael Elk, et al. 2013. “The Impact of Silver Nanoparticles on the Composting of Municipal Solid Waste The Impact of Silver Nanoparticles on the Composting of Municipal Solid Waste.” *Environmental Science & Technology* Just Accep.
Giuliodori, Anna Maria, Claudio O. Gualerzi, Sara Soto, Jordi Vila, and María M. Tavío. 2007. “Review on Bacterial Stress Topics.” *Annals of the New York Academy of Sciences* 1113: 95–104. doi:10.1196/annals.1391.008.
Grkovic, S, M H Brown, and R a Skurray. 2001. “Transcriptional Regulation of Multidrug Efflux Pumps in Bacteria.” *Seminars in Cell & Developmental Biology* 12

(3): 225–37. doi:10.1006/scdb.2000.0248.
Gudipaty, Swapna Aravind, Andrew S Larsen, Christopher Rensing, and Megan M McEvoy. 2012. “Regulation of Cu(I)/Ag(I) Efflux Genes in Escherichia Coli by the Sensor Kinase CusS.” *FEMS Microbiology Letters* 330 (1): 30–37. doi:10.1111/j.1574-6968.2012.02529.x.
Gupta, Kalpana, Thomas M Hooton, and Walter E Stamm. 2001. “Increasing Antimicrobial Resistance and the Management of Uncomplicated Community-Aquired Urinary Tract Inf.” *Annals of Internal Medicine* 135 (1): 41–50. doi:10.7326/0003-4819-135-1-200107030-00012.
Ha, Un-hwan, Yanping Wang, and Shouguang Jin. 2003. “DsbA of *Pseudomonas aeruginosa* Is Essential for Multiple Virulence Factors.” *American Society of Microbiology* 71 (3): 1590–95. doi:10.1128/IAI.71.3.1590.
Harrison, Joe J, Howard Ceri, and Raymond J Turner. 2007. “Multimetal Resistance and Tolerance in Microbial Biofilms.” *Nature Reviews. Microbiology* 5 (12): 928–38. doi:10.1038/nrmicro1774.
Harrison, Joe J, Raymond J Turner, and Howard Ceri. 2005. “High-Throughput Metal Susceptibility Testing of Microbial Biofilms.” *BMC Microbiology* 5 (January): 53. doi:10.1186/1471-2180-5-53.
Hasman, Henrik, and Frank M. Aarestrup. 2002. “Tcrb, a Gene Conferring Transferable Copper Resistance in Enterococcus Faecium: Occurrence, Transferability, and Linkage to Macrolide and Glycopeptide Resistance.” *Antimicrobial Agents and Chemotherapy* 46 (5): 1410–16. doi:10.1128/AAC.46.5.1410-1416.2002.
Hassan, M T, D van der Lelie, D Springael, U Römling, N Ahmed, and M Mergeay. 1999. “Identification of a Gene Cluster, Czr, Involved in Cadmium and Zinc Resistance in *Pseudomonas aeruginosa*.” *Gene* 238 (2): 417–25. http://www.ncbi.nlm.nih.gov/pubmed/10570969.
Hawkey, Peter M. 1998. “The Origins and Molecular Basis of Antibiotic Resistance.” *BMJ (Clinical Research Ed.)* 317 (7159): 657–60. doi:10.1136/bmj.317.7159.657.
Hay, Thomas, Sebastien Fraud, Calvin Ho Fung Lau, Christie Gilmour, and Keith Poole. 2013. “Antibiotic Inducibility of the mexXY Multidrug Efflux Operon of *Pseudomonas aeruginosa*: Involvement of the MexZ Anti-Repressor ArmZ.” *PLoS ONE* 8 (2): 20–23. doi:10.1371/journal.pone.0056858.
He, Di, Shikha Garg, and T. David Waite. 2012. “H 2O 2-Mediated Oxidation of Zero-Valent Silver and Resultant Interactions among Silver Nanoparticles, Silver Ions, and Reactive Oxygen Species.” *Langmuir* 28 (27): 10266–75. doi:10.1021/la300929g.
Hendren, Christine Ogilvie, Appala R. Badireddy, Elizabeth Casman, and Mark R. Wiesner. 2013. “Modeling Nanomaterial Fate in Wastewater Treatment: Monte Carlo Simulation of Silver Nanoparticles (Nano-Ag).” *Science of the Total Environment* 449. Elsevier B.V.: 418–25. doi:10.1016/j.scitotenv.2013.01.078.
Ho-Fung Lau, Calvin, Sebastien Fraud, Marcus Jones, Scott N. Peterson, and Keith Poole. 2013. “Mutational Activation of the AmgRS Two-Component System in Aminoglycoside-Resistant *Pseudomonas aeruginosa*.” *Antimicrobial Agents and*

Chemotherapy 57 (5): 2243–51. doi:10.1128/AAC.00170-13.
Ho, Chi-Ming, Sammi King-Woon Yau, Chun-Nam Lok, Man-Ho So, and Chi-Ming Che. 2010. "Oxidative Dissolution of Silver Nanoparticles by Biologically Relevant Oxidants: A Kinetic and Mechanistic Study." *Chemistry, an Asian Journal* 5 (2): 285–93. doi:10.1002/asia.200900387.
Horszczaruk, Elzbieta, Jolanta Baranowska, Roman Jedrzejewski, Pawel Sikora, Krzysztof Cendrowski, and Ewa Mijowska. 2017. "Properties of Cement Composites Modified with Silica-Magnetite Nanostructures." *Procedia Engineering* 196 (June). Elsevier B.V.: 105–12. doi:10.1016/j.proeng.2017.07.179.
Hu, Nan, and Bin Zhao. 2007. "Key Genes Involved in Heavy-Metal Resistance in Pseudomonas Putida CD2." *FEMS Microbiology Letters* 267 (1): 17–22. doi:10.1111/j.1574-6968.2006.00505.x.
Hwang, Ee Taek, Jin Hyung Lee, Yun Ju Chae, Yeon Seok Kim, Byoung Chan Kim, Byoung-In Sang, and Man Bock Gu. 2008. "Analysis of the Toxic Mode of Action of Silver Nanoparticles Using Stress-Specific Bioluminescent Bacteria." *Small (Weinheim an Der Bergstrasse, Germany)* 4 (6): 746–50. doi:10.1002/smll.200700954.
Idsa. 2004. "Bad Bugs, No Drugs As Antibiotic Discovery Stagnates ...A Public Health Crisis Brews," no. July: 1–35.
Imlay, James A. 2008. "Cellular Defenses against Superoxide and Hydrogen Peroxide." *Annual Review of Biochemistry* 77 (217): 755–76. doi:10.1146/annurev.biochem.77.061606.161055.
Institute, Clinical and Laboratory Standards. 2012. *Methods for Dilution Antimicrobial Susceptibility Tests for Bacteria That Grow Aerobically ; Approved Standard — Ninth Edition*. Vol. 32.
Jacob, Claus, Gregory I. Giles, Niroshini M. Giles, and Helmut Sies. 2003. "Sulfur and Selenium: The Role of Oxidation State in Protein Structure and Function." *Angewandte Chemie - International Edition* 42 (39): 4742–58. doi:10.1002/anie.200300573.
Ji, Jun Ho, Jae Hee Jung, Sang Soo Kim, Jin-Uk Yoon, Jung Duck Park, Byung Sun Choi, Yong Hyun Chung, et al. 2007. "Twenty-Eight-Day Inhalation Toxicity Study of Silver Nanoparticles in Sprague-Dawley Rats." *Inhalation Toxicology* 19 (10): 857–71. doi:10.1080/08958370701432108.
Jinks-Robertson, Sue, and Ashok S. Bhagwat. 2014. "Transcription-Associated Mutagenesis." *Annual Review of Genetics* 48 (1): 341–59. doi:10.1146/annurev-genet-120213-092015.
Jung, Ae, Young Jik, Ae Jung Huh, Young Jik Kwon, Ae Jung, and Young Jik. 2011. "'Nanoantibiotics': A New Paradigm for Treating Infectious Diseases Using Nanomaterials in the Antibiotics Resistant Era." *Journal of Controlled Release : Official Journal of the Controlled Release Society* 156 (2). Elsevier B.V.: 128–45. doi:10.1016/j.jconrel.2011.07.002.
Jung, Woo Kyung, Hye Cheong Koo, Ki Woo Kim, Sook Shin, So Hyun Kim, and Yong Ho Park. 2008. "Antibacterial Activity and Mechanism of Action of the Silver Ion in

Staphylococcus Aureus and Escherichia Coli." *Applied and Environmental Microbiology* 74 (7): 2171–78. doi:10.1128/AEM.02001-07.
Kachur, Alexander V, Cameron J Koch, and John E Biaglow. 1998. "Mechanism of Copper-Catalyzed Oxidation of Glutathione." *Free Radical Research* 28 (3). Taylor & Francis: 259–69. doi:10.3109/10715769809069278.
Kamat, P. V. 2007. "Meeting the Clean Energy Demand: Nanoestructure Architectures for Solar Energy Conversion." *Phys. Chem.* 392: 2834–60. doi:10.1002/adma.200902096.
Kang, Guo-dong, and Yi-ming Cao. 2012. "Development of Antifouling Reverse Osmosis Membranes for Water Treatment: A Review." *Water Research* 46 (3). Elsevier Ltd: 584–600. doi:10.1016/j.watres.2011.11.041.
Kapoor, Sudhir. 1998. "Preparation , Characterization , and Surface Modification of Silver Particles." *Langmuir* 3 (17): 1021–25.
Khan, Iftheker A, A R M Nabiul Afrooz, Joseph R V Flora, P Ariette Schierz, P Lee Ferguson, Tara Sabo-attwood, and Navid B Saleh. 2013. "Chirality A Ff Ects Aggregation Kinetics of Single-Walled Carbon Nanotubes."
Khan, Iftheker A, Nicole D Berge, Tara Sabo-attwood, P Lee Ferguson, and Navid B Saleh. 2013. "Single-Walled Carbon Nanotube Transport in Representative Municipal Solid Waste Land Fi Ll Conditions."
Kim, Jeonghwan, and Bart Van Der Bruggen. 2010. "The Use of Nanoparticles in Polymeric and Ceramic Membrane Structures: Review of Manufacturing Procedures and Performance Improvement for Water Treatment." *Environmental Pollution* 158 (7). Elsevier Ltd: 2335–49. doi:10.1016/j.envpol.2010.03.024.
Kim, Shin Woong, Yong-Wook Baek, and Youn-Joo An. 2011. "Assay-Dependent Effect of Silver Nanoparticles to Escherichia Coli and Bacillus Subtilis." *Applied Microbiology and Biotechnology* 92 (5): 1045–52. doi:10.1007/s00253-011-3611-x.
Kirisits, Mary Jo, Lynne Prost, Melissa Starkey, and Matthew R Parsek. 2005. "Characterization of Colony Morphology Variants Isolated from *Pseudomonas aeruginosa* Biofilms." *American Society of Microbiology* 71 (8): 4809–21. doi:10.1128/AEM.71.8.4809.
Kittler, S., C. Greulich, J. Diendorf, M. Köller, and M. Epple. 2010. "Toxicity of Silver Nanoparticles Increases during Storage Because of Slow Dissolution under Release of Silver Ions." *Chemistry of Materials* 22 (16): 4548–54. doi:10.1021/cm100023p.
Knapp, Charles W., Seánín M. McCluskey, Brajesh K. Singh, Colin D. Campbell, Gordon Hudson, and David W. Graham. 2011. "Antibiotic Resistance Gene Abundances Correlate with Metal and Geochemical Conditions in Archived Scottish Soils." *PLoS ONE* 6 (11). doi:10.1371/journal.pone.0027300.
Knetsch, Menno L W, and Leo H. Koole. 2011. "New Strategies in the Development of Antimicrobial Coatings: The Example of Increasing Usage of Silver and Silver Nanoparticles." *Polymers* 3 (1): 340–66. doi:10.3390/polym3010340.
Knibbe, Carole, Antoine Coulon, Olivier Mazet, Jean Michel Fayard, and Guillaume Beslon. 2007. "A Long-Term Evolutionary Pressure on the Amount of Noncoding DNA." *Molecular Biology and Evolution* 24 (10): 2344–53.

doi:10.1093/molbev/msm165.
Kohanski, Michael, Mark a. DePristo, and James J. Collins. 2010. "Sublethal Antibiotic Treatment Leads to Multidrug Resistance via Radical-Induced Mutagenesis." *Molecular Cell* 37 (3). Elsevier Ltd: 311–20. doi:10.1016/j.molcel.2010.01.003.
Kohanski, Michael, Daniel Dwyer, and James Collins. 2010. "How Antibiotics Kill Bacteria : From Targets to Networks." *Nature Publishing Group* 8 (6). Nature Publishing Group: 423–35. doi:10.1038/nrmicro2333.
Kohanski, Michael, Daniel Dwyer, Boris Hayete, Carolyn Lawrence, and James Collins. 2007. "A Common Mechanism of Cellular Death Induced by Bactericidal Antibiotics." *Cell* 130 (5): 797–810. doi:10.1016/j.cell.2007.06.049.
Kohanski, Michael, Daniel J. Dwyer, Jamey Wierzbowski, Guillaume Cottarel, and James J. Collins. 2008. "Mistranslation of Membrane Proteins and Two-Component System Activation Trigger Antibiotic-Mediated Cell Death." *Cell* 135 (4): 679–90. doi:10.1016/j.cell.2008.09.038.
Krahn, Thomas, Christie Gilmour, Justin Tilak, Sebastien Fraud, Nicholas Kerr, Calvin H.-F. Ho Fung Lau, and Keith Poole. 2012. "Determinants of Intrinsic Aminoglycoside Resistance in *Pseudomonas aeruginosa*." *Antimicrobial Agents and Chemotherapy* 56 (11): 5591–5602. doi:10.1128/AAC.01446-12.
Kumar, Ayush, and Herbert P. Schweizer. 2005. "Bacterial Resistance to Antibiotics: Active Efflux and Reduced Uptake." *Advanced Drug Delivery Reviews* 57 (10): 1486–1513. doi:10.1016/j.addr.2005.04.004.
Kumari, Avnesh, Sudesh Kumar Subhash C. Yadav, and Sudesh Kumar Subhash C. Yadav. 2010. "Biodegradable Polymeric Nanoparticles Based Drug Delivery Systems." *Colloids and Surfaces B: Biointerfaces* 75 (1): 1–18. doi:10.1016/j.colsurfb.2009.09.001.
Kuzminov, A. 1999. "Recombinational Repair of DNA Damage in Escherichia Coli and Bacteriophage Lambda." *Microbiology and Molecular Biology Reviews : MMBR* 63 (4): 751–813, table of contents. http://www.pubmedcentral.nih.gov/articlerender.fcgi?artid=98976&tool=pmcentrez&rendertype=abstract.
Kuzminov, Andrei. 1994. "Homologous Recombination - Experimental Systems, Analysis and Significance" 4 (4): 765–70. doi:10.1128/ecosalplus.7.2.6.Homologous.
Kvítek, L, A Panácek, Jana Soukupova, M Kolar, R Vecerova, Robert Prucek, Mirka Holecova, et al. 2008. "Effect of Surfactants and Polymers on Stability and Antibacterial Activity of Silver Nanoparticles." *The Journal of Physical Chemistry* 112 (15): 5825–34. doi:10.1021/jp711616v.
Laban, Geoff, Loring F. Nies, Ronald F. Turco, John W. Bickham, and Maria S. Sepúlveda. 2010. "The Effects of Silver Nanoparticles on Fathead Minnow (Pimephales Promelas) Embryos." *Ecotoxicology* 19 (1): 185–95. doi:10.1007/s10646-009-0404-4.
Laffite, Amandine, Pitchouna I. Kilunga, John M. Kayembe, Naresh Devarajan, Crispin K. Mulaji, Gregory Giuliani, Vera I. Slaveykova, and John Poté. 2016. "Hospital

Effluents Are One of Several Sources of Metal, Antibiotic Resistance Genes, and Bacterial Markers Disseminated in Sub-Saharan Urban Rivers." *Frontiers in Microbiology* 7 (JUL): 1–14. doi:10.3389/fmicb.2016.01128.

Langmead, Ben, and Steven L. Salzberg. 2012. "Fast Gapped-Read Alignment with Bowtie 2." *Nature Methods* 9 (4): 357–59. doi:10.1038/nmeth.1923.

Łasica, Anna M., and Elzbieta K. Jagusztyn-Krynicka. 2007. "The Role of Dsb Proteins of Gram-Negative Bacteria in the Process of Pathogenesis." *FEMS Microbiology Reviews* 31 (5): 626–36. doi:10.1111/j.1574-6976.2007.00081.x.

Lau, Calvin Ho-fung, Daniel Hughes, and Keith Poole. 2014. "MexY-Promoted Aminoglycoside Resistance in *Pseudomonas aeruginosa*: Involvement of a Putative Proximal Binding Pocket in Aminoglycoside Recognition." *mBio* 5 (2): e01068. doi:10.1128/mBio.01068-14.

Lau, Calvin Ho Fung, Thomas Krahn, Christie Gilmour, Erin Mullen, and Keith Poole. 2015. "AmgRS-Mediated Envelope Stress-Inducible Expression of the mexXY Multidrug Efflux Operon of *Pseudomonas aeruginosa*." *MicrobiologyOpen* 4 (1): 121–35. doi:10.1002/mbo3.226.

Laubacher, Mary E., and Sarah E. Ades. 2008. "The Rcs Phosphorelay Is a Cell Envelope Stress Response Activated by Peptidoglycan Stress and Contributes to Intrinsic Antibiotic Resistance." *Journal of Bacteriology* 190 (6): 2065–74. doi:10.1128/JB.01740-07.

Lee, Chang Ro, Ill Hwan Cho, Byeong Chul Jeong, and Sang Hee Lee. 2013. "Strategies to Minimize Antibiotic Resistance." *International Journal of Environmental Research and Public Health* 10 (9): 4274–4305. doi:10.3390/ijerph10094274.

Lee, Hyang Yeon, Hyoung Kun Park, Yoon Mi Lee, Kwan Kim, and Seung Bum Park. 2007. "A Practical Procedure for Producing Silver Nanocoated Fabric and Its Antibacterial Evaluation for Biomedical Applications." *Chemical Communications*, no. 28(July). The Royal Society of Chemistry: 2959–61. doi:10.1039/B703034G.

Lee, Samuel, Aaron Hinz, Elizabeth Bauerle, Angus Angermeyer, Katy Juhaszova, Yukihiro Kaneko, Pradeep K Singh, and Colin Manoil. 2009. "Targeting a Bacterial Stress Response to Enhance Antibiotic Action." *Proceedings of the National Academy of Sciences of the United States of America* 106 (34): 14570–75. doi:10.1073/pnas.0903619106.

Lee, Yvonne M., Patricia a. DiGiuseppe, Thomas J. Silhavy, and Scott J. Hultgren. 2004. "P Pilus Assembly Motif Necessary for Activation of the CpxRA Pathway by PapE in Escherichia Coli." *Journal of Bacteriology* 186 (13): 4326–37. doi:10.1128/JB.186.13.4326-4337.2004.

Legatzki, Antje, Gregor Grass, Andreas Anton, Christopher Rensing, and Dietrich H. Nies. 2003. "Interplay of the Czc System and Two P-Type ATPases in Conferring Metal Resistance to Ralstonia Metallidurans." *Journal of Bacteriology* 185 (15): 4354–61. doi:10.1128/JB.185.15.4354-4361.2003.

Lencastre, H De, S W Wu, M G Pinho, a M Ludovice, S Filipe, S Gardete, R Sobral, S Gill, M Chung, and A Tomasz. 1999. "Antibiotic Resistance as a Stress Response: Complete Sequencing of a Large Number of Chromosomal Loci in Staphylococcus

Aureus Strain COL That Impact on the Expression of Resistance to Methicillin." *Microbial Drug Resistance* 5 (3): 163–75. doi:10.1089/mdr.1999.5.163.

Leung, Emily, Diana E. Weil, Mario Raviglione, Hiroki Nakatani, Health Organization, Mario Raviglione, Hiroki Nakatani, and Health Organization. 2011. "The WHO Policy Package to Combat Antimicrobial Resistance." *Bulletin of the World Health Organization* 89 (5): 390–92. doi:10.2471/BLT.11.088435.

Levard, Clément, E. Matt Hotze, Gregory V. Lowry, and Gordon E. Brown. 2012a. "Environmental Transformations of Silver Nanoparticles: Impact on Stability and Toxicity." *Environmental Science and Technology* 46 (13): 6900–6914. doi:10.1021/es2037405.

Levard, Clément, E Matt Hotze, Gregory V Lowry, and Gordon E Brown. 2012b. "Environmental Transformations of Silver Nanoparticles: Impact on Stability and Toxicity." *Environmental Science & Technology* 46 (13): 6900–6914. doi:10.1021/es2037405.

Levard, Clément, Sumit Mitra, Tiffany Yang, Adam D Jew, Appala Raju Badireddy, Gregory V Lowry, and Gordon E Brown. 2013. "Effect of Chloride on the Dissolution Rate of Silver Nanoparticles and Toxicity to E. Coli." *Environmental Science & Technology* 47 (11): 5738–45. doi:10.1021/es400396f.

Li, X Z, D M Livermore, and H Nikaido. 1994. "Role of Efflux Pump(s) in Intrinsic Resistance of *Pseudomonas aeruginosa*: Resistance to Tetracycline, Chloramphenicol, and Norfloxacin." *Antimicrobial Agents and Chemotherapy* 38 (8): 1732–41. doi:10.1128/aac.38.8.1732.

Li, X Z, H Nikaido, and K E Williams. 1997. "Silver-Resistant Mutants of Escherichia Coli Display Active Efflux of Ag+ and Are Deficient in Porins." *Journal of Bacteriology* 179 (19): 6127–32. http://www.pubmedcentral.nih.gov/articlerender.fcgi?artid=179518&tool=pmcentrez&rendertype=abstract.

Li, Xian-Zhi., Christopher A. Elkins, and Helen I. Zgurskaya. 2007. *Antimicrobial Resistance in Bacteria*. doi:10.1007/978-3-319-39658-3.

Li, Xian-Zhi, Christopher A. Elkins, and Helen I. Zgurskaya. 2016. *Efflux-Mediated Antimicrobial Resistance In Bacteria: Mechanisms, and Clinical Implications*. 1st ed. New York, NY: Springer. https://books.google.com/books?id=FkF4DQAAQBAJ&pg=PA118&lpg=PA118&dq=asymmetric+muxABC&source=bl&ots=sY2fFyakrQ&sig=OUsMsomchxjvwkIYQjGjc-g6faA&hl=en&sa=X&ved=2ahUKEwjNvsDVgf7ZAhUD7awKHSIHA1kQ6AEwAHoECAAQKw#v=onepage&q=asymmetric muxABC&f=false.

Li, Xian-Zhi Z, Xian-Zhi Z Li, Hiroshi Nikaido, and Hiroshi Nikaido. 2004. *Efflux-Mediated Drug Resistance in Bacteria*. *Drugs*. Vol. 64. doi:10.2165/11317030-000000000-00000.Efflux-Mediated.

Li, Xuan, John J. Lenhart, and Harold W. Walker. 2012. "Aggregation Kinetics and Dissolution of Coated Silver Nanoparticles." *Langmuir* 28 (2): 1095–1104. doi:10.1021/la202328n.

Li, Xuan, John J Lenhart, and Harold W Walker. 2010. “Dissolution-Accompanied Aggregation Kinetics of Silver Nanoparticles.” *Langmuir : The ACS Journal of Surfaces and Colloids* 45 (22): 16690–98. doi:10.1021/la101768n.

Li, Y., P. Leung, L. Yao, Q. W. Song, and E. Newton. 2006. “Antimicrobial Effect of Surgical Masks Coated with Nanoparticles.” *Journal of Hospital Infection* 62 (1): 58–63. doi:10.1016/j.jhin.2005.04.015.

Li, Yang, Wen Zhang, Junfeng Niu, and Yongsheng Chen. 2013. “Surface-Coating-Dependent Dissolution, Aggregation, and Reactive Oxygen Species (ROS) Generation of Silver Nanoparticles under Different Irradiation Conditions.” *Environmental Science & Technology* 47 (18): 10293–301. doi:10.1021/es400945v.

Liang, Zhihua, Atreyee Das, and Zhiqiang Hu. 2010. “Bacterial Response to a Shock Load of Nanosilver in an Activated Sludge Treatment System.” *Water Research* 44 (18). Elsevier Ltd: 5432–38. doi:10.1016/j.watres.2010.06.060.

Lin, Jun, Kunihiko Nishino, Marilyn C. Roberts, Marcelo Tolmasky, Rustam I. Aminov, and Lixin Zhang. 2015. “Mechanisms of Antibiotic Resistance.” *Frontiers in Microbiology* 6 (February): 2013–15. doi:10.3389/fmicb.2015.00034.

Liu, Jingyu, Robert H Hurt, Nanoscale Innovation, and Rhode Island. 2010. “Ion Release Kinetics and Particle Persistence in Aqueous Nano-Silver Colloids.” *Environmental Science & Technology* 44 (6): 2169–75. doi:10.1021/es9035557.

Liu, Jingyu, David a Sonshine, Saira Shervani, and Robert H Hurt. 2010. “Controlled Release of Biologically Active Silver from Nanosilver Surfaces.” *ACS Nano* 4 (11): 6903–13. doi:10.1021/nn102272n.

Liu, Shaobin, Li Wei, Lin Hao, Ning Fang, Matthew Wook Chang, Rong Xu, Yanhui Yang, and Yuan Chen. 2009. “Sharper and faster ‘Nano Darts’ kill More Bacteria: A Study of Antibacterial Activity of Individually Dispersed Pristine Single-Walled Carbon Nanotube.” *ACS Nano* 3 (12): 3891–3902. doi:10.1021/nn901252r.

Livermore, D M. 1995. “Beta-Lactamases in Laboratory and Clinical Resistance.” *Clinical Microbiology Reviews* 8 (4): 557–84.

Lo, Shu-fen Fen, Chee-jen Jen Chang, Wen-yu Yu Hu, Mark Hayter, and Yu-ting Ting Chang. 2009. “The Effectiveness of Silver-Releasing Dressings in the Management of Non-Healing Chronic Wounds: A Meta-Analysis.” *Journal of Clinical Nursing* 18 (5): 716–28. doi:10.1111/j.1365-2702.2008.02534.x.

Loewen, P C, J Switala, and B L Triggs-Raine. 1985. “Catalases HPI and HPII in Escherichia Coli Are Induced Independently.” *Archives of Biochemistry and Biophysics* 243 (1): 144–49. http://www.ncbi.nlm.nih.gov/pubmed/3904630.

Lok, Chun-nam CN, Chi-ming CM Ho, Rong Chen, Paul Kwong-hang Tam, Jen-fu Chiu, and Chi-ming Che. 2008. “Proteomic Identification of the Cus System as a Major Determinant of Constitutive Escherichia Coli Silver Resistance of Chromosomal Origin.” *Journal of Proteome …*, 2351–56. http://pubs.acs.org/doi/abs/10.1021/pr700646b.

Lok, Chun-nam, Chi-ming Ho, Rong Chen, Qing-yu He, Wing-Yiu Yu, Hongzhe Sun, Paul Kwong-Hang Tam, Jen-Fu Chiu, and Chi-ming Che. 2006. “Proteomic Analysis of the Mode of Antibacterial Action of Silver Nanoparticles.” *Journal of*

Proteome Research 5 (4): 916–24. doi:10.1021/pr0504079.
Lok, Chun-Nam, Chi-Ming Ho, Rong Chen, Qing-Yu He, Wing-Yiu Yu, Hongzhe Sun, Paul Kwong-Hang Tam, Jen-Fu Chiu, and Chi-Ming Che. 2007. "Silver Nanoparticles: Partial Oxidation and Antibacterial Activities." *Journal of Biological Inorganic Chemistry : JBIC : A Publication of the Society of Biological Inorganic Chemistry* 12 (4): 527–34. doi:10.1007/s00775-007-0208-z.
Long, Yan Min, Li Gang Hu, Xue Ting Yan, Xing Chen Zhao, Qun Fang Zhou, Yong Cai, and Gui Bin Jiang. 2017. "Surface Ligand Controls Silver Ion Release of Nanosilver and Its Antibacterial Activity against Escherichia Coli." *International Journal of Nanomedicine* 12: 3193–3206. doi:10.2147/IJN.S132327.
Luoma, S.N. 2008. "Silver Nanotechnologies and the Environment: Old Problems or New Challenges." Project on Emerging Nanotechnologies of the Woodrow Wilson International Center for Scholars. http://scholar.google.com/scholar?hl=en&btnG=Search&q=intitle:SILVER+NANOTECHNOLOGIES+AND+THE+ENVIRONMENT+:+OLD+PROBLEMS+OR+NEW+CHALLENGES+?#0.
Macak, J. M., H. Tsuchiya, A. Ghicov, K. Yasuda, R. Hahn, S. Bauer, and P. Schmuki. 2007. "TiO2 Nanotubes: Self-Organized Electrochemical Formation, Properties and Applications." *Current Opinion in Solid State and Materials Science* 11 (1–2): 3–18. doi:10.1016/j.cossms.2007.08.004.
Macomber, L., and J. A. Imlay. 2009. "The Iron-Sulfur Clusters of Dehydratases Are Primary Intracellular Targets of Copper Toxicity." *Proceedings of the National Academy of Sciences* 106 (20): 8344–49. doi:10.1073/pnas.0812808106.
Maier, Tobias, Marc Güell, and Luis Serrano. 2009. "Correlation of mRNA and Protein in Complex Biological Samples." *FEBS Letters* 583 (24). Federation of European Biochemical Societies: 3966–73. doi:10.1016/j.febslet.2009.10.036.
Maillard, Jean-Yves, and Philippe Hartemann. 2013. "Silver as an Antimicrobial: Facts and Gaps in Knowledge." *Critical Reviews in Microbiology* 39 (4): 373–83. doi:10.3109/1040841X.2012.713323.
Manzur, TNVIR, Nur Yazdani, and Md. Abul Bashar Emon. 2016. "Potential of Carbon Nanotube Reinforced Cement Composites as Concrete Repair Material." *Journal of Nanomaterials* 2016. doi:http://dx.doi.org/10.1155/2016/1421959.
Marinus, M. G. 2012. "DNA Mismatch Repair." *EcoSal Plus* 5 (1): 87–100. doi:10.1037/a0038432.Latino.
Markowska, Katarzyna, Anna M Grudniak, Krzysztof Krawczyk, Izabela Wróbel, and Krystyna I Wolska. 2014. "Modulation of Antibiotic Resistance and Induction of a Stress Response in *Pseudomonas aeruginosa* by Silver Nanoparticles." *Journal of Medical Microbiology* 63 (Pt 6): 849–54. doi:10.1099/jmm.0.068833-0.
Markowska, Katarzyna, Anna M Grudniak, and Krystyna I Wolska. 2013. "Silver Nanoparticles as an Alternative Strategy against Bacterial Biofilms." *Acta Biochimica Polonica* 60 (4): 523–30. http://www.ncbi.nlm.nih.gov/pubmed/24432308.
Maseda, Hideaki, Isao Sawada, Kohjiro Saito, Hiroo Uchiyama, and Taiji Nakae. 2004.

"Enhancement of the mexAB - oprM Efflux Pump Expression by a Quorum-Sensing Autoinducer and Its Cancellation by a Regulator , MexT , of the mexEF - oprN Efflux Pump Operon in *Pseudomonas aeruginosa* Enhancement of the mexAB - oprM Efflux Pump Expression by." *Antimicrob. Agents Chemother. 2004*, 48 (4): 1320–28. doi:10.1128/AAC.48.4.1320.

Masuda, Nobuhisa, Eiko Sakagawa, Satoshi Ohya, Naomasa Gotoh, Hideto Tsujimoto, and Takeshi Nishino. 2000. "Substrate Specificities of MexAB-OprM, MexCD-OprJ, and MexXY-OprM Efflux Pumps in *Pseudomonas aeruginosa*." *Antimicrob. Agents Chemother.* 44 (12): 3322–27. doi:10.1128/aac.44.12.3322-3327.2000.

Maynard, Andrew D. 2007. "Nanotechnology: The next Big Thing, or Much Ado about Nothing?" *Annals of Occupational Hygiene* 51 (1): 1–12. doi:10.1093/annhyg/mel071.

Mazel, D, and J Davies. 1999. "Antibiotic Resistance in Microbes." *Cellular and Molecular Life Sciences : CMLS* 56 (9–10): 742–54. doi:10.1007/s000180050021.

McNeil, Nicole M.R., Ciara McDonnell, Miranda Hambrook, and Thomas G. Back. 2015. "Oxidation of Disulfides to Thiolsulfinates with Hydrogen Peroxide and a Cyclic Seleninate Ester Catalyst Peroxide and a Cyclic Seleninate Ester Catalyst." *Molecules* 20 (6): 10748–62. doi:10.3390/molecules200610748.

Meyer, Joel N., Christopher A. Lord, Xinyu Y. Yang, Elena A. Turner, Appala R. Badireddy, Stella M. Marinakos, Ashutosh Chilkoti, Mark R. Wiesner, and Melanie Auffan. 2010. "Intracellular Uptake and Associated Toxicity of Silver Nanoparticles in Caenorhabditis Elegans." *Aquatic Toxicology* 100 (2). Elsevier B.V.: 140–50. doi:10.1016/j.aquatox.2010.07.016.

Mileykovskaya, Eugenia, and William Dowhan. 1997. "The Cpx Two-Component Signal Transduction Pathway Is Activated in Escherichia Coli Mutant Strains Lacking Phosphatidylethanolamine." 179 (4): 1029–34.

Miller, Jennifer H., John T. Novak, William R. Knocke, Katherine Young, Yanjuan Hong, Peter J. Vikesland, Matthew S. Hull, and Amy Pruden. 2013. "Effect of Silver Nanoparticles and Antibiotics on Antibiotic Resistance Genes in Anaerobic Digestion." *Water Environment Research* 85 (5): 411–21. doi:10.2175/106143012X13373575831394.

Mima, Takehiko, Swati Joshi, Margarita Gomez-Escalada, and Herbert P. Schweizer. 2007. "Identification and Characterization of TriABC-OpmH, a Triclosan Efflux Pump of *Pseudomonas aeruginosa* Requiring Two Membrane Fusion Proteins." *Journal of Bacteriology* 189 (21): 7600–7609. doi:10.1128/JB.00850-07.

Mima, Takehiko, Naoki Kohira, Yang Li, Hiroshi Sekiya, Wakano Ogawa, Teruo Kuroda, and Tomofusa Tsuchiya. 2009. "Gene Cloning and Characteristics of the RND-Type Multidrug Efflux Pump MuxABC-OpmB Possessing Two RND Components in *Pseudomonas aeruginosa*." *Microbiology* 155 (11): 3509–17. doi:10.1099/mic.0.031260-0.

Misra, Superb K., Agnieszka Dybowska, Deborah Berhanu, Samuel N. Luoma, and Eugenia Valsami-Jones. 2012. "The Complexity of Nanoparticle Dissolution and Its Importance in Nanotoxicological Studies." *Science of the Total Environment* 438.

Elsevier B.V.: 225–32. doi:10.1016/j.scitotenv.2012.08.066.
Mols, Maarten, and Tjakko Abee. 2011. “Primary and Secondary Oxidative Stress in Bacillus.” *Environmental Microbiology* 13 (6): 1387–94. doi:10.1111/j.1462-2920.2011.02433.x.
Moore, Jessica M., Raul Correa, Susan M. Rosenberg, and P. J. Hastings. 2017. “Persistent Damaged Bases in DNA Allow Mutagenic Break Repair in Escherichia Coli.” *PLoS Genetics* 13 (7): 1–27. doi:10.1371/journal.pgen.1006733.
Mor, Gopal K., Oomman K. Varghese, Maggie Paulose, Karthik Shankar, and Craig A. Grimes. 2006. “A Review on Highly Ordered, Vertically Oriented TiO2 Nanotube Arrays: Fabrication, Material Properties, and Solar Energy Applications.” *Solar Energy Materials and Solar Cells* 90 (14): 2011–75. doi:10.1016/j.solmat.2006.04.007.
Morita, Yuji, Lily Cao, Virginia C. Gould, Matthew B. Avison, and Keith Poole. 2006. “nalD Encodes a Second Repressor of the mexAB-oprM Multidrug Efflux Operon of *Pseudomonas aeruginosa*.” *Journal of Bacteriology* 188 (24): 8649–54. doi:10.1128/JB.01342-06.
Morones, Jose Ruben, Jose Luis Elechiguerra, Alejandra Camacho, Katherine Holt, Juan B Kouri, Jose Tapia Ram, Miguel Jose Yacaman, Jose Tapia Ramírez, Miguel Jose Yacaman, and Jose Tapia Ram. 2005. “The Bactericidal Effect of Silver Nanoparticles.” *Nanotechnology* 16 (10): 2346–53. doi:10.1088/0957-4484/16/10/059.
Mryasov, O., and A. Freeman. 2001. “Electronic Band Structure of Indium Tin Oxide and Criteria for Transparent Conducting Behavior.” *Physical Review B* 64 (23): 233111. doi:10.1103/PhysRevB.64.233111.
Mueller, Nicole C, and Bernd Nowack. 2008. “Exposure Modeling of Engineered Nanoparticles in the Environment.” *Environmental Science & Technology* 42 (12): 4447–53. http://www.ncbi.nlm.nih.gov/pubmed/18605569.
Mulvaney, Paul, Thomas Linnert, and Arnim Henglein. 1991. “Surface Chemistry of Colloidal Silver in Aqueous Solution: Observations on Chemisorption and Reactivity.” ... *Journal of Physical Chemistry* 95 (20): 7843–46. http://pubs.acs.org/doi/abs/10.1021/j100173a053.
Murthy, Shashi K. 2007. “Nanoparticles in Modern Medicine: State of the Art and Future Challenges.” *International Journal of Nanomedicine* 2 (2): 129–41. http://www.pubmedcentral.nih.gov/articlerender.fcgi?artid=2673971&tool=pmcentrez&rendertype=abstract.
Musee, Ndeke, Melusi Thwala, and Nomakhwezi Nota. 2011. “The Antibacterial Effects of Engineered Nanomaterials: Implications for Wastewater Treatment Plants.” *Journal of Environmental Monitoring : JEM* 13 (5): 1164–83. doi:10.1039/c1em10023h.
Nagy, Amber. 2010. “Characterization and Interactions of Nanoparticles in Biological Systems.” *The Ohio State University*. doi:10.1017/CBO9781107415324.004.
Nel, Andre. 2007. “Toxic Potential of Materials.” *Science* 311 (5726): 622–27. doi:10.1126/science.1114397.

Nel, Andre E, Lutz Mädler, Darrell Velegol, Tian Xia, Eric M V Hoek, Ponisseril Somasundaran, Fred Klaessig, Vince Castranova, and Mike Thompson. 2009. "Understanding Biophysicochemical Interactions at the Nano-Bio Interface." *Nature Materials* 8 (7). Nature Publishing Group: 543–57. doi:10.1038/nmat2442.

Nies, D. H. 1999. "Microbial Heavy-Metal Resistance." *Applied Microbiology and Biotechnology* 51 (6): 730–50. doi:10.1007/s002530051457.

Nies, Dietrich. 2003. "Efflux-Mediated Heavy Metal Resistance in Prokaryotes." *FEMS Microbiology Reviews* 27 (2–3): 313–39. doi:10.1016/S0168-6445(03)00048-2.

Nishino, Kunihiko, Eiji Nikaido, and Akihito Yamaguchi. 2007. "Regulation of Multidrug Efflux Systems Involved in Multidrug and Metal Resistance of Salmonella Enterica Serovar Typhimurium." *Journal of Bacteriology* 189 (24): 9066–75. doi:10.1128/JB.01045-07.

Norrby, S Ragnar, Carl Erik Nord, Roger Finch, S Ragnar Norrby, Carl Erik Nord, and Roger Finch. 2005. "Lack of Development of New Antimicrobial Drugs: A Potential Serious Threat to Public Health." *The Lancet. Infectious Diseases* 5 (2): 115–19. doi:10.1016/S1473-3099(05)01283-1.

Nowack, Bernd. 2010. "Chemistry. Nanosilver Revisited Downstream." *Science (New York, N.Y.)* 330 (6007): 1054–55. doi:10.1126/science.1198074.

Otto, Karen, and Thomas J Silhavy. 2002. "Surface Sensing and Adhesion of Escherichia Coli Controlled by the Cpx-Signaling Pathway." *Proceedings of the National Academy of Sciences of the United States of America* 99 (4): 2287–92. doi:10.1073/pnas.042521699.

Owens, Robert C. 2008. "Antimicrobial Stewardship: Concepts and Strategies in the 21st Century." *Diagnostic Microbiology and Infectious Disease* 61 (1): 110–28. doi:10.1016/j.diagmicrobio.2008.02.012.

Panáček, Aleš, Libor Kvítek, Robert Prucek, Milan Kolář, Renata Večeřová, Naděžda Pizúrová, Virender K. Sharma, Tat'Jana Nevěčná, and Radek Zbořil. 2006. "Silver Colloid Nanoparticles: Synthesis, Characterization, and Their Antibacterial Activity." *Journal of Physical Chemistry B* 110 (33): 16248–53. doi:10.1021/jp063826h.

Papp-Wallace, Krisztina M., Andrea Endimiani, Magdalena A. Taracila, and Robert A. Bonomo. 2011. "Carbapenems: Past, Present, and Future." *Antimicrobial Agents and Chemotherapy* 55 (11): 4943–60. doi:10.1128/AAC.00296-11.

Park, Hee-jin, Jaeeun Jee Yeon Jaeeun Jee Yeon Kim, Jaeeun Jee Yeon Jaeeun Jee Yeon Kim, Joon-hee Lee, Ji-Sook Hahn, Man Bock Gu, Jeyong Yoon, et al. 2009. "Silver-Ion-Mediated Reactive Oxygen Species Generation Affecting Bactericidal Activity." *Water Research* 43 (4). Elsevier Ltd: 1027–32. doi:10.1016/j.watres.2008.12.002.

Peng, Xiaogang, Michael C. Schlamp, Andreas V. Kadavanich, and A. P. Alivisatos. 1997. "Epitaxial Growth of Highly Luminescent CdSe/CdS Core/shell Nanocrystals with Photostability and Electronic Accessibility." *Journal of the American Chemical Society* 119 (30): 7019–29. doi:10.1021/ja970754m.

Perron, Karl, Olivier Caille, Claude Rossier, Christian Van Delden, Jean Luc Dumas, and Thilo Köhler. 2004. "CzcR-CzcS, a Two-Component System Involved in Heavy

Metal and Carbapenem Resistance in *Pseudomonas aeruginosa*." *Journal of Biological Chemistry* 279 (10): 8761–68. doi:10.1074/jbc.M312080200.
Piddock, Laura J V. 2006. "Multidrug-Resistance Efflux Pumps - Not Just for Resistance." *Nature Reviews. Microbiology* 4 (8): 629–36. doi:10.1038/nrmicro1464.
Poole, Keith. 2001. "Multidrug Efflux Pumps and Antimicrobial Resistance in *Pseudomonas aeruginosa* and Related Organisms." *J. Mol. Microbiol. Biotechnol.* 3 (2): 255–64. http://www.ncbi.nlm.nih.gov/pubmed/11321581.
———. 2004. "Efflux-Mediated Multiresistance in Gram-Negative Bacteria." *Clinical Microbiology and Infection* 10 (1): 12–26. doi:Doi 10.1111/J.1469-0691.2004.00763.X.
———. 2008. "Bacterial Multidrug Efflux Pumps Serve Other Functions" 3 (4): 179–85.
———. 2012a. "Stress Responses as Determinants of Antimicrobial Resistance in Gram-Negative Bacteria." *Trends in Microbiology* 20 (5). Elsevier Ltd: 227–34. doi:10.1016/j.tim.2012.02.004.
———. 2012b. "Bacterial Stress Responses as Determinants of Antimicrobial Resistance." *The Journal of Antimicrobial Chemotherapy* 67 (9): 2069–89. doi:10.1093/jac/dks196.
———. 2014. "Stress Responses as Determinants of Antimicrobial Resistance in *Pseudomonas aeruginosa*: Multidrug Efflux and More." *Canadian Journal of Microbiology* 60 (12): 783–91. doi:10.1139/cjm-2014-0666.
Poole, Keith, K Krebes, C McNally, and S Neshat. 1993. "Multiple Antibiotic Resistance in *Pseudomonas aeruginosa*: Evidence for Involvement of an Efflux Operon." *J Bacteriol* 175 (22): 7363–72.
Potvin, Eric, Roger C Levesque, François Sanschagrin, and Roger C Levesque. 2008. "Sigma Factors in *Pseudomonas aeruginosa*." *FEMS Microbiology Reviews* 32 (1): 38–55. doi:10.1111/j.1574-6976.2007.00092.x.
Poveda, A, M Le Clech, and P Pasero. 2010. "Transcription as a Source of Genomic Instability during S Phase." *Transcription* in press (3): 204–14. doi:10.1038/nrg3152.Transcription.
Pratsinis, Sotiris E, Georgios a Sotiriou, and Sotiris E Pratsinis. 2010. "Antibacterial Activity of Nanosilver Ions and Particles." *Environmental Science & Technology* 44 (14): 5649–54. doi:10.1021/es101072s.
Qi, Lifeng, Zirong Xu, Xia Jiang, Yan Li, and Minqi Wang. 2005. "Cytotoxic Activities of Chitosan Nanoparticles and Copper-Loaded Nanoparticles." *Bioorganic & Medicinal Chemistry Letters* 15 (5): 1397–99. doi:10.1016/j.bmcl.2005.01.010.
Radzig, M a, V a Nadtochenko, O a Koksharova, J Kiwi, V A Lipasova, and I a Khmel. 2013. "Antibacterial Effects of Silver Nanoparticles on Gram-Negative Bacteria: Influence on the Growth and Biofilms Formation, Mechanisms of Action." *Colloids and Surfaces. B, Biointerfaces* 102 (February). Elsevier B.V.: 300–306. doi:10.1016/j.colsurfb.2012.07.039.
Rai, M K, S D Deshmukh, a P Ingle, and a K Gade. 2012. "Silver Nanoparticles: The Powerful Nanoweapon against Multidrug-Resistant Bacteria." *Journal of Applied*

Microbiology 112 (5): 841–52. doi:10.1111/j.1365-2672.2012.05253.x.
Raivio, Tracy L., Shannon K. D. Leblanc, and Nancy L. Price. 2013. "The Escherichia Coli Cpx Envelope Stress Response Regulates Genes of Diverse Function That Impact Antibiotic Resistance and Membrane Integrity." *Journal of Bacteriology* 195 (12): 2755–67. doi:10.1128/JB.00105-13.
Ramos, Juan L., Estrella Duque, María-Trinidad Gallegos, Patricia Godoy, María Isabel Ramos-González, Antonia Rojas, Wilson Terán, and Ana Segura. 2002. "Mechanisms of Solvent Tolerance in Gram-Negative Bacteria." *Annual Review of Microbiology* 56 (1): 743–68. doi:10.1146/annurev.micro.56.012302.161038.
Ratte, HT. 1999. "Bioaccumulation and Toxicity of SIlver Compounds: A Review." *Environmental Toxicology and Chemistry* 18 (1): 89–108. http://onlinelibrary.wiley.com/doi/10.1002/etc.5620180112/full.
Reibold, M., P. Paufler, A. A. Levin, W. Kochmann, N. Pätzke, and D. C. Meyer. 2006. "Materials: Carbon Nanotubes in an Ancient Damascus Sabre." *Nature* 444 (7117): 286. doi:10.1038/444286a.
Rodriguez-Montelongo, Luisa, Lilia C. de la Cruz-Rodriguez, Ricardo N. Farías, and Eddy M. Massa. 1993. "Membrane-Associated Redox Cycling of Copper Mediates Hydroperoxide Toxicity in Escherichia Coli." *BBA - Bioenergetics* 1144 (1): 77–84. doi:10.1016/0005-2728(93)90033-C.
Roe, David, Balu Karandikar, Nathan Bonn-Savage, Bruce Gibbins, and Jean-baptiste Roullet. 2008. "Antimicrobial Surface Functionalization of Plastic Catheters by Silver Nanoparticles." *The Journal of Antimicrobial Chemotherapy* 61 (4): 869–76. doi:10.1093/jac/dkn034.
Römer, Isabella, Thomas a White, Mohammed Baalousha, Kevin Chipman, Mark R Viant, and Jamie R Lead. 2011. "Aggregation and Dispersion of Silver Nanoparticles in Exposure Media for Aquatic Toxicity Tests." *Journal of Chromatography. A* 1218 (March): 4226–33. doi:10.1016/j.chroma.2011.03.034.
Ron, EZ. 2006. "Bacterial Stress Response." *The Prokaryotes*, 1012–27. http://link.springer.com/10.1007/0-387-30742-7_32.
Rowley, Gary, Michael Spector, Jan Kormanec, and Mark Roberts. 2006. "Pushing the Envelope: Extracytoplasmic Stress Responses in Bacterial Pathogens." *Nature Reviews. Microbiology* 4 (5): 383–94. doi:10.1038/nrmicro1394.
Sawa, Justyna, Alexander Heuck, Michael Ehrmann, and Tim Clausen. 2010. "Molecular Transformers in the Cell: Lessons Learned from the DegP Protease-Chaperone." *Current Opinion in Structural Biology* 20 (2). Elsevier Ltd: 253–58. doi:10.1016/j.sbi.2010.01.014.
Schellhorn, HE. 1995. "Regulation of Hydroperoxidase (Catalase) Expression in Escherichia Coli." *FEMS Microbiology Letters* 131 (1994): 113–19. http://onlinelibrary.wiley.com/doi/10.1111/j.1574-6968.1995.tb07764.x/abstract.
Schweizer, Herbert P. 2003. "Efflux as a Mechanism of Resistance to Antimicrobials in *Pseudomonas aeruginosa* and Related Bacteria: Unanswered Questions." *Genetics and Molecular Research : GMR* 2 (1): 48–62. http://www.ncbi.nlm.nih.gov/pubmed/12917802.

Séverine, Aendekerk, Bart Ghysels, Pierre Cornelis, Christine Baysse, Bart Ghysels, Pierre Cornelis, and Christine Baysse. 2002. “Characterization of a New Efflux Pump, MexGHI-OpmD, from *Pseudomonas aeruginosa* That Confers Resistance to Vanadium.” *Microbiology (Reading, England)* 148 (Pt 8): 2371–81. doi:10.1099/00221287-148-8-2371.

Sheng, Zhiya, and Yang Liu. 2011. “Effects of Silver Nanoparticles on Wastewater Biofilms.” *Water Research* 45 (18). Elsevier Ltd: 6039–50. doi:10.1016/j.watres.2011.08.065.

Shouldice, Stephen R., Begoña Heras, Patricia M. Walden, Makrina Totsika, Mark A. Schembri, and Jennifer L. Martin. 2011. “Structure and Function of DsbA, a Key Bacterial Oxidative Folding Catalyst.” *Antioxidants & Redox Signaling* 14 (9). Mary Ann Liebert, Inc. 140 Huguenot Street, 3rd Floor New Rochelle, NY 10801 USA : 1729–60. doi:10.1089/ars.2010.3344.

Sidoli, Simone, Katarzyna Kulej, and Benjamin A. Garcia. 2017. “Why Proteomics Is Not the New Genomics and the Future of Mass Spectrometry in Cell Biology.” *Journal of Cell Biology* 216 (1): 21–24. doi:10.1083/jcb.201612010.

Silver, S, A Gupta, K Matsui, and J F Lo. 1999. “Resistance to Ag(i) Cations in Bacteria: Environments, Genes and Proteins.” *Metal-Based Drugs* 6 (4–5): 315–20. doi:10.1155/MBD.1999.315.

Silver, Simon. 2003. “Bacterial Silver Resistance: Molecular Biology and Uses and Misuses of Silver Compounds.” *FEMS Microbiology Reviews* 27 (2–3): 341–53. doi:10.1016/S0168-6445(03)00047-0.

Simon-Deckers, a. 2009. “Size-, Composition-and Shape-Dependent Toxicological Impact of Metal Oxide Nanoparticles and Carbon Nanotubes toward Bacteria.” ... *Science & Technology*, 1–6. http://pubs.acs.org/doi/full/10.1021/es9016975.

Simon-deckers, Lique, Nathalie Herlin-boime, and Pierre Marie. 2009. “Shape-Dependent Toxicological Impact of Metal Oxide Nanoparticles and Carbon Nanotubes toward Bacteria,” 8423–29.

Simoncic, Barbara, and Brigita Tomsic. 2015. “Structures of Novel Antimicrobial Agents for Textiles – A Review.” *Textile Research Journal* 0 (0): 1–17. doi:10.1177/0040517510363193.

Singh, Nina, and Pamela J. Yeh. 2017. “Supressive Drug Combination and Their Potential to Combat Antibiotic Resistance.” *The Journal of Antibiotics* 70 (11): 1033–42. doi:10.1016/j.nurpra.2015.12.013.

Sondi, Ivan, and Branka Salopek-Sondi. 2004. “Silver Nanoparticles as Antimicrobial Agent: A Case Study on E. Coli as a Model for Gram-Negative Bacteria.” *Journal of Colloid and Interface Science* 275 (1): 177–82. doi:10.1016/j.jcis.2004.02.012.

Stark, G. 2005. “Functional Consequences of Oxidative Membrane Damage” 16: 1–16. doi:10.1007/s00232-005-0753-8.

Stepanauskas, Ramunas, Travis C. Glenn, Charles H. Jagoe, R. Cary Tuckfield, Angela H. Lindell, Catherine J. King, and J. V. McArthur. 2006. “Coselection for Microbial Resistance to Metals and Antibiotics in Freshwater Microcosms.” *Environmental Microbiology* 8 (September 2005): 1510–14. doi:10.1111/j.1462-

2920.2006.01091.x.
Stock, Ann M, Victoria L Robinson, and Paul N Goudreau. 2000. “Two-Component Signal Transduction.” *Reactions* 69: 183–215. doi:10.1146/annurev.biochem.69.1.183.
Stohs, S. J., and D. Bagchi. 1995. “Oxidative Mechanisms in the Toxicity of Metal Ions.” *Free Radical Biology and Medicine* 18 (2): 321–36. doi:10.1016/0891-5849(94)00159-H.
Storz, Gisela, and Regine Hengge. 2000. *Bacterial Stress Responses*. 1st ed. American Society For Microbiology Press.
———. 2011. *Bacterial Stress Response*. 2nd ed.
Stover, C K, X Q Pham, a L Erwin, S D Mizoguchi, P Warrener, M J Hickey, F S L Brinkman, et al. 2000. “Complete Genome Sequence of *Pseudomonas aeruginosa* PAO1, an Opportunistic Pathogen.” *Nature* 406 (6799): 959–64. doi:10.1038/35023079.
Sun, Tianmeng, Yu Shrike Zhang, Bo Pang, Dong Choon Hyun, Miaoxin Yang, and Younan Xia. 2014. “Engineered Nanoparticles for Drug Delivery in Cancer Therapy.” *Angewandte Chemie - International Edition* 53 (46): 12320–64. doi:10.1002/anie.201403036.
Szczepanowski, R, S Braun, V Riedel, S Schneiker, I Krahn, A Pu, a Pühler, and a Schlüter. 2005. “The 120 592 Bp IncF Plasmid pRSB107 Isolated from a Sewage-Treatment Plant Encodes Nine Different Antibiotic-Resistance Determinants, Two Iron-Acquisition Systems and Other Putative Virulence-Associated Functions.” *Microbiology (Reading, England)* 151 (Pt 4): 1095–1111. doi:10.1099/mic.0.27773-0.
Taniguchi, Yuichi, Paul J Choi, Gene-wei Li, Huiyi Chen, Mohan Babu, Jeremy Hearn, Andrew Emili, and X Sunney Xie. 2011. “Sensitivity in Single Cells.” *Science (New York, N.Y.)* 329 (5991): 533–39. doi:10.1126/science.1188308.
Teitzel, Gail M G.M., and Matthew R M.R. Parsek. 2003. “Heavy Metal Resistance of Biofilm and Planktonic *Pseudomonas aeruginosa*.” *Appl. Environ. Microbiol.* 69 (4): 2313–20. doi:10.1128/AEM.69.4.2313.
Tepper, James M, and Kurt Schlesinger. 1980. “Acoustic Priming and Kanamycin-Induced Cochlear Damage.” *Brain Research* 187 (1): 81–95. doi:10.1016/0006-8993(80)90496-5.
Thaden, Joshua T., Stephen Lory, and Timothy S. Gardner. 2010. “Quorum-Sensing Regulation of a Copper Toxicity System in *Pseudomonas aeruginosa*.” *Journal of Bacteriology* 192 (10): 2557–68. doi:10.1128/JB.01528-09.
Thannickal, Victor J, and Barry L Fanburg. 2000. “Reactive Oxygen Species in Cell Signaling.” *American Journal of Physiology Lung Cell Molecular Physiology*, no. 78.
Tian, Zhe Xian, Xue Xian Yi, Anna Cho, Fergal O’Gara, and Yi Ping Wang. 2016. “CpxR Activates MexAB-OprM Efflux Pump Expression and Enhances Antibiotic Resistance in Both Laboratory and Clinical nalB-Type Isolates of *Pseudomonas aeruginosa*.” *PLoS Pathogens* 12 (10). doi:10.1371/journal.ppat.1005932.

Toh, Her Shuang, Christopher Batchelor-Mcauley, Kristina Tschulik, and Richard G. Compton. 2014. “Chemical Interactions between Silver Nanoparticles and Thiols: A Comparison of Mercaptohexanol against Cysteine.” *Science China Chemistry* 57 (9): 1199–1210. doi:10.1007/s11426-014-5141-8.

Tseng, Tsai-tien T, Kevin S Gratwick, Justin Kollman, Daniel Park, Dietrich H Nies, André Goffeau, and Milton H Saier. 1999. “The RND Permease Superfamily: An Ancient, Ubiquitous and Diverse Family That Includes Human Disease and Development Proteins.” *Journal of Molecular Microbiology and Biotechnology* 1: 107–25.

Vaccaro, Brian J., W. Andrew Lancaster, Michael P. Thorgersen, Grant M. Zane, Adam D. Younkin, Alexey E. Kazakov, Kelly M. Wetmore, et al. 2016. “Novel Metal Cation Resistance Systems from Mutant Fitness Analysis of Denitrifying Pseudomonas Stutzeri.” *Applied and Environmental Microbiology* 82 (19): 6046–56. doi:10.1128/AEM.01845-16.

Vance, Marina E., Todd Kuiken, Eric P. Vejerano, Sean P. McGinnis, Michael F. Hochella, and David Rejeski Hull. 2015. “Nanotechnology in the Real World: Redeveloping the Nanomaterial Consumer Products Inventory.” *Beilstein Journal of Nanotechnology* 6 (1): 1769–80. doi:10.3762/bjnano.6.181.

Walsh, Christopher. 2000. “Molecular Mechanisms That Confer Antibacterial Drug Resistance.” *Nature* 406 (6797): 775–81. doi:10.1038/35021219.

Wassarman, Karen M., Gisela Storz, Jörg Vogel, Karen M. Wassarman, Gisela Storz, Jörg Vogel, Karen M. Wassarman, and Gisela Storz. 2011. “Regulation by Small RNAs in Bacteria: Expanding Frontiers.” *Molecular Cell* 43 (6): 880–91. doi:10.1016/j.molcel.2011.08.022.

Waxman, D J, and J L Strominger. 1983. “Penicillin-Binding Proteins and the Mechanism of Action of Beta-Lactam Antibiotics1.” *Annual Review of Biochemistry* 52 (1): 825–69. doi:10.1146/annurev.bi.52.070183.004141.

Wigginton, Nicholas S, Alexandre De E Titta, Flavio Piccapietra, Jan A N Dobias, Victor J Nesatyy, Marc J F Suter, and Rizlan Bernier-Latmani. 2010. “Binding of Silver Nanoparticles to Bacterial Proteins Depends on Surface Modifications and Inhibits Enzymatic Activity.” *Environmental Science & Technology* 44 (6): 2163–68. doi:10.1021/es903187s.

Wildgoose, Gregory G., Craig E. Banks, and Richard G. Compton. 2006. “Metal Nanoparticles and Related Materials Supported on Carbon Nanotubes: Methods and Applications.” *Small* 2 (2): 182–93. doi:10.1002/smll.200500324.

Williams, Gareth J., Steven D. Breazeale, Christian R H Raetz, and James H. Naismith. 2005. “Structure and Function of Both Domains of ArnA, a Dual Function Decarboxylase and a Formyltransferase, Involved in 4-Amino-4-Deoxy-L-Arabinose Biosynthesis.” *Journal of Biological Chemistry* 280 (24): 23000–8. doi:10.1074/jbc.M501534200.

Winsor, Geoffrey L., Emma J. Griffiths, Raymond Lo, Bhavjinder K. Dhillon, Julie A. Shay, and Fiona S.L. Brinkman. 2016. “Enhanced Annotations and Features for Comparing Thousands of *Pseudomonas* genomes in the *Pseudomonas* Genome

Database." *Nucleic Acids Research* 44 (D1): D646–53. doi:10.1093/nar/gkv1227.
World Health Organization, and Theresa Braine. 2011. "Race against Time to Develop New Antibiotics." *Bulletin of the World Health Organization* 89 (2): 88–89. doi:10.2471/BLT.11.030211.
Wu, Dong, Zhiting Huang, Kai Yang, David Graham, and Bing Xie. 2015. "Relationships between Antibiotics and Antibiotic Resistance Gene Levels in Municipal Solid Waste Leachates in Shanghai, China." *Environmental Science and Technology* 49 (7): 4122–28. doi:10.1021/es506081z.
Wulf, Peter De, and E. C C Lin. 2000. "Cpx Two-Component Signal Transduction in Escherichia Coli: Excessive CpxR-P Levels Underlie CpxA* Phenotypes." *Journal of Bacteriology* 182 (5): 1423–26. doi:10.1128/JB.182.5.1423-1426.2000.
Wurtzel, Omri, Deborah R. Yoder-himes, Kook Han, Ajai a. Dandekar, Sarit Edelheit, E. Peter Greenberg, Rotem Sorek, and Stephen Lory. 2012. "The Single-Nucleotide Resolution Transcriptome of *Pseudomonas aeruginosa* Grown in Body Temperature." *PLoS Pathogens* 8 (9). doi:10.1371/journal.ppat.1002945.
Wylie, John L, and Elizabeth A Worobec. 1995. "The OprB Porin Plays a Central Role in Carbohydrate Uptake in Pseudomonas These Include : The OprB Porin Plays a Central Role in Carbohydrate Uptake in *Pseudomonas aeruginosa*." *Journal of Bacteriology* 177 (11): 3021–26. doi:10.1128/JB.177.11.3021-3026.1995.
Xia, Tian, Michael Kovochich, Monty Liong, Lutz Mädler, Benjamin Gilbert, Haibin Shi, Joanne I Yeh, Jeffrey I Zink, and Andre E Nel. 2008. "Comparison of the Mechanism of Toxicity of Zinc Oxide and Cerium Oxide Nanoparticles Based on Dissolution and Oxidative Stress Properties." *ACS Nano* 2 (10): 2121–34. doi:10.1021/nn800511k.
Xiu, Zong-Ming, Jie Ma, and Pedro J. J. Alvarez. 2011a. "Differential Effect of Common Ligands and Molecular Oxygen on Antimicrobial Activity of Silver Nanoparticles versus Silver Ions." *Environmental Science & Technology* 45 (20): 9003–8. doi:10.1021/es201918f.
Xiu, Zong-Ming, Jie Ma, and Pedro J J Alvarez. 2011b. "Differential Effect of Common Ligands and Molecular Oxygen on Antimicrobial Activity of Silver Nanoparticles versus Silver Ions." *Environmental Science & Technology* 45 (20): 9003–8. doi:10.1021/es201918f.
Xiu, Zong-Ming, Qing-bo Zhang, Hema L. Puppala, Vicki L. Colvin, and Pedro J. J. Alvarez. 2012. "Negligible Particle-Specific Antibacterial Activity of Silver Nanoparticles." *Nano Letters* 12 (8): 4271–75. doi:10.1021/nl301934w.
Xiu, Zong Ming, Qing Bo Zhang, Hema L. Puppala, Vicki L. Colvin, and Pedro J J Alvarez. 2012. "Negligible Particle-Specific Antibacterial Activity of Silver Nanoparticles." *Nano Letters* 12 (8): 4271–75. doi:10.1021/nl301934w.
Yamamoto, Kaneyoshi, and Akira Ishihama. 2005. "Transcriptional Response of *Escherichia coli* to External Copper." *Molecular Microbiology* 56 (1): 215–27. doi:10.1111/j.1365-2958.2005.04532.x.
Yang, Xinyu, Andreas P. Gondikas, Stella M. Marinakos, Melanie Auffan, Jie Liu, Heileen Hsu-Kim, and Joel N. Meyer. 2012. "Mechanism of Silver Nanoparticle

Toxicity Is Dependent on Dissolved Silver and Surface Coating in *Caenorhabditis elegans*." *Environmental Science and Technology* 46 (2): 1119–27. doi:10.1021/es202417t.

Yang, Yu, and Pedro J.J. Alvarez. 2015. "Sublethal Concentrations of Silver Nanoparticles Stimulate Biofilm Development." *Environmental Science and Technology Letters* 2 (8): 221–26. doi:10.1021/acs.estlett.5b00159.

Yin, Liyan, Yingwen Cheng, Benjamin Espinasse, Benjamin P. Colman, Melanie Auffan, Mark Wiesner, Jerome Rose, Jie Liu, and Emily S. Bernhardt. 2011. "More than the Ions: The Effects of Silver Nanoparticles on Lolium Multiflorum." *Environmental Science and Technology* 45 (6): 2360–67. doi:10.1021/es103995x.

Yoneda, Kazuhiko, Hiroki Chikumi, Takeshi Murata, Naomasa Gotoh, Hiroyuki Yamamoto, Hiromitsu Fujiwara, Takeshi Nishino, and Eiji Shimizu. 2005. "Measurement of *Pseudomonas aeruginosa* Multidrug Efflux Pumps by Quantitative Real-Time Polymerase Chain Reaction." *FEMS Microbiology Letters* 243 (1): 125–31. doi:10.1016/j.femsle.2004.11.048.

Yoneyama, Hiroshi, and Taiji Nakae. 1996. "Protein C (OprC) of the Outer Membrane of *Pseudornonas aeruginosa* Is a Copper-Regulated Channel Protein." *Microbiology* 142 (1 996): 2137–44.